

On The Integrated Analysis And Forensic Interpretation Of Gunshot Residues

By

Callum Michael Bonnar
BSc (Hons) (Analytical Chemistry)

*Thesis Submitted to Flinders University
for fulfilment of the degree of
Doctor of Philosophy
March 2023*

College of Science and Engineering
Flinders University
Adelaide, South Australia

Table of Contents

LIST OF FIGURES	5
LIST OF TABLES	7
DECLARATIONS	9
ACKNOWLEDGEMENTS	10
ABSTRACT	11
CHAPTER 1: BACKGROUND, LITERATURE REVIEW AND RESEARCH AIMS	13
1.1 Criminal use of firearms in Australia and worldwide	14
1.2 Firearms and the Production of GSR Traces	15
1.3 Collection of GSR Traces for Forensic Purposes	17
1.3.1 Wax Fixation	17
1.3.2 Adhesive Lifting	17
1.3.3 Wet Swabbing.....	17
1.3.4 Vacuum Lifting	18
1.3.5 Vapour Trapping	18
1.4 Forensic Interpretation of GSR	18
1.4.1 Identification of material as GSR	19
1.3.2 Distribution and Deposition	19
1.4.2 Secondary and Subsequent Transfers of GSR	20
1.4.3 Persistence of GSR	20
1.4.4 Contamination and Pollution	21
1.4.5 Source-Attribution or Linking Exhibits.....	23
1.4.6 Memory Effect	24
1.5 Chemistry and Classification of GSRs	25
1.5.1 Inorganic GSR.....	25
1.5.2 Organic GSR	28
1.6 GSR-Like Material	32
1.7 Analytical Methods.....	33
1.7.1 Analysis of Inorganic GSR	34
1.7.2 Analysis of Organic GSR	38
1.7.3 Holistic Analyses	50
1.8 Summary and Research Objectives	52
1.8.1 Assessment of the state-of-the-art	52
1.8.2 Research Objectives	53
CHAPTER 2: TECHNICAL METHOD DEVELOPMENT	56
2.1 Background:.....	57
2.2 Tandem detection of organic and inorganic gunshot residues using LC-MS and SEM-EDS.....	58
2.2.1 Abstract	58

2.2.2 Introduction	58
2.2.3 Experimental.....	63
2.2.4 Results and Discussion.....	67
2.2.5 Conclusions.....	75
2.2.6 Acknowledgements	76
2.3 Further Refinement & Investigation of Efficacy	76
2.3.1 Adjusted LC-MS instrumental settings	76
2.3.2 GSR collected from surfaces other than human hand skin	78
2.3.3 Testing of specimens with delay between GSR exposure and sampling	82
2.3.4 Results	84
2.3.5 Summary.....	88
2.4 Conclusions.....	88
CHAPTER 3: ENVIRONMENTAL PREVALENCE OF GSR OR GSR-LIKE TRACES	90
3.1 Background.....	91
3.2 Aims	97
3.3 Methods	98
3.3.1 Sample Collection	98
3.3.2 Instrument Settings	98
3.4 Results	99
3.4.1 LC-MS.....	100
3.4.2 SEM-EDS	103
3.5 Discussion	105
3.5.1 Samples from known shooters.....	105
3.5.2 Samples from non-shooters	106
3.6 Conclusions.....	107
CHAPTER 4: STATISTICAL INTERPRETATION OF INTEGRATED GSR DATA	108
4.1 Introduction.....	109
4.2 Background.....	110
4.2.1 Evaluative Reporting.....	110
4.2.2 Conditional Probability	112
4.2.3 Bayesian Networks for GSR evidence evaluation.....	114
4.2.4 Probability Distribution Functions.....	115
4.2.5 Multivariate Data: Machine Learning, Neural Networks, and Score-Based Approaches.....	116
4.3 Aims	119
4.4 Calculations and Discussion.....	119
4.4.1 Predictive Power of Diagnostic Tests	119
4.4.2 Independence of Diagnostic Results	126
4.4.3 Summary of Qualitative Results	127
4.5 Univariate, Quantitative Models of GSR Evidence	128

4.6 Multivariate Models of GSR Evidence	133
4.6.1 Pre-processing and Exploratory Analysis.....	133
4.6.2 Partial least squares discriminant analysis (PLS-DA)	136
4.6.3 Artificial Neural Networks	140
4.7 Conclusions.....	144
CHAPTER 5: GSR IN VEHICLES	147
5.1 Background.....	148
5.2 Vehicles as a potential source of “GSR-like” material:.....	149
5.2.1 Brake Pads:	149
5.2.2 Airbags:.....	150
5.2.3 Tyre Rubber:	151
5.3 Background surveys of vehicles for GSR traces.....	153
5.4 Published case studies featuring specific GSR/Vehicle interactions:	155
5.4.1 Discharge of a Pistol Out a Car Window with the Breech Within the Interior of the Car: Analysis of Gunshot Residue on a Car’s Interior Surfaces (2017), Burnett & Lebieczik ^[299]	155
5.4.2 A case of alleged discharge of a firearm within a vehicle (2018), Burnett ^[300]	156
5.4.3 Gunshot residue and airbags: Part II. A case study (2019), Denis & Hearn ^[301]	157
5.5 Aims	158
5.6 Methods	159
5.6.1 Positive Control Scenario.....	159
5.6.2 Survey	159
5.7 Results and Discussion:.....	160
5.7.1 Positive Control Scenario.....	160
5.7.2 Survey of privately-owned vehicles.....	164
5.7.3 Evaluating and Assigning Weight to Analytical Observations	169
5.8 Conclusions:.....	174
CHAPTER 6: ANALYSIS OF OGSR BY AMBIENT MASS SPECTROMETRY	175
6.1 Background.....	176
6.2 Armed with the Facts: A Method for the Analysis of Smokeless Powders by Ambient Mass Spectrometry.....	178
6.2.1 Abstract	178
6.2.2 Introduction.....	178
6.2.3 Experimental.....	184
6.2.4 Results and Discussion.....	188
6.2.5 Conclusions.....	202
6.2.6 Acknowledgments	202
6.3 Direct Analysis in Real-Time (DART)	203
6.3.1 Introduction:.....	203
6.3.2 Experimental:	204
6.3.3 Results and Discussion.....	205

6.3.4 Conclusions.....	220
6.4 Conclusions.....	220
CHAPTER 7: GENERAL CONCLUSIONS	221
7.1 Themes	222
7.2 Technical method development.....	222
7.3 Collecting representative data from real GSR traces	224
7.3.1 Samples Collected from Hands.....	225
7.3.2 Samples collected from Vehicles.....	226
7.4 Investigating how these new data could be interpreted	227
7.4.1 Technical Interpretation of GSR Evidence	227
7.4.2 Evaluative Interpretations of Quantitative and Multivariate GSR Data.....	229
7.5 Further Research Directions and Future Prospects.....	230
CHAPTER 8: BIBLIOGRAPHY AND APPENDICES.....	232
8.1 Reproduced Figures.....	232
8.2 Bibliography.....	233
8.3 Appendices	248
Appendix 2-1.....	248
Appendix 3-1.....	249
Appendix 5-1.....	251
Appendix 5-2.....	253
Appendix 6-1.....	255
Appendix 6-2.....	256

List of Figures

Figure 1-1: Trends in Australian firearm fatalities to 2019 (data from Australian Bureau of Statistics).....	14
Figure 1-2: Components of ammunition and stages of firing process. Example shows a rimfire-style cartridge.	16
Figure 1-3: Molecular Structures of nitroglycerin (NG, left) and nitrocellulose (NC, right)	28
Figure 1-4: Formation of by-products in diphenylamine-stabilised propellant	30
Figure 1-5: Images showing the superficial damage to carbon stub surface after analysis for GSR by LIBS. Reproduced from Trejos <i>et al.</i> , (2018).	36
Figure 1-6: A GSR particle pre- and post- exposure to laser ablation. Reproduced from Dona-Fernandez <i>et al.</i> , (2018).	37
Figure 1-7: Cyclic Voltammogram showing response to GSR standards. Reproduced from Vuki <i>et al.</i> , (2012).	41
Figure 1-8: A representation of the principles behind a) Electrospray- and b) Plasma- based ambient desorption/ionisation instruments. Reproduced from Cooks <i>et al.</i> , (2006).	46
Figure 2-1: Secondary Electron image of a hand sampling stub, both pre-solvent (left) and post-solvent (right). Red circle indicates a slight visible change to the stub, potentially attributable to solvent contact.....	68
Figure 2-2: Particle from 0.40 calibre ammunition, collected on the right hand of a volunteer shooter, pre- solvent (left) and post-solvent (right).	68
Figure 2-3: Characteristic PbSbBa particle (approx. 18 μm diameter) originating from 0.40 calibre ammunition, detected on the sampling stub following organic extraction. This is the same particle displayed in Figure 2-2.	69
Figure 2-4: "Characteristic" particle distribution map of sampling stub from the shooter's left hand following discharge of 6x 0.22LR rounds from a revolver. Pre-solvent (black) and Post-solvent (red, offset).....	71
Figure 2-5: "Characteristic" particle distribution map of sampling stub from the shooter's left hand following discharge of 6x 0.22LR rounds from a revolver. Pre-solvent (black) and Post-solvent (red, offset).....	73
Figure 2-6: Mean recovery values from three stub surfaces, each doped with a selection of OGSR compounds at different concentrations. Error bars represent 3 standard deviations.	73
Figure 2-7: Overlaid extracted ion chromatograms of OGSR standards, after additional refinement of solvent profiles.	77
Figure 2-8: Interchangeable target setup, here holding a blood-smear paper substrate.....	80
Figure 2-9: (left) Plain paper target displaying presence of bullet wipe and dark GSR material.	80
Figure 2-10: Comparison of OGSR recovered from different substrates, including textiles and grease-proof paper swabbed with various liquids.	82
Figure 2-11: Image showing representative PDMS collection patch and their orientation relative to firearm (slide has been manually retracted).	84
Figure 2-12 a): Normalized recovery of OGSR compounds vs time to sampling.....	86
Figure 3-1: This particle was found on an individual who declared that they had not discharged a firearm for more than two years. The distribution of elements within the particle was largely homogenous, with Pb (red), Sb (pink), Ba (blue) and Cu (purple) shown.	104
Figure 4-1: Hierarchy of propositions in a forensic case involving trace evidence, applied to GSR.	111
Figure 4-2: A generalized Bayesian network for the evaluation of GSR evidence, reproduced from Seyfang <i>et al.</i> , (2019).	115
Figure 4-3: Tree diagram displaying the steps needed to calculate positive predictive value when the base rate, sensitivity and selectivity of the test are known.	123

Figure 4-4: Tree diagram displaying the steps needed to calculate a posterior predictive value, when the outcome of a previous test is already known.	124
Figure 4-5 a-c: Quantized observations of GSR loading, and calculated PDFs	130
Figure 4-6: Partial least squares discriminant analysis (PLS-DA) plot of GSR survey data	136
Figure 4-7: Plot of scores assigned to survey samples, using the first PLS-DA vector (t_1).	137
Figure 4-8: Sensitivity and specificity of decision thresholds applied to PLS-DA scores	138
Figure 4-9: Likelihood ratios assigned to survey samples using PLS-DA modelling	139
Figure 4-10: General form of an artificial neural network. The modelling program will apply prospective weightings to the measurements taken from each sample iteratively, until the training data can be correctly categorized based upon their output scores. Weightings calculated for this experiments' data set can be found in Table 4-8.....	141
Figure 4-11: Sensitivity and specificity of decision thresholds applied to ANN scores	143
Figure 4-12: Likelihood ratios assigned to survey samples using ANN modelling	144
Figure 5-1: Diphenylamine (DPA) and related compounds with known or suspected association with tyre-rubber.....	153
Figure 5-2: An arbitrarily selected particle recovered from cartridge debris shown in back-scatter and selected elemental maps reconstructed from EDX spectra. This particle appears to consist of a glassy core partially encapsulated by a Ba/Pb shell. Further analogous particles were also observed.	163
Figure 5-3: Observed distribution of characteristic particles within vehicles.	165
Figure 5-4: EDX Spectrum and SEM imaging for characteristic GSR particle located in a vehicle belonging to a survey respondent stating that they had never had contact with firearms.	168
Figure 5-5: Summary of GSR examination results from different subpopulations within the survey, identified <i>via</i> written responses.	170
Figure 5-6: Probability distribution functions describing the estimated probability of observing a given number of characteristic particles, in samples taken from different subpopulations.....	172
Figure 6-1: Schematic view of a DART-MS ion source, one example of AIMS technology. Reproduced from Cody, Laramée & Durst, (2005).	177
Figure 6-2: Negative-ion DSA-ToF-MS Spectrum for the analysis of trinitroglycerin.....	190
Figure 6-3: a) DSA Spectra of co-analysed methyl- (5 ng) and ethyl- (2ng) centralite, with observed accurate m/z values. b, c) Proposed fragmentation patterns, with calculated exact m/z values.	191
Figure 6-4: a) Plot of the raw peak areas obtained for deposits of both the d6-DPA internal standard (1.0 ng) and DPA calibration (0.25, 0.5, 0.75, 1.0, 1.5, 2.0 and 2.5 ng, 4 replicates of each). b) Mean corrected peak area plotted against DPA mass deposited to mesh. Error bars represent three standard deviations ($n=4$).196	196
Figure 6-5: Powder sample extracts #3 (a), #22 (b) and #26 (c), analysed in both positive- and negative- ion modes. Spectra are normalised to the most abundant peak in each.	198
Figure 6-6: a): comparison between spectra obtained from a clean sampling stub, and one exposed to GSR. b): High-resolution excerpt of the same spectra.....	201
Figure 6-7: (left) Perkin-Elmer AxION® Direct Sample Analysis (DSA™) system with enclosed mesh sample mount and (right) JEOL USA Direct Analysis in Real Time (DART®) ion-source and Vapor® interface, in transmission or reflectance configurations.....	204
Figure 6-8: (Top) Sum of parent and product ions for each analyte plotted by desorption temperature. (Bottom): Ratio of parent ion to product ion with increasing desorption temperature.	206
Figure 6-9: Peaks for protonated diphenylamine measured using two settings of an ion-trap MS with DART, compared to the same peak by DSA-AccuToFMS (normalised by intensity).	207

Figure 6-10: Total ion intensity observed as four mesh positions moved between the DART source and the Vapur interface, when using either helium or nitrogen feed gasses. The first three positions for each test contained the same amount of OGSR reference mixture, while the fourth position was blank/untreated mesh.	208
Figure 6-11: Spectra from powder extracts #3 (a), #22 (b), and #26 (c) in Table 6-7. Each was analysed in both positive- and negative- ion modes. Spectra are normalized to the most abundant peak.	212
Figure 6-12: a) Comparison of pre-shooting and post-shooting DART-MS spectra from hand samples collected with adhesive stubs supplied by Pelco. No differences signifying detection of OGSR were observed.	216
Figure 6-13: a) Spectra collected from extracted post-shooting hand-samples using DART-AccuToFTM MS. Spectrum A from blank stub, supplied by Ted Pella. The author would like to thank Dr. R. Cody and colleagues for their valuable contribution of these data (R. Cody, personal communications, February 2020).	218

List of Tables

Table 1-1: Relative Value and Categorisation of OGSR Compounds	31
Table 1-2: Ionisation Pathways Initiated by DART Ion Source [196, 198]	49
Table 2-1: Set-up and Operating Conditions for SEM-EDS Analysis	65
Table 2-2: HPLC Solvent Profile	65
Table 2-3: OGSR Compounds Targeted in this Study	66
Table 2-4: Pre- and post- solvent particle counts for 0.22 calibre ammunition, from the dominant hand of the shooter	70
Table 2-5: Pre- and post- solvent particle counts for 0.40 calibre ammunition, from the dominant hand of the shooter	70
Table 2-6: Compounds detected in residue <i>via</i> stub collection after firing two separate firearms, compared to the propellant powders recovered from the same lot of ammunition	74
Table 2-7: HPLC-MS Setup and operation	77
Table 2-8: Replicates showing detectable amounts of all OGSR markers.....	84
Table 2-9: IGSR particles found on PDMS patches	85
Table 3-1: Published Surveys of GSR on Randomly or Selectively Sampled Persons	93
Table 3-2: Separate Prevalence Values for Individual Analytes	96
Table 3-3: Solvent Profile	98
Table 3-4: Simplified Survey Results.....	99
Table 3-5: OGSR Marker Compounds Detected in Shooter Samples	101
Table 4-1: Verbal equivalent scale for numerical likelihood ratios. H_p = prosecution hypothesis, H_d = defence hypothesis	113
Table 4-2: Observed Results for Each Test and Subgroup.....	120
Table 4-3: Predictive Values (Single Test).....	121
Table 4-4: Predictive Values after Sequential Re-Testing	125
Table 4-5: p - values calculated for the data under each parametric PDF	129
Table 4-6: LRs applied to characteristic IGSR data under two different parametric models.....	132
Table 4-7: Correlation matrix between indicators of GSR exposure collected from the samples in Chapter 3:.. Pearson coefficients are displayed above the diagonal, with associated p values below the diagonal.	135

Table 4-8: ANN Weightings using GSR Survey Training Data	142
Table 5-1: Observations of DPA & NO _x DPA in Urban Dust by Liu <i>et al.</i> ^[295]	152
Table 5-2: Summary of studies reporting on GSR detected in police vehicles.....	154
Table 5-3: GSR samples reported in the case.....	157
Table 5-4: Approximate concentrations of each smokeless powder stabiliser in extracts recovered <i>via</i> adhesive stub, separated by location.....	160
Table 5-5: Particle Loadings by Location and Classification	162
Table 5-6: OGSR marker compounds detected in shooter's vehicles	166
Table 5-7: Likelihood ratios estimated under mixed-PDF model	173
Table 6-1: Goudsmits <i>et al.s'</i> proposed hierarchical classification of compounds associated with propellant ^[85]	180
Table 6-2: Charged species representing targeted analytes as observed when using DSA-ToF-MS	188
Table 6-3: Mass Accuracy and Resolution of DSA-MS System	194
Table 6-4: Observed Composition of 30 smokeless powders, representing past and present products accessible in Australia.....	199
Table 6-5: Mass-resolution (FWHM, amu) of OGSR reference compounds using two Velos Pro operating modes	207
Table 6-6: Accurate-mass measurement of OGSR molecules by DART-MS	210
Table 6-7: Observed composition of 30 smokeless powders using DART-MS	213

Declarations

Academic Integrity

I certify that this thesis does not incorporate without acknowledgment any material previously submitted for a degree or diploma in any university; and that to the best of my knowledge and belief it does not contain any material previously published or written by another person except where due reference is made in the text.

Signed: Callum Bonnar

Date: December 1st, 2022

Funding Sources

This research was supported by an Australian Government Research Training Program (RTP) Scholarship.

Additional funding was provided by the Ross Vining Memorial Research Fund (administered by Forensic Science South Australia).

Generous in-kind support was provided by both ChemCentre and Forensic Science South Australia.

Part-funding to allow attendance at the Australian and New Zealand Forensic Science Society's 2018 Symposium was provided by the Flinders University Student Association (FUSA) Development Grants program.

Publications

The following peer-reviewed publications were created by the author and have been reproduced as part of this thesis. Details on how these texts fit within the larger body of research are given as they appear in the document.

- C. Bonnar, E. Moule, N. Lucas, K. Seyfang, R. Dunsmore, R. Popelka-Filcoff, K. Redman, K.P. Kirkbride. Tandem detection of organic and inorganic gunshot residues using LC-MS and SEM-EDS. *Forensic Science International*, **2020** (314).
- C. Bonnar, R. Popelka-Filcoff, K.P. Kirkbride. Armed with the Facts: A Method for the Analysis of Smokeless Powders by Ambient Mass Spectrometry. *Journal of the American Society for Mass Spectrometry*, **2020** (31).

Further contributions were made by the author to the following publications, during the course of this research:

- K. Pitts, C. Bonnar. Gunshot Residue. *Encyclopedia of Forensic Sciences, Third Edition*. Elsevier, **2023** (vol. 3, p63-74).
- K-A. Stark, J. Gascooke, C. Gibson, C. Lenehan, C. Bonnar, M. Fitzgerald, K.P. Kirkbride. Xylitol Pentanitrate – Its characterization and analysis. *Forensic science international*, **2020** (316).

Acknowledgements

“Education never ends, Watson. It is a series of lessons with the greatest for the last. This is an instructive case. There is neither money nor credit in it, and yet one would wish to tidy it up.”

- Arthur Conan Doyle, 1911.

While no brief dedication can adequately convey the thanks I owe to many, I shall attempt to do so here.

Firstly, to my primary supervisor K. Paul Kirkbride – When I initially considered undertaking a PhD, everyone with whom I spoke recommended that I should seek to learn from your wisdom. I honestly believe that following those endorsements was one of the best decisions I have ever made. If there are any limits to your knowledge of academic forensic science, or to your interest in my research ideas, I certainly did not find them. Your support, guidance, and encouragement have been invaluable to this project, and to me personally. You have my wholehearted gratitude.

To my co-supervisor Rachel Popelka-Filcoff – thank you for all your insight, advice, and video call discussions. You have often been the first to spot potential problems before they arose, in both my research and when navigating university systems. I appreciate your help in avoiding those pitfalls. Thank you for encouraging me to be a more diligent scientist.

To John Coumbaros and Kahlee Redman, my industry supervisors from ChemCentre and Forensic Science South Australia respectively – The introductions, infrastructure, and resources you arranged have been enormously helpful to me, and the quality of my project has been greatly improved by your personal involvements. I am also sincerely grateful for all the time you managed to find to assist me with my research, above and beyond your many other duties.

To Rob, Kari and David – I am amazed at the technical knowledge you collectively hold. Thank you for everything that you have taught me and for always taking the time to stop and chat. I am particularly indebted to you for the many hours spent in fieldwork or wrangling temperamental equipment on my behalf. To you and everyone else in the Forensic Chemistry teams at ChemCentre, thank you for your friendly and patient hospitality while sharing your lab spaces with me.

To those recent Flinders alumni whose ranks I hope to soon join - thank you for the warm welcome into PhD life and to Adelaide. You helped me feel at home very quickly. In no particular order, I'm glad to have met you Nick, Kelsey, Eliza, Kelly-Anne, Shaun, Jo, Jennie, Tim and Tristan. Here's to crossing paths again at conferences and in more new cities.

Additional thanks are owed to the many enthusiastic, yet anonymous, volunteers who participated in the surveys conducted for this project. I would also like to take this opportunity to acknowledge all members of the Australian and New Zealand Forensic Science Society for the work they have contributed to build such a lively and inclusive forensic community.

To my family – I am grateful for all the years of care and encouragement you have given me. Thank you for always asking about my research with sincerity. Seeing your work ethic always motivates me. To my parents especially, this dissertation stands as a testament to the value you have always placed on my education.

Finally to Karin - I feel blessed to have gone through the PhD process with a partner who understands contemporary academia by my side. Thank you for your patience during the many occasions when research has taken up more than its fair share of my time and attention. Your friendship, support, and reminders to “be kind to myself” continue to sustain me and inspire me to be my happiest self. I love you very much.

Abstract

Gunshot residue (GSR) is a type of trace material that can be very important to the investigative, coronial, or criminal justice outcomes of incidents involving firearms. If scientists can identify and interpret these traces, they can contribute valuable information to the forensic process. The intent of this body of work was to improve the capabilities available to forensic practitioners, regarding this particular category of trace evidence.

Specifically, it was identified that contemporary GSR analyses largely target the inorganic portion of gunshot residues (IGSR). Forensic scientists already recognize that firearms also produce organic residues (OGSR). Research into the exploitation of OGSR traces as evidence has been well documented in academic literature, but as yet no single technique has been adopted into routine laboratory use. It is even rarer for an integrated (IGSR/OGSR) methodology, using data on both components of the trace, to be used forensically for either detection or evaluation of traces. The original contribution to knowledge made by this PhD project was the exploration of options for this unified approach.

New data on the subject were generated using combinations of laboratory experimentation, firing range fieldwork, and collection of survey samples. Authentic GSR samples were collected both from shooting experiments performed under controlled conditions and also following “natural” shooting activities undertaken by recreational shooters. It was found that liquid chromatography-mass spectrometry instrumentation, already available to forensic chemistry laboratories, could detect known OGSR compounds from recovered traces. A process for preparing subsamples for this organic analysis, while still retaining the possibility of inorganic analysis by scanning electron microscopy (SEM-EDS), was developed. Further samples were collected alongside written surveys asking about recent firearm use. Analysis of the pool of “non-shooter” background samples gave confidence that the combination of analytical methods was specific for the detection of GSR, with few to no false positives. This tandem approach offers potential improvement over current methodologies, as it increases the mass of material that can be targeted for detection. It also allows greater confidence when discriminating between GSR and inorganic, environmental GSR-like interferences by providing more chemical data to the analyst from each trace. These data are applicable to sub-source and activity-level evaluations used by experts in some jurisdictions when presenting their findings.

Next, different strategies for combining the outputs of each test into a single reportable result were investigated. Initially, the inorganic and organic laboratory tests were judged to indicate whether samples were either “positive” or “negative” for GSR using separate, predetermined categorical requirements. A Bayesian updating approach was then used to show that a statistical improvement in diagnostic accuracy was achieved when using two categorical tests in tandem. More advanced statistical methods including both

univariate and multivariate models were also used to generate likelihood ratios representing the potential strength of evidence that could be provided to an investigator or courtroom. Of several techniques evaluated, artificial neural networks were chosen as the preferred method for synthesising multivariate data into a cohesive output without needing to discard any underlying information. Some perceived advantages and disadvantages of choosing categorical or likelihood ratio-based reporting are discussed. Data were also used as examples to perform certain sub-source and activity-level evaluations.

Finally, two separate spectrometers featuring ambient-ionisation capability were assessed for possible use as rapid and selective detectors for analysing GSR. Both “Direct Sample Analysis” (DSA™) and “Direct Analysis in Real-Time” (DART®) ion-sources were found to be capable of desorbing and ionising relevant OGSR compounds. Either instrument was suitable for analysing, and potentially discriminating between, smokeless powders collected in their unburned state. However, the outcomes for GSR samples collected using adhesive stubs were poor due to a significant background signal arising from the adhesive in the stubs themselves. Therefore it is suggested that any future efforts to incorporate AIMS into a GSR detection procedure should focus on sample collection or isolation procedures.

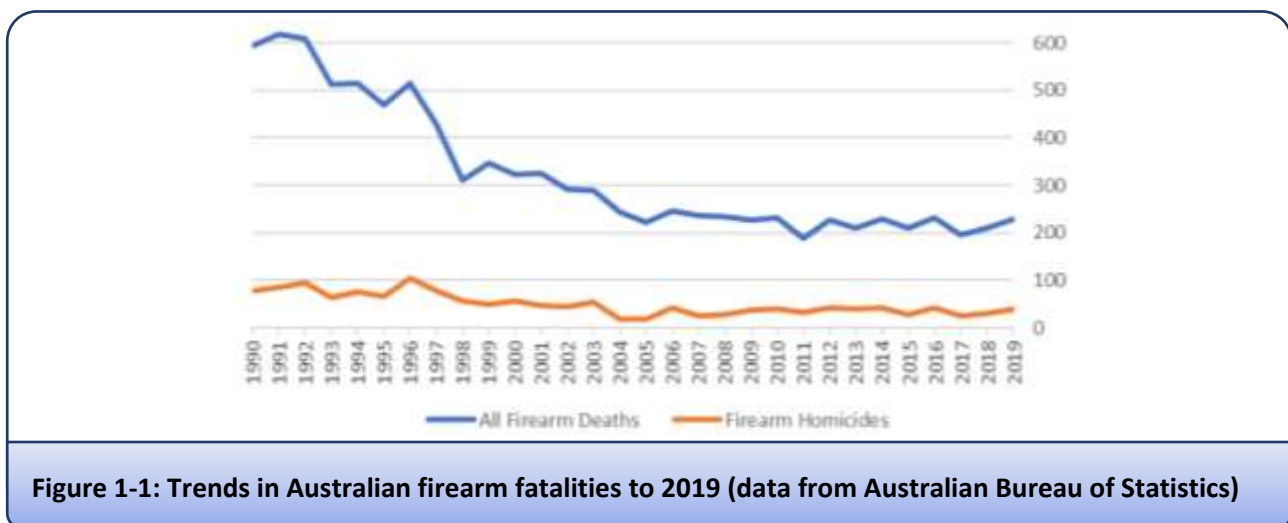
In summary, the integrated analysis of GSR traces was found by the author to both be technically feasible and to offer greater value to forensic scientists than the sum of its parts.

Chapter 1:

Background, Literature Review and Research Aims

1.1 Criminal use of firearms in Australia and worldwide

Of all the matters in which forensic scientists are called upon to provide their expertise, those involving firearms are among the most serious. Australia experiences a comparatively low rate of gun crime, often attributed to legal reforms enacted between 1996 and 1998 [1, 2]. However, incidents involving firearms continue to occur. Figure 1-1 shows the number of fatalities in Australia caused by gunshot between 1990 and 2019. Suicide was the leading reason for death by firearm (79% in 2019), followed by homicide (13%), with the remainder recorded as either accidental deaths or undetermined causes [3]. Additional data from the Australian Bureau of statistics suggest that firearms were used in 22% of homicides, 5% of kidnappings and 6% of robberies in 2019 [4].



For contrast, approximately three quarters of homicides and half of suicides involve firearms in the U.S.A., where controls are less strict and private ownership rates are much higher. Over 45,000 people (13.6 per 100,000 people) were recorded as having died by gunshot in the United States during 2020 [5]. There were 15,070 homicides, 189,718 aggravated assaults, and 125,289 robberies recorded as being committed with guns in 2016 [6]. Use of firearms in crime is more difficult to measure in the European Union, due to differences in reporting practices between member states. It is estimated that there are approximately 1,000 firearm homicides in Europe per year [7]. A potential comparison can be made with England and Wales, where 9,406 incidents involving firearms were recorded in the year to March 2020. The weapon was discharged in 27% of those events, and 316 resulted in serious or fatal injuries [8].

While these figures may represent a small portion of total crimes committed, the investigation of such incidents is an important public safety objective because firearms have considerable potential to cause injury or death. There are multiple sub-disciplines of forensic science concerned with firearms. These include reconstruction of ballistic trajectories, distance-determination, comparison of striations on found on barrels and projectiles, or examination of firing pin indentations. This project specifically concentrates on the analysis of gunshot residue or GSR.

1.2 Firearms and the Production of GSR Traces

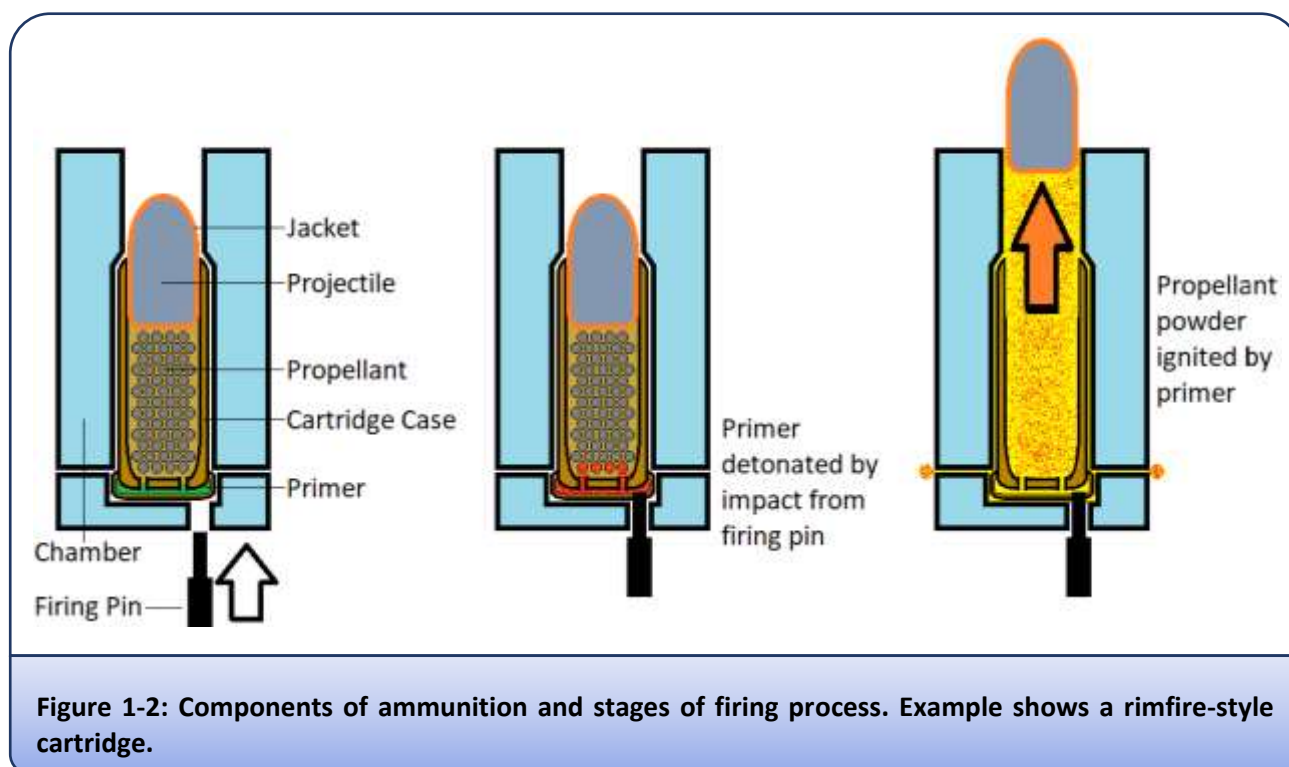
The term gunshot residue is broadly used to refer to substances, aside from projectiles, that are released from guns as they are fired. Detectable GSR traces occur when partially unburnt material or the condensed by-products of combustion reactions settle from the air onto nearby surfaces. Traces can be deposited on anyone or anything within close enough proximity to the discharging firearm. The presence and composition of these traces may then be used by forensic scientists to understand and reconstruct incidents involving firearms [\[9\]](#).

For general information regarding the operation of firearms and how this influences resultant GSR traces, readers are referred to the relevant chapter of the Encyclopedia of Forensic Sciences (Third Edition), edited by M. Houck, towards which the author of this thesis contributed [\[10\]](#). For a briefing on how these traces can be interpreted in a courtroom, see also Expert Evidence, edited by Freckleton & Selby [\[11\]](#). An informative summary of recent academic literature can be found in the review “Fate and Behaviour of Gunshot Residue” by Blakey *et al.* (2018) [\[12\]](#). An overview of some relevant concepts is given as follows.

Almost all contemporary small arms (excluding air rifles) are designed to use self-contained cartridges as ammunition, and thus are, at least theoretically, capable of producing GSR. When a firearm is discharged, a series of mechanical and chemical events take place to force the projectile from the gun barrel (Figure 1-2). Firstly the trigger mechanism causes a firing pin to strike the base of an ammunition cartridge. This impact detonates a small amount shock-sensitive explosive, known as the primer, to initiate combustion. The energy and molten matter released by detonation of the primer ignites the second stage of the ammunition; propellant powders largely based on nitrate esters. Propellants are intended to deflagrate rather than explode, releasing a much larger volume of hot gasses than is occupied by the solid propellant in its unfired state. It is the expansion of these gasses within the constrained environment of a gun barrel that produces the force expelling a projectile at high speed. The morphology of propellant particles is determined during manufacturing to impart an even burn and thus control rates of change in barrel pressure. Ammunition is usually designed so that combustion continues until the moment the projectile leaves the barrel. At this time, the sudden drop in both temperature and pressure can quench the reaction, leaving partially unburned particles of propellant.

Each step of the process described above can create material that is released and later detected as GSR. The inorganic primer is initially vaporised through detonation, and the products condense into randomly distributed, typically spheroidal particles containing metallic elements. Additional metallic GSR is contributed by the interaction of bullet and gun barrel, as friction removes matter from the surface of each. These elements can later be found in microscopic particles, also called inorganic- or primer- GSR (IGSR & PGSR). Not all propellant is consumed, leaving some partially unburned pieces that reflect the composition of the original product. Other organic compounds may be contributed from lubricants, cleaning oils, and combustion

products including carbon soot and polycyclic aromatic hydrocarbons [13, 14]. These collectively comprise organic GSR (OGSR).



The type and design of a firearm will affect the way in which all of this residual matter is released and distributed in the immediate environment during shooting [12, 15]. A portion of GSR is propelled at speed from the muzzle, trailing the projectile in a conical pattern. Consequently, long arms such as rifles and shotguns will have different dispersal patterns to handguns. This plume becomes more turbulent and less defined as it travels. Smaller particles can fit through gaps in a firearm's mechanisms to create a lateral plume nearer shooters' hands. It is reasonable to expect that this plume will consist of both larger and more numerous particles when a firearm with an open construction i.e. a revolver is involved [15]. Many firearms feature an ejection port to remove spent cartridge cases from the breech, and further GSR is released as cases tumble through the air from this opening. Bolt-action, break-action or belt-fed mechanisms will have separate influences again. As ammunition is designed to be compatible with particular firearms, deliberate or accidental mismatches can also affect the GSR observed. Rifle and shotgun ammunitions contain more propellant, to provide an even burn throughout a long barrel. If they are used in a firearm fitted with a short barrel (or a gun barrel has been cut down for concealment), a greater mass of material consistent with the original propellant composition will result [12].

1.3 Collection of GSR Traces for Forensic Purposes

Before analysis of a suspected GSR trace can proceed, the trace must first be collected from some underlying substrate. Recovery of traces is complicated by the fact that GSR is not usually visible to the unaided eye. The location and distribution of particles on an exhibit or person are also often of great importance, and care should be taken to avoid loss or redistribution of material. Therefore, deliberate consideration of the sampling process is a vital step for GSR and indeed all forensic trace analysis (Schwartz et al., 2020). The physical nature of the substrate will impact the likelihood of that surface retaining GSR and the collection equipment that may be suitable. For example, different techniques may be used for a permeable, loose or dirty surface compared to an unbroken, impermeable one. Rival sampling platforms also lend themselves to different analytical techniques to a greater or lesser degree. A brief overview of the sampling tools available to forensic practitioners is given as follows:

1.3.1 Wax Fixation

The earliest method used by law enforcement officers to collect GSR traces involved painting layers of softened paraffin wax onto a surface, such as the hands of a suspected shooter. As the wax cooled and hardened into a cast, it could any trap particles of residue present. This cast was carefully removed and treated with colour-changing reagents to detect and visualize GSR. This method is no longer in general use, as the reagents were susceptible to false positives caused by non-GSR materials.

1.3.2 Adhesive Lifting

The most common sampling technique contemporary to this research is adhesive lifting. This approach efficiently removes loose particulates including GSR from substrates and fixes them into place (cite Taudte 2016). Typical platforms consist of conductive, carbon-based discs mounted to small aluminium stubs that can be easily placed into an electron microscope for analysis (more in section X.Y). These stubs are simple to use and convenient to transport. Adhesives are typically pressed against a surface 50–100 times with a dabbing motion when collecting a sample, or until the stub is no longer subjectively sticky. Samples can be recovered from solid surfaces including hands, faces, or clothing (cite shirt sleeves paper). Adhesives may however become ineffective very quickly if an attempt is made to sample dirty, wet, or loose surfaces.

1.3.3 Wet Swabbing

Swabbing involves firmly rubbing a questioned surface with materials such as small sponges, cloth patches, or cotton wool. These can be moistened to improve recovery and are best suited to low-porosity substrates (cite swab touch spray paper and one other). Dilute acids were formerly popular solvents for the recovery of inorganic GSR, being well-aligned with later analysis using bulk techniques such as atomic absorption spectroscopy (cite). Research indicates that swabs wetted with organic solvents can efficiently collect the residues produced by both explosives and GSR (cite). Depending on the intended analytical process, residues may need to be dislodged and/or dissolved from the swab before their composition can be ascertained.

1.3.4 Vacuum Lifting

Vacuum lifting is achieved by connecting a vacuum pump to a sampling unit containing a series of inert filters of decreasing pore size. The airflow helps to dislodge any residues that are subsequently caught by the filters. It may be an appropriate alternative for collecting GSR trapped within the weave of a textile, for items such as fleecy clothing that will shed large amounts of fibers, or substrates that are otherwise particularly dirty (Andrasko and Pettersson, 1991). While efficient at collecting GSR, it will also collect a population of extraneous particulates that may overshadow the desired GSR traces.

1.3.5 Vapour Trapping

Some organic components of GSR exert sufficient vapour pressure to naturally volatilise and release matter into the atmosphere around them. Heating will increase the effect, at the risk of degrading any thermally sensitive analytes (cite). The vapours can be concentrated by drawing a volume of headspace gas across a trapping material in a process called solid phase micro-extraction (SPME) (Dalby and Birkett, 2010). Analytes are then be recovered for instrumental analysis by solvent extraction or reheating. However vapor trapping and subsequent analyte recovery are equilibrium processes – under any given set of conditions, only a portion of the material will progress through each of the various stages. If vapour analysis is to be attempted, the exhibit item (e.g., an expended cartridge case) must be stored in an airtight container as soon as possible after collection.

1.4 Forensic Interpretation of GSR

Once samples have been collected for analysis, the tasks facing forensic scientists can be separated into two key areas. The first covers detection and formal identification of suspect material as GSR. The second involves evaluating how these traces might be interpreted in the context of the case. It is disingenuous to simply state that the detection of GSR on an individual is proof that they have fired a gun. Even if this were possible, both the investigative effort and judicial proceedings are more likely to be interested in questions about the activity of persons of interest (POIs) – was an individual involved in a specific shooting event, and what were their actions immediately before and afterwards? The location, magnitude and pattern of any detected traces can provide invaluable information. Key to these discussions is the transfer and persistence of GSR traces, which do not remain static and may exhibit behaviours specific to this form of trace evidence ^[16]. Narrowing down residues to potential sources (i.e. brands of ammunition) can also provide actionable information to investigators in both forensic and counter-terrorism roles. Therefore, interpretative matters must be considered as part of the analytical process, as the way in which data are collected and the conclusions drawn from that data are dependent on one another.

1.4.1 Identification of material as GSR

The first and most important step in forensic GSR analysis is formal identification of the presence or absence of any GSR in a sample. Just as ammunition and firearms all share specific design features, residues typically consist of similar chemical compositions originating in components of the ammunition and firearm. The chemistry of these, and the laboratory methods used for analysis, will be discussed in further detail below. Natural and manufactured products containing some of the same elements used in ammunition (separately) are common. There is a risk that this background material may cause false positives, particularly when analytical methods with insufficient specificity (such as “colour tests”) are applied. The likelihood of observing traces caused by these sources must be accounted for. A hierarchical system for describing the exclusivity of traces has been established amongst GSR analysts. Substances with a composition that is known to frequently arise from firearms use, without having any other known sources, is now called *characteristic of* GSR. Other materials typical of firearm discharge, but also known to arise from some other items or processes, can only be considered *consistent with* GSR.

1.3.2 Distribution and Deposition

When a firearm is discharged, particulate GSR is dispersed throughout the immediate vicinity. This can result in traces being transmitted to shooters, victims, and bystanders; all are considered examples of primary transfer. Proximity and orientation to the firearm at the time of discharge generally, but not always, influences the likelihood of exposure to the GSR plume ^[17]. The fraction of GSR emitted from the barrel is propelled at high speed and may be found adhering to distant surfaces in the direction of fire. The spread of this material can be measured and used to estimate the distance between an object and firearm at the time of shooting. Residues not immediately encountering a surface will settle from the air over time. This deposition is innately variable, being influenced by factors including type/condition of the firearm, hand positioning and ambient air movement. ^[12, 14, 15, 17, 18]. To better interpret GSR traces, it would be desirable to determine some approximation of the amount of residue likely to be found immediately after firing. Unfortunately, this has repeatedly been found to be highly unpredictable and irreproducible even under controlled conditions ^[19]. Nonetheless, many hundreds or even thousands of characteristic IGSR particles can be found in samples collected post-shooting ^[17, 19].

With a comprehensive combination of sampling strategies, Wingfors *et al.* (2013) found that a particular lead-free rifle ammunition produced 30±2 milligrams/round particulate matter, several hundred micrograms of volatile organic vapours and >1000 milligrams of inorganic gasses (n=3) ^[14]. A figure combining deposition mass and collection efficiency from hands is a more relevant reflection of case work; for example Gauriot *et al.* (2013) found when five volunteers each fired a single shot from the same 0.38 cal revolver, the number of characteristic particles detected by SEM-EDS varied from 87 to 133 ^[20]. Furthermore, an increasing number of shots before sampling only loosely correlates to an increase in detected GSR. ^[21-23]. In fact, it is possible to find no characteristic GSR even in situations where residues are expected to reflect a potential maximum.

This was illustrated during a meta-study of 71 coronial cases of known suicide by firearm in South Australia, where post-firing activity by the victim (causing loss of evidence) can be assumed to be minimal [24]. The study was designed such that only cases in which there was no doubt that the victim fired the fatal shot were considered. Unexpectedly there were no characteristic particles detected on 5% of samples, meaning there is clear potential for false negative results in forensic case work. It is speculated that atypical positioning and lack of cycling for bolt-action guns may have contributed to this result.

1.4.2 Secondary and Subsequent Transfers of GSR

GSRs are readily transferred between surfaces *via* physical contact, following Locard's oft-cited principle of exchange [25]. Particulates are gradually lost from initial sources, and subsequently gained by other people, items, or locations. This can result in the spread of traces within and well beyond the context of any specific shooting events. For that reason, the presence of GSR (especially when found in small amounts) cannot be considered proof of a direct link between surfaces.

Academic studies have modelled GSR transfer using actions such as handshakes between shooters and non-shooters, or non-shooters handling firearms shortly after discharge. Two studies by French, Morgan and Davy (2013 & 2015) used counts of inorganic GSR particles to demonstrate secondary and tertiary transfer [16, 19]. As many as 129 particles were detected on the recipients' hands after one handshake, and between 12-22 particles after a chain of two handshakes between non-shooters. Gassner *et al.* (2019) used similar scenarios to demonstrate transfers of OGSR [26].

In practice, the dynamics of transfer events can be difficult to reconstruct *post hoc* as there are no inherent features that allow discrimination between primary and subsequent transfers. Probabilistic approaches based upon the magnitude of observed traces have been suggested; empirical studies like the ones cited above suggest distributions will skew larger for samples representing surfaces closer to the initial incident, compared to surfaces further along a chain of transfer events.

1.4.3 Persistence of GSR

After initial deposition, any recoverable GSR traces on a surface will start to diminish. Offenders may also undertake deliberate countermeasures to avoid detection, such as washing, changing clothes, or wearing gloves. Consequently, the absence of detectable GSR is not sufficient to indicate that no contact with firearms has occurred. It is difficult to isolate the variables of initial deposition mass, rates of secondary transfer, and collection efficiency experimentally [18, 21, 22].

Individual IGSR particles are considered stable in the environment and may essentially persist indefinitely once collected. However, the population of particles on any given surface is finite and can be reduced by transfer events. This includes both physical activity and environmental factors such as wind and rain. Hands are a frequent choice of substrate for collecting GSR samples from suspected shooters, as they are likely to

be in immediate contact with the firearm. Numerous studies have attempted to quantify the persistence of IGSR particles on hands, to better inform forensic sampling practices. According to a review by Blakey *et al.* (2018), empirical detection windows can end at between four- and ten-hours post-discharge [12]. For example, Brozek-Mucha (2011) measured the persistence of GSR on volunteers' hands after firing a single round from a semi-automatic pistol [27]. Samples were taken in half-hour increments and in the intervening time participants performed regular clerical work. The greatest losses occurred in the first 30-minute interval, and a half-life of approximately one hour was estimated. At the longest time interval observed (four hours), all five replicates contained much reduced, but still non-zero amounts of GSR.

Alternatively, OGSR is theorised to degrade due to a combination of mechanisms such as secondary transfer, evaporation, and skin permeation [18, 21, 23, 26, 28-31]. Specifically considering OGSR persistence, Maitre *et al.* (2018) again found that the greatest amount of residue was lost from hands during the first hour, but traces greater than the limit of detection by liquid-chromatography/mass spectrometry (LC-MS) were still observable up to four hours post discharge [31].

Detectable OGSR will also decrease from the surface of inanimate objects. Samples taken from spent ammunition cartridges may be used in estimation of time since firing has occurred. Each component within OGSR is "lost" from the cartridge at a different rate, posited to depend largely on volatility. By comparing the ratios of volatile ammunition components, a rough estimation can be made of the elapsed time since that cartridge was used. However, inaccuracies of up to 50% of the estimated time have been observed even under controlled conditions [29]. This technique requires an aging curve to be constructed that matches the specific situation of each questioned case sample i.e. the exact same ammunition and storage conditions. Aging profiles are known to be especially sensitive to temperature, and the thermal history of questioned samples may not be known to any degree of accuracy. Therefore the conclusions that can be drawn from cartridge ageing are likely to remain broad (hours, days or weeks) [29, 32, 33].

1.4.4 Contamination and Pollution

Frequent firearm users may carry a background loading of residue and can unknowingly distribute this amongst their surrounds. As most ammunitions are chemically very similar, their residues are generally not distinctive enough to conclusively connect traces with specific shooting events (although it is sometimes attempted – see below). The potential for detecting traces arising from firearms use, unrelated to the incident of interest, can further complicate interpretation of GSR evidence.

This contamination can occur *via* family members, colleagues or other associates that use firearms in the course of their employment or sporting pursuits. Stamouli *et al.* (2021) conducted a population study to assess the background of GSR traces. Of 252 firearm owners that were sampled, approximately half were found to have one or more GSR particles on their person. One-quarter had more than ten particles, including

6.5% found to have >101 particles [34]. Increased amounts of GSR were found to correlate with handling firearms within the five hours preceding sample collection. Brozek-Mucha (2014) was able to show that GSR traces propagated throughout households where one member was a recreational hunter. Individuals not themselves involved in hunting were found to carry small numbers of particles (between 1-4) in four of five households examined during the hunting season [35].

Some have argued that a distinction should be drawn between contamination forming part of the natural background of a crime-scene, and potential pollution contributed after the fact [36]. Law-enforcement personnel also often carry firearms as part of their duties. Sampling studies have shown that police equipment, vehicles and facilities can be sources of GSR contamination to suspects taken into custody. For example, Charles and Geusens (2012) found that more heavily armed members of police special forces units were likely to carry a greater number of characteristic IGSR particles than general duties officers or administrative staff [37]. Berk *et al.* collected 201 samples from within police vehicles and detention facilities in Chicago. From these, 56 characteristic particles were recovered across 23 samples [38]. Most were found on samples taken from table-tops and restraining bars to which handcuffs could be attached. They stated that the likelihood of large numbers of particles being transferred to POIs was small and suggested using a threshold of three characteristic particles before reporting a result as “positive”. In a similar study, Ali *et al.* (2016) collected 70 samples from police stations and vehicles in Pittsburgh then tested them for both inorganic and organic GSR [39]. They found one characteristic IGSR particle and quantifiable amounts of organic GSR markers in two further samples. It is notable that the instances of OGSR were collected from the hands of non-shooting individuals after they spent ten minutes in the rear of a police vehicle – suggesting that a transfer has taken place. Cook (2016) instead directly sampled 33 Australian police officers’ hands, following collection of duty firearms at the start of their shifts. At least one particle was found in 85% of samples, with an average of 65 particles detected across all participants [40]. Cook also found that handwashing was sufficient to remove almost all of this material, thus reducing the risk of polluting POIs.

Separately Lucas *et al.* (2019) and Maitre *et al.* (2019) simulated the effects of GSR-contaminated Australian police officers performing “mock arrest” scenarios and handcuffing POIs. Using electron microscopy, Lucas *et al.* found that less than 25% of IGSR particles were transferred from the arresting officer to the volunteer [41]. Since the average initial loading of GSR was five particles, this suggests a measurable but low risk of traces falsely being interpreted to support narratives where the POI has discharged a firearm. Maitre *et al.* found similar results for OGSR [30]. Samples taken from hands immediately after shooting three rounds were used as a baseline, with three organic GSR compounds detected by LC-MS. After completing the mock arrest scenario (n=5), the average amounts found in samples from the “arresting officers” had reduced to between 23-68% of the baseline. Amounts of OGSR on the non-shooting “detainees” had increased from nil, to between 8-55% of baseline. The estimated amounts of transfer varied widely depending on the location of sampling (dominant vs. non-dominant hand) and the compound in question. Gassner *et al.* (2019) found that

when one subject fired three rounds, then immediately proceeded to “arrest” a second subject in a different location, the level of OGSR on the arrestee could be almost as high as that on the shooter [26]. In fact the observed values were highly variable (n=12), and in some cases a greater amount of residue was detected on the non-shooter compared to the shooter. While this approach demonstrates the mechanism and potential for contamination of POIs to occur, the rates of occurrence for such events are currently not known. Further population tests would be required to assess the actual detection rates for GSR subsequent to POIs entering a police station or vehicle.

The inclusion of taggants may help to chemically mark GSRs originating from police-officers’ ammunition. Elements from the lanthanide group are typically chosen as dopants for primers as they are readily detected by SEM-EDS, and are unlikely to be found in other firearm applications [42, 43]. Luminescent markers can also aid in detection of traces [44]. If used as intended, analysts should be able to recognise that a population of GSR particles may at least partially come from pollution of the scene and adjust their interpretation accordingly.

Aside from the risk of pollution to POIs from police officers’ duty firearms, cross-contamination of samples must also be avoided in laboratory environments. The adhesive stubs used to collect GSR samples are typically housed in plastic enclosures, so movement of particles between samples is not possible during storage. However, it is sometimes desirable to simultaneously load many samples from either the same, or even different cases, into the vacuum chamber of a scanning electron microscope (SEM). To assess the risk of inter-stub transfer during analysis, Rosengarten *et al.* (2021) placed both clean and heavily GSR-laden stubs onto a twenty-position SEM stage using three different patterns [45]. Despite running the electron beam for over 220 hours on samples collectively containing greater than one hundred thousand particles, no instances of transfer to blank stubs were observed. As the normal number of particles in GSR analyses are likely to be several orders of magnitude smaller, the risk of pollution within the SEM chamber was determined to be negligible.

1.4.5 Source-Attribution or Linking Exhibits

Attempts may be made to link specific firearms and ammunition either to one another, or to an event, to inform lines of enquiry. Arguably the modular design of ammunition presents a barrier to classification of the total population of existing ammunition. That would require maintaining a database of all ammunitions (often in circulation for extended periods of time), as well ensuring the database reflected changes in the market over time [46-48]. It is also possible to “mix and match” primer, propellant and projectiles from different suppliers especially when the end consumer is using reloaded cartridges. The practice of “handloading” is well described in shooting textbooks and by hobbyists online, although there does not appear to be any literature in peer reviewed journals on the subject whatsoever [49]. Manufacturers have no obligation to disclose formulations beyond basic material safety data requirements as this represents their intellectual

property. Changes have been observed between production batches of the same merchandise, presumably either for economic reasons or to improve product performance [\[17, 50\]](#).

The problem becomes simpler, although not trivial, if case-specific comparison samples are available due to the course of police investigations. It is easier to assign particles belonging to one of a few well characterised sources (i.e. a constrained dataset), compared to the myriad of ammunition combinations that may occur in the broader market. This type of comparison is applicable if a POI is found to have ready access to particular types/brands of ammunition, or better yet is apprehended immediately after a shooting with ammunition in their possession. The composition and behaviour of these “known” ammunitions can be tested to assess whether the questioned sample is consistent with those sources. Some stipulations apply when trying to determine a link; the ratio of components to one another may not be maintained during the firing process.

Categorization issues aside, it is analytically possible to differentiate between some classes of ammunitions from their residues. Certain studies have observed a similar chemical profile pre- and post- firing, but this cannot be assumed as a matter of course [\[51-54\]](#). Raw data are often interrogated using chemometrics; a process of statistically determining which variables give the greatest discriminating power and then using these variables to sort samples into groups satisfying a given threshold of distinctiveness. A diverse range of analytical techniques have been used to generate the input data: SEM-EDS, ICP-MS, Raman & FTIR spectroscopy, voltammetry and mass spectrometry [\[55-61\]](#). Further details on these are given below in section 1.5. In the largest study of this kind, Dennis *et al.* (2015) published results comparing gas chromatography – mass spectrometry data from 726 casework samples, largely from Federal Bureau of Investigation laboratories [\[62\]](#). These samples were intact grains of propellant powder, but the principle would also apply to GSR. The authors concluded that there was a limited range of probability ratios between same-source or different-source allocations, and therefore while discrimination was possible the statistical strength of these associations needed improvement. Further issues may also arise as analytical methods are updated or even individual instruments are replaced at the end of their service life; re-analysis of old samples might be required.

1.4.6 Memory Effect

Another complicating factor is the “memory effect” of firearms that have been used with different ammunitions during their service history. Residue from previous shots can be deposited within the firearm itself, and can then be dislodged upon subsequent firing. An incorrect assessment of consistency may be made if compounds are detected that originate from an earlier firing, but those compounds are not associated with the specific ammunition being questioned [\[50\]](#). As with many aspects of GSR formation this memory effect is unpredictable, but it has been observed despite mechanical cleaning, disassembly, sonication and acid cleaning of firearm components [\[18, 50, 52, 63-65\]](#).

1.5 Chemistry and Classification of GSRs

As stated above, recognising material as GSR is the most important stage of analysis; from there, other aspects of interpretation can follow. While there are many different types of firearms and ammunition available, the chemical composition of their components has remained largely consistent over the last century. Recognition of these commonalities has allowed forensic scientists to develop guidelines for recognizing GSR. The following sections describe aspects of the chemistry of GSR, followed by the contemporary system for assigning forensic value to traces exhibiting these compositions. By current convention, organic and inorganic substances are considered independently ^[9].

1.5.1 Inorganic GSR

During combustion, metallic elements from the primer (and other components to a lesser extent) are vaporized. The vapours subsequently condense into solid particles of between approximately 0.1 and 20 microns (μm) in size, although larger accumulations can also be observed. Each particle can contain multiple elements of interest due to mixing at high temperatures, followed by rapid cooling and accretion ^[64, 66]. It is this mixing and condensation that makes analysis based on individual particles so powerful for the unambiguous identification of GSR.

The introduction of practical, non-corrosive, non-mercuric initiators for use in cartridges is credited to German chemists who patented "Sinoxid" -type primers in 1928 ^[67, 68]. These were subsequently adopted as the most common design for all small-arms ammunition. Many contemporary centrefire primers contain lead styphnate as the main explosive, barium nitrate as an oxidiser and antimony sulphide to provide fuel and sensitise the mixture. Consequently, traces containing comingled Pb, Sb and Ba are considered particularly characteristic of GSR. Other common ingredients that may also be present in primers include tetrazene (1-(5-tetrazolyl)-3-guanyl tetrazene hydrate) and/or aluminium powder. Antimony compounds might instead be replaced with ground glass frictionators, creating another type of distinctive trace ^[69-71]. This is particularly relevant to many of the small-calibre rimfire ammunitions frequently used in Australia, such as 0.22 LR.

Health concerns associated with exposure to airborne heavy metals have prompted interest in the development of less toxic primers ^[72, 73]. These have been variously called Pb-free or heavy metal free (HMF) ammunitions. Analysis of residues produced by HMF primers will therefore reveal a different composition to those having Pb-based primers, with Al, Si, Cu, and Zn particles being common features ^[74]. For example, Federal Ammunition's "Catalyst" branded primers reportedly use a combination of nitrocellulose, aluminium, and bismuth oxides to create a thermite reaction that ignites the propellant ^[75]. Formulations containing DDNP (2-diazo-4,6-dinitrophenol), zinc peroxide, strontium nitrate, manganese oxide, boron and titanium have also been reported in various commercial products ^[68, 76]. However, firearms that have a history of shooting both Sinoxid and HMF ammunitions may produce a population of particles that reflects both compositions. While not currently considered reliable enough for use in high-risk applications, HMF primers

may be used to protect frequent shooters during training. Due to greater overlap in composition with other non-firearm particulates, Pb-free ammunition is expected to contribute to additional challenges to GSR interpretation if or when it influences a greater segment of the ammunition market.

Projectiles are commonly made from lead, hardened by varying quantities of antimony, due to its high density. They can be partially or fully enclosed with jackets of harder metal alloys, with copper alloyed with zinc and/or tin being the most common materials. Some military-style ammunition may also have a steel or tungsten core, to improve penetration. Shotgun pellets can be entirely steel rather than lead, especially when used for hunting, to prevent the spread of heavy metals into sensitive ecosystems or game intended for human consumption. Traces of molybdenum or selenium from gun-bluing or blacking agents may be transferred from the firearm when shooting. These elements can all contribute to GSR, although are less directly indicative of a firearm source.

The foundational basis of the current classification system for IGSR particles was developed by Wolten and colleagues at The Aerospace Corporation (U.S.A.) in the 1970s, under contract with the National Institute of Law Enforcement and Criminal Justice [77-79]. Particles containing Pb,Ba,Sb or Ba,Ca,Si or Ba,Sb were designated as “unique” to firearms, as no other sources were known to produce particles with matching composition and appearance. A lesser category of particles, distinguished by composition, were described as “consistent with but not unique to gunshot residue” [77]. This hierarchical approach was incorporated into the field of GSR examination and remains current, although terminology and classifications for specific particle compositions have evolved over time. Studies into occupational and industrial sources of particulate matter, sharing chemical similarities with GSR, have contributed to the refinement of these classifications. Influential publications include those by Wallace and McQuillen (1984), Garofano *et al.* (1999), and Torre *et al.* (2002) [80-82].

Since 1994, the American Society for Testing and Materials (ASTM International) has produced a codified standard for the analysis and classification of GSR traces [83]. This document, which is regularly updated, perhaps represents the best single depiction of contemporary views amongst expert GSR analysts. Many laboratories base their manuals or standard operating procedures on the ASTM’s guide. As the classifications and language from the 2020 edition of ASTM-E1588 will be used frequently throughout this thesis, a summary is provided as follows:

1.5.1.1. Summary of the ASTM's Criteria for classification of recovered material as IGSR:

- The population of recovered particles should be considered in its totality, as some observations can counter-indicate a firearm source.
- There are three levels of classification, indicating relative rarity and importance, based on elemental composition.
- Particles should have a generally rounded morphology. However, morphology is of lesser importance than composition.
- Characteristic Particles, containing Pb/Ba/Sb or Pb/Ba/Ca/Si/Sn, are the most probative. These are not considered to have prevalent non-firearm sources.
- Pb or heavy-metal free ammunitions may instead produce particles of Gd/Ti/Zn or Ga/Cu/Sn.
- Consistent Particles contain combinations of Pb/Ba/Ca/Si, Pb/Ba, Pb/Sb, Ba/Sb, Ba/Al, Ti/Zn or Sr, with or without inclusions of Sn and Al. These are very likely to be found in connection to firearm sources but may also have some known or suspected non-firearm sources.
- Commonly associated particles, the least valuable class, predominantly consist of a single element such as Pb, Sb or Ba. These can be found in association with firearm use, and contribute to the overall population of observed particles. However they have many additional non-firearms source and add little value when not found in the presence of the previous two classes.

1.5.2 Organic GSR

Up to 136 organic compounds have been associated with discharging firearms [14, 84]. These originate from the propellant powder, its additives and degradation products, lubricants, cleaning oils, and their respective combustion products. Not all of these are suitable targets for forensic analysis, as many are ubiquitous in the environment and would not offer any discriminating information [85].

Propellant powders for civilian use are typically based on the nitrate esters nitrocellulose (NC) and nitroglycerin (NG) (Figure 1-3). These compounds are chosen because the “fuel” and “oxidiser” ingredients for combustion are components of the same molecule, allowing for rapid deflagration. Propellants are formed into grains, the size and shape of which will have a marked influence on the rate of burning and maximum pressure generated in a gun barrel. Each particle of the propellant burns inwards from exposed surfaces, where a layer up to 100 μm under the surface begins to melt, thermally decompose and release combustible gasses in an initial “foaming” mechanism [86].

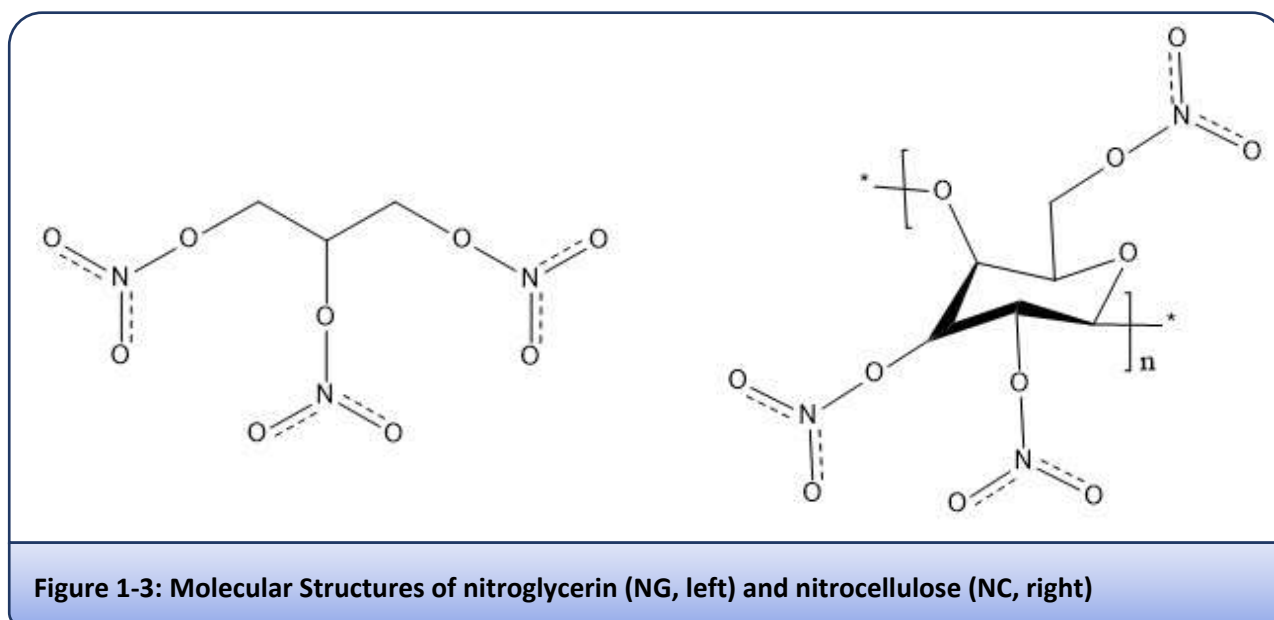


Figure 1-3: Molecular Structures of nitroglycerin (NG, left) and nitrocellulose (NC, right)

A key indicator for performance is the ratio of nitric oxide to carbon moieties, as greater proportions of oxygen create more gaseous products to increase barrel pressure. Conversely, increased carbon contributes to undesirable sooty by-products. Basing a decision on this metric alone would indicate that NG is a preferable choice for propellants over NC, as it has a much higher oxygen/nitrogen content. However, the maximum pressure that can be safely constrained by the barrel of a firearm must be taken into consideration. As an example, each monomer of the cellulose chain has three hydroxyl substituents that can be nitrated. For propellant, the cellulose is typically nitrated to around 13% nitrogen content (somewhere between 2 or 3 -OH groups replaced with NO₂), as the theoretical maximum degree of nitration creates a product that is too dangerous [87]. Using NG as the basis for smokeless powder risks detonation within the material rather than controlled deflagration. As the share of NG as a proportion of the total increases, so too does the risk of barrel pressure rising too quickly and causing the entire firearm to explode. Therefore “double base”

powders combining NC and NG allow the tuning of performance (along with powder morphology and inhibitors). Pure NG is also liquid at room temperature, whereas NC is a fibrous solid. Nitroguanidine may be added as a flash suppressor in powders intended for large bore artillery, or alkali salts such as potassium sulfate, nitrate or cryolite (K_3AlF_6) may be used for the same purpose in small arms ammunition [88].

NC and NG deteriorate during storage, which at best may limit performance or at worst create a danger of unplanned fire or explosion. FTIR experiments on artificially aged NC show that the basic carbon skeleton does not change during degradation. The reaction starts spontaneously at the O-NO₂ bond, producing NO₂ radicals followed by other nitric oxides and acids [89]. Continued degradation is autocatalytic and occurs *via* at least two pathways with NC in isolation, although more have been proposed when combined with other ingredients in smokeless powders [90]. Stabilisers are added to scavenge the nitric oxides, inhibiting the catalytic cycle and prolonging ammunition's shelf life.

Many additives are typically included into propellants with the aim of modifying manufacturing characteristics, increasing shelf life, inhibiting accidental ignition or improving firearm performance. Some additives contribute to multiple roles simultaneously. Stabilisers are chemicals added to delay the chemical aging process of propellant powders. In most cases this is achieved by "soaking up" free nitrogen oxides using aromatic amines/amides such as diphenylamine (DPA) or ethyl centralite (EC), although other emerging stabilisers were reviewed by Trache and Tarchoun in 2018 [91]. The pathway for reaction between DPA and nitrogen oxides is shown in Figure 1-4, and illustrates why simultaneous detection of the original compound and its nitrated derivatives is highly indicative of OGSR [85]. Nitrated toluenes are another nitro-aromatic species added to propellant, acting simultaneously as plasticisers, propellants and flash suppressors. Phthalate plasticisers may be added to modify burn rates or make the product more amenable to machining; however these are likely to be found in other polymer products and thus are not good indicators of contact with firearms if found in isolation [92]. Propellant grains may be coated in graphite powder to reduce build-up of static electricity, and to reduce initial exposed surface area to modify burn rates.

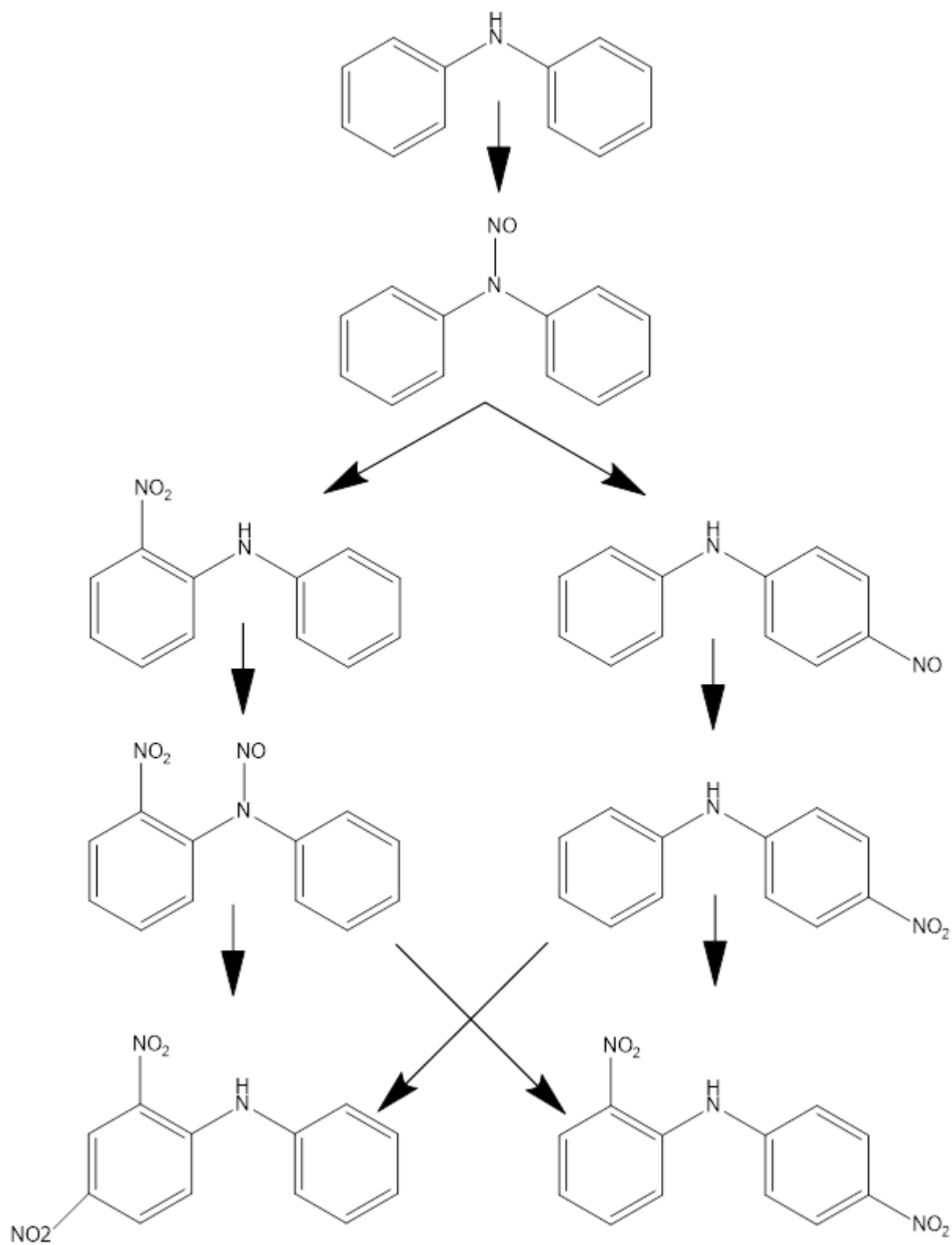


Figure 1-4: Formation of by-products in diphenylamine-stabilised propellant

Of all the organic compounds associated with GSR in literature, it has been said that only approximately 20 of these are of high probative value for the purpose of detection [85]. The criteria for selecting these compounds were that a) they should have a strong observational association with ammunition components, b) the origin of the compounds within the ammunition is well understood, and C) there should be a limited occupational and environmental prevalence of those compounds. A formalized hierarchy for evaluating the presence of OGSR compounds, reflecting the approach used for IGSR, is under development by the Gunshot Residue Subcommittee of NIST (ASTM 2020). An excerpt of the preliminary document, current at the time of writing, is provided as follows:

1.5.2.1. Excerpt of criteria proposed for the classification of recovered material as OGSR, by the GSR subcommittee of the Organization of Scientific Area Committees for Forensic Science. Taken from section 10 [93]:

- “Based on the classification scheme for compounds identified... minimum criteria to report OGSR has been identified are:
 - At least two category I compounds, with or without a category II compound, the residue is characteristic of OGSR;
 - One category I compound and at least one category II compound, the residue is consistent with OGSR.
 - If less than the minimum is identified, each compound identified may be listed but an inconclusive result should be reported. The reason for the inconclusive results shall be included for any inconclusive result.
 - If no OGSR components are detected, a negative result should be reported.”

Category	Compound
1	Methyl Centralite
	Ethyl Centralite
	Nitroglycerine
	Nitroso-diphenylamine
	Nitro-diphenylamine
2	Nitrocellulose
	Akardite
	Diphenylamine
	"Other" Diphenylamine derivatives
	2,4, Dinitrotoluene
"Other" Dinitrotoluene derivatives	

1.6 GSR-Like Material

Forensic GSR examination can be complicated by the fact that some non-firearm sources may produce materials with similar qualities to actual GSR. These “GSR-like” traces may potentially be detected on members of the general population without involvement of firearms. Consequently, the forensic significance of any GSR trace is inversely proportional to the prevalence of similar material arising from occupational, industrial, or environmental sources. Competent GSR analysts should have an awareness of both the specific known sources of GSR-like material, and the likelihood of encountering them during analyses. Depending on the level of evaluation requested, this may require some communication of case-specific information between analysts and investigators. Importantly, separate studies have repeatedly found features by which it is possible to distinguish IGSR from common occupational interferences despite structural or chemical similarities [\[34, 81, 94, 95\]](#).

For example, cartridge-operated tools (i.e. nail guns) may produce particles that are essentially the same as firearm-derived residues, as the cartridges are not essentially different from those used in ammunition. For this reason, it has been suggested that the terms “cartridge residues” or “primer residues” may be more accurate than GSR in many circumstances [\[80\]](#). Vehicle brake pads are also frequently cited as sources of GSR-like material, as they can produce particles containing Pb, Ba & Sb [\[82\]](#). More recent research suggests that changing manufacturing trends and improved analyses have decreased the risk of impact on casework [\[95\]](#). Pyrotechnic devices such as fireworks, sparklers, or airbag initiators produce particles containing metallic elements through high-temperature processes. These will often contain elements unusual to GSR but may have some overlap in composition, especially with lead-free primers [\[71\]](#).

NC and NG are the largest contributors to propellant powder by mass and are frequently found as partially intact flakes following controlled shooting experiments [\[12\]](#). Other uses for these compounds include historical film stock, fixatives for biological assays, and in medicinal products. It follows that there may be a risk of detecting NC and NG from non-firearm sources [\[96\]](#). Diphenylamine (DPA) is one of the most commonly stabilisers used for NC propellants, and is included in most lists for compounds indicative of GSR. It is also a priority pollutant according to the European Union, having uses in polymer, agricultural and perfume industries [\[97\]](#). Perhaps even more problematic for the detection of GSR, nitrated derivatives of DPA are used as feedstock in the production of azo-dyes and may include the compounds formed during propellant decomposition [\[97\]](#). Ethyl- or methyl- centralite, other predominant stabiliser choices, are not reported to have industrial applications aside from in propellants. The detection of these compounds in the general population due to non-firearm sources is not expected to be prevalent; accordingly, the presence of centralite compounds is of more probative value than DPA alone [\[39, 98\]](#). Plasticiser compounds and combustion products are even more ubiquitous in the environment. These may be helpful in discriminating

between different GSR traces or smokeless powders, but are not exclusive enough to aid in the identification of GSR.

One method of estimating the likelihood of finding “innocent” GSR traces is through the use of population surveys, although investigation of mechanisms leading to secondary transfer are also important [\[12\]](#). These studies require collection of samples from members of a relevant community and can either target those at elevated risk of contamination, or the population at large. A key distinction also needs to be made between non-firearm sources of traces that appear similar to GSR, and non-criminal use of firearms for employment or recreational purposes. Both may contribute to a “positive” detection during criminal cases, but neither are evidence of involvement with a criminal act. The observed rate of detection creates an empirical and quantifiable basis upon which to estimate the background prevalence of GSR and GSR-like traces. Such surveys have been conducted previously, particularly investigating sources of metallic particles [\[34\]](#). Greater detail on the results of these surveys will be given in Chapter Three of this thesis.

1.7 Analytical Methods

Specific laboratory methods used for GSR analysis form the core focus of thesis. The evolution of these procedures already has a long history, reportedly beginning around the early 1910s [\[76\]](#). The first tests intended to signify use of a firearm required the application of reagents that changed colour in the presence of specific GSR components [\[99, 100\]](#). Compared to more modern techniques, these provided rapid results and could be carried out with little specialist equipment. However, colour tests are susceptible to false positives and have poor sensitivity [\[101, 102\]](#). Many of the reagents are also toxic. Consequently, they are now used primarily for visualising GSR to facilitate distance-determination investigations, although they may serve a rapid screening role requiring further confirmation [\[103\]](#). As with all forms of forensic trace analysis, there has been a general trend to move away from such techniques. Instead, instrumental analyses are now preferred. These can offer much more sensitive, selective, and repeatable observations for trained analysts, despite significant purchase and upkeep costs. The following sections will give an overview of instrumental techniques that have either been adopted or proposed for use in GSR analysis.

There have been a number of previous reviews on the field of GSR analysis, some being comprehensive and others dedicated to more specific aspects. The broadest of the recent reviews was published by Dalby *et al.* in 2010, detailing the state of literature on formation, collection, analysis and interpretation [\[9\]](#). This has been updated and expanded upon by authors such as Taudte *et al.* (2014), Goudsmits *et al.* (2015) and Brozek-Mucha (2017), as well as a review released as part of the 19th Interpol International Forensic Science Managers Symposium in 2020 [\[84, 104-106\]](#).

1.7.1 Analysis of Inorganic GSR

1.7.1.1. “Bulk” Techniques

The first instrumental method for analysing IGSR was neutron activation analysis (NAA), followed by atomic absorption spectroscopy (AAS) and inductively coupled plasma mass spectrometry (ICP-MS) ^[107]. ICP-MS and AAS require dissolution of samples. These are all examples of bulk analyses that treat the entire sample as a homogenous entity. Bulk analyses may allow for better quantification of the amounts of each element in the overall sample compared to particulate analysis. On the other hand, they are usually destructive and lack specificity due to loss of morphological information. The detection of Pb, Ba and Sb in a homogenous solution does not have the same probative value for GSR analysis compared to finding these elements within microscopic particulates. These techniques have largely fallen out of favour, but are still reported in some literature ^[9, 108-110].

1.7.1.2. Particulate Analysis by Electron Microscopy

Scanning electron microscopes fitted with energy-dispersive spectrometers (SEM-EDS) have been the preeminent technology for particulate analysis of GSR since the 1980s ^[80]. SEMs function by sweeping a beam of high-energy electrons across the surface of the sample, overcoming the fundamental limits on image resolution achievable using wavelengths of visible light. Returning electrons are detected to build up an image, while emitted x-ray radiation is used to determine composition. This means both chemical and structural information can be collected simultaneously. As well as listing features required for reporting a positive result, minimum instrument performance standards are guided by international bodies such as the American Society for Testing and Materials (ASTM) or European Network of Forensic Science Institutes (ENFSI) ^[111, 112].

SEM-EDS analysis has advantages that make it particularly powerful for GSR analysis. Firstly, microscopy is non-destructive, preserves the particulate structure of the residue and allows particle morphology to be photographed. Secondly, adhesive-topped aluminium stubs are used widely in electron microscopy and make convenient forensic sampling platforms. As the elements in IGSR particles have greater atomic masses than the carbon substrate, each particle appears as a bright spot against the darker background when using backscatter imaging. The difference in brightness enhances visibility to analysts, and the addition of commercial image-processing software means that particle-searching process can be automated. Most importantly, each element emits characteristic wavelengths of x-ray radiation when stimulated by incident electrons. It is on this basis that the chemical composition of each particle can be recorded. SEM-EDS has overall limits of detection that are many orders of magnitude worse than the bulk analytical techniques described above. However, the electron beam can be focussed on individual particles, and the elements of interest exist within these particles at part-per-hundred- rather than part-per-million- concentrations. Therefore, the limits of detection are more than adequate. Finer chemical detail exists in particulate IGSR

than can be shown by SEM-EDS, prompting research into complimentary techniques such as time-of-flight secondary ion mass spectrometry (ToF-SIMS) or focused ion beam (FIBS) sectioning [70, 105, 113].

Despite its strengths, there are some weaknesses of relying solely on SEM/EDS for GSR detection. Although automated, analysis of samples is time consuming. Initial scans may take between 2-8 hours, followed by manual evaluation requiring skilled operators. There are also diverse environmental sources of metallic particles unrelated to firearm use, which may complicate interpretation of data. The instrumentation is expensive to purchase and maintain, so jurisdictions with low caseloads may not wish to carry this cost [114]. Ammunition manufacturers now sell products that do not contain lead or other heavy metals due to health and environmental impacts. Detection and interpretation of residues created by this “green” ammunition is possible, but potentially problematic under the existing paradigm. Finally, there is also an organic component to GSR originating in the propellant powder, which cannot be analysed using SEM-EDS. Potentially probative information is lost when this organic gunshot residue (OGSR) is not analysed.

1.7.1.3. Laser-Ablation Sampling

Methods using laser-ablation (LA) sampling fall somewhere between bulk- and particulate- analysis. Inside LA instruments, lasers are used to focus brief but very intense bursts of energy into a sample at a spatial domain of at least 10-20 µm. This causes localised heating, and finite volumes of the sample are near-instantly converted from their native solid state to either a vapour or plasma for detection. The approach reduces requirements for digestion or extraction of the whole trace and is destructive only on a microscopic scale. While ablation is not precise enough for detection of single particles, the association of indicative elements (i.e. Pb, Ba & Sb) within micron-scale areas is more precise than finding those same elements in totally dissolved samples. Advantages of LA include speed, surface sensitivity, and the ability to analyse substances that are otherwise largely chemically inert. The application of LA for trace analysis is well described in literature, especially in instances involving inorganic material such as glass, paint and soils [115-118]. Two common techniques for chemical analysis featuring LA are laser-induced breakdown spectroscopy (LIBS) and laser-ablation inductively-coupled plasma mass spectrometry (LA-ICP-MS). These were recently compared directly by Vander Pyl *et al.* (2021), using standardized primer samples from leaded and unleaded ammunition, and also post-shooting hand samples [119].

LIBS is a form of atomic emission spectroscopy, with the laser providing excitation energy. LA is used to create a micro-plasma environment from a sample’s surface. This plasma only exists for microseconds before cooling. Excited analyte species then return to their ground states and emit characteristic wavelengths of electromagnetic radiation. The application of LIBS to GSR was first demonstrated in literature by Rosenberg and Dockery in 2003 [120]. A succession of publications by different research groups followed, each describing different sampling media. These included Rosenberg & Dockery (2008, PTFE tape), Silva *et al.* (2009, resin or 3M scotch tape) and Tarifa & Almirall (2015, PTFE following cotton swabbing) [121-123]. Classification accuracies

up to 100% were achieved in some instances. In addition to Pb, Ba & Sb, other metallic elements can also be detected simultaneously; this broadens applicability to non-traditional primer formulations [124].

Rather than using the more common grid pattern, Trejos *et al.* (2018) chose instead to ablate a continuous line measuring 100 μm by 7mm (or 0.6%) into a SEM stub (pictured in Figure 1-5) [125]. This platform is convenient for later confirmatory analyses. Using LIBS, samples were screened in less than one minute. False positive rates of 5% ($n = 20$) and false negative rates of 25% ($n = 92$) were observed. Building upon these results, Menking-Hoggatt (2019) returned to the grid-like approach, collecting 25 spectra from 100 μm -diameter ablation spots (0.2% of the surface) [126]. Classification accuracy of 100% was achieved ($n = 326$).

[125]

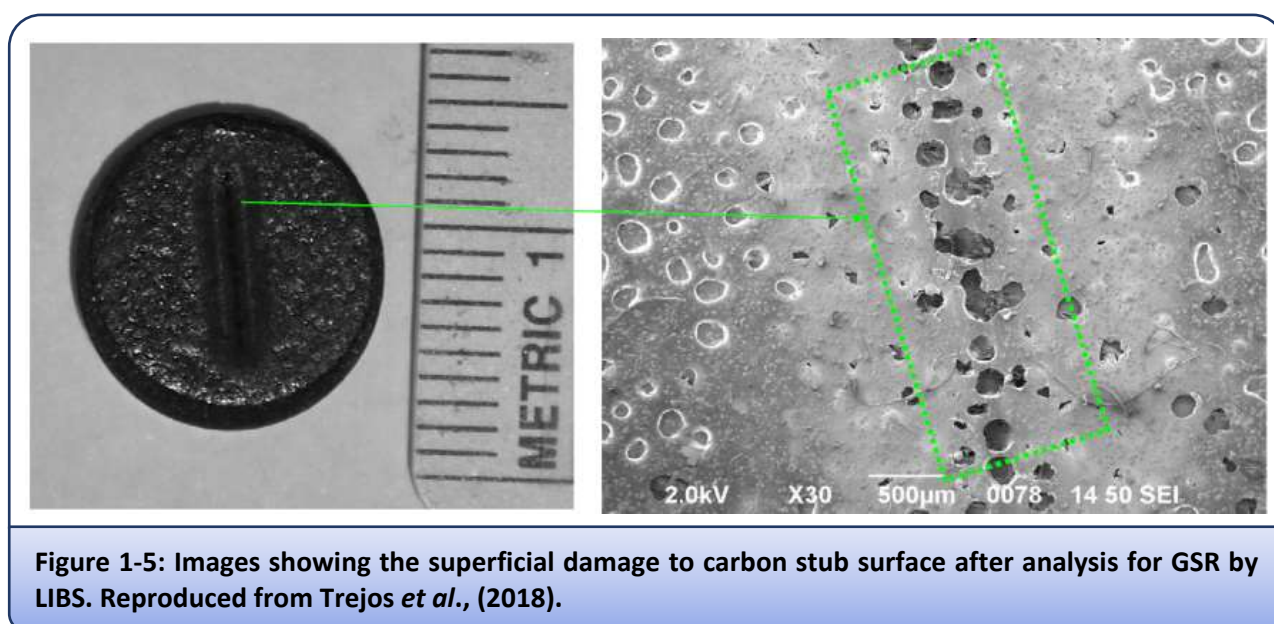


Figure 1-5: Images showing the superficial damage to carbon stub surface after analysis for GSR by LIBS. Reproduced from Trejos *et al.*, (2018).

Separate studies by Fambro *et al.* (2017) and Dona-Fernandez *et al.* (2018) have established that characteristic GSR particles do remain intact after ablation conducted directly on SEM sampling stubs [124, 127]. In particular, Dona-Fernandez *et al.* demonstrated the use of a backpack-style portable LIBS system that could be used to screen samples for GSR directly at the site of crime-scenes. All samples containing at least three characteristic particles could be recognized as “positives” on the basis of their LIBS spectra. Of 135 stubs collected, 22 were sequentially analysed by SEM-EDS, then LIBS, then re-acquired by SEM-EDS. It was found that the majority of particles $<2 \mu\text{m}$ in size were fully ablated, causing a reduction in total detected particle numbers. Conversely, at least some particles $>2 \mu\text{m}$ could be located following exposure to the ablation beam. These exhibited changes in morphology, including expansion and fragmentation, compared to their original presentation (Figure 1-6).

Aside from being an excitation source for atomic emission spectroscopy, laser ablation can also be used as a sample introduction system for inductively-coupled plasma (ICP) torches. As material is removed from samples' surfaces, it is flushed out of the sampling cell and into the torch using a flow of inert gasses (i.e. He,

Ar). In turn, ICP torches are used as ion-sources coupled to mass spectrometers, allowing elemental analysis. Collectively, these systems are referred to by the acronym LA-ICP-MS. While they are technologically complex and expensive, LA-ICP-MS systems are very sensitive and can also provide isotopic information. Their operating principles and forensic applications were thoroughly described by Trejos and Almirall in 2010 [117].

[127]

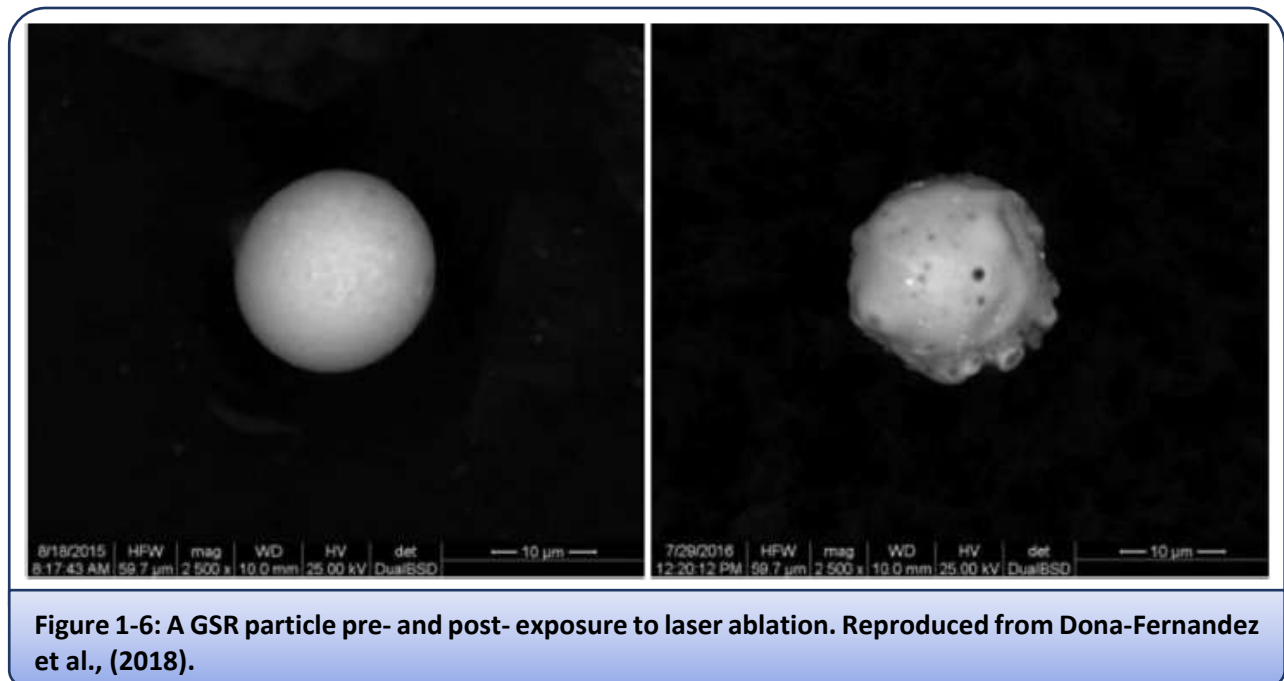


Figure 1-6: A GSR particle pre- and post- exposure to laser ablation. Reproduced from Dona-Fernandez et al., (2018).

Abrego *et al.* described a method for GSR detection using LA-ICP-MS in 2012 [128]. They used a 160 μm spot size traversing at 20 μs^{-1} , and compared three different raster patterns affecting 5-10% of 12.7 mm SEM stubs. When signals >10 standard deviations from the blank were simultaneously observed for Pb, Ba & Sb, it was inferred that a characteristic GSR particle had been ablated. Summarized data from twelve additional elements were also reported. In 2014 the same research group proposed a modified sampling device to allow parallel analyses of hand swabs by both LA-ICP-MS and Raman spectroscopy [129]. Consequently, the suite of analytes could be expanded to 20 elements plus organic stabiliser compounds and their derivatives. This is particularly useful for the detection or characterisation of Pb-free ammunition residues, four of which were examined in that publication. No universal criteria for particle detection were set; instead, comparisons were made with compositions known to be associated with the ammunitions of interest.

Pluháček *et al.* (2018) described an innovative use for LA-ICP-MS's capabilities, in addition to the more commonly proposed GSR-screening role [130]. Hyperspectral imaging showed that Pb, Ba, Sb, Cu, Zn & Hg were transferred from shooters' hands into latent fingermarks. At 110 μm -resolution, sufficient ridge detail was available to enable forensic feature comparison. When all these elements were detected following a single ablation event, it was again inferred that a particle had been found. The use of development powders reportedly did not interfere with spectra collection, presumably so long as the powder does not contain any

elements of interest to GSR examiners. While still insufficient to settle many activity-level enquiries, finding GSR-laden fingermarks implies links between an individual, firearms, and the surface from which the fingermark was lifted.

Two recent publications have addressed the efficacy of LA-ICP-MS when discriminating between samples provided by shooters or non-shooters. Ferreira *et al.* (2021) used a targeted approach and a noticeably higher-resolution ablation size than their contemporaries (20 μm) [131]. They sampled the hands of five recent shooters and fifteen non-shooters considered at risk for occupational exposure to GSR-like material. While automotive workers were found to have greater average amounts of Ba on their hands than recent shooters, spectral maps and ternary plots for each group could be distinguished by visual inspection. Vander Pyl *et al.* (2021) conducted a larger study involving 119 samples, comprising three groups: non-shooters, shooters using traditional ammunition, and shooters using Pb-free ammunition [119]. They also used LIBS and SEM-EDS analyses to cross-check LA-ICP-MS data. Reported performance rates (for LA-ICP-MS) included 6.6% false positives, 91.8% true positives when the shooters used leaded ammunition, and 85.2% true positives for Pb-free ammunition.

1.7.2 Analysis of Organic GSR

Instrumental analysis of the organic fraction within GSR traces (OGSR) has generally lagged inorganic methods, both in technical progress and application to casework by practitioners. For many years instrumentation was not sensitive enough to detect the available amounts of each compound, particularly propellant additives present as small percentages of smokeless powder. However, some examples of OGSR detection capability can be found in active forensic laboratories [84]. As increasingly powerful technology continues to be developed, there has been a renewed interest in organic GSR analysis largely led by research scientists. As of the early 2020s, scientific working groups are seeking to establish an international consensus on industry best-practice to develop more standardized OGSR detection procedures.

1.7.2.1. Fieldable Ion Mobility Spectroscopy

Ion mobility spectroscopy (IMS) is already applied as a rapid screening technique for illicit drugs and explosives, especially in security applications. Volatile analytes are ionised at atmospheric pressure using ^{63}Ni or electrical discharge, which can be enhanced by the application of reagent gasses. Compounds are then separated by the amount of time it takes ions to move through a counter-flow of gas under applied electric field. Molecular mass, morphology and charge state can affect drift times [132]. The instrument output is similar to a chromatographic retention time, allowing identification of previously characterised compounds. Benefits such as high sensitivity, low cost, portability, and ease of use for non-scientist operators have led to deployment of tens of thousands of these devices for airports and military users [133]. As IMS is capable of detecting trace level vapours originating from explosives, it is a short step to possible application to OGSR [134-136]. Additives in authentic smokeless powder samples (EC, DPA, NDPAs) were qualitatively detected by

IMS, and LODs determined at 1-2ng by West *et al.* (2007) [137]. Like GC-MS, IMS has also been coupled to SPME to concentrate volatile markers of explosives [84, 134, 138, 139]. The use of headspace sampling may be more applicable to the detection of explosive devices or post blast residue containing smokeless powder, rather than post-firing GSR on a POI.

Yeager *et al.* (2015) have thoroughly validated an IMS method that could be applied to routine and presumptive hand swab testing for OGSR, although this was not integrated with IGSR testing [140]. Their results show that in about 70% of known shooter samples, peaks were detected in the expected drift-time windows for DPA, N-nDPA and dimethyl phthalate (as determined by a previous experiment by the same laboratory) [28]. The authors argue for pattern matching rather than an assessment of individual peaks due to high variability within shooter and non-shooter samples. This viewpoint was repeated by Bell and Seitzinger (2016) because IMS spectra are generated with all analytes and matrix interferences competing with one another during the ionization process [141]. Specificity can be an issue with IMS detection, with false positives for simulated explosive/interferant combinations as high as 21% [142]. All papers on the topic of propellant powder detection by IMS propose a presumptive or screening role, rather than confirmatory analysis (unless an orthogonal method is added).

1.7.2.2. Capillary Electrophoresis

Capillary electrophoresis (CE) has been proposed as a separation technique for investigating smokeless powders and OGSR. Using Micellar Electrokinetic CE with a UV detector, limits of detection in the low-picogram range have been achieved with an injection volume of 11 nL [143]. Less sensitivity but greater specificity was achieved using less common instrumentation - capillary electrochromatography/mass spectrometry (capillary electrophoresis using a chromatography column supporting a stationary phase with embedded charges), with 0.1-5.5 $\mu\text{g mL}^{-1}$ limits of detection [144]. The benefit of capillary electrophoresis appears to be minimal sample mass requirements, which could be advantageous in the common occurrence of only tiny amounts of GSR recovery during sampling. These masses must be concentrated into an equally tiny injection volume, so a preconcentration step would be needed to reduce volume from a swab designed to have large sampling coverage. Typical CE papers describe a degree of sample preparation that may be unsuitable for routine use [145]. On the other hand, CE could potentially be used to profile the additives in intact smokeless powder samples at lower cost than High-Performance Liquid Chromatography (HPLC) [145-147]. Publication of studies in CE for GSR analysis appears minimal in the last 5 years.

1.7.2.3. Vibrational Spectroscopy

One tactic described in literature is to spectroscopically detect the chemical bonds of OGSR compounds by their vibrational energy. In related literature, Raman detection of organic explosives for military and security applications is well described. For these purposes where stand-off distance, speed and minimization of false negatives (at the expense of false positives) are key, portable Raman detectors are strong contenders [148].

Applying Raman spectroscopy to GSR, Lopez-Lopez *et al.* (2012) compared the spectra of dissolved residues after firing six different ammunition types with their original powders. They found a high degree of similarity between these paired spectra [52]. They were also able to visually differentiate the Raman response of those six samples from one another. Bueno, Sikirzhyski and Lednev, a very active research group in this area, have used Fourier-Transform Infrared (FT-IR) and Raman spectroscopy to discriminate GSR resulting from the discharge of a 9mm and a 0.38 calibre firearm [57, 149, 150]. This group have also demonstrated the possibility, through the use of micro-Raman mapping and image processing software, of producing an automated GSR particle searching system similar to that in use with SEM-EDS [58]. A point for consideration is that vibrational spectroscopy produces a single spectrum even when mixtures are present. Therefore, spectra can be dominated by a few abundant compounds, with trace inclusions contributing less to the overall shape. This is pertinent to GSR, which has major concentrations of propellant alongside smaller amounts of additives.

1.7.2.4. Electrochemistry

Electrochemical approaches to GSR detection have been demonstrated since 1977, with early experts performing anodic stripping voltammetry (ASV) using mercury electrodes [151]. This process pre-concentrates metallic ions onto the electrodes, then measures the resultant current produced at each analytes' characteristic oxidation potential. The technique is sensitive for measurement of metals in general, but has some deficiencies for detection of GSR. Firstly, it requires dissolved samples rather than particulates. More concerningly, ASV is unsuited to detection of barium, a key analyte. The potential required to strip this element from electrodes is so negative that breakdown of solvent solutions can occur [152].

Publications on the subject appeared sporadically in the literature until 2013, when they were reviewed by O'Mahoney and Wang [152]. Around this time the same authors and their colleagues prompted a meaningful change in approach by applying disposable sensor strips, also known as screen-printed electrodes (SPEs), to electrochemical GSR detection. SPEs open opportunities for decentralized, rapid screening tests without reliance on colour-change reactions. Rather than using delicate glassware, these disposable strips feature metallic or carbon electrode surfaces and are much more readily transported to local police stations or even crime scenes. Vuki *et al.* (2012) describe the detection of GSR analytes using square-wave voltammetry on disposable electrodes [153]. Either Pb, Sb, DNT & NG or Pb, Sb, Zn & DPA could be detected simultaneously in a single run, albeit from laboratory standards rather than from post-shooting GSR samples. This is a rare example of a single chemical technique being used to simultaneously indicate the presence of both organic and inorganic GSR (Figure 1-7). Furthermore, O'Mahoney *et al.* (2014) showed that SPEs could be integrated with SEM-EDS for a complementary screening and confirmatory process using authentic samples [154]. Conductive carbon tape was affixed to SPE strips to create a platform that could be used sequentially for sampling, voltammetry and electron-microscopy. This approach not only introduced orthogonal confirmation, but also improved the signal observed in voltametric analyses.

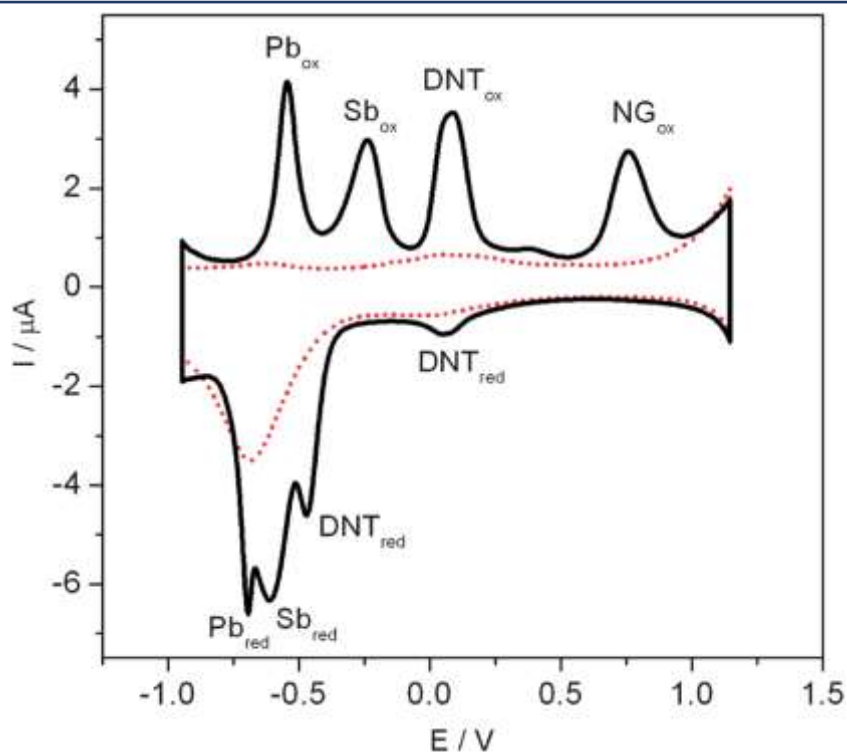


Figure 1-7: Cyclic Voltammogram showing response to GSR standards. Reproduced from Vuki et al., (2012).

Trejos, Arroyo and colleagues have continued to develop the approach described above [125]. Rather than using the modified SPEs to collect samples directly, publications by this group favour extraction from standard SEM stubs using a combination of organic and aqueous washes. The resulting stubs and solutions are then available for many other analytical techniques including voltammetry [155]. This has shown promise for large-scale screening surveys to estimate the prevalence of GSR or GSR-like materials, particularly because the speed and portability of electrochemical sensors enables laboratories to process far greater sample volumes than would be possible by SEM-EDS [156].

While a promising screening technique, electrochemistry does not match the specificity of SEM-EDS as a confirmatory method. For example, Ott and co-authors (2020) interpreted electrochemical data as “positive” for GSR when at least two of the following analytes were present above critical thresholds: Pb, Sb, Cu, DNT, DPA and/or EC [156]. Current GSR analysis guidelines place more weight on the association of metallic elements within particles, than on the detection of those same elements within a sample at large [157]. Also, the capability to resolve organic molecules having similar redox potentials but differing association with GSR does not appear to have been investigated specifically. The use of *ad hoc* classification criteria in academic work does not necessarily mean that the specific conclusions reached are any less unreliable. However, it may cause issues if judicial end-users do not apply a nuanced distinction between preliminary and confirmatory testing.

1.7.2.5. “Hyphenated” Mass Spectrometry

Mass spectrometry (MS) is recognized as one of the gold standards for instrumental analysis in many applied scientific fields. Mass spectrometers operate by first ionising the individual molecules or atoms that comprise a sample, and then measuring the mass-to-charge ratio of those ions. They are notable for their sensitivity and selectivity, particularly when coupled with chromatographic separation in so-called “hyphenated” systems. Hyphenated instruments dominate commercial laboratory usage because they can separate mixtures of compounds, and they can also resolve structural isomers (whereas MS generally cannot). From the outset, research groups have also used tandem mass spectrometry (MS/MS) to provide more certain OGSR compound identification [23, 158, 159]. Tandem mass spectrometry also allows for lower limits of detection by reducing instrumental noise. So-called direct and ambient mass spectrometers have also been investigated for OGSR analysis. The application of MS techniques to OGSR was thoroughly reviewed by Taudte *et al.* in 2014 [104]. Some specific examples, and more recent publications, are examined below.

Chromatographic separation is a technique notable for high discriminating power, and as such chromatographs are often the staple instrument by which large numbers of samples are analysed in forensic laboratories. They improve robustness by reducing the effects of potential interferences introduced during sampling, and allow some flexibility towards unexpected inclusions in ammunition formulation [106]. There are many commercially available systems that allow for straightforward coupling of chromatographs and mass spectrometers.

Use of gas chromatographs (GCs) to separate the components of smokeless powders has been demonstrated since the 1970s. While using GC-MS for smokeless powder was first reported by Mach *et al.* in 1978, thermal energy analyser (TEA) detectors were reportedly more common than MS detectors prior to Dalby *et al.*'s 2010 review, [9, 160, 161]. In 2003, Zeichner *et al.* compared GC-TEA, GC-MS and IMS for the detection of GSR vacuum-collected from clothing. They concluded that GC-MS was less sensitive than GC-TEA. Also in 2003, Andrasko *et al.* compared GC-TEA and GC-MS for detecting and characterising the OGSR found in firearms' barrels post-shooting [162]. They likewise found that TEA was more sensitive, but MS provided more structural information about molecules in the residue. Therefore, systems using MS had a greater scope for selectivity and characterisation. This was best illustrated in a later publication by Pigou *et al.* (2016), who made extensive use of mass spectra to investigate the identity of an artefact formed during the GC analysis of smokeless powders containing DPA [163].

One of the noteworthy advantages of GC is that it can easily accept samples by thermally desorbing them from solid adsorbents. These can be effective pre-concentration devices for collecting semi-volatile materials, such as the components of OGSR. Using 100 mg of unburned powder (a large mass compared to amounts expected in shooting cases), Dalby and Birkett (2010) developed a solid-phase micro extraction (SPME) method to detect and identify 27 compounds during a 32 minute GC-MS run [164]. Using a similar headspace

extraction process, Joshi *et al.* (2011) applied a combination of SPME, ion mobility spectrometry and GC-MS to characterise the composition of 65 smokeless powders [134]. SPME-GC-MS has also been used to detect NG, DPA and EC traces resulting from a smokeless powder pipe bomb explosions [165]. A sampling device demonstrating greater sensitivity than SPME, called capillary micro-extraction of volatiles (CMV), was proposed by Tarifa and Almirall in 2015 [123]. This setup was used to pre-concentrate the volatile components of GSR from hand swabs for 2 minutes, and resulted in detection of 3 ng diphenylamine (DPA) and 8 ng nitroglycerin (NG) by GC-MS. In a different approach, Stevens *et al.* (2016) directly interfaced authentic post-firing hand swabs with a GC inlet by thermal desorption. Due to high signal/noise ratios, LODs varied widely across several orders of magnitude (0.05ng for EC and DBP to 500ng for DNT and NDPA) [92]. Sample preparation was minimal and up to 10 compounds were targeted.

While having some deficiencies for detection of OGSR traces, GC-MS appears to excel in providing data for the niche application of estimating the time-since-discharge from recovered items. Early work on this approach was conducted by Andrasko, Norberg, and Stahling, examining both spent cartridges and firearm barrels [32, 162, 166]. More recently, extensive investigations into the aging kinetics of OGSR within spent cartridges have been conducted by Gallidabino, Romolo, Weyermann and colleagues [29, 167-169].

Unfortunately, a number of the key compounds in GSR are not easily amenable to analysis by gas chromatography. GC uses a heated inlet and column to volatilise sample into the gas phase for separation. N-nitroso DPA (N-nDPA), the first intermediate in propellant degradation, thermally decomposes to diphenylamine under these conditions and NG also partly decomposes. Nitrocellulose (a polymer) is not sufficiently volatile, and DPA may form unfamiliar artefacts within the instrument [92, 129, 163].

Despite increased solvent usage and more complex mobile phase chemistry, ultra-high performance liquid chromatography – mass spectrometry (UHPLC-MS) has advantages over GC-MS for the detection and characterisation of OGSR. Crucially, LC-MS allows analysis of thermally sensitive analytes such as N-nDPA and nitro- explosives, without causing additional decomposition. This was first suggested by Meng & Caddy in 1997, but had not been demonstrated by the time of that review [160]. Concerns over potential problems for efficient separation by LC have been raised as smokeless powder additives can encompass a wide range of different polarities [170, 171]. Nevertheless the number of examples continuing to appear in literature suggests that those concerns were unfounded. LC-MS methods appear to be the front-runners for adoption into practicing forensic laboratories, especially if holistic integration with SEM is successful. Firstly, detection limits are low enough to detect the deposition mass typically seen in casework samples. Secondly, the use of orthogonal information being a) chromatographic retention times and b) compound-specific fragmentation patterns contributes to a good confirmatory technique. Thirdly, the instruments and expertise to operate them are already widely available in forensic labs.

Electrospray ionisation (ESI) is the most reported approach to interfacing LC with a MS instrument for GS. Analyte ions are ejected from solvent droplets as they vaporize due to combined forces of electrostatic repulsion and change in pressure [172]. Atmospheric pressure chemical ionisation (APCI) is also applicable; charged chemical species are used to ionise analytes, often resulting in the formation of adducts. These are softer technique leaving a greater proportion of molecular ions intact for detection [104].

Application of LC-MS to smokeless powder samples initially arose as a technique for the identification and characterisation of explosive devices. An influential early publication was provided by Mathis and McCord in 2003 [171]. These authors used reverse-phase gradient LC and ESI-MS to quantitatively measure the additives in 11 unfired smokeless powders to generate profiles for comparison. Analytical sensitivity and the number of compounds under observation have continued to improve incrementally ever since. In 2013 Thomas *et al.* described a UHPLC-MS/MS method targeting a panel of 20 compounds specifically relevant to smokeless powder [173]. Their LODs varied between 64 ng (NG) and 0.4 ng (3,4 dinitrotoluene) injected into the system. Meanwhile, DeTata *et al.* characterised the retention times, accurate mass measurements and fragmentation data for >50 explosive and additive compounds using APCI and quadrupole time-of-flight mass spectrometry (LC-QToF-MS) [174].

LC-MS has also proven capable of detecting OGSR traces recovered from the hands of people who have discharged or handled firearms. Laza *et al.* (2007) used triple quadrupole LC-MS/MS to analyse samples collected using cotton swabs moistened with 75% isopropyl alcohol and 25% water, followed by solid-phase concentration on bonded octadecyl (C18) sorbent cartridges [158]. They reported limits of detection at 5, 6, 20, 27, 32, 34, and 115 µg injected onto the column for EC, MC, 2-NDPA, N-nDPA, 4-NDPA, DPA, and AK II, respectively. Swab recovery was estimated between 57% to 89% using dried aliquots of standard solutions. At least one compound of interest was detected from each of the post-shooting hand swabs from 15 ammunition lots in various calibres [158]. Perret *et al.* (2008) also utilized triple quadrupole LC-MS/MS, operating in both positive and negative polarity modes, for the detection of explosives residues. Cotton swabs were collected from volunteers after they had handled commercial/military explosive formulations. Nitro-explosives including NG and two stabilisers relevant to OGSR were included in this study (DPA, EC). Detection of NG in particular was reportedly possible after 6 hours post handling, or after hands had been washed with soap and water. In 2015 Taudte *et al.* reported that they used a form of artificial intelligence (artificial neural networks, ANN), in their experimental design to estimate the most efficient LC separation parameters for OGSR samples. Their chosen method was able to resolve 32 compounds with a 27-minute chromatographic runtime. Hand samples were then collected using medical swabs, after volunteers discharged a selection of twelve different ammunitions using eight firearm models. Although all ammunitions used double-base powder, NG was only detected in 62% of samples. MC, EC and 2-NDPA were each detected in approximately ¾ of samples.

Proof-of-concept studies have been presented for many approaches towards detecting or characterising OGSR traces. However, recent trends in academic literature suggest that LC-MS is increasingly becoming the technique of choice for this application. There are a growing number of publications reporting the use of LC-MS data to investigate other aspects of GSR collection or evaluation, without focussing solely on the analytical method itself. For example, Gassner & Weyermann (2016) used UHPLC-MS/MS to compare the collection efficiency of sampling materials, finding that adhesive stubbing outperformed swab-type sampling [53]. Taudte *et al.* (2016) then studied the stability of OGSR once collected, again using UHPLC-MS/MS to analyse extracts made from either adhesive stubs or wetted wipes [175]. Recently Hofstetter *et al.* (2017) reported results from their studies on the transfer and prevalence of OGSR traces, while Maitre *et al.* (2018) modelled the retention of OGSR on the hands of shooters [23, 31]. Again, both used LC-MS to quantify organic compounds that signified the magnitude of the entire GSR trace. The relative scarcity of publications investigating similar issues using other instruments suggests that, at least amongst academic institutions, LC-MS is likely to be the most-favoured approach in the near future.

The trade-off with LC-MS is that while very comprehensive, it is also intensive. Workflow could be improved either by using a screening technique to reduce the number of samples submitted for confirmatory analysis, or by using a different confirmatory-level method that allows for higher throughput.

1.7.2.6. Ambient Ionisation Mass Spectrometry

Ambient ionisation mass spectrometry (AIMS) is the collective term for instrumental techniques that near-simultaneously desorb and ionise analytes directly from a samples' surfaces, without significant preparatory steps and at atmospheric pressure [176]. Those ions are then introduced into the vacuum chamber of a mass spectrometer for detection and chemical characterisation. Sampling in this way is inherently rapid, and permits analysis on items of unusual size or morphology without previous dissolution or exposure to vacuum [177]. Ambient ionisation can also be coupled to miniaturised, portable MS instruments. As such, it was identified by Correa *et al.* (2016) as a strong contender for "everything-everyone-everywhere" use in forensic analysis [178].

The field of AIMS developed rapidly, with a myriad of instruments operating on similar principles described in literature. Early publications focussed on novel applications rather than mechanistic studies, leading to many competing naming conventions for closely related techniques. The complexity of categorising these instruments was highlighted by Javanshad & Venter (2017) [176]. However, the landmark publications introducing AIMS' capabilities were released by Takats & *et al.* (2004) and Cody & Laramée (2005), using streams of ionising liquid- and gas-phase reactants respectively [179, 180]. The general principles of each design are shown in Figure 1-8:. The following discussion will therefore be organized along similar lines.

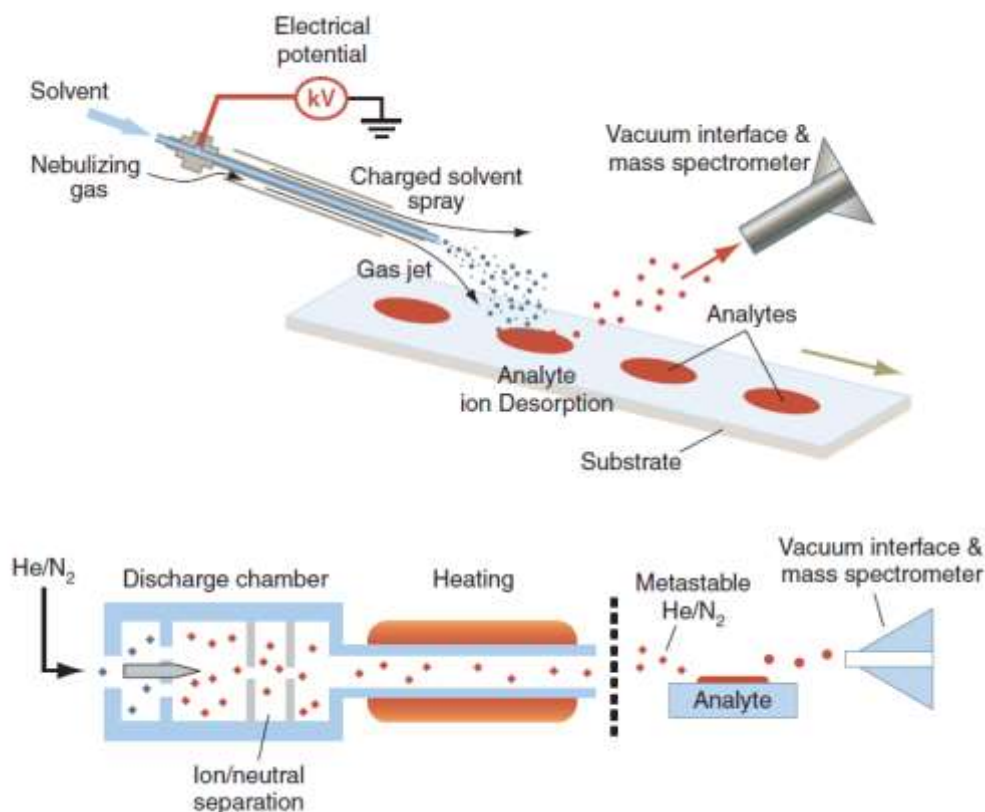


Figure 1-8: A representation of the principles behind a) Electro spray- and b) Plasma- based ambient desorption/ionisation instruments. Reproduced from Cooks et al., (2006).

Electrospray Desorption/Ionisation:

Electrospray ionisation (ESI) instruments produce ions by passing liquids through a capillary under strong electric fields. The analyte can be present in solution before being passed through the capillary, which means electrospray is sometimes used as a direct-injection sample introduction system for mass spectrometry. On the other hand, desorption-ESI (DESI) allows ambient sampling without the need to collect and dissolve samples. Introduced by Takats *et al.* in 2004, a jet of charged solvent is sprayed onto a solid surface, where droplets impact the surface and desorb analyte under electrostatic and pneumatic forces [179, 182]. Both are discussed as follows.

A direct-injection ESI-MS/MS apparatus was used by researchers at Tsinghua University, Beijing to detect several different compounds associated with OGSR, both from spiked swabs and post-firing hand swab extracts. In separate papers released in 1999 and 2001, the group described detection of methyl centralite and DPA with nitrated DPA derivatives. Detection limits as low as 60 pg were achieved for injected MC by using MS/MS to remove interfering signals [183]. The method was sensitive enough that serious contamination issues were observed after multiple post-firing samples were analysed, and traces of MC built up in the sampling columns. Reported limits of detection were higher for DPA (1.0 ng mL^{-1}), N-nDPA (0.5 ng mL^{-1}) and 4-NDPA (2.5 ng mL^{-1}) [184]. In 2009 Scherperel *et al.* published results of experiments using nanospray ESI with

ion trap MS/MS to analyse smokeless powders and GSR extracted from cotton target cloth [170]. EC, DPA, N-nDPA, 4NDPA and dibutyl phthalate were all detected in a single run for 0.1 mg mL⁻¹ extracts of unburned powder, but only EC was detected in post-shooting GSR samples. A notable amount of interference was observed when the target cloths had not been washed prior to use as shooting targets, or had been machine washed using detergent. The background could be minimised by washing with deionised water, but this must occur before the shooting event to avoid loss of analyte compounds. This is not something that can be controlled in the context of a forensic investigation.

Detection of explosives on various surfaces was one of the first proposed applications for DESI [182, 185]. In 2007 Justes *et al.* reported the ability to identify explosives including TNT, RDX, HMX and PETN spiked at “a few ng” directly onto skin. A volunteer placed their finger 3-5mm from the mass spectrometer inlet during the experiment, without discomfort [186]. Zhao *et al.* (2008) were also able to desorb compounds of interest directly from the skin after a controlled shooting event, specifically EC and MC [98]. Direct detection was still possible despite a range of potential confounding influences, including waiting for 12 hrs between shooting and analysis, repeated hand washing, and deliberate application of interferences such as milk or soft drink. Other surfaces (hair, glass, rubber, leather and cotton) were spiked with EC and MC standards, with LODs of 5-70 pg depending on the surface. Improved S/N ratio was achieved using tandem mass spectrometry. A deliberate decision was made to target only centralite compounds for this study, as other compounds were considered to have greater environmental abundance. Expanding the list of targets would increase probative value, especially as MC is allegedly only associated with ammunition of Chinese provenance [187].

Morelato *et al.* (2012) demonstrated that detection of key OGSR compounds by DESI on standard SEM stubs is possible with no modification, and does not preclude later analysis by SEM-EDS [188]. MC, EC, DPA and nitrated DPA were detected in positive ionisation mode, although contrary to the research presented by Zhao *et al.*, certain centralite ion fragments (m/z 134 and 148) were not seen [98]. For an unknown reason and despite intensive attempts, NG could not be detected even from standard solution. While detection of stabilisers was possible, unfortunately it was noted that weak and unstable signals were obtained from the surface of stubs. This contradicted promising earlier results during optimisation from standards doped to approximately 260ng/mm² on a Teflon surface. Proposed explanations included “...instability of the solvent layer under high nitrogen flow, the sticky characteristics of the stub surface, the conductivity of the stub itself or a combination of these factors” (Morelato *et al.*, 2012) [188]. No specific figures of merit were given, but their final verdict was that high limits of detection caused by stubs’ physio-chemical properties were such that routine OGSR screening would not be viable. Improved results may be possible using tandem mass spectrometry to reduce signal-to-noise ratios.

Another distinct technique that has been suggested since Taudte *et al.*'s 2014 review is swab touch spray mass spectrometry. Following a procedure first reported by Pirro *et al.* (2015), medical swabs with an absorbent tip wrapped around an aluminium handle are used to swab the area of interest (without solvent). High voltage can then be applied directly to the aluminium handle to promote ionisation, while solvent is sprayed onto the absorbent tip in the vicinity of the mass spectrometer inlet [189]. Fedick and Bain used a rayon fibre swab with this setup to detect both MC and EC as proof-of-principle with both tandem mass spectrometry and a miniature, portable mass spectrometer. Advantageously medical swabs are sold in individual sterile, tamper-proof packaging and can be used without preparatory steps, leading to their description as "ideal forensic sampling device(s)" [190]. Positive detections of MC and EC were made from shooters' hands, a variety of glove materials, clothing and fired cartridges. Unfortunately the involvement of additional sampling devices is likely to interfere or compete with existing protocols using SEM stubs, as mentioned previously.

Plasma Desorption/Ionisation:

Rather than using solvents as charge carriers, AIMS can also be achieved using heated streams of plasma or meta-stable gas species. This approach was initially developed by Laramée and Cody at JEOL USA Inc. in the early 2000s [180]. Their product, sold under the name "Direct Analysis in Real Time" (DART), was the first commercially available AIMS source and has been used in a large share of subsequent publications. DART and other AIMS ion sources featuring plasma ionisation are regularly reviewed, with examples published by Ding & Duan in 2015 and Chen *et al.* in 2017 [191, 192].

In plasma AIMS, the flow of heated reagent gas helps to desorb and volatilise analytes from the surface of samples. For DART-MS, which can produce either positively- or negatively- charged ions, helium is the normal reagent. Ionisation then occurs in the gas phase *via* collisions between the analyte and reactive species originating from an electronic excitation source. A cascade of reactions ensues as electronically excited He* encounters atmospheric N₂, O₂ and water vapour (reactions R1-1 to R1-13, Table 1-2). These reactions are rapid even at ambient pressure, with ~10⁹ to 10¹⁰ collisions occurring per second [193]. Both Penning ionisation and atmospheric-pressure chemical ionisation (APCI) can play a role in transferring charges from the reagent gas to the sample. Ionisation using AIMS instruments is typically considered "softer" or lower-energy than ionisation in systems using electron impact mechanisms, avoiding excessive molecular fragmentation.

The utility of AIMS towards forensic and security applications was immediately recognised, with initial exploration for use in the detection of chemical warfare agents preceding academic publication [180]. Other forensic applications include screening of explosives, suspected illicit drug products, or detection of these drugs and their metabolites in biological fluids [177, 178, 191, 193-199]. There have also been proof-of-concept studies specifically investigating the detection of smokeless powder and GSR with plasma desorption/ionisation reported in literature.

Table 1-2: Ionisation Pathways Initiated by DART Ion Source [196, 198]			
Positive Mode		Negative mode	
R1-1	$\text{He}^* + \text{N}_2 \rightarrow \text{He} + \text{N}_2^+ + \text{e}^-$		
R1-2	$\text{N}_2^+ + \text{N}_2 + \text{N}_2 \rightarrow \text{N}_4^+ + \text{N}_2$	R1-8	$\text{O}_2 + \text{e}^- \rightarrow \text{O}_2^-$
R1-3	$\text{N}_4^+ + \text{H}_2\text{O} \rightarrow 2\text{N}_2 + \text{H}_2\text{O}^+$	R1-9	$\text{O}_2^- + \text{M} \rightarrow [\text{M}+\text{O}_2]^-$
R1-4	$\text{H}_2\text{O}^+ + \text{H}_2\text{O} \rightarrow \text{H}_3\text{O}^+ + \text{OH}^\cdot$	R1-10	$[\text{M}+\text{O}_2]^- \rightarrow \text{M}^-$
R1-5	$\text{H}_3\text{O}^+ + n\text{H}_2\text{O} \rightarrow [(\text{H}_2\text{O})n + \text{H}]^+$	R1-11	$\text{M} + \text{e}^- \rightarrow \text{M}^-$
R1-6	$\text{M} + [(\text{H}_2\text{O})n + \text{H}]^+ \rightarrow (\text{M}+\text{H})^+ + n\text{H}_2\text{O}$	R1-12	$\text{MX} + \text{e}^- \rightarrow \text{M}^- + \text{X}^\cdot$
R1-7	$\text{M} + [\text{X}]^+ \rightarrow (\text{M}+\text{X})^+$	R1-13	$\text{M} + \text{X}^\cdot \rightarrow [\text{M}+\text{X}]^-$

The ability of DART-MS to desorb and ionise the components of undetonated smokeless powders, both from single grains and from solvent extracts, has been established and compared to a representative GC-MS method by Lennert and Bridge (2018) [61]. Their study analysed 33 smokeless powders by both instruments, and then investigated the ability to discriminate between samples with up to five chemometric models. A time-of-flight mass spectrometer was interfaced with the DART source, as accurate mass measurement and isotopic profiles are used to identify compounds. Analytical figures of merit were not reported, but 20 mg samples were used to produce 600 microliter extracts. Only a tiny fraction of this extract, enough to coat the tip of a glass capillary, was actually exposed to the ionisation stream. Therefore the technique is likely to be sensitive enough to also detect OGSR after smokeless powder has been ignited, depending on collection and sample introduction efficiency. The study concluded that spectra produced by DART-MS and GC-MS are equivalent in discriminating power, while DART was significantly faster at ~2min per sample. This is important both for application as a screening method, and because smokeless powder samples are likely to degrade over time even in solution.

The authors Bridoux *et al.* (2016), Li *et al.* (2016) and Williamson *et al.* (2018) each described coupling AIMS to an additional preconcentration step for the detection of explosives devices, smokeless powders, or OGSR standards respectively [199-201]. Techniques included vacuum lifting and solid-phase sorbents. Clemons *et al.* (2013) took this to an extreme, manually using a nano-manipulator device to collect single crystals of explosive compounds evaporated from solvent before analysing them by DART-MS [201]. This is certainly an impressively precise sampling method and may find use in extreme circumstances where notable contamination is closely intermingled with analyte particles. It is also probably not appropriate as a routine sampling strategy.

Black *et al.* (2017) described a method more closely mirroring the direction taken for hyphenated LC-MS protocols (see section 1.7.2.5), by extracting SEM stubs with 50 μL of methanol after dabbing a cotton shooting target [202]. The methanol/GSR solution was immediately withdrawn by syringe and 1-3 μL aliquots ionised *via* DART. They reported detection of very small signals for MC and DPA, and larger signals for EC. This paper also raises interesting questions about what may be considered GSR in future, as test firings were carried out using a firearm 3D printed from online plans using a variety of polymers. The polymers could then be characterized using DART-MS on cartridge scrapings, or on the surface of the projectile itself. At the present time there has been no mention of using DART for directly detecting GSR on the stub surface itself (as was suggested by Morelato *et al.* (2012) using DESI) [188]. Rowell *et al.* (2012) used DART-MS to look for nitro-organic explosive residue transferred by touch and collected on fingerprint lifting tape, a potentially analogous underlying surface. Unfortunately they also reported that characteristic explosive fragment ion peak signals were very weak, and difficult to distinguish from a complex background spectra created by the adhesive surface [198].

1.7.3 Holistic Analyses

Methods capable of characterising both the organic and inorganic portions of the same GSR trace are rarely applied in forensic casework. This is mostly driven by incompatibilities between SEM-EDS, the preferred confirmatory technique for GSR detection, and meaningful analysis of organic compounds. There are two approaches that could lead to a more holistic use of recovered GSR traces; either the traces can be split into sub-samples for separate laboratory analysis, or instrumental techniques other than SEM-EDS can be used to characterise both portions of the trace. In this document the former group are considered to be “integrated” analyses.

1.7.3.1. Return to Bulk Analysis

There are some analytical techniques capable of detecting inorganic and organic matter simultaneously. However, most require the dissolution of the sample, and therefore represent a return to bulk methods in a move against the general trend of forensic GSR examination. For example, the work of Vuki *et al.* (2012) (as previously described in section 1.7.2.4) showed that it is possible to concurrently detect Sb, Pb, DNT and NG or Sb, Pb, Zn and DPA in solution, using electrochemical methods.

Dissolved metal ions can also be encapsulated by organic molecules through electrostatic forces in a process called complexation. This allows separation and detection *via* methods typically considered appropriate for organic compounds only. In 2004 Morales & Vazquez used diaminocyclohexane tetraacetic acid (CDTA) as a pre-treatment step to form complexes with metal ions associated with GSR [145]. They then used micellar capillary electrophoresis to separate and detect 11 OGSR compounds and 10 metal-ion complexes. However, the process was not sensitive enough to detect OGSR in authentic post-shooting hand samples. Very recently, Feeney *et al.* (2021) have revisited the complexation approach to allow simultaneous analysis of inorganic

GSR by LC-MS [155]. They found that 18-crown-6-ether effectively formed complexes with Pb and Ba, while Sb was chelated by tartaric acid. In a two-part study of post-shooting samples, GSR was successfully detected in 95% and 100% of instances.

1.7.3.2. Sequential Non-Destructive Imaging

Bueno and Lednev (2014) described a method combining hyperspectral Raman microscopy and image processing software to produce an automated OGSR particle-searching system [58]. While the sensitivity of this system was not directly compared to methods requiring extraction, the non-destructive nature means that subsequent analysis by SEM might be implemented without meaningful disruption.

1.7.3.3. Split-sampling methods

The chief advantage of producing subsamples from a trace is that the most appropriate laboratory method can be applied to each type of material that the trace contains. The corresponding disadvantage is that increased handling and manipulation increases the risk of losing recovered materials, in effect decreasing the sensitivity of combined methods. The simplest application of this approach would be to collect two samples from a questioned surface, i.e. a tape lift for SEM-EDS and a wetted swab for OGSR analysis [160]. However much of the material will be collected onto whichever device is used first, leaving less for collection by the second. This was specifically demonstrated by Gassner *et al.* in 2016 [18]. Instead, two 2014 papers from researchers at the University of Basque Country demonstrated that SEM stubs could be modified by covering half of the adhesive surface with a polymer (polytetrafluoroethylene, PTFE). The two halves could then be separately analysed using combinations of either LA-ICP-MS and Raman microscopy, or else SEM-EDS and LC-MS for washings taken from the modified half [128, 129]. However, this again essentially halves the collection surface for each type of residue. It is also possible to use a single collection device, and then separate the trace into organic and inorganic fractions afterwards. In 2019 Goudsmits *et al.* reported using solid-phase microextraction followed by GC-MS to achieve this fractionation [203]. As this method is not expected to disturb any inorganic particulates, conventional SEM-EDS analysis can follow. However, as SPE is an equilibrium process, complete recovery of the OGSR compounds cannot be expected [22].

Zeichner and Eldar (2004) conducted typical SEM analysis on their samples first, then used a two-stage solvent extraction to recover and concentrate OGSR [204]. They also found that performing extraction of adhesive stubs under sonication helped to maximise recovery. This preserves the integrity of the sample for the initial examination but is somewhat destructive in the second phase. Later, a similar approach using a single solvent was applied by Ali *et al.* (2016), and this was also subsequently recommended by Minziere *et al.* (2020) when compared against analogous procedures [39, 205]. In 2016 Taudte *et al.* reported that liquid extraction from adhesive stubs outperformed swabbing for OGSR collection efficiency [22]. However, they used swabs to demonstrate that a single liquid sample could encompass both an organic solution of OGSR,

and a suspension of IGSR particulates. The latter then were recovered using 0.8 µm PTFE syringe filters and could be re-mounted onto adhesive stubs with observed densities between 0.6 – 1.3 particles/mm².

Black *et al.* (2017) omitted sonication, but still used solvent extraction to recover OGSR compounds for analysis by AIMS [202]. They reported using a pipette to deposit 50 µL of methanol onto the adhesive stub, sufficient volume to cover the surface without overflowing. The droplet was then withdrawn into the same pipette, with 1-3 µL analysed by DART-MS. While OGSR (specifically the stabiliser EC) was detected in this extract, there was only a passing mention of SEM-EDS and an accompanying figure suggesting that an accompanying inorganic analysis could also be completed.

1.8 Summary and Research Objectives

1.8.1 Assessment of the state-of-the-art

There is a substantial body of extant academic literature concerning the theory and forensic application of chemical sciences to gunshot residues. The collection and laboratory examination of samples for inorganic GSR is a mature process, supported by international norms and published standards. Identification of inorganic gunshot residue by SEM-EDS is an established technique in routine use. However, the procedure is time-consuming and requires specialized equipment. There are some limitations on the range conclusions that can be drawn using data from this source, particularly in the absence of significant numbers of “characteristic” three component (Pb, Sb, Ba) particles.

On the other hand, few of the numerous methods proposed for organic GSR analysis are used in regular forensic practice. These have included instrumental techniques such as: Raman spectroscopy, electrochemistry, capillary electrophoresis, ion mobility spectroscopy, gas/liquid chromatography coupled to mass spectrometry, or ambient ionisation mass spectrometry. However each thus far has exhibited flaws such as high limits of detection, lack of specificity and sensitivity, or disruption of the process currently in place for SEM-EDS. This is despite previous research characterising the organic materials typically associated with firearm use. Key compounds include nitrocellulose, nitroglycerin, nitrotoluenes, diphenylamine, centralites, and their nitric-oxide derivatives. These substances have the potential to increase the forensically-relevant information available to police officers and courts *via* expert analysts. In particular, characterisation of OGSR can help to discriminate between true IGSR and IGSR-like interferences. This may become a deciding factor in future casework, if a general shift towards heavy-metal free ammunition begins to impact criminal firearm usage. Including OGSR also increases the mass of material available for detection, a worthwhile consideration when working with trace evidence.

It is apparently even rarer to apply an analytical workflow incorporating both inorganic and organic gunshot residue examination holistically. To illustrate why this may have a significant impact on GSR casework, attention should be given to the results of a 2016 survey for GSR traces amongst the Australian public,

conducted by Lucas *et al.* and colleagues from Australian state police departments [206]. In one instance, three particles each containing the elements Pb, Ba and Sb were detected on the hands of a randomly selected member of the public who reported no firearm use and listed their occupation as “retail worker”. These particles were not of a morphology typical to GSR, were not found in abundance, and were not associated with other particles of a supportive nature. However, in the relevant jurisdiction they meet the definition of “characteristic” GSR and would have been reported as such to a court of law. There was some contention that in fact these particles were not from a firearm and at best their presence is hard to account for with available information. The concurrent detection of compounds identified as OGSR would allow for a more confident assessment; perhaps the volunteer was untruthful, or else had been unknowingly exposed. Conversely, the absence of organic compounds from propellant or its stabilisers points towards either a non-firearm source or an unexplained secondary transfer. Therefore while anecdotal, this example highlights the potential for OGSR testing to add value under the current paradigm of GSR examination.

Nevertheless, the identification of a given trace as GSR is only one aspect of the role that may be required of a GSR expert. The development of mathematical models and theoretical frameworks to support sound evaluation of traces is also an area of active research. This supports recommendations from the European Network of Forensic Science Institutes stating that evaluative reporting should be favoured over technical reporting whenever case-specific circumstances allow. Again, much of the experimental work supporting evaluative models for GSR evidence has been focussed solely on the inorganic portion of traces.

1.8.2 Research Objectives

1.8.2.1. General aims

Additional potential for OGSRs to aid in forensic investigations is well described in literature, and the technical capability to detect and analyse these traces is an area of maturing research. If such under-utilised traces are made accessible to the toolbox of forensic analysts, successful resolution of a greater number of cases may be possible. However, processes targeting OGSR are unlikely to supplant particle-mapping by SEM-EDS in routine casework. Consequently, the overarching premise of this thesis was to develop an integrated forensic approach to both the organic and inorganic portions of GSR traces. This required laboratory experimentation on technical processes, and also new ways of thinking about the evaluation of laboratory data to support the provision of expert knowledge to end-users.

1.8.2.2. Chapter Two: Technical Method Development

Prior literature suggested that LC-MS was the most promising approach to OGSR analysis. Benefits of these instrumental systems include the ability to reach sufficient limits of detection, and the discriminating power provided by orthogonal measurements of retention time and molecular mass-to-charge ratio. Adhesive stubs are the preferred sample-collection media for SEM analysis, and have also been shown to efficiently collect OGSR. However, previous work rarely gave more than cursory attention to the effect that procuring OGSR

extracts had on IGSR collected by adhesive stubs. In several examples SEM-EDS was performed first, risking loss of volatile OGSR components to the vacuum and incident electron beam. IGSR particles were then potentially lost/discarded in the process of isolating OGSR through sonication. Chapter Two documents the development of a method allowing tandem analysis by SEM-EDS and LC-MS/MS, while retaining existing adhesive stubs for later re-analysis if required. Efforts were made to determine the robustness of the process to real-world sampling conditions, such as the collection of traces from dirty surfaces or after delays post-deposition.

1.8.2.3. Chapter Three: Background Prevalence of GSR or GSR-like Traces

Selection of a suitable analytical technique provides only part of the information needed for forensic analysis. Defensible estimates of the background prevalence of GSR are also crucial, especially on the body and personal effects of people in the general population. Without such information the importance that can be placed on a “positive” detection is unknown or unsupported. Background frequency is inextricably linked to analytical method due to associated limits of detection and rates of false positive/negative results. “Random person” sampling and targeted testing of high-risk contamination scenarios has been conducted to cover IGSR in some situations. More work is still needed, as results cannot necessarily be extrapolated between jurisdictions. Comparable data for OGSR is lacking and would be required for any meaningful interpretation of findings during casework. Background testing for OGSR has been comparatively minimal, especially in Australia. Combined detection organic and inorganic traces from non-firearm sources or innocent firearm use in any population set is almost entirely unexplored. Chapter Three aims to contribute to addressing this shortfall. Data collected from a small-scale survey of the background prevalence of O- and I- GSR traces amongst Australians is provided. Samples were collected both from the hands of recent recreational shooters and from non-shooters for comparison purposes.

1.8.2.4. Chapter Four: Evaluative Reporting and Statistical Modelling

In the sub-discipline of chemical criminalistics, raw instrumental data are rarely reported directly to end users. Instead, part of the role of forensic scientists is to interpret the data using their expert knowledge. A typical report for GSR examination will start by stating the quantity of characteristic and/or consistent particles, and in some cases a minimum number of these are required before the sample can be considered “positive”. This approach does not account for OGSR under current published standards, although similar categories have been proposed in order to assign relative value to organic compounds connected with GSR. The first part of Chapter Four uses this qualitative, proscriptive approach to evaluate the same data collected for preceding chapters. Using a Bayesian updating model, positive and negative predictive values were calculated for each instrumental test separately and in combination. The results were then used to establish whether there was any improvement in detection accuracy.

The second part of the chapter instead explored the possibility of creating statistical models from the quantitative data collected in preceding chapters. These models form the basis underpinning evaluative reporting. Prior models for the evaluation of GSR traces have been published, but these only include either inorganic or organic markers in isolation. The contents of Chapter Four instead explore if multivariate machine-learning algorithms could be trained to allow more holistic use of the data collected from each trace.

1.8.2.5. Chapter Five: GSR Traces Recovered from Vehicles

Surfaces other than the hands of suspected shooters are routinely sampled and submitted for analysis in shooting cases. Some of these, such as the interior of passenger vehicles, are suspected of representing an increased risk of contamination with GSR-like interferences. That is, some materials and components used in vehicle manufacture may generate traces that are difficult to distinguish from GSR. In addition, vehicles belonging to frequent firearm-carriers such as police officers will develop a loading of transferred GSR over time. However there has been no prior survey of the background loading of GSR within vehicles *unless* those vehicles were already explicitly associated with firearm users. Chapter Five compares the analytical results obtained after sampling vehicles belonging to either shooters or non-shooters, considering both OGSR and IGSR.

1.8.2.6. Chapter Six: Ambient-Ionisation Mass Spectrometry

AIMS is a potential competitor to LC-MS for the analysis of OGSR. The combination of speed and sensitivity make it an attractive proposition as a screening technique, and with appropriate validation and trials it may also prove accurate and selective enough for use as a confirmatory technique for OGSR in its own right. While proof-of-concept has been demonstrated, more thorough investigation of this application is currently unreported. If found to be fit for purpose, it could potentially offer a significant reduction to demands on laboratory workload. Due to its versatile nature, it is proposed that sequential analysis by AIMS and SEM-EDS analyses may be possible with minimal adjustment to existing sample collection protocols. In consideration of the above, further research into the use of AIMS as a technique for the detection and analysis of organic gunshot residues was conducted.

Chapter 2:
Technical Method Development

2.1 Background:

Gunshot residues (GSRs) are physical traces that are important to the forensic investigation of crimes (or suspected crimes) involving firearms. Early GSR detection strategies relied upon colorimetric reactions, but these were nonspecific and are now generally considered unreliable for uses other than distance-determination or simple visualisation. The prevailing benchmark for GSR identification is scanning electron microscopy (SEM) of samples collected using adhesive stubs, having progressively been adopted across various jurisdictions since the 1980s. This method specifically targets residues originating from the inorganic primers commonly used in cartridge-based ammunition. Electron microscopy is used to detect micron-sized particles, with elemental composition verified by energy dispersive spectroscopy (EDS). It then falls to expert analysts, using their experience and working within established standards, to determine the extent to which a sample is characteristic of GSR.

More recently, there has been academic and practitioner interest in improved capabilities for detecting the organic portion of gunshot residue, or OGSRs, typically originating from smokeless propellant powders. Compounds such as nitroglycerine and chemical stabilisers have been identified as key targets in this regard. While several laboratory-based methods have been shown to be sufficiently selective and sensitive to detect OGSRs collected post-shooting, these are yet to be standardised to the same extent seen for IGSR analysis by SEM-EDS. Despite a healthy and growing collection of academic literature specifically examining OGSR for forensic purposes, comparatively fewer studies address the issues of integrating both the laboratory workflows and resulting information into a coherent outcome.

A combined approach to both portions of a given GSR trace offers several benefits. Firstly, a greater fraction of each trace's total mass becomes available to potentially find and analyse. Secondly, it is less likely that non-firearm sources will exhibit chemical similarities to both primer and propellant residues simultaneously. Finding both together can therefore increase analysts' confidence that they have indeed detected GSR. Finally attempts at source-attribution, either through databases or comparison with known specimens, can be improved when more identifying features are available to discriminate between sources.

One approach to integrated analysis was described in the article titled "Tandem detection of organic and inorganic gunshot residues using LC-MS and SEM-EDS" (Bonnar *et al.*, 2020, Forensic Science International, DOI: <https://doi.org/10.1016/j.forsciint.2020.110389>). The full text of this article has been reproduced in section 2.2, with minor changes to formatting to maintain consistency. The study outlines a process of collecting GSR samples from the hands of a recent shooter using adhesive stubs. Extracts containing OGSR are prepared by pipetting organic solvent onto the stubs' surface, gently agitating the droplets, then recovering the liquid. OGSR was identified from the extracts using liquid-chromatography and mass spectrometry. Once dried, the adhesive stubs can be examined by SEM-EDS in the normal manner. It was observed that the extraction process did not interfere with analysis of IGSR particles for practical purposes.

Following publication of the proof-of-concept study, some minor adjustments were made to the analytical method. Subsequently, a series of samples were collected to assess the robustness of the process to conditions that may be encountered during “real-world” investigations. The results of these experiments are outlined in section 2.3. Concluding remarks can then be found in section 2.4.

2.2 Tandem detection of organic and inorganic gunshot residues using LC-MS and SEM-EDS

2.2.1 Abstract

Gunshot residue (GSR) is a valuable form of forensic trace evidence in the investigation of firearms crime. The current gold-standard approach does not include the analysis of organic components of the residues, which may be a deficiency, particularly in cases where there is little to no inorganic gunshot residue (IGSR) present or its attribution to a firearm source is ambiguous. A solvent extraction method was used for the extraction of organic GSR (OGSR) from the most common sampling device used to collect IGSR (i.e., SEM stubs with double-sided carbon adhesive tape). It was found that extraction did not significantly disturb inorganic GSR present on stubs, which raises the possibility that a valuable, comprehensive tandem analysis of both organic and inorganic GSR may be implemented using a single residue collection device.

The organic extract was analysed using Ultra High Performance Liquid Chromatography coupled to an Ion Trap Mass Spectrometer using Electrospray Ionisation (UHPLC-ESI-MS/MS), with preliminary results indicating that organic components can be extracted and detected at levels appropriate to casework GSR analysis. Testing of traces collected from the hands of recent shooters showed detection of stabiliser compounds typical of OGSR, which were confirmed to be present in the test ammunition’s propellant. Extraction of OGSR from SEM stubs is rapid and simple to integrate into typical existing inorganic GSR analysis workflows. Total analysis time is approximately 30 minutes per specimen, including preparation, instrumental analysis and data review. As the first step in the examination of GSR stubs in relation to a shooting case, extraction of organics and analysing them for the presence of OGSR may bring two operational benefits. First, that approach may be a useful way to determine which stubs warrant priority examination for IGSR, and second, it offers the possibility of providing relatively rapid case information to investigators.

2.2.2 Introduction

Gunshot residue (GSR) refers to materials generated during the discharge of a firearm. This residue is released as a plume that subsequently settles on nearby surfaces, which can include the target, and is often used in the investigation of firearms crime. Conventionally, forensic analysis of GSR has been focussed on the inorganic gunshot residue (IGSR), which is primarily generated from components of the ammunition’s primer but may also contain traces of the projectile, the gun’s barrel and the cartridge case. For IGSR analysis, the composition and morphology of the individual particles and the overall particle population composition are

considered when identifying residue as being GSR and when evaluating the significance of the residue collected. Scanning electron microscopy with energy dispersive X-ray analysis (SEM-EDS) is the current industry standard for the analysis of GSR casework specimens, and has been since the 1980s [77]. ASTM International produced and periodically updates a guide for GSR analysis [142], which defines particle types and compositions considered most likely to be associated with the discharge of a firearm, the ones of highest probative value being individual particles that possess a composition containing Pb, Ba and Sb or Pb, Ba, Ca, Si and Sn present in the same particle. This same standard defines a variety of other particle elemental compositions and the relative strengths of their association with a firearms discharge.

In addition to the inorganic traces targeted for detection thus far, organic compounds are also expelled during the discharge of a firearm. These originate from the propellant's energetic components and the various additives used to improve the ammunition's performance and longevity. Previous reviews have demonstrated that a wide variety of different organic compounds may be included in propellant and primer formulations, and may therefore contribute to GSR [9, 104, 152]. As is well understood in the interpretation of IGSR traces, the evidential value of detecting organic compounds associated with GSR is inversely proportional to those compounds' abundance in sources beyond firearms. This concept has been used to propose a preliminary list that may form the basis of a more formal classification scheme of forensic value [85]. Diphenylamine (DPA) and its nitrated derivatives, N-nitrosodiphenylamine (N-NDPA), methyl centralite (MC, 1,3-diethyl-1,3-diphenylurea), ethyl centralite (EC, 1,3-diethyl-1,3-diphenylurea), akardite-II (AK-II, 3-methyl-1,1-diphenylurea), dinitrotoluenes (DNT), nitroglycerine (NG) and nitrocellulose (NC) are frequently selected as targets for organic GSR (OGSR) analysis [9, 61, 129, 207]. Of these, the centralites and AK-II have scarce reported usage outside the industrial manufacture of propellants. N-NDPA and nitro-derivatives of DPA can be produced as by-products in the manufacture of certain dyestuffs, but also arise as a result of smokeless powder's decomposition. Detection of one or more of these compounds in traces related to shooting investigations is therefore very significant [158].

Combination of OGSR and IGSR evidence in tandem should have a greater probative value than either one of the two pieces of evidence in isolation, as articulated by authors such as Morelato *et al.*, Taudte *et al.*, and Goudsmits *et al.* [22, 188, 203]. This increased value stems from an improved capability to discriminate between material truly originating from a firearm, and material originating from environmental sources but exhibiting similar chemical composition. Firstly, a firearm may have been fired but subsequently low numbers of particles 'characteristic' of GSR or only particles 'consistent' with GSR are detected, either due to usage of atypical ammunition (including rimfire ammunition and heavy metal-free ammunition) or losses from secondary transfer. In this situation the detection of OGSR gives more certainty to the proposition that a sampled surface has been associated with the discharge of a firearm. Secondly, in the situation where only particles 'consistent' with GSR are detected (such as those containing Ba and Pb), the absence of OGSR may

add weight to the proposition that the sampled surface was associated with environmental particles rather than GSR. Therefore, the integration of testing for both types of evidence is a subject worthy of investigation.

Various approaches have been attempted for the analysis of OGSR, including colour tests, electrochemical detection, Fourier-Transform Infrared (FTIR) spectroscopy, ion mobility spectrometry, gas- and liquid-chromatography (GC & LC), and various applications of mass spectrometry (MS), many of which were outlined in a recent review [84]. At this time, there is no method accepted as a standard for forensic OGSR analysis in the same manner as SEM-EDS is for IGSR. Solid phase micro-extraction (SPME) sampling coupled to GC-MS has found some utility as a technique for the comparative analysis of intact smokeless powders and swab samples collected from post-blast residues [164, 165]. However, some key compounds are not well-suited to analysis by GC-MS; N-NDPA in particular is known to degrade to DPA when it is exposed to the heat of injection and NG also partially degrades [92, 129, 163]. LC-MS methods such as used in Taudte *et al.* 2017 [22] are considered to have the best limits of detection for most analytes, and appears to be the technique of choice for research groups seeking to address OGSR activity-level and interpretive issues [208].

The collection of GSR can be performed either by application of double-sided adhesive tapes mounted on SEM pin stubs, or absorbent swabs wetted by solvent. Of these options, stubs are reported to be more efficient overall [22]. This offers the elegant possibility that tandem analysis of OGSR and IGSR may be possible using a single sampling device. In early attempts to undertake tandem OGSR and IGSR analysis, two separate sampling devices were used, i.e., SEM stubs for IGSR and swabs for OGSR analysis [160]. More recent approaches have used a single sampling device, either by modifying the standard GSR aluminium and carbon tape stubs [22, 128, 129], by removing the organic components off the stub using various solvent extraction procedures [129, 205], or by attempting to detect the organic components with a non-destructive beam technique [22, 129]. For example, Abrego *et al.* [128] used micro-Raman spectroscopy coupled to scanning laser-ablation ICP-MS, to enable analysis of both OGSR and IGSR from lead-free ammunition. While the procedure was completed in under 2 hrs from a single sampling device, their claims of “non-destructive” testing are debatable as it is mentioned that the power of the laser had to be tuned in order to avoid penetration through the carbon sampling tape into the aluminium stub beneath and of course particles had to be destroyed by ablation for detection. Benito *et al.* demonstrated that modifying a SEM stub, by covering half of the adhesive surface with PTFE film, produced a viable collection device resulting in inorganic and organic subsamples [129]. However, this was recently shown to decrease sampling efficiency as the residue-collecting surface of the sampler is effectively halved for each type of residue [205]. In another strategy, UPLC-MS has been integrated with SEM-EDS by extracting OGSR in solvent under sonication, then filtering out suspended IGSR particles [22]. This may compromise any inorganic trace that was collected, as the additional handling may cause inadvertent loss of particles.

Some approaches to simultaneous OGSR/IGSR analysis in a single run have been examined. In 2004 Morales & Vazquez [\[145\]](#) established the separation of 11 organic and 10 inorganic species associated with GSR by capillary electrophoresis. However, the method required significant sample preparation and, more crucially, sensitivity was not sufficient to detect many key residue components from real shooting residues. Vuki *et al.* in 2012 [\[153\]](#) showed that it was possible to use cyclic and square-wave voltammetry to concurrently detect Sb, Pb, DNT and NG or Sb, Pb, Zn and DPA. However, the ability of this technique to cope with environmental interferences is unknown, as “clean” standard mixtures were used to generate voltammograms rather than GSR case specimens. A significant issue with simultaneous analytical approaches is that the ones reported rely on complete dissolution of samples, which destroys particle morphology and elemental composition. This is of particular relevance because components of IGSR in isolation have common environmental sources, and it is their association within single particles that is most indicative of a firearm being the likely source. The research group of Lednev *et al.* have demonstrated the possibility, through the use of micro-Raman mapping and image processing software, of producing an automated OGSR particle searching system [\[149\]](#). However, in that work the examination of the selectivity of the technique towards GSR only involved consideration of dust from automotive brakes, which would not usually be confused with IGSR [\[82, 95\]](#). Furthermore, Raman is not capable of gathering analytical data for metal particles (such as brass, Fe, and Pb), which is vital for the differentiation between IGSR and environmental dusts. In 2019, Goudsmits *et al.* [\[203\]](#) reported that OGSR could be collected from adhesive stubs using solid-phase microextraction followed by GC-MS. This method should not disrupt any IGSR present on the stubs therefore conventional IGSR analysis can follow. However, as described previously, GC-MS is not ideal for the comprehensive analysis of OGSR as certain analytes are heat-sensitive.

One characteristic of all the techniques described above is that they involve significant analysis time, either due to sample preparation or a requirement to scan collection devices at high spatial resolution. In 2018 a more rapid approach was presented by Gandy *et al.* [\[207\]](#), who investigated sodium borohydride as a fieldable presumptive test reagent for GSR that produces a colour change in the presence of DPA and poly-nitro diphenylamines. The colourimetric test was shown to accurately and sensitively react with common organic components but was not tested on the surface of adhesive stubs. Gandy *et al.* [\[207\]](#) also examined the effects this testing had on the subsequent detection of Pb, Ba and Sb using SEM-EDS. While the presumptive testing for OGSR did not appear to degrade the IGSR components, no evaluation of the effect of these reagents on the morphology of the IGSR particles was performed, as the EDS analysis was performed on IGSR simulant comprising barium nitrate, lead nitrate and antimony sulfide. Nonetheless, the intention of the study was to develop a rapid IGSR/OGSR test on the same sampling platform, allowing tandem analysis without the need to for a separate sampling platform.

In another example of research that shows promise for tandem OGSR and IGSR analysis present on SEM stubs, Black *et al.* (2017) [\[202\]](#) were able to detect NG, EC, MC DPA, and monomethylphthalate by ambient

mass spectrometry, specifically using a Direct Analysis in Real-Time (DART) ion source. Their approach appears to be both very rapid and elegantly simple. Stubs were used to collect GSR from cotton fabric, OGSR was extracted from the stub using solvent, and extracts were evaporated on the tip of a sealed glass capillary and presented to the DART-MS. While SEM-EDS was successfully used to detect IGSR on stubs used for OGSR detection, it was not the focus of the study. In particular, there was no exploration into the effects of OGSR extraction on subsequent IGSR detection capability or conversely whether exposure of stubs to the high vacuum of the SEM chamber causes sufficient loss of OGSR to render their subsequent detection impossible by DART-MS. Lennert *et al.* have also shown that it is possible to rapidly identify and classify smokeless powders using DART-MS techniques [\[61\]](#) but did not explore the compatibility of the technique with subsequent IGSR detection.

Three different protocols for interfacing SEM-EDS and UHPLC-MS/MS for GSR analysis were very recently published by Minziere *et al.* [\[205\]](#). In the first, two separate adhesive stubs were used to sequentially sample the area of interest, with each being analysed in a separate instrument. The second protocol involved a single stub, with the adhesive layer being physically cut into two subsamples, reminiscent of the strategy used by Benito *et al.* [\[129\]](#). Each of these methods had lower recovery efficiency, attributed to the effect of spreading the recovered material across two sampling surfaces. The third protocol, found to be the most effective by the authors of that publication, was to first analyse the whole stub surface by SEM-EDS in the typical manner. The carbon adhesive was then removed from the aluminium backing and sonicated in a solvent to produce an OGSR solution

An optimal solution to the problem of tandem IGSR/OGSR analysis would be to find a technique with simple preparation and fast analysis times, but with high analytical selectivity and a wider scope of detectable compounds, thus giving comprehensive OGSR data without adding large amounts of time or sample handling to the process involved in collection of IGSR data. Such a solution would allow analysts to provide rapid preliminary results to investigators and would also be a valuable capability when triaging multiple GSR samples. Those that show the presence of OGSR may be the most valuable ones to prioritise for IGSR analysis. As SEM-EDS is well established as the method of choice for IGSR analysis, an optimal tandem IGSR/OGSR approach must be compatible with SEM-EDS.

Of the OGSR recovery methods described in the current literature, the solvent droplet extraction method proposed by Black *et al.* [\[202\]](#) offers elegant simplicity and rapidity. The present study investigates the use of droplet-based stub extraction in conjunction with UHPLC-ESIMS/MS and explores its impact upon subsequent SEM-EDS examination of IGSR. As an approach to tandem analysis of OGSR and IGSR present on a single sampling device, the method described maximizes analytical results and for practical purposes preserves IGSR traces.

2.2.3 Experimental

2.2.3.1. Standards and Solvents

Reference Standards: Trinitroglycerin ($1,000 \mu\text{g mL}^{-1}$) in acetonitrile and a mixed GSR surveillance standard containing dimethylphthalate ($200 \mu\text{g mL}^{-1}$), diphenylamine ($200 \mu\text{g mL}^{-1}$), n-nitrosodiphenylamine ($75 \mu\text{g mL}^{-1}$), two isomers of nitrodiphenylamine ($50 \mu\text{g mL}^{-1}$ each) and four isomers of dinitrodiphenylamine ($50 \mu\text{g mL}^{-1}$ each) in acetonitrile were purchased from Cerilliant, *via* Sigma Aldrich, Sydney, Australia. Single standards of diphenylamine and nitrosodiphenylamine were also purchased from Sigma Aldrich, and their deuterated analogues (d_6) were purchased from CDN Isotopes *via* SciVac Vacuum Components, Sydney. Methyl- and ethyl- centralite standards (1.0 mg mL^{-1}) were purchased from Accustandard, *via* Novachem, Melbourne, Australia. Acetonitrile, acetone, methanol and dichloromethane were used as solvents in this work. All were listed as chromatography grade > 99.9% and purchased from Sigma-Aldrich.

2.2.3.2. Sample Collection

Carbon adhesive tabs affixed to aluminium SEM stubs (Pelco *via* Ted Pella Inc., USA) were used to represent a typical forensic GSR sampling device. Stubs known to be positive for GSR were collected from the hands of experienced shooters after separately firing 0.22 calibre, 0.38 calibre, 9mm, and 0.40 calibre ammunitions.

For the preliminary (IGSR) study, samples were collected from the hands of a shooter after separately firing 0.40 calibre and 0.22 calibre ammunitions. First, the volunteer thoroughly washed their hands, and a blank was collected from each hand. Specimens of 0.22LR Winchester XTR ammunition (Batch No.1DTM62) were discharged from a Smith and Wesson Model 63 revolver. Six rounds were discharged into a bullet recovery tank. Immediately following, the hands of the shooter were sampled using GSR stubs, first from the right hand, then the left. Two stubs were used for each hand; one to sample the palm, index finger, thumb and their webs and one to sample the back of the hand, index finger, thumb and their webs. Hands were dabbed on the approximately 50 times or until the adhesive lost its tackiness. This process was then repeated two more times, with hand washing between each batch of six shots, totalling 18 rounds of ammunition discharged and 12 stubs collected.

The shooter then thoroughly washed and dried their hands before a second blank sample was collected. Six rounds of 0.40 S&W Federal Premium Law Enforcement ammunition (Batch No. V42Z458) were discharged from a 0.40 calibre Smith and Wesson M&P (Military and Police) semi-automatic pistol into a bullet recovery tank. The sampling protocol and replicate procedure was then repeated as above until 18 rounds of ammunition had been discharged and 12 stubs collected.

For further (OGSR) studies, specimens of 9mm Winchester Defender ammunition (Batch No. S9MMPDB1) were discharged from a CZ-brand semi-automatic target pistol (Shadow 2 model). This pistol was thoroughly cleaned and freshly lubricated prior to use. Sets of either a single round or six rounds were discharged at a

sport shooting club's outdoor range. Immediately afterwards the hands of the shooter were sampled using a single GSR stub, first from the right hand, then the left. The hands and wrists were then thoroughly cleaned with domestic pre-moistened wipes and allowed to air-dry before continuing. This process was then repeated until 5 "single shot" (1a-e) and 4 "six shot" (6a-d) samples were collected, totalling 29 rounds of ammunition discharged. The final round of the box was disassembled, and extracts made from recovered smokeless powder for chemical comparison. Further blanks were collected periodically, to ensure that carry-over effects were not a contributing factor.

One week later, the shooter repeated the above steps using a Smith & Wesson Model 686 0.38/0.357 calibre revolver. This firearm was loaded with custom target-shooting ammunition made in-house, using a 120 grain, 0.38 calibre projectile (Westcastings, Australia) loaded with 2.3 grains of Hodgdon "Trail Boss" smokeless powder.

In order to confirm the qualitative findings, 10 mg of the smokeless powder from each ammunition was extracted in 300 µL dichloromethane as recommended by the National Center for Forensic Science at the University of Central Florida [\[209\]](#). An aliquot of these extracts was diluted 1:100 in a solution of 1 ppm *d6*-DPA in acetonitrile for instrumental analysis.

Specimens were stored at 4°C until analysis by either SEM-EDS or UHPLC-ESI-MS/MS and between analysis types. Stubs were extracted within 24 hours of collection, and extracts were analysed within eight hours of preparation.

2.2.3.3. Extraction protocol

The following extraction protocol is intended to minimise disruption to inorganic material present on the stub surface, rather than to maximise recovery of organic material. 100 µL of acetonitrile containing a deuterated internal standard (*d6*-diphenylamine, 1 ppm) was used as the extraction solvent. A pipette with disposable tip was used to apply the liquid such that it pooled on the surface of the SEM stub, which was then slightly tilted, and the plastic holder rolled gently between finger and thumb to ensure complete coverage. The solvent was allowed to interact with the surface for 30-35 seconds, and was then recovered by pipetting from the edge, to ensure that any IGSR present on the surface was not disrupted by contact with the pipette tip. Any solvent unable to be recovered from the surface of the stub was allowed to evaporate to dryness before the stubs were resealed.

Recovery tests were also performed, by depositing aliquots of target compounds onto the surface of clean stubs in the following amounts: DPA (100 ng), N-NDPA (100 ng) NO₂DPA (100 ng), MC (10 ng) EC (10 ng), AK (0.1 ng). Each test was repeated in triplicate (three separate stubs doped then extracted), then each extract analysed in triplicate.

2.2.3.4. SEM Details

Inorganic GSR analysis was conducted using an FEI Inspect F50 SEM system with EDAX elemental analysis capability. Particle identification was performed using GSR Magnum automated particle analysis software. The brightness and contrast settings of the particle analysis system were calibrated using a Au/Nb/Ge/Si/C calibration standard (Eastern Analytical). A Synthetic Particle Standard (PLANO W. Plannet GmbH, Wetzlar, Germany, SPS-5P-2a-X02-Y03) was analysed at the start and end of each run as a positive control. Further SEM operating and analysis parameters can be seen in Table 2-1. Carbon coating, a common preparatory step prior to SEM, was not applied to any of the stubs to minimise disruption of the stub surface prior to analysis.

Parameter	Setting
Accelerating Voltage	25 kV
Working Distance	10 mm
Emission Current	~110 μ A
Magnification	486 x
Min. Particle Size	0.5 μ m
Dwell Time	10 μ s

2.2.3.5. HPLC Details

Analysis of OGSR extracts was performed on a Thermo Fisher Velos Pro linear ion trap mass spectrometer interfaced to a Thermo Scientific Vanquish UHPLC using an electrospray ion source. This system allows for identification of target analytes through a combination of retention time, parent m/z isolation, and specification of molecular fragments. A 100mm x 3.0mm ACE Excel 3 Super C18 column was used, with the following solvent profile (Table 2-2) at 0.5mL min⁻¹ flow:

Minutes	10mM Aqueous Ammonium Formate	Methanol
0	50 %	50 %
6	15 %	85 %
15	15 %	85 %

A series of selected ion monitoring (SIM) channels were created using the Thermo TunePlus software, with each of the target compounds' nominal $[M+H]^+$ mass-to-charge ratio (\pm 0.5 Da) isolated for 0.010 seconds with a fragmentation energy of 35 V. A full scan for fragment ions was performed for each parent mass, rather than specifying individual target fragments. A nontargeted, full scan across the m/z range of 100 – 500 Da was also performed during the same chromatographic run. The system cycled through all the targeted m/z values approximately ten times per second. Limits of detection were calculated using a 7-point calibration series, with the area of the most abundant fragment peak as the response variable (Table 2-3).

Table 2-3: OGSR Compounds Targeted in this Study				
Compound	Protonated Parent Mass (m/z)	Fragment used for EIC Quantification (m/z)	Retention Time (min)	Instrumental LOD (ppb)
Deuterated Diphenylamine (d6-DPA)	176.1346	95	5.6	(Internal Standard)
Akardite II (AK)	227.1184	196	1.2	0.1
Methyl Centralite (MC)	241.1341	134	1.8	9
Ethyl Centralite (EC)	269.1654	148	7.6	11
Diphenylamine (DPA)	170.0970	92	5.6	96
N-Nitrosodiphenylamine (N-NDPA)	199.0871	169	3.7	9
Nitrodiphenylamine (NO ₂ .DPA)	215.0821	198	3.7	10
Dinitrodiphenylamine ((NO ₂) ₂ .DPA)	260.0671	214	6.3	Undetermined

2.2.3.6. Data Analysis

Inorganic: Particles were classified as “characteristic” of firearms origin or “consistent” with firearms origin in accordance with ASTM E1588-17 [\[112\]](#). Following the automated system’s classification, all GSR classifications were verified by an operator prior to further data treatment. Multiple hits on the same particles were excluded from further particle counts, and exemplar spectra and particle images were collected where appropriate. Particles considered ‘commonly associated’ with a firearms origin were classified by the system, but not manually reviewed.

Organic: LC-MS data files were initially processed through the software Thermo TraceFinder 4.1, with additional manual verification using XCalibur QualBrowser. Each data channel recorded by the mass spectrometer was checked for the presence of a peak at the correct retention time, corresponding to the transition of a targeted parent ion to the most abundant fragment ion. A fragment extracted ion chromatogram (EIC) was prepared from each parent ion SIM chromatogram. Peak spectra were also visually compared to positive controls.

2.2.4 Results and Discussion

2.2.4.1. Effect of solvent extraction on inorganic GSR trace detection

As the volatility of compounds likely to be found in OGSR is non-negligible [\[134, 210\]](#), it is possible that a fraction of them may be lost if stubs are exposed to the electron beam and high vacuum of the SEM used for IGSR detection prior to extraction of stubs for OGSR detection. Therefore, it was decided that extraction of OGSR should be carried out prior to exposure of the stub to SEM-EDS analysis. In practice, the most pragmatic approach may also involve initial cursory examination of the stub surface using a stereomicroscope to assess if fragments of partially burned propellant or similar are present, prior to a final decision on analysis order.

In order to test whether a solvent extraction process presents an undue risk of altering the stub surface or dislodging IGSR, four stubs collected from a volunteer's hands immediately post-firing were first examined by SEM-EDS, then extracted with solvent and subsequently re-analysed using SEM-EDS. Regarding their gross features, no damage to the adhesive surfaces was apparent by SEM, and surface debris (presumably dust, hairs, skin cells *etc.*) were still clearly present and in their original location. Of the four stubs examined only one displayed any indication of change; a pitted feature on the stub as manufactured has been occluded after extraction (Figure 2-1). The mechanism of this change is unknown, but the overall analysis was not impacted. Individual particles could also be relocated in their initial positions following the extraction procedure (Figure 2-2 and Figure 2-3).

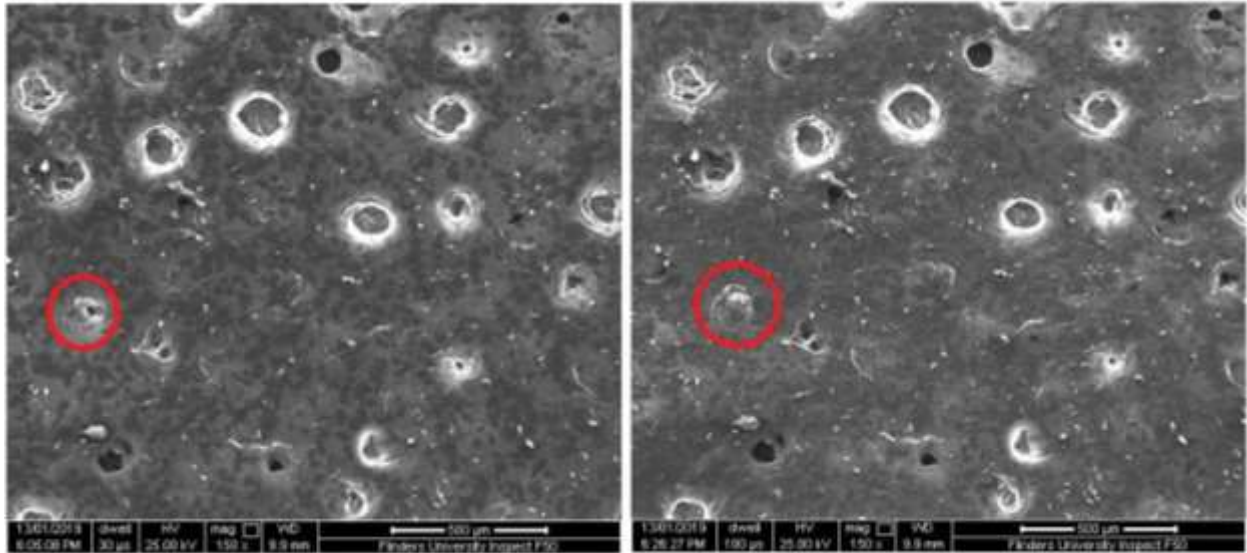


Figure 2-1: Secondary Electron image of a hand sampling stub, both pre-solvent (left) and post-solvent (right). Red circle indicates a slight visible change to the stub, potentially attributable to solvent contact.

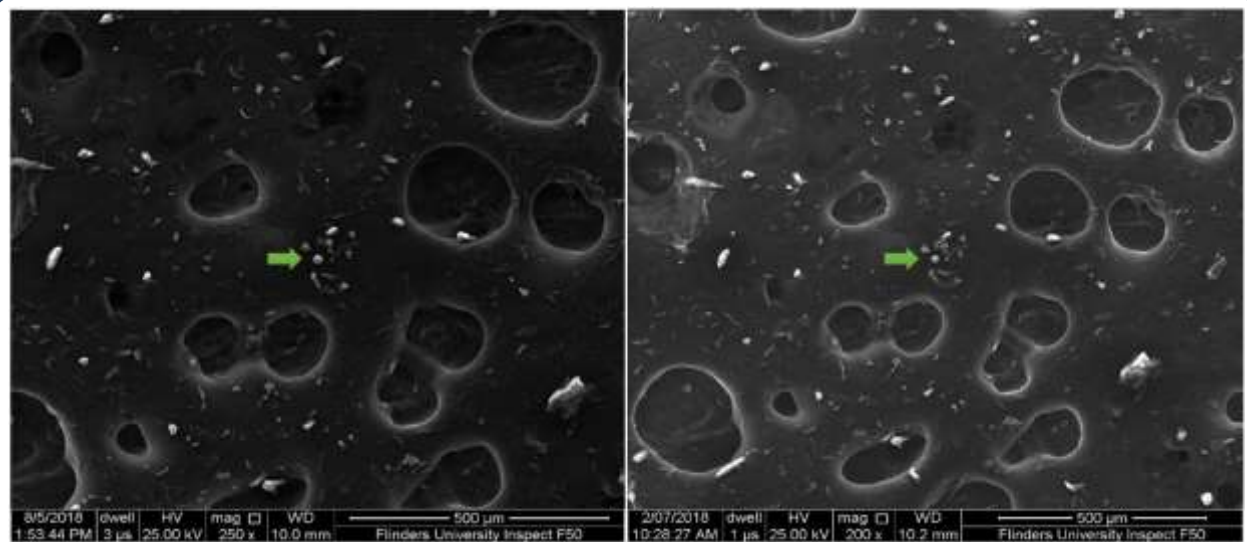


Figure 2-2: Particle from 0.40 calibre ammunition, collected on the right hand of a volunteer shooter, pre-solvent (left) and post-solvent (right).

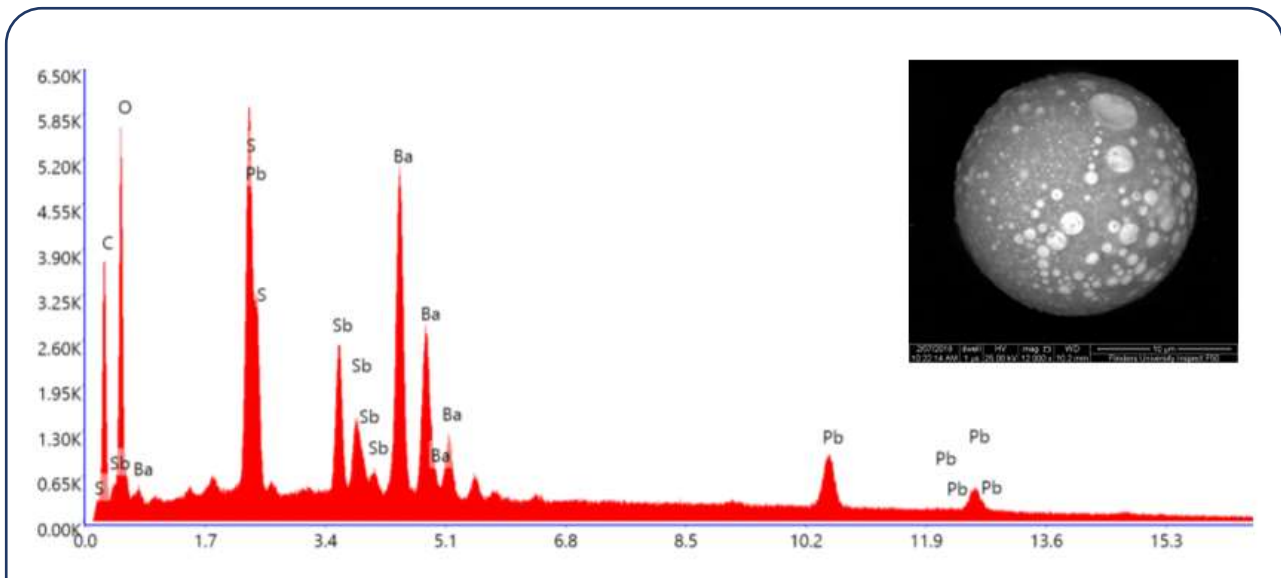


Figure 2-3: Characteristic PbSbBa particle (approx. 18 μm diameter) originating from 0.40 calibre ammunition, detected on the sampling stub following organic extraction. This is the same particle displayed in Figure 2-2.

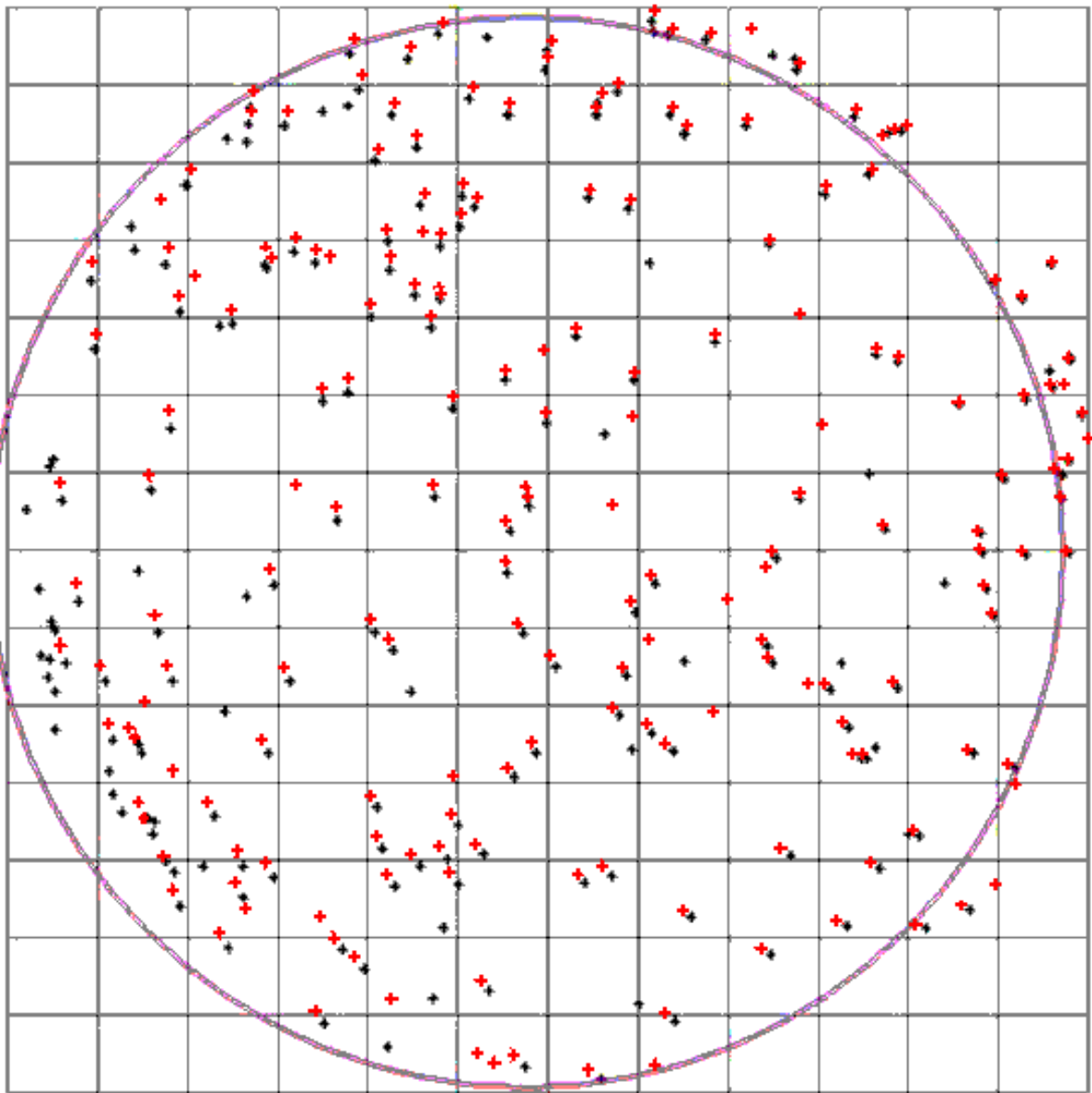
Automated particle analysis software (GSR Magnum) results were compared pre- and post- solvent extraction. Stubs had heavy particle loadings due to the fact these samples were collected moments after firearm discharge, and as a consequence an 8 hour search time limit was applied to each stub rather than searching their entire surface area. Despite this, in some cases more than 5,000 total hits and several hundred “characteristic” particles were logged on a single stub, and therefore a good representative sub-sample of the expected residue present on the stub was obtained. Typical examples of pre- and post-solvent extraction particle counts for 0.22 and 0.40 calibre ammunition types can be seen in Tables Table 2-4 and Table 2-5. Direct comparison of the particle counts shows there is reasonable concordance between the number of particles present before and after solvent extraction for all stubs examined. The differences between particle numbers observed in both tables are consistent with instrument variability for classifying composition of particles sub- $0.5\mu\text{m}$ in size. This accounts for the apparent reduction of particles in specific categories while the total particle counts increased. Even if taking a conservative interpretation that application of solvent, (or additional manipulation of the stub) may result in some particle loss, there is a net overall benefit of significantly strengthening the GSR evidence obtained by including OGSR data.

Table 2-4: Pre- and post- solvent particle counts for 0.22 calibre ammunition, from the dominant hand of the shooter		
Composition	Pre-solvent count	Post-solvent count
PbBaSb	38	40
BaSb	45	45
PbSb	70	63
BaCaSi	4	4
BaAl	18	19
Pb	523	626
Total particle count	3529	3650

Table 2-5: Pre- and post- solvent particle counts for 0.40 calibre ammunition, from the dominant hand of the shooter		
Composition	Pre-solvent count	Post-solvent count
PbBaSb	341	256
BaSb	439	429
PbSb	191	245
BaCaSi	7	10
BaAl	2	6
Pb	2075	1268
Total particle count	4586	5320

In addition to counting the raw number of particles present before and after extraction, their locations were also recorded, further confirming that solvent extraction potentially has minimal impact on IGSR collected with stubs. This can be seen in the overlaid particle map of Figure 2-4, which for brevity depicts only those particles classified as “characteristic” under the ASTM definition that were present on a typical stub. The majority of particles are clearly being re-detected in their previous positions (note that a minor image off-set was added post analysis for visual clarity in Figure 2-4). Several specific GSR particles were manually reacquired and examined by the analysts to determine whether solvent extraction caused changes to the morphology or composition of particles (e.g. Figure 2-3). Changes were not apparent and the spheroidal particles continued to cover a broad size distribution relevant to GSR (>1 µm to tens of µm).

These findings demonstrate that the frugal solvent extraction process proposed by Black *et al.* seems to have minor impact, if any, upon the IGSR traces present on GSR stubs [202]. This is in contrast to methods of OGSR extraction that involve sonication of the entire stub in solvent in order to extract OGSR followed by collection of IGSR by filtration, which may present the risk of particle loss and in any event are somewhat tedious.



Post-solvent
Pre-solvent

Figure 2-4: “Characteristic” particle distribution map of sampling stub from the shooter's left hand following discharge of 6x 0.22LR rounds from a revolver. Pre-solvent (black) and Post-solvent (red, offset)

2.2.4.2. Organic GSR Compounds

Once the use of solvent extraction of OGSR from stubs was found to be compatible with subsequent SEM-EDS analysis of IGSR, the efficacy this approach for OGSR analysis was evaluated. The compounds targeted for detection by UHPLC-ESI-MS/MS in this set of experiments were AK, MC, EC, DPA, N-NDPA, NO₂.DPA and (NO₂)₂.DPA. Figure 2-5 displays overlaid extracted-ion chromatograms obtained using individual reference standards. While two compounds (N-NDPA and NO₂.DPA) co-elute, they are easily distinguishable by their mass spectra.

Target compounds from standard solutions were deposited onto the surface of clean stubs and allowed to dry. Recovery efficiencies were in the range of 50-100% when each deposit was extracted immediately after drying, with results shown in Figure 2-6. Contributing factors to these losses were likely to include a combination of evaporative loss of compounds along with the carrier solvent, and absorption into the sponge-like carbon substrate of the stub. The long-term stability of organic material on the stub surface was not tested, as standards in liquid form were considered to be poor substitutes for solid particles of partially burned propellant powder. They do however have one advantage; their initial deposition mass can be controlled, which is not possible for true GSR.

Once conditions to detect OGSR were determined, test firings and recovery of GSR from a volunteer's hands using standard adhesive stubs were carried out. All 9 specimens collected after discharge of a 9mm semi-automatic returned positive results, and furthermore the compounds detected remained consistent across each extract. The compounds detected were AK, EC, DPA, N-NDPA and NO₂.DPA. Upon initial observation the presence of such a large variety of stabilisers within a single residue sample seemed unlikely, and either contamination or a firearm-memory effect was suspected. However, analysis of powder taken from a disassembled round of the same batch of ammunition ruled out these causes as all these compounds were also present in the powder (see Table 2-6). Further investigation of literature suggests that the stabiliser akardite forms diphenylamine as a decomposition product [\[91, 211, 212\]](#). It is therefore proposed that the smokeless powder in the ammunition may have either initially contained DPA as well as AK and EC, or DPA may have formed in-situ as the powder aged. To the authors' knowledge, this has not been reported previously for recovered post-shooting residues and further investigation into the aging of AK-stabilised propellants is warranted.

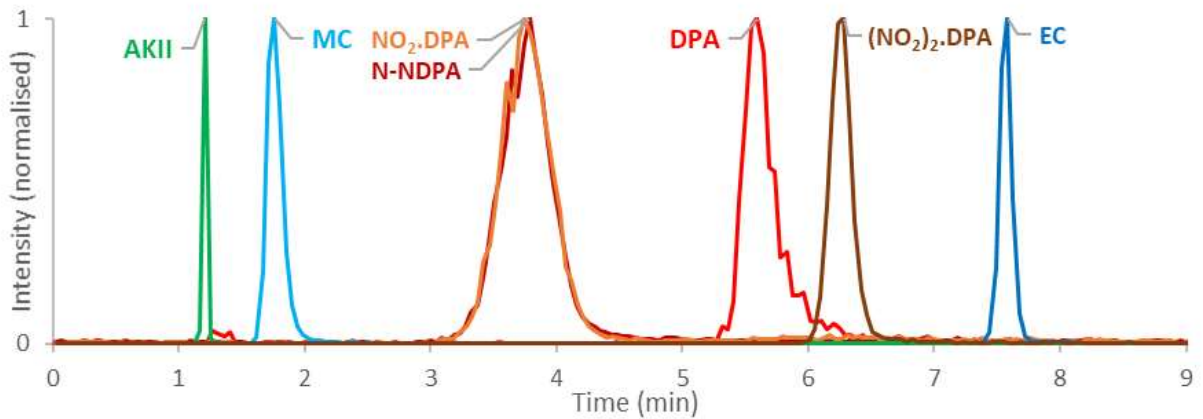


Figure 2-5: “Characteristic” particle distribution map of sampling stub from the shooter's left hand following discharge of 6x 0.22LR rounds from a revolver. Pre-solvent (black) and Post-solvent (red, offset)

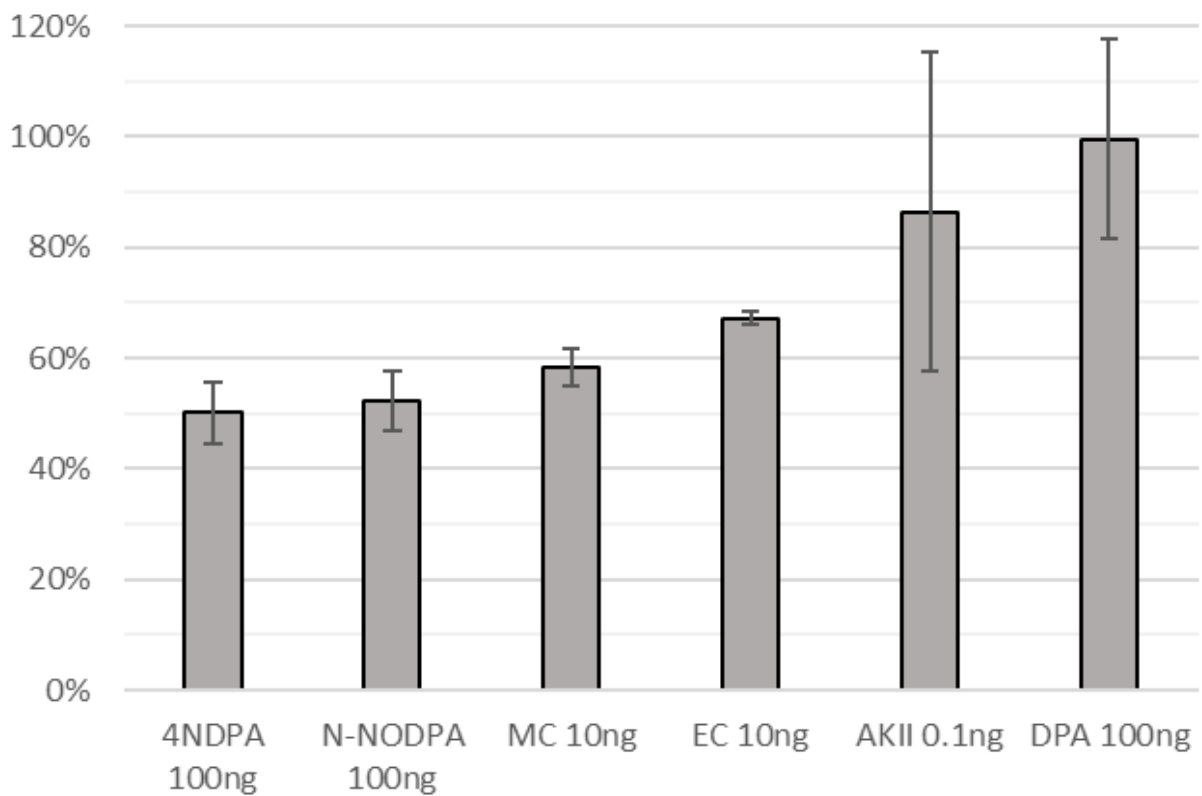


Figure 2-6: Mean recovery values from three stub surfaces, each doped with a selection of OGSR compounds at different concentrations. Error bars represent 3 standard deviations.

Results from the 9 0.38 calibre revolver samples were less consistent. Of the single-shot specimens, 1 returned a negative result for all target compounds, 3 returned a positive result for DPA only, and 1 returned a positive result for DPA, N-NDPA, and NO₂.DPA. Of the six-shot specimens, 1 returned a negative result, 1 returned a positive result for DPA only, and 2 returned a positive result for DPA, N-NDPA, and NO₂.DPA. Results from propellant recovered from unfired 0.38 calibre ammunition, along with the hand-stub extract showing the greatest number of compounds, are summarized in Table 2-6. Several factors may have contributed to the poorer detection rate of the six shot specimens. Firstly, the ammunition was hand loaded for the specific purpose of accurate competition shooting, with a lighter-than-typical powder load to reduce recoil. This smaller amount of initial material may have resulted in a lesser amount of residue, which dropped below the analytical capability of the mass spectrometer after recovery. The comparatively open construction of the revolver-style pistol may have also contributed; while this is generally expected to create a larger plume of residue, it may disperse material more widely and forward of the shooter’s hands. Video recordings of the shooting session showed a visible plume drifting upwards and to the left of the shooter as the rounds exited the barrel, due to natural air movement around the outdoor range facilities at the point of collection. As the variability in GSR deposition is widely acknowledged amongst analysts, the additional analytical step was still considered to be successful and beneficial as a majority of collected specimens returned a positive result for one or more stabiliser compounds.

As qualitative OGSR results provide the information required to supplement IGSR analysis, quantitative analysis was not performed on any shooting specimen for the purpose of these proof-of-concept demonstrations. For both firearm types, the chromatograms resulting from stub extracts correlated with the extracts prepared from unfired powder. It also provides support for the potential to discriminate residues by composition, as has been previously reported for intact smokeless powders [\[61\]](#).

Table 2-6: Compounds detected in residue <i>via</i> stub collection after firing two separate firearms, compared to the propellant powders recovered from the same lot of ammunition								
Specimen		AK	EC	MC	DPA	N-NDPA	NO ₂ DPA	(NO ₂) ₂ DPA
Winchester "Defender" 9 mm	Unfired Powder	√	√	x	√	√	√	x
	Recovered Residue	√	√	x	√	√	√	x
Hodgdon "Trail Boss" 0.38 cal	Unfired Powder	x	x	x	√	√	√	x
	Recovered Residue	x	x	x	√	√	√	x

2.2.5 Conclusions

A method for the recovery of OGSR from industry-standard SEM stubs that can integrate unobtrusively with current practices for the detection of IGSR has been explored; that method involves a rapid and simple extraction of OGSR from the stub using a minimal amount of solvent.

In a small trial of stubs collected from the hands of a shooter it was determined that there was practically no loss or movement of IGSR particles brought about by the solvent extraction process nor did it impede IGSR analysis. Although the solvent was only allowed to contact the stub for less than 1 minute, sufficient OGSR was extracted for successful detection using LC-MS. With further development, a tandem approach such as this that does not come with a significant penalty from effort expended in GSR case investigations or require a shift in IGSR examination methodology will allow forensic labs to maximize the probative value of GSR examination, especially in those cases where IGSR results are equivocal, such as when heavy metal-free ammunition is involved or when characteristic particles are not detected.

Logically, solvent extraction of OGSR could be carried out either before or after attempts to detect IGSR, but our research only focussed on extraction of OGSR prior to IGSR analysis. That decision was made for three main reasons: it was felt that the high vacuum of the SEM may cause loss of OGSR traces, thus compromising their detection; as some laboratories routinely carbon-coat specimens prior to IGSR examination additional research into the impacts of the coating process would have been required; and extraction and analysis of OGSR prior to IGSR examination was expected to offer additional benefits to GSR examination. The latter reason was of particular importance to our research. For the approach investigated, the entire extraction and LC-MS process could be carried out in much less than 1 hour; this is significantly shorter than the time required for examination of stubs for IGSR, which can take many hours. With further development, an effective tandem approach involving extraction of OGSR as the first step in GSR case investigation may add value to operations. In a typical shooting case where numerous stubs are collected from one or more persons of interest, the application of a rapid solvent extraction and LC-MS method would allow investigators to be advised within a relatively short time as to whether the person of interest, or whom of the persons of interest, may have been associated in some way with the shooting. Furthermore, the availability of reliable OGSR results could be valuable in triage of items for IGSR examination. In the specific case mentioned above, the availability of OGSR results will assist in the identification of stubs that should be prioritized for IGSR analysis in order to provide rapid confirmative results to investigators. In a more general triage sense with regards to laboratory GSR case management, the availability of reliable OGSR guidance as to which of the stubs on-hand show positive results can be used to inform decisions as to which stubs warrant valuable SEM-EDS analysis time.

In the experiments described here, GSR collection was carried out immediately after test firings. This was carried out in order to maximize the number of IGSR particles collected and maximize any particle losses

arising from solvent extraction. However, this would also maximize OGSR traces collected, possibly to levels beyond those collected from typical shooting incidents. In order to determine whether the process described really can contribute effectively to triage and investigative support, further experiments involving realistic delays between firearm discharge and trace collection are warranted.

2.2.6 Acknowledgements

Research relating to this article was supported by a Premier's Research and Industry Fund grant provided by the South Australian Government Department of Further Education, Employment, Science and Technology and the Ross Vining Research Fund, which is administered by Forensic Science SA.

The authors acknowledge the expertise, equipment, and support provided by the Australian Microscopy and Microanalysis Research Facility (AMMRF), the Australian National Fabrication Facility (ANFF), and ChemCentre Western Australia (CCWA).

We are extremely grateful for the support provided to this research by SA Police, and in particular Brevet Sergeant Andrew Plummer, PhD.

We also thank the Port Bouvard Pistol & Small Bore Rifle Club and their members for providing practical assistance.

2.3 Further Refinement & Investigation of Efficacy

After initial proof-of-concept trials were published, several further experiments were conducted. These were intended to both refine technical aspects of the chosen analytical process, and also to generate GSR specimens that more closely reflect those that could be encountered as real-world, forensically relevant traces. The trials covered the following issues:

1. Adjustments were made to LC-MS run settings
2. GSR specimens were collected from a broader collection of substrates (that may be considered more challenging)
3. Specimens were left for varying periods of time after being exposed to GSR, and were then sampled later

2.3.1 Adjusted LC-MS instrumental settings

Analysis of the organic components of recovered GSRs was in large part conducted using a LC-MS system consisting of a Thermo Scientific Vanquish UHPLC interfaced to a Velos Pro linear ion trap mass spectrometer using a heated electrospray ion source. Following a course of routine maintenance, the opportunity arose to further refine several parameters on the instrument in question. Where not explicitly specified otherwise, the conditions summarised in Table 2-7 should be assumed throughout this thesis. The most consequential of the changes involved the mobile-phase profile used for LC elution, with an increase to the proportion of

methanol at the end of each run. This meant that every run ended with the same proportions of each solvent used for the start of the next run. The overall chromatographic runtime was also reduced from 15 minutes to 12 minutes per sample. Compared to previous settings, these changes resulted in sharper elution peaks, better separation between the of nitroso- and nitro- derivatives of DPA (Figure 2-7, compared to Figure 2-5), and also eliminated a minor creep in elution time previously seen for all compounds (~2 seconds per run).

Table 2-7: HPLC-MS Setup and operation			
Component	Setting		
Column:	100 mm x 3.0 mm ACE Excel 3 Super C18		
Total Flow Rate:	0.5 mL min ⁻¹		
HESI Temp:	350° C		
MS Transfer Capillary Temp:	275° C		
In-source Fragmentation:	OFF		
MSn Normalized Collision Energy:	35		
Solvent Profile	Minutes	10 mm Aqueous Ammonium Formate	Chromatography-Grade Methanol
	0	40%	60%
	1	15%	85%
	10	15%	85%
	12	40%	60%

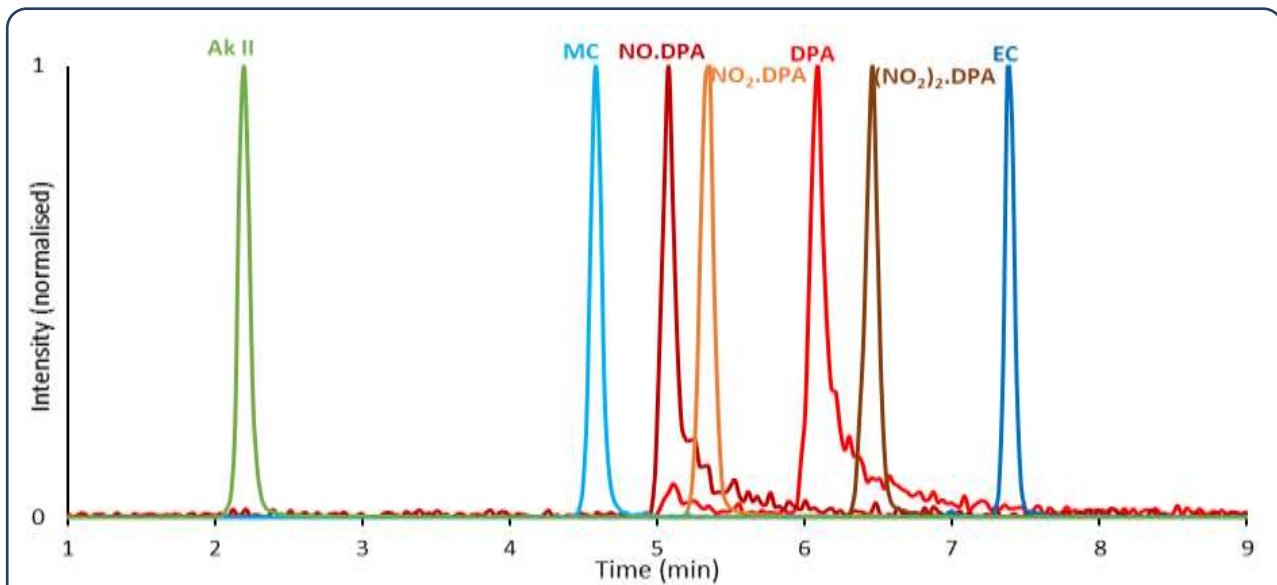


Figure 2-7: Overlaid extracted ion chromatograms of OGSR standards, after additional refinement of solvent profiles.

2.3.2 GSR collected from surfaces other than human hand skin

Human tissue is a highly relevant substrate in relation to recovery of GSR traces. For instance, various methods of GSR detection can be applied to a deceased victim to inform scene reconstruction [108, 213-215]. Additionally, when an individual is suspected of involvement with a shooting, their hands will often be the first site from which samples are sought -- particularly when the time interval between shooting and sampling events is brief. This application for the proposed tandem OGSR/IGSR analysis procedure was demonstrated in the preceding sections.

However, GSR traces may be co-mingled with any number of environmental substances that could impede physical collection by an adhesive stub, or otherwise obstruct detection by chemical means. There is a significant body of research on the effect of textiles on recovered GSR, as "*most gunshot entrance sites on human victims are localized in clothed body regions*" (Pircher *et al.* 2019) [216]. GSR may also be retained on shooters' clothing for longer than their hands [23]. As a general disclaimer, the enormous variation in measured OGSR under controlled conditions has by necessity led to reporting of observed trends in broad, intuitive terms rather than strongly supporting quantitative models. A distinction is also drawn here between analyses for the purpose of visualisation, and more binary assessments as to the presence of specific OGSR markers.

Instrumental techniques of distance determination *via* GSR on textiles were reviewed by Lopez-Lopez & Garcia-Ruiz in 2014 [213]. Hofstetter *et al.* (2017) offer the most direct comparison of textiles with skin surfaces sampled under similar conditions. Among other findings, they showed that a greater amount of OGSR was recovered from gloves and sleeves than bare hands and bare forearms respectively [23]. Gassner *et al.* (2016) report being able to detect OGSR traces on a shooter's sleeve (cotton-polyester blend) at least two hours post-shooting using adhesive stubs and UHPLC triple-quadrupole MS [18]. Black *et al.* (2017) instead used similar stubs to recover OGSR from a cotton target [202]. Most recently Fabbris *et al.* (2020) used a combination of optical microscopy and stylus profilometry to characterise the morphology of six different textile targets and thus propose a trend to their IGSR retention capability. They found that IGSR was retained in the order of elastane > linen > cotton > polyester ~viscose ~ silk, ascribed to a combination of greater weave density and thread thickness helping to trap particulate GSR [217].

Aside from textiles, other substances have previously been identified as potentially problematic for OGSR detection. Early colourimetric methods such as the dermal-nitrate paraffin test were insufficiently specific to avoid false positives from either fertilisers or urine [218]. There has also been at least one reported case of a POI attempting to remove GSR from their hands *via* urination, more hygienic methods of hand-washing being denied to them [219]. Blood is likely to be present in large quantities at shooting scenes, potentially hindering location of probative GSR traces or interfering with analysis [216, 220, 221]. Finally, Zhao *et al.* claimed in 2008 to

be able to detect centralites directly on hands contaminated with dust, milk, soda or juice using DESI-MS, although no example data were shown in that publication [\[98\]](#).

In order to demonstrate some level of robustness of the method towards “dirty” or difficult specimens, GSR was deposited onto a collection of substrates; namely common textiles and greaseproof paper onto which a variety of liquids had been deposited. The GSR specimens were generated by discharging a firearm through each target at a muzzle-to-target distance of 0.75m. The targets were collected and later sampled with adhesive stubs. The short distance was chosen to ensure a large amount of material was present, such that the target’s composition might have more impact on the observed GSR traces rather than variations in its travel across the intervening distance.

2.3.2.1. Materials

A selection of textiles were purchased from online crafting suppliers and used with no further washing or preparation. These included tanned leather, nylon canvas, cotton denim, felted wool and a polyester fabric. A synthetic urine substitute (Surine™) was purchased from Cerilliant Corporation, Texas. Mixed multi-donor blood that had exceeded its permitted storage time for medical use was donated as a laboratory matrix from the Australian Red Cross. An ethanol-based hand sanitiser (Dettol “Healthy Touch”) was purchased from a local pharmacy. Orange juice was applied directly from a fresh fruit.

2.3.2.2. Method

Tests using live ammunition were conducted at a private, outdoor, recreational shooting range. Three square pieces (15cm x 15cm) of each target material listed in section 2.3.2.1 were prepared and mounted on paper backing. Liquids were applied to several by means of a moistened cotton ball and allowed to air-dry. Each was sampled with an adhesive swab that was then extracted for potential OGSR interferants; none caused a false positive by LC-MS. They were then individually clipped onto a corrugated plastic holder prior to each replicate, with the centre of the target approximately level with the shooters eyeline (Figure 2-8). A CZ (Ceská Zbrojovka) branded, Shadow 2 model, 9mm semi-automatic pistol was cleaned and lubricated immediately prior to testing. It was then loaded with a single round of Winchester-branded 147 grain 9mm luger jacketed hollow point ammunition. The shooter took up position with the muzzle of the firearm level at a pre-measured mark 0.75m from the target, fired, and then the target was recovered. Each was placed into a separate plastic sleeve and transported away from the range for sampling. Adhesive stubs (Pelco/Ted Pella) were used to collect GSR samples with approximately 100 dabbing motions, avoiding the obvious bullet-wipe in the immediate vicinity of the hole made by the projectile.

The surfaces were stubbed approximately 8 hours after the first shots were fired. 24 hours later each stub was extracted for 1 minute with a solution of 100 uL of 1ppm d6 diphenylamine in acetonitrile. These extracts were analysed by LC-MS as described previously.



Figure 2-8: Interchangeable target setup, here holding a blood-smeared paper substrate

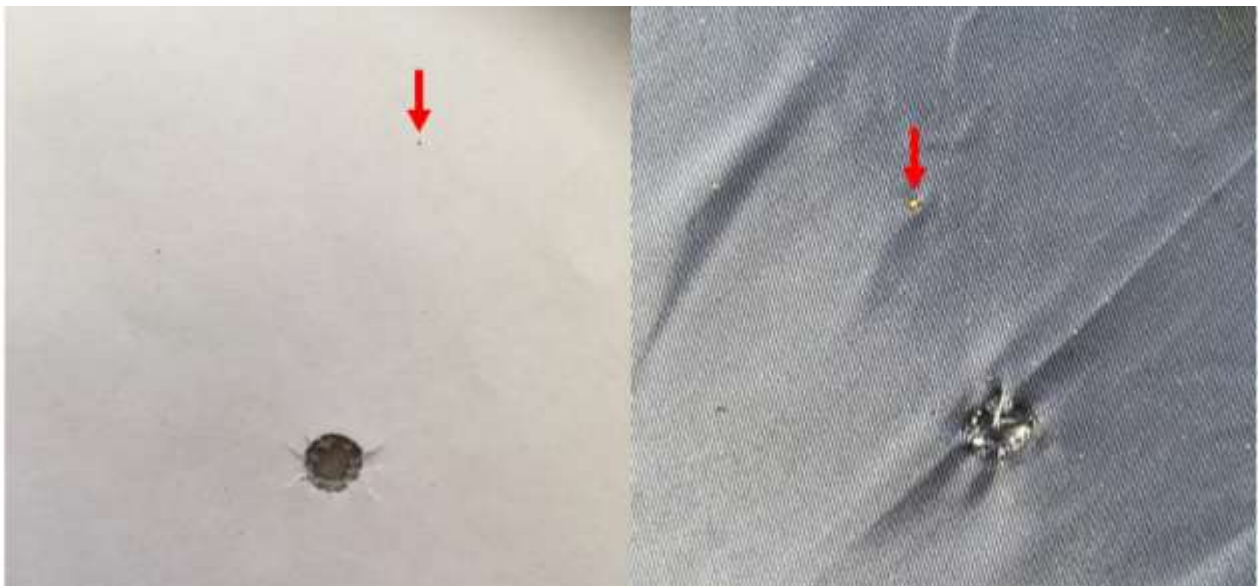


**Figure 2-9: (left) Plain paper target displaying presence of bullet wipe and dark GSR material.
(right) Polyester target showing paler, less burned propellant pieces**

2.3.2.3. Results

Fine black sooty residue was visibly dispersed on the surface of many of the materials tested, along with a darkened outline of “bullet wipe” in the immediate vicinity of the projectiles’ path (Figure 2-9, left). Some targets, notably the polyester and nylon textiles, also had larger pale- or yellow- coloured spherical pieces superficially embedded into them (Figure 2-9, right). These particles are assumed to be unburned propellant powder, and extracts prepared from those stubs were later found to have a higher concentration of stabiliser compounds compared to substrates with less visible GSR. Unsurprisingly it was also noted that adhesive stubs could be overloaded by extraneous material before the entire surface was sampled – this was most noticeable on the target made of felted wool.

Upon analysis by LC-MS, all target samples returned indications of multiple stabiliser compounds and thus were easily distinguishable from stubs taken from initial backgrounds. There was substantial variation in the measured peak areas when comparing the same compound on different replicates of the same substrate type. While in some instances the three measurements made on the same surface type were similar, on other sets of identical targets the highest recorded amount of a compound could be 2-4 times the magnitude of the lowest recorded amount. This was expected due to the well-known variability in GSR deposition, coupled with the effects of a multi-stage sampling and extraction process. Nonetheless, there was a general trend that could be described for the effect of target material on the measured GSR. The perforated targets underwent some degree of handling before sampling - removal from the support clips and placement into plastic sleeves for preservation. Greater amounts of OGSR were measured from woven textiles, with the porous and more flexible substrates appearing to trap both the burned and unburned propellant particles and retain them throughout transport. The liquid-doped paper targets bore lesser amounts of GSR as particles were less likely to be retained on the smoother, less yielding surface. The least GSR was measured on pieces of tanned leather, the least flexible substrate tested and the only non-woven garment material.

The concentrations of each stabiliser in the extract solutions were calculated using external calibration curves, with the average value summarising the three replicates for each target material displayed in Figure 2-10. These values should be considered indicative only, as significant extrapolation above the upper bound of the calibration range was required. However, it appeared that diphenylamine, *n*-nitrosodiphenylamine and akardite were present at the greatest concentrations. There was then a noticeable step-down to the concentrations of ethyl centralite and nitro-diphenylamine. Chromatographic peaks for dinitro-diphenylamine were intermittently observed across the sample set, but were barely above instrumental noise level. No peaks corresponding to methyl centralite were observed.

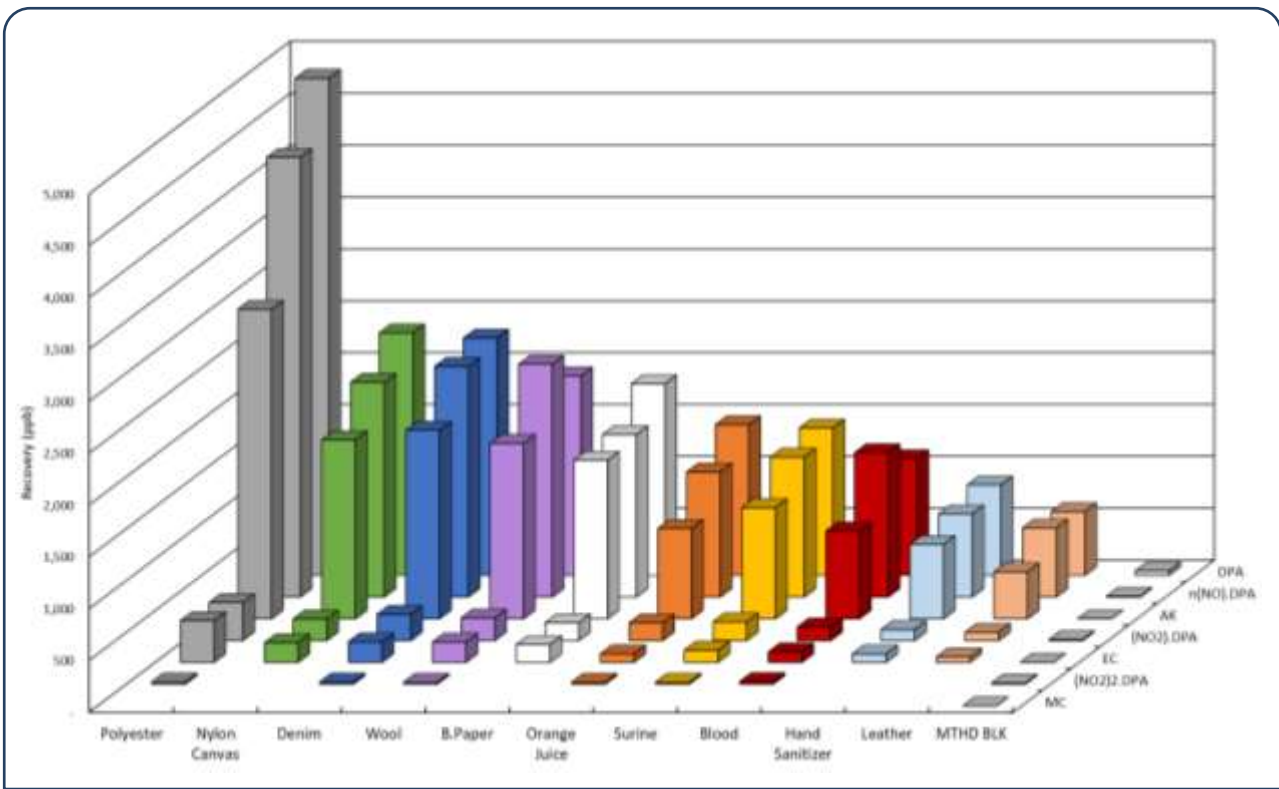


Figure 2-10: Comparison of OGSR recovered from different substrates, including textiles and grease-proof paper swabbed with various liquids.

This test showed that OGSR can be recovered from underlying surfaces that are not “clean” using adhesive stubs, without causing undue risk of either false positive or false negative results. This would present an improvement on the specificity of commonly applied chemographic tests such as the modified Griess Test, although does not replace the latter’s ability to visualize dispersion of GSR across the surface. It remains essential to collect appropriate case-specific reference samples to control for as many environmental factors as possible.

2.3.3 Testing of specimens with delay between GSR exposure and sampling

Experiments on the viability of stub-extraction for tandem OGSR-IGSR analysis described in section 2.2 involved collecting samples from shooters’ hands immediately subsequent to discharging firearms. This is unlikely to occur in the context of a forensic investigation, as identification and apprehension of persons of interest can take some time. Therefore, questions were raised about the effectiveness of the proposed method under more challenging but realistic circumstances. There is a growing collection of studies on the rate of OGSR loss from hands, with prevailing advice suggesting sample collection within 4 hours offers the greatest chance of successful detection. This appears to stem partially from early results of analysis by ion-mobility spectrometry, and also because it is in agreement with IGSR persistence studies [21, 27, 28, 135]. The model put forward by Moran & Bell in 2014 favours evaporation from, and absorption into, skin as major drivers of OGSR loss [24]. Conversely, evidence has been shown by Gassner, Maitre and colleagues using more sensitive HPLC-MS instrumentation that secondary transfer of OGSR does occur [26, 30]. This may be linked to

levels of physical activity, as shown when comparing samples taken from the dominant and nondominant hands after the same firing event [208]. These later studies also support the potential for persistence greater than 4 hours, absent deliberate countermeasures, as a high proportion of specimens analysed at that time interval still returned a “positive” designation [31]. Zhao *et al.* have even reported that when 240 ng of MC standard was applied to human hands, it could still be detected using DESI-MS up to 12 hours later, or after the subject washed their hands six times [98].

The presumption that rate-of-loss appears to be linked to activity level presents difficulties for direct comparison in controlled experiments. To alleviate both logistical challenges and the unpredictable effects of physical activity, a surrogate hand-sampling platform was utilized. Previous research suggests that polydimethyl siloxane (PDMS, or silicone) membranes might be suitable replacements for human skin in pharmaceutical trials as they can mimic the absorption of lipophilic compounds. Moran and Bell used thin PDMS membranes to model the rate at which stabilisers could be absorbed into skin, finding the “steady state flux” (J_{ss}) rate, measured in $\text{mg cm}^{-2} \text{h}^{-1}$, of DPA (8.3), EC (3.8) and 4NDPA (9.2) [21, 28]. The use of silicone wristbands as personal OGSR exposure monitors has also been suggested in literature, but the application was not investigated in a manner consistent with likely forensic scenarios [222]. A similar approach was used here, with sections of PDMS polymer used as collection patches affixed directly to the shooter’s hands in the vicinity of the firearm’s ejection port. In this way GSR could be deposited onto the polymer in the same manner as would be expected under normal shooting conditions, with evaporative and absorptive losses potentially occurring over time. Conversely, physical activity of the patch was more restricted and more consistent across specimens compared to natural hand movement.

2.3.3.1. Method:

Thirty collection patches (5 cm x 10 cm) were cut from a larger sheet of 1mm thick silicone rubber (purchased online from Gecko Optical) with protective backing on both sides. Stub extracts were taken to check that no compounds inherent in the product caused a false positive for targeted organic smokeless powder stabilisers. A single patch was affixed to the upper portion of the shooter’s gloved right hand with double sided tape (Figure 2-11). The protective backing was then removed from the exposed outer face of the patch, and the shooter discharged a single round from a “CZ Shadow 2” 9 mm semi-automatic pistol. The patch was removed, then placed in a covered but non-airtight aluminium tray stored outside for a prescribed time period. Triplicate specimens were stored together and sampled with adhesive stubs after 1, 2, 3, 4, 5, 6, 8, 12 and 24 hour delays respectively. Each stub was extracted with 100 μL of acetonitrile as previously described, approximately 48 hours after the shots were fired. The extracts were concentrated under nitrogen and reconstituted in 10 μL of a solution containing 1 ppm *d*6DPA in acetonitrile for analysis by LC-MS. Three stubs were then selected for carbon-coating and SEM-EDS analysis (The first replicates left for 4 hrs, 12 hrs & 24 hrs respectively). In the interest of time, the SEM search function was limited to finding 50 particles identified to contain Pb, Ba and Sb simultaneously.



Figure 2-11: Image showing representative PDMS collection patch and their orientation relative to firearm (slide has been manually retracted).

2.3.4 Results

Specimens were designated positive when LC-MS peaks were present for DPA, NO₂.DPA, Ak and EC simultaneously. Under this definition, at least one replicate from every time point returned a positive finding for smokeless powder stabilisers, even up to 24 hours post-firing (Table 2-8). A more lenient definition requiring the presence of fewer compounds increases the count for most time intervals – see Appendix 2-1.

Table 2-8: Replicates showing detectable amounts of <u>all</u> OGSR markers										
Time (hrs)	0	1	2	3	4	5	6	8	12	24
# Positive / Replicates	3/3	2/3	1/3	3/3	1/3	2/3	3/3	1/3	2/3	2/3

On a basic level, these findings agree with literature in showing that silicone patches are a useful tool that can be applied when studying OGSR [21, 28, 222]. More conceptually it offers evidence that the proposed sampling method (using adhesive stubs and then extracting them) can be used to detect OGSR after realistic time-delays. However, there was significant variation both between the number of compounds and the amount of each compound detected when comparing between replicates of the same time point. This is conveyed by Figure 2-12, where the response variable (chromatographic peak area) has been normalized as following:

$$Response = \frac{Peak Area_{Sample} - (Mean Peak Area_{Blank} + 3 \times STD DEV_{Blank})}{Peak Area_{d6DPA (I.S.)}}$$

The variability was such that there was only a weak correlation between increasing time-to-sample-collection and decreasing signal intensity.

Data were also collected for inorganic GSR particles deposited onto the PDMS collection surfaces. The mechanism for loss of particulates is presumed to be influenced by physical activity; the particles themselves are considered to be chemically stable, and resistant to both evaporation and skin absorption, under the conditions likely to be relevant to sample collection from hands. Therefore a thorough investigation of particle loading vs. time was not conducted under the contrived low-activity conditions of this test. However the results presented in Table 2-9 firstly support the prior assertion that detection and analysis of inorganic GSR *via* SEM-EDS can proceed subsequent to solvent extraction. The same results also demonstrate that inorganic primer residue will settle onto PDMS collection surfaces and be retained for some time, and thus the material may be a suitable surface for use in other experiments.

Table 2-9: IGSR particles found on PDMS patches				
Stub Collection Interval (hr)	Total particles found	“Characteristic” Particles found	Search Duration (min)	Amount of stub surface searched (%)
4	84	50	9.4	1.9
12	86	50	10.8	2.6
24	182	50	61.3	25.6

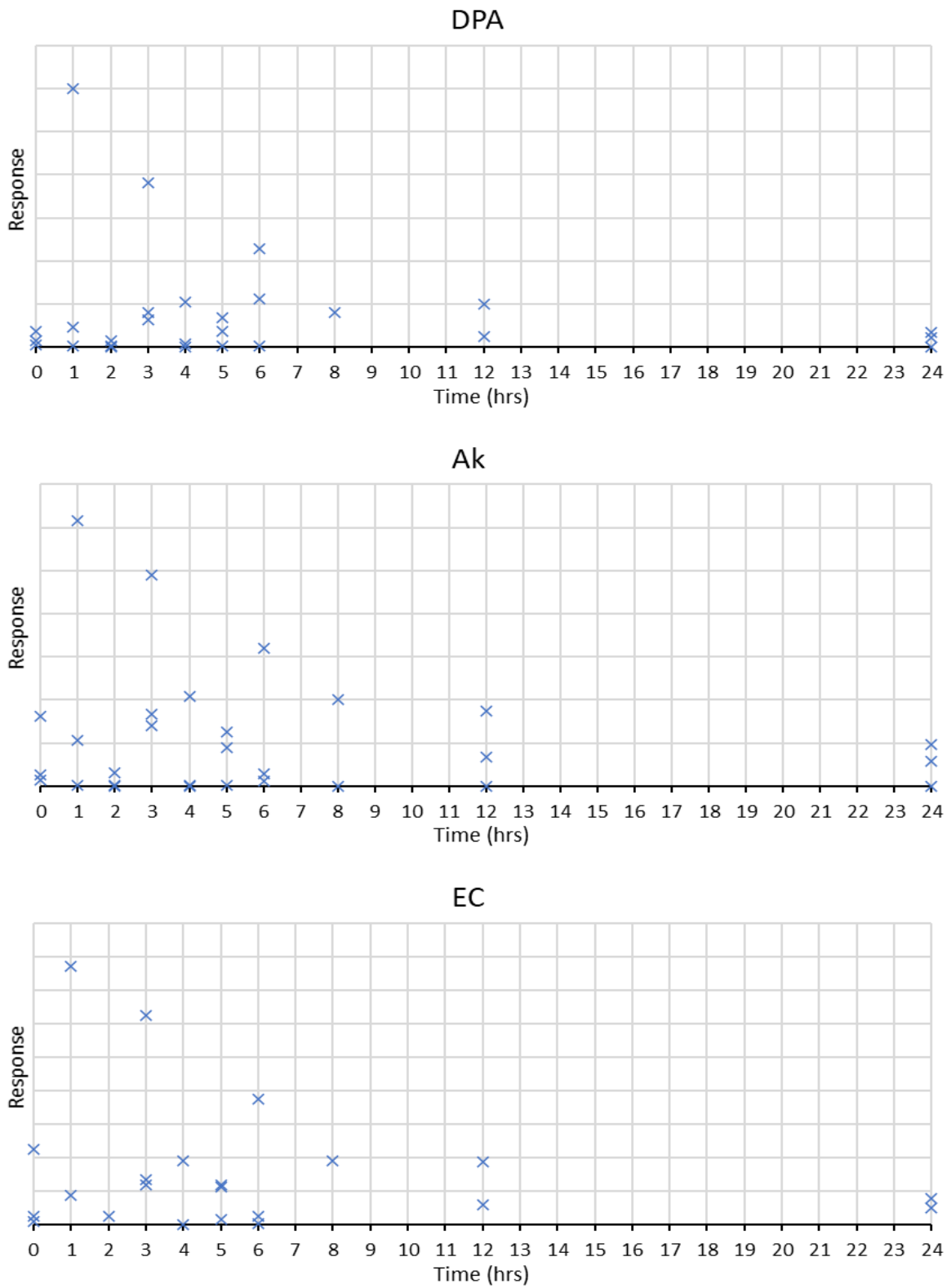


Figure 2-12 a): Normalized recovery of OGSR compounds vs time to sampling

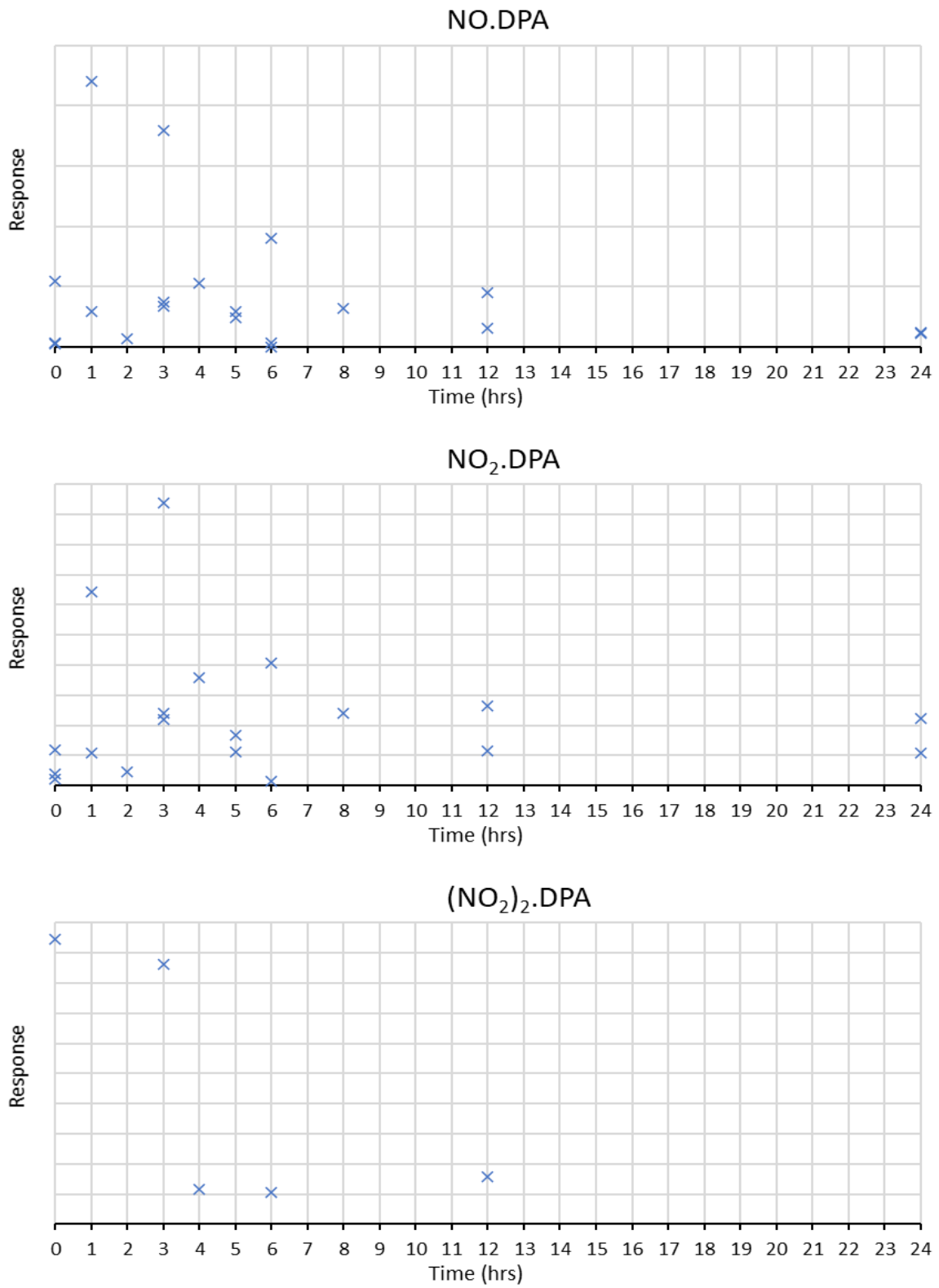


Figure 2-12 b): Normalized recovery of OGSR compounds vs time to sampling

2.3.5 Summary

The second part of this chapter addressed the robustness of the chosen sampling method. Traces collected during police investigations are likely to originate from dirtier and more chaotic environments than controlled laboratory conditions. It is impossible to predict and pre-emptively test all of these experimentally, and case-specific controls should be considered wherever possible. However, it was deemed important to test the sampling and analysis method, from start to finish, after the introduction of at least some complicating factors.

The process proved capable of detecting GSR from shooter's hands, downrange textiles, and surfaces that had been deliberately dirtied. The propensity of textiles to trap propellant particles appeared to have a greater effect on eventual *in silico* concentrations of OGSR, compared to the rate of "overloading" adhesive stubs with loose fibres. None of the dried liquids added to the surface of targets led to inability to detect any of the OGSR compounds known to be present in the ammunition.

Compounds representing OGSR were also detected up to 24 hours post-shooting when deposited on undisturbed surfaces, although reductions in signal intensity occurred as the sampling delay increased. Further experiments modelling the effects of daily activity have been conducted by other authors, but typically extend to approximately four hours.

2.4 Conclusions

A tandem approach was proposed to allow analysis of both organic and inorganic portions of GSRs collected using adhesive sampling stubs. This sample-collection platform is already in common use during investigation of shooting incidents. Extracts were prepared from the stubs for analysis by HPLC-MS/MS, while the stubs were dried and used for SEM-EDS following standard procedures. The impact of the extraction procedure on inorganic particles appeared to be low, with maps of particle locations prepared pre- and post- extraction being largely similar [\[223\]](#). Using the extracts to ascertain information on the OGSR content of a recovered trace provides valuable orthogonal information [\[9, 22, 155, 188, 203\]](#).

The procedure allowed recovery and isolation of OGSRs to a sufficient degree to that they could be detected by HPLC-MS/MS. Key compounds were observed in samples collected from diverse substrates, representing preliminary simulations of potential operational uses. Detection of OGSR was also achieved from samples taken after time-delays of up to 24 hrs after a shooting event, although the loss of material caused by movement was not modelled. This is an important aspect of forensic investigations, as a significant delay may occur between an incident and opportunities to collect trace material [\[31\]](#). Further studies, including sampling surveys of known firearm users, will help to increase confidence that OGSR can be detected from shooter's hands despite them having undertaken routine physical activities.

An admitted flaw of the stubbing/solvent extraction approach is its semi-destructive nature. Samples analysed by SEM-EDS post-extraction have consistently been shown to contain particulate IGSR, proving that this material is not stripped from adhesive stubs wholesale. On the other hand, it is not possible to guarantee that every single particle initially present will be retained throughout the extraction. The risk of mistakenly identifying a stub as “negative” for IGSR due to particle loss may exist, particularly if very small numbers of particles were originally collected.

While inorganic particles can remain on the stubs’ surface unchanged, any organic particulates such as partially unburned propellant fragments are expected to dissolve. This prevents subsequent application of alternative strategies such as hyperspectral imaging ^[58]. Extracts are also consumed during LC-MS analyses, although sufficient volume is typically available for several replicates. This contrasts with SEM-EDS samples that can be stored and re-tested where necessary, an asset of current standard procedures that is retained by the process investigated herein.

This method development has been undertaken from the perspective of an independent analytical laboratory providing expert analysis. In Australia it is usual for these laboratories to work with samples or exhibits provided by law-enforcement officers, who undertake the direct searches of incident/crime scenes. In this work, the effects of intervals up to 24 hours between a shooting event and collection of samples by these crime-scene personnel have been modelled.

However, there may then be substantial delays before samples are transported to a laboratory, and a further interval before the laboratory is able to perform analyses. There is no practical risk of this second interval affecting the integrity of IGSR particles, as they are considered stable essentially indefinitely once fixed to an adhesive surface ^[45]. However, the impact on OGSR traces is an area of active research. Existing publications indicate that sample transport and preservation practices may have an impact on the viability of OGSR traces as good candidates for laboratory analyses. For example, the work of Gassner et al. (2016) and Taudte et al. (2017) suggests that refrigeration and swift transport of adhesive specimens are likely to yield a greater amount of usable OGSR material ^[18, 175]. This information should be passed on to crime-scene officers by scientists. Further research and consultation between stakeholders may confirm that changes to current forensic workflow are desirable, to translate the methods investigated above into operational practice. The study contained within this thesis does not seek to make any specific recommendations in this regard.

Chapter 3:

Environmental Prevalence of GSR or GSR-like Traces

3.1 Background

When a criminal offence involving the use of a firearm is under investigation, samples may be collected to ascertain whether a surface or person of interest have been exposed to traces that reflect firearm use. The most probative of these traces, referred to as gunshot residue (GSR), consist of inorganic and organic material originating in ammunition's primer and propellant respectively ^[9]. However, the forensic value of suspected GSR material is inversely proportional to the prevalence of indistinguishable traces in the environment. This is well accepted amongst qualified GSR examiners, leading to the development of guidelines such as *ASTM-E1588* by the American Society for Testing and Materials or the *Best Practice Manual in the Forensic Examination of Gunshot Residues* by the European Network of Forensic Science Institutes ^[111, 112]. These standards apply a hierarchical classification system for inorganic GSR (IGSR) particles based on their chemical composition; particles with a composition that is rarely encountered outside of firearm use are assigned greater value than particles which could be generated by a firearm, but could also come from diverse other sources. The ASTM's classification system and naming conventions have been, and will continue to be, used to describe IGSR throughout this document.

Although the forensic evaluation of persistence, transfer, and pollution events (see section 1.4) is under continual development, the collection and analysis of IGSR is a mature and relatively settled process. This is evident in, and supported by, the existence of published standards like the ones referenced above. Conversely, more diverse strategies for collection, analysis and interpretation of organic GSR (OGSR) are being explored, particularly as analytical instruments have increased in sensitivity (see section 1.7.2) ^[84, 104, 105, 157, 224]. Some of these have found use in laboratories actively conducting forensic casework, often on a case-by-case basis and without a unified approach amongst organisations. This situation may be changing. A comprehensive summary of organic compounds linked to ammunition (fired and unfired) was published by Goudsmits *et al.* in 2015, with the same authors proposing a preliminary list of high-value compounds in 2016 ^[84, 85]. A formal classification hierarchy, an excerpt of which is included in the introduction to this thesis, is under development by the Gunshot Residue Subcommittee of NIST ^[93]. These endeavours suggest that a consensus amongst stakeholders on the relative value of certain compounds may be achievable in the short to medium term.

While essential, a standardised list of target compounds does not in itself meet the objectives of GSR evidence for a judicial system. If the proposed methodologies are applied to casework, it is equally important to understand the likelihood of determining a "positive" result from collected specimens not directly linked to a specific criminal act under investigation. The dangers of not clearly

communicating this to a court were highlighted by a recently published case study from the United Kingdom [\[225\]](#). Put simply even if a laboratory could assign traces as having firearm or non-firearm origins with perfect accuracy, there will be some portion of the community that may carry GSR acquired from contact with firearms that has no relation to the matter under investigation. “Background” levels of GSR have previously been investigated empirically by directly collecting samples from volunteers in the community. There is also the possibility that the actions of law enforcement personnel may cause GSR to be transferred to a person prior to sample collection [\[26, 30, 37, 41\]](#). Together these will indicate a general likelihood of observing a positive result from any given person of interest, if in fact they were not involved in a crime. This may be used as the denominator for a likelihood ratio in order to formally evaluate the strength of a piece of evidence. It is important to note that surveys will likely reflect local trends in firearm legislation and usage, and as such careful consideration should be undertaken before applying generalised data to clarification of any specific case.

Previously published sampling surveys, summarized in Table 3-1, can be divided into three broad target groups. The first (category 1) is defined here as those having a high probability of testing positive for actual GSR – those who use firearms as part of their employment or hobbies. Examples are police officers, hunters, competition shooters and the like. Examination of these population groups, particularly police officers, has been most frequent in literature due to the risk of polluting POIs during arrest or transport. The second group (category 2) are those who are suspected to have a high probability of encountering “GSR-like” materials, such as pyrotechnicians, industrial manufacturers, welders, and automotive technicians. These individuals may have a higher-than-average risk of returning a false positive if tested for GSR. Either of the preceding groups are also a potential source of contamination to others, as it has been firmly established that people can be indirectly exposed to GSR through secondary or subsequent transfers from a residue-bearing source [\[16, 23, 26, 30, 40, 157\]](#). The final group (category 3) encompasses all other randomly selected participants, upon whom the presence of GSR or even GSR-like substances is considered less likely. This third group will form the primary focus of the following discussion.

Table 3-1: Published Surveys of GSR on Randomly or Selectively Sampled Persons

Study	Technique	Targets	Exposure Category*	Population Surveyed	# Samples (% positive)
Gialamas <i>et al.</i> 1995 (U.S.A.) [226]	SEM-EDX	IGSR	1	Police	43 (6.97%)
Garofano <i>et al.</i> 1999 (Italy) [81]	SEM-EDX	IGSR	2	Mechanical Occupations i.e vehicle repair, construction <i>etc.</i>	175 (N/A)
Northrop 2001 (U.S.A.) [227]	MEKC	OGSR	3	General Population	100 (0%)
Cullum <i>et al.</i> 2004 (U.K.) [228]	IMS	NG, TNT, PETN, RDX, HMX, 2,4-DNT	3	Public areas	493 (0.61%)
Lohoda <i>et al.</i> 2008 (U.S.A.) [229]	GC	“10 explosive organic nitrate compounds”	3	Public areas (outdoor)	333 (0%)
Lindsay <i>et al.</i> 2011 (Canada) [230]	SEM-EDX	IGSR	2	Firearm factory employees - assembly	7 (85.71%)
				Firearm factory employees - administration	6 (50.00%)
Gerard <i>et al.</i> 2012 (Canada) [231]	SEM-EDX	IGSR	1	Police - On Duty	30 (76.67%)
			1	Forensic Service - Police	36 (25.00%)
			3	Forensic Service - Administrative	28 (0%)
Charles & Guesens 2012 (Belgium) [37]	SEM-EDX	IGSR	1	Police Special Forces (low scenario)	12 (66.66%)
				Police Special Forces (high scenario)	12 (83.33%)
			3	Simulated suspect (low scenario)	12 (41.66%)
				Simulated suspect (high scenario)	12 (91.66%)
Brozek Mucha <i>et al.</i> 2014 (Poland) [35]	SEM-EDX	IGSR	1	Habitual Shooters	50 (36.00%)
			3	Non-Shooters	100 (1.00%)
			3	Laboratory Surfaces	55 (0%)
Hannigan <i>et al.</i> 2015 (Ireland) [232]	SEM-EDX	IGSR	3	Garments submitted to laboratory	100 (2.00%)

Bell & Seitzinger 2016 (U.S.A.) ^[141]	IMS	OGSR	3	University Students & Police	73 (5.48%)
Lucas <i>et al.</i> 2016 (Australia) ^[206]	SEM-EDX	IGSR	3	Market/Shopping centre	289 (0.35%)
Cook 2016 (Australia) ^[40]	SEM-EDX	IGSR	1	Police	33 (84.855)
Ali <i>et al.</i> 2016 (U.S.A) ^[39]	SEM-EDX and LC-MS	IGSR and AK, EC, DPA, NnDPA, NDPA	3	Simulated POIs and detention facilities	70 (1.43%)
Hoffstetter <i>et al.</i> 2017 (Switzerland) ^[23]	LC-MS	OGSR	3	General Population	27 (0%)
			1	Police Lab Personnel	25 (8.00%)
Manganelli <i>et al.</i> 2019 (Switzerland) ^[233]	LC-MS	OGSR	3	Police	115 (36.5%)
			1	General Population	122 (18%)
Lucas <i>et al.</i> 2019 (Australia) ^[41]	SEM-EDX	IGSR	1	Police	75 (7.90%)
Seyfang <i>et al.</i> 2019 (Australia) ^[71]	SEM-EDX	Glassy-GSR	2	Fireworks - technicians & spectators	20 (0%)
Ott <i>et al.</i> 2020 (U.S.A.) ^[156]	Anodic stripping voltammetry	Pb, Sb, Cu, 2,4-DNT, DPA, NG, EC	1	Shooters	395 (93.42%)
			3	Non-Shooters	350 (6.58%)
Stamouli <i>et al.</i> 2021 (24 countries, predominantly European) ^[34]	SEM-EDX	IGSR	1	Arresting Police Officers	339 (28.5%)
			1	Firearm Owners	252 (51.3%)
			2	Car Mechanics	153 (0%)

*Category 1. Known association with firearms

*Category 2. Known association with specific environmental sources of GSR-like material

*Category 3. Including all other members of society, and those whose status in the previous categories is not known

Regarding background IGSR distribution amongst the public (Category 3), SEM-EDX studies indicate that prevalence is low across multiple countries for which data are available (0-2% returning at least one characteristic Pb/Ba/Sb particle ^[34, 35, 41, 231, 232]. Comparatively fewer studies have been conducted to address the same issue for OGSR. Initial results appear to suggest equally low background prevalence could be observed for these compounds, although notable variation exists in both detection methodologies and stated rates. The earliest studies applicable to background OGSR prevalence in fact aimed to detect explosives, but results for relevant organic nitrate compounds such

as NG and DNT were reported therein. Separately Northrop (U.S.A., 100 specimens) and Lohoda *et al.* (U.S.A., 333 specimens) did not find any reportable positive results using capillary electrophoresis and gas-chromatography respectively [227, 229]. Cullum *et al.* (U.K., 493 specimens) reported detection of NG twice and DNT once for a prevalence rate of 0.61% using an ion-mobility spectrometer (IMS) [228]. Specifically considering GSR but also using IMS, Bell & Seitzinger (U.S.A., 73 specimens) instead reported a rate of ~5% using neural-network pattern matching to discriminate “shooter” and “non-shooter” categories. However, this value was shown to be significantly affected by the statistical threshold chosen by the examiner; at a likelihood ratio of 10:1 (shooter/non-shooter) the rate dropped to 2% [141].

Two interrelated Swiss studies evaluated extracts collected from adhesive stubs by LC-MS/MS, representing the direction in which OGSR research appears to be moving [234]. IGSR was not examined in either survey. The first, by Hofstetter *et al.* (2017), found none of the targeted OGSR compounds in 27 samples collected from members of the public [23]. The second by Manganelli *et al.* (2019) found a much higher prevalence within their sample population [233]. From a pool of 122 volunteers, 17% stated that they owned a firearm, 5% stated that they regularly used firearms, and 5% declared contact with other potential sources of GSR contamination. One participant had been practicing shooting immediately prior to providing their sample, and unsurprisingly was found to have six OGSR compounds on their hands. The authors went on to report that 14.8% of participants’ hand specimens tested positive to a single OGSR compound, and 2.5% had two compounds. Akardite II and nitro-diphenylamine were the most encountered analytes. Interestingly, positive detections appeared to be more closely associated with a participant’s occupation involving automotive repair rather than their status as a firearm user. This potentially has quite significant implications for the interpretation of combined OGSR-IGSR traces, as both brake-pads and airbags have previously been raised as hypothetical sources of environmental IGSR-like material [95, 235, 236]. However a high rate of gun ownership in the relevant population (17% reported in this study) may create a follow-on effect due to transfer events, especially if firearms are regularly transported in personal vehicles.

The combined OGSR & IGSR survey with the largest pool of sampled volunteers at the time of writing was conducted by Ott *et al.* in West Virginia, published in 2020 [156]. This study included specimens from 395 shooters and 350 non-shooters, and investigated both portions simultaneously using an electrochemical sensor. This approach departs from current GSR reporting guidelines in that it is a bulk technique and a “positive” result was determined to be any sample that exhibited at least two of the following markers: Pb, Sb, Cu, (2,4)-DNT, DPA, NG and/or EC. Various statistical techniques were also explored for making a binary shooter/non-shooter classification. A notable feature is the

substitution of Cu for Ba as an inorganic GSR marker, as the device in question was previously shown to be unsuitable for Ba detection [125]. However, performing 745 analyses using the preferred confirmatory technique of SEM-EDS would be wildly impractical using current technology. Therefore, use of an electrochemical screening technique is more defensible in this circumstance, particularly as it appears to be compatible with subsequent confirmatory tests if required.

Ott *et al.* reported several values representing method accuracy, but the most relevant to the current discussion is the “false positive” rate which could be reframed as the background prevalence of detection among the non-shooter volunteer pool. This value was reported as 2.67% under each of the three statistical treatments investigated (Naïve Bayes, Logistic Regression and Neural Network). Rather than representing false positives in the analytical sense, these could equally likely be reflecting environmental exposure to the targeted compounds, especially as the two groups of participants were likely to mingle under the circumstances studied (an outdoor scouting event). Detection rates of selected single analytes are shown in Table 3-2. The original authors also stated that “*the combined incidence of IGSR and OGSR markers was not observed on the background samples*” [156].

Table 3-2: Separate Prevalence Values for Individual Analytes			
	Pb	NG	Cu
Shooter	93.7%	43.5%	57.0%
Non-Shooter	4.9%	4.3%	6.3%

Thus far, one limited prevalence survey has been reported including data from both SEM-EDS and LC-MS/MS in tandem. In that study, Ali *et al.* (2016) collected adhesive stub samples from multiple locations within Pittsburgh police facilities to assess the risk of pollution on POIs during forensic investigations [39]. Also sampled were the hands of simulated “suspects” who spent ten minutes handcuffed in the rear of a police vehicle. Of 70 stub specimens, one Pb/Ba/Sb particle was found on an interview desk and two samples from volunteers’ hands were deemed positive for EC (1.4%). However, most extracts including controls had a chromatographic peak consistent with EC but below the LOQ. As with Ott *et al.* (2020), Ali *et al.* (2016) did not observe any specimens concurrently presenting detection of both IGSR and OGSR.

There are many gaps in the existing knowledge base regarding background prevalence of GSR traces. Most notably, detection rates for individual compounds representing OGSR have only been evaluated to a limited extent. This information represents a basic requirement for evaluative approaches to providing expert advice about GSR. To expand upon this same line of enquiry, there have been no prior studies on prevalence that describe the simultaneous measurement of IGSR and OGSR markers

using the best-practice methods for each. Ott *et al.* (2020) surveyed both shooters and non-shooters using a screening method, but did not follow up with confirmatory SEM-EDS on that occasion ^[156]. The work of Ali *et al.* (2016) specifically examined POIs *after* arrest simulations; this models pollution but not background contaminants ^[39]. If a holistic approach to GSR analysis is to be used, data on the co-occurrence of the constituent parts is necessary to understand the forensic significance of laboratory observations.

3.2 Aims

The study described in this chapter had two major aims. The immediate aim was to collect data on the background prevalence of organic GSR compounds amongst the Australian public, while also increasing the number of samples tested for IGSR particles. This helps to expand upon previous publications by broadening the pool of surveyed populations. Specifically, most prior data have been collected in North American and European countries. The Australian context is notable because of a perception of low firearm usage rates, and a bias towards lower-calibre guns in private possession. Both factors suggest that less GSR material is in circulation to cause contaminating transfers. Therefore, samples were sought from members of the general Australian public. Each participant was requested to self-report any association with firearms or potential sources of environmental pollution. Data of this type can be used in the estimation of likelihood ratios when determining the forensic value of recovered traces.

The more academic aim of the survey was to investigate the relationship between observing OGSR and IGSR traces in any given sample. If a sample was collected from a known shooter after a brief interval, it would be expected that both types of residues should be present. This assumption may not in fact hold true, depending on the relative persistence or transferability of each type of material and the subject's actions during the intervening time. Observation of O- and I- GSR residues simultaneously in a non-shooter's sample could also be correlated if there is secondary transfer from a shooter. However, evaluation of this scenario may be complicated if there exists some source of environmental pollution common to the two. It must also be considered that two separate sources of GSR or GSR-like material, one organic and one inorganic, may contribute to a detected trace. In that instance, the prevalence of each component should be considered unconnected and statistically independent. Each sample was first analysed by LC-MS/MS, and then subsequently examined by SEM-EDS. The relative performance of the two instruments in the "detection" role were monitored.

3.3 Methods

3.3.1 Sample Collection

Approval to conduct surveys was granted by Flinders University's Social and Behavioural Research Ethics Committee under application #6870. Samples were collected from 60 volunteers in Perth, Western Australia and Adelaide, South Australia, evenly split between recent shooters and non-shooters. Participants were asked to complete a questionnaire self-reporting previous firearm use if applicable, and any circumstances considered as potential vectors for a false positive result. Hand-samples were then collected using adhesive carbon tabs mounted to 12.5mm aluminium stubs (Ted Pella, USA) which were stored in individual plastic housings and refrigerated until analysis. Each sample was extracted according to the procedures set forth in Bonnar *et al.* 2020 [223], with minor modifications. Briefly, 100 μL of acetonitrile was pipetted to cover the stub surface and allowed to remain for 1 minute. The solvent was then recovered, reduced under N_2 , reconstituted in 10 μL of acetonitrile containing 1 $\text{ng } \mu\text{L}^{-1}$ of *d6*-diphenylamine, and 1 μL was injected for analysis by UHPLC-ESI-MS/MS. Solvent blanks and extracts prepared from clean stubs were also collected as negative controls. Each stub was allowed to dry at room temperature before being re-capped in its plastic housing for storage. The stubs were later analysed by SEM-EDS microscopy according to the guidelines set out by the ASTM [112].

3.3.2 Instrument Settings

3.3.2.1. UHPLC-ESI-MS/MS

Analyses of the liquid extracts were performed using a Thermo Scientific Vanquish UHPLC fitted with a 100 mm x 3.0 mm ACE Excel 3 Super C18 column. The total flow rate was 0.5 mL min^{-1} and the solvent profile was as follows:

Table 3-3: Solvent Profile		
Minutes	10 mm Aqueous Ammonium Formate	Chromatography-Grade Methanol
0	40%	60%
1	15%	85%
10	15%	85%
12	40%	60%

The LC was interfaced to a Velos Pro linear ion trap mass spectrometer *via* a heated electrospray ion-source at 350° C. A series of selected ion monitoring (SIM) channels were created using the Thermo TunePlus software, with each of the target compounds' nominal $[\text{M}+\text{H}]^+$ mass-to-charge ratio (+/- 0.5 Da) isolated for 0.010 s with a normalized fragmentation energy (CID) of 35 V. A full scan for fragment ions was performed for each parent mass. An extracted ion chromatogram was then created for the

diagnostic fragment ions as per Bonnar *et al.* (2020) [223]. Each solution was determined to contain an analyte of interest if there was a peak >3 standard deviations above the mean value of extracts collected from clean stubs (n=4), and corresponding to the retention time of reference standards. A provisional classification of samples following the proposed NIST guidelines was performed (see above). Samples meeting the criteria of “characteristic” and “consistent” were afterwards referred to as “positive” for OGSR, and samples defined as “inconclusive” were combined with the GSR OSAC’s “negative” category.

3.3.2.2. SEM-EDS

Microscopic analysis was conducted using a Tescan MIRA field-emission SEM, equipped with two Oxford Instruments Ultimex100 EDS detectors for X-ray spectroscopy. The instruments were operated using Tescan Essence software, and Oxford’s Aztec automated particle analysis software with additional GSR suite. System settings were defined in accordance to ASTM E1588-17 and ChemCentre’s internal standard operating procedures for GSR analysis in casework [112]. Brightness and contrast settings were set using a standard containing cobalt, rhodium and gold. A positive control consisting of three small, pre-characterised Pb or PbSb particles were automatically re-acquired between every two experimental samples to monitor instrument performance.

All samples were carbon-coated prior to SEM analysis. Working distances were manually set by the operator for each sample stub, at approximately 6-8 mm. A time limit of four hours was applied for each of the samples belonging to known shooters, due to an expectation that these would be heavily loaded with GSR. An eight-hour time limit was used for all non-shooter samples.

3.4 Results

Table 3-4 is provided to guide the reader through the results of sequential GSR tests for the survey population. More detailed information on these results is available in sections 3.4.1 and 3.4.2.

Table 3-4: Simplified Survey Results		
	Shooters (n = 30)	Non-shooters (n = 30)
Positive for OGSR by LC-MS/MS	20	0
Positive for IGSR by SEM-EDS	30	1

3.4.1 LC-MS

Of the 30 extracts representing shooter participants, 20 were found to contain at least two of the specified OGSR marker compounds required for the sample to be designated positive using the pre-established criteria chosen for this study (66.67%). A further 8 samples (26.67%) returned peaks for only a single compound, being designated as “inconclusive”. This left only two samples for which no indication of contact with OGSR was discernible. A breakdown of compounds detected in individual shooter extract samples is given in Table 3-5. Many extracts were found to contain more than 5 target compounds, with the most common combination being ethyl centralite, akardite, and diphenylamine along with its derivatives. Responses to the written survey were checked, and it was found that a common factor was attendance to either marksmanship competitions or a proficiency training course that involved handling and discharging a multitude of firearms. Samples were provided at the end of the days’ shooting events, after a variable but brief (<1 hr) delay. This is likely to have contributed to the diversity of stabilisers present within individual samples, although there is no reason that a mixture of compounds cannot be used within singular examples of propellant powder.

None of the 30 samples collected from non-shooters gave rise to OGSR results that were statistically significant (+ three standard deviations above mean blank measurements), and thus results for individual non-shooter samples are not shown.

Table 3-5: OGSR Marker Compounds Detected in Shooter Samples									
Sample Name	Diphenylamine	Nitroso-diphenylamine	Nitro-diphenylamine	Dinitro-diphenylamine	Akardite	Methyl Centralite	Ethyl Centralite	Count of Compounds Detected	Provisional NIST Classification
HS 081	√	√	√	x	√	√	√	6	Characteristic
HS 093	√	√	√	x	√	√	√	6	Characteristic
HS 083	√	√	√	x	√	x	√	5	Characteristic
HS 087	√	√	√	x	√	x	√	5	Characteristic
HS 090	√	√	√	x	√	x	√	5	Characteristic
HS 095	√	√	√	x	√	x	√	5	Characteristic
HS 102	√	√	√	x	√	x	√	5	Characteristic
HS 104	√	√	√	x	√	x	√	5	Characteristic
HS 107	√	√	√	x	√	x	√	5	Characteristic
HS 108	√	√	√	x	√	x	√	5	Characteristic
HS 109	√	√	√	x	√	x	√	5	Characteristic
HS 110	√	√	√	x	√	x	√	5	Characteristic
HS 082	√	x	x	x	√	x	√	3	Consistent
HS 086	x	x	√	x	√	x	√	3	Consistent
HS 099	√	√	x	x	x	x	√	3	Consistent
HS 085	x	x	x	x	√	x	√	2	Consistent
HS 088	x	x	x	x	√	x	√	2	Consistent
HS 096	x	x	x	x	√	x	√	2	Consistent
HS 097	x	x	x	x	√	x	√	2	Consistent
HS 101	x	x	x	x	√	x	√	2	Consistent
HS 084	x	x	x	x	x	x	√	1	Inconclusive
HS 089	x	x	x	x	x	x	√	1	Inconclusive
HS 091	x	x	x	x	x	x	√	1	Inconclusive
HS 094	x	x	x	x	x	x	√	1	Inconclusive
HS 100	x	x	x	x	x	x	√	1	Inconclusive

HS 103	x	x	x	x	√	x	x	1	Inconclusive
HS 105	x	x	x	x	√	x	x	1	Inconclusive
HS 106	x	x	x	x	x	x	√	1	Inconclusive
HS 092	x	x	x	x	x	x	x	0	Negative
HS 098	x	x	x	x	x	x	x	0	Negative

3.4.2 SEM-EDS

Of the 30 stubs collected from shooter participants, all were found to bear particulate matter confirmed to correspond with IGSR of both “characteristic” and “consistent” classifications (as expected). The mean number of characteristic particles was 483, with standard deviation of 570. The distribution of particle counts across the samples was best fit by a log-normal model ($\mu = 5.5$, $\sigma = 1.23$, $p = 0.63$). A more detailed record of the individual stub’s particle population is given in Appendix 3-1.

Notably one single particle meeting the requirements for classification as “characteristic” was located on a stub originating from a participant who declared themselves not to be a recent shooter (last reported contact with a firearm was two years prior to sampling). This particle, shown in Figure 3-1, contained Pb, Ba, & Sb, with minor contributions from Cu, Fe & Si. Under microscopic examination it measured approximately 100 μm by 50 μm , with a smooth surface disrupted intermittently by circular holes. A combination of back-scatter imaging and EDS X-ray mapping indicated that its chemical composition was mostly homogenous, with a nodule enriched in Pb present on one side. Therefore this sample was considered as a false positive for iGSR for the purpose of the following discussion. However, the presence of only a single particle in the absence of a greater supporting population would likely be evaluated using extreme caution when reporting this result in the context of a police investigation or court proceeding.

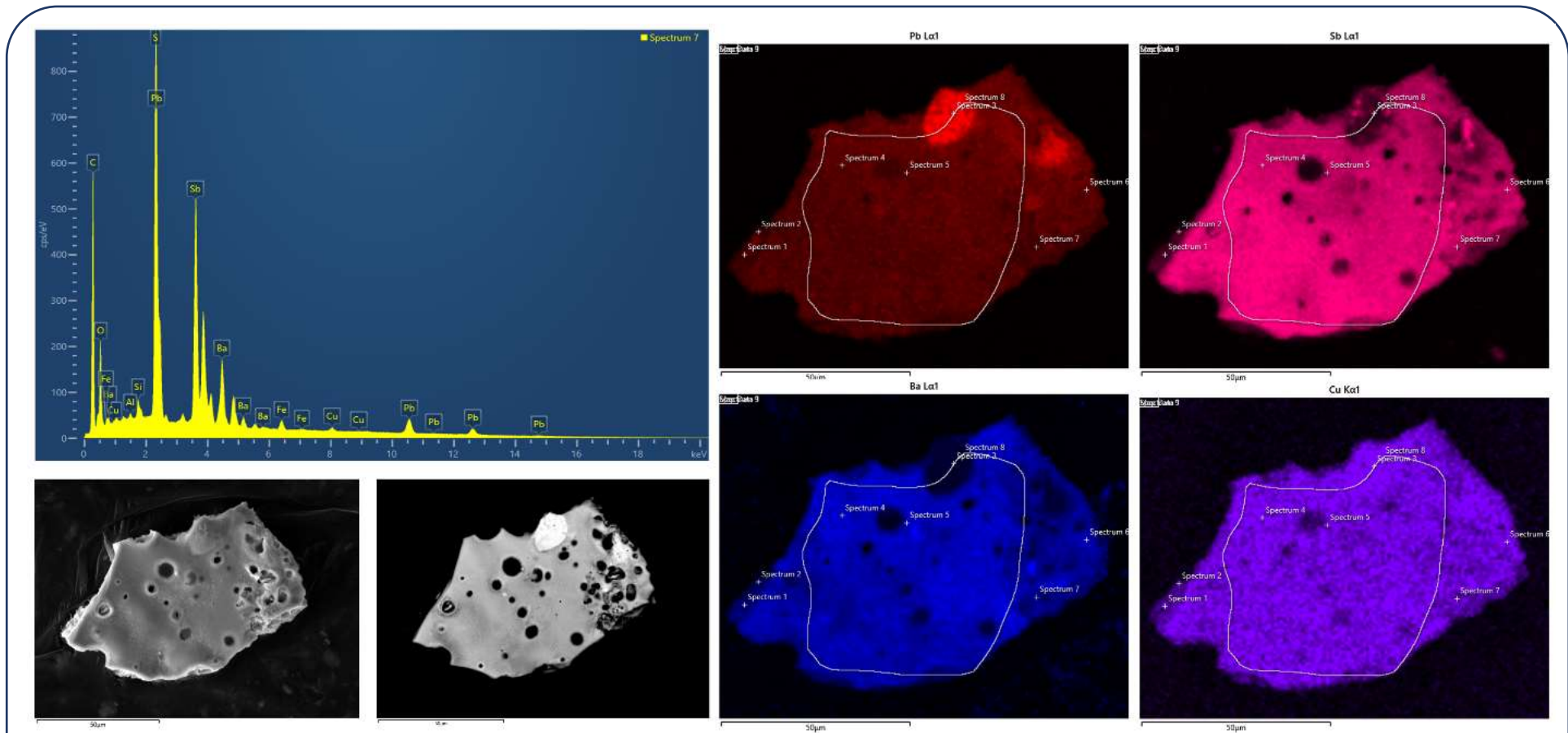


Figure 3-1: This particle was found on an individual who declared that they had not discharged a firearm for more than two years. The distribution of elements within the particle was largely homogenous, with Pb (red), Sb (pink), Ba (blue) and Cu (purple) shown.

3.5 Discussion

3.5.1 Samples from known shooters

The 30 samples collected from shooters' hands for this survey were generated by volunteers following "natural" behaviours, with no prior knowledge of forensic GSR collection. This was done to avoid any subconscious efforts to maximise GSR exposure or minimise losses post-shooting. Often there were delays of approximately 15-30 minutes between the cessation of shooting and collection of stub samples, during which the participants packed away their firearms, manipulated door handles and handled scoring paperwork etc. Unsurprisingly, all these individuals' samples were found by SEM-EDS to contain numerous IGSR particles meeting the ASTM's definitions for both "characteristic" and "consistent" classifications. This further corroborates SEM's already strong reputation as the confirmatory technique of choice.

Additionally, 28 of the 30 samples were found to contain at least one of the stabiliser compounds selected to represent OGSR. These findings support the assertion that additional chemical information can be obtained from traces collected using existing practices. This additional information has two potential benefits. Firstly, it allows better recognition of GSR, particularly if large numbers of nuisance particles such as Fe are present, or characteristic particles are absent. Secondly, it is currently difficult to discriminate between ammunition sources based on IGSR, as many products use similar formulations in their primers. A more thorough characterisation of the trace using OGSR could allow analysts to classify GSRs according to the presence of individual stabiliser compounds.

However, analysis using LC-MS/MS alone failed to indicate association with firearms for two shooter's stubs (6.67%) entirely. A further 8 of 30 were classified as "inconclusive", as only a single OGSR compound was detected from them. There are several possible explanations for this outcome:

1. Insufficient propellant material may have been present on some of the shooters' hands, because:
 - a. OGSR was present, but was below the relevant instrumental LODs
 - b. Material may have been lost due to post-shooting activity
 - c. A mixture of firearms including 0.22 calibre bolt-action rifles and pump- or lever- action shotguns were used by some participants. The comparatively long barrel lengths and enclosed actions may have caused OGSR to be distributed in the direction of aim, and away from the shooter [\[15\]](#).
2. The increased manual handling required to extract, concentrate and transfer liquids to form a viable specimen for LC-MS analysis magnifies the chances of unnoticed gross error
3. Only seven marker compounds were targeted by the method and in particular the energetic compound nitroglycerin was not included in the test. A more inclusive suite of indicative compounds may improve detection rates. Also, some ammunition may have only included a single stabiliser, and thus would never attain the two-compound threshold.

For these reasons, LC-MS/MS may have an unacceptably high false-negative rate for forensic casework if used in isolation, at least using the subsampling configuration described above. Further advances in sample collection and extraction, or refinement of instrumental methods, may improve upon the detection rates observed in this study. This does not mean that LC-MS/MS as described above cannot play any part in GSR trace detection. Considering the relative resource requirements of SEM and LC-MS analysis, there is scope for using liquid extraction as a triaging tool i.e., as a relatively rapid test that indicates an order of priority for later SEM-EDS analysis. The frequency of observing IGSR from any given sample under the SEM was 31/60 (51.67%) when no prior information was considered. This increased to 28/28 (100%) if at least one OGSR compound had previously been observed in the sample. If no OGSR compounds were recorded using LC-MS, the frequency of observing characteristic IGSR particles was only 3/32 (9.38%). This concept will be explored in greater detail under a Bayesian framework in following chapters.

3.5.2 Samples from non-shooters

A further 30 samples were collected from the hands of individuals declaring that they had no recent contact with firearms, nor exposure to potential sources of contamination as described in a questionnaire. In general, this group could be described as students and administrative workers. Survey samples such as these can be used to represent the expected background frequency of detection, against which specific case samples might be compared in a forensic case. In this instance, SEM was found to have a measurable false positive rate (1/30, 3.33%). This rate is broadly in agreement with previous studies [34, 35, 206, 232]. A false positive does not necessarily mean that the test is falsely labelling non-GSR material as originating from a firearm. That explanation may form part of the answer, but background distribution of GSR due to transfer events cannot be ruled out. Furthermore, the sample in question was found to contain only a single particle meeting the requirements to be classified as “characteristic” under ASTM standard E1588-17. Policies on the minimum number of particles required for a “positive” result differ between jurisdictions, but single particles have previously been used as evidence of contact with firearms. In the absence of a population of supporting particles, it is unlikely that an analyst would provide an opinion indicating strong association between the sample and a shooting. In this instance the inclination is to believe the participant when they stated they had not recently handled any firearms, as they had no incentive to offer a false statement. Within the context of this study, it is particularly interesting to note that the IGSR findings were not supported by the concurrent presence of OGSR.

No OGSR was detected on declared non-shooters, suggesting that the prevalence of OGSR-like material among the sampled population was low (<3.33%, n=30). This was equally true for each of the seven compounds chosen to represent OGSR, and thus individual rates could not be calculated. The findings broadly concur with previous studies and indicates that the detection of OGSR may be a strong indicator of contact with firearms under an evaluative reporting framework [23, 141, 156, 157, 227].

3.6 Conclusions

The survey work described in this chapter was based upon the collection of 60 samples, with their origins evenly divided between shooters and nonshooters. Of the 30 nonshooter samples, none were found to contain stabiliser compounds linked to OGSR. While it is unwise to draw broad conclusions from such a limited survey, these data at least suggest low background prevalence of the compounds in Australia. This includes cross-contamination from actual shooters, and sources of these compounds in applications unrelated to firearms. It is suggested that these results be interpreted as a pilot study demonstrating the soundness of the approach for surveys with a greater number of participants. Several “detections” in a much larger sample population would be required to estimate an accurate base rate for each individual compound. The study was also conducted primarily in an urban environment, with participants’ occupations including students, laboratory staff, and office workers. Other relevant populations may exhibit a greater prevalence of transferred GSR or interfering substances.

For the samples collected from shooters, analysis by SEM-EDS performed as expected by detecting and characterising many IGSR particles. As each stub had been extracted for OGSR prior to SEM analysis, and since no false negatives resulted, these data further support for the inference that solvent extraction does not preclude conventional IGSR examination. In many instances LC/MS could also be used to detect the presence of a GSR trace and to generate an orthogonal set of analytical data. However, it could not be relied upon for a detection role to the same extent as microscopy. Therefore, chromatography and mass spectrometry were judged to add value as complementary techniques to increase the depth of characterisation that can be performed on a given sample, and as tools to aid in decisions on the priority of samples delivered to a laboratory for analysis. It is not uncommon for crime scene officers to submit large numbers of sampling stubs for analysis during a single investigation. Some of these are determined by the expert as *prima facie* unlikely to provide information commensurate with the effort of analysis. The option for analysts to perform highly selective “screening” tests, the results of which can be obtained much more rapidly than is currently the norm, may prove attractive in operational settings. This is not intended to suggest that samples should be discarded on the basis of negative or inconclusive results by LC-MS, but rather they may be of lower priority for analysis by SEM compared to other samples within the context of the same case.

The results obtained from this survey work are seen by the author to support the possibility of greater use of tandem OGSR and IGSR analysis in forensic case work. However, benefits to forensic scientists and the wider judicial system have been described in general terms only. The content of Chapter Four represents an effort to quantify this potential, and to describe the tools which may be used.

Chapter 4: **Statistical Interpretation of Integrated GSR Data**

4.1 Introduction

The preceding chapters in this thesis focussed on practical aspects of integrating chemical analyses for both organic and inorganic components of GSRs. This entailed development of a multi-instrumental laboratory method, and the demonstration of that method on samples representative of those submitted to laboratories. However, laboratory results must be communicated to various stakeholders for use in forensic contexts. This presents a potential issue when providing information to end-users in law-enforcement or judicial settings, who may lack the technical background required to interpret such findings. Therefore, this chapter explores various approaches to combining separate laboratory observations into a useful and coherent output.

Background information is provided on the practice of evaluative reporting for trace evidence in general, and for GSR evidence in particular. Bayesian approaches including conditional probability and likelihood ratios are summarised. These provide a necessary framework for understanding what constitutes the “strength” of evidence, and how trace evidence can be used by triers of fact to evaluate competing hypotheses. Laboratory data previously described in Chapter Three were first assessed under a qualitative and categorical approach, whereby set criteria must be reached before each sample can be considered “positive” for GSR. Using this approach, it was shown that detection of OGSR and detection of IGSR are not statistically independent. It was also shown that testing for both types of GSR provides better predictive value as to a person’s status as a shooter or non-shooter, compared to either test alone.

Next, the same sample set was divided into subsets according to shooter/non-shooter status and the results were instead assessed using quantitative models. Various probability distribution functions were tested against the data for each variable, to see if any parametric functions accurately modelled the observations. This approach has been previously discussed in literature by several authors specifically considering univariate IGSR particle-counts. The outcome of this modelling was generally poor, with few sets described well by parametric distributions. This is a distinct hazard of trying to model rare events when only small sample sets are available. PDFs constructed separately for each variable are also difficult to combine rationally when dependencies exist between the data.

Finally, machine learning algorithms were used as intermediary steps to reduce data dimensionality so that each sample could be summarized with as few parameters as possible. Due to dependencies between observations, partial-least squares regression and artificial neural networks were selected as classification tools. Both were able to provide information that would allow forensic scientists to correctly classify all samples as either shooters or non-shooters under the conditions of the experiment. Of the two, the neural network was considered to deliver more useful information about the relative strength of support provided to either proposition.

4.2 Background

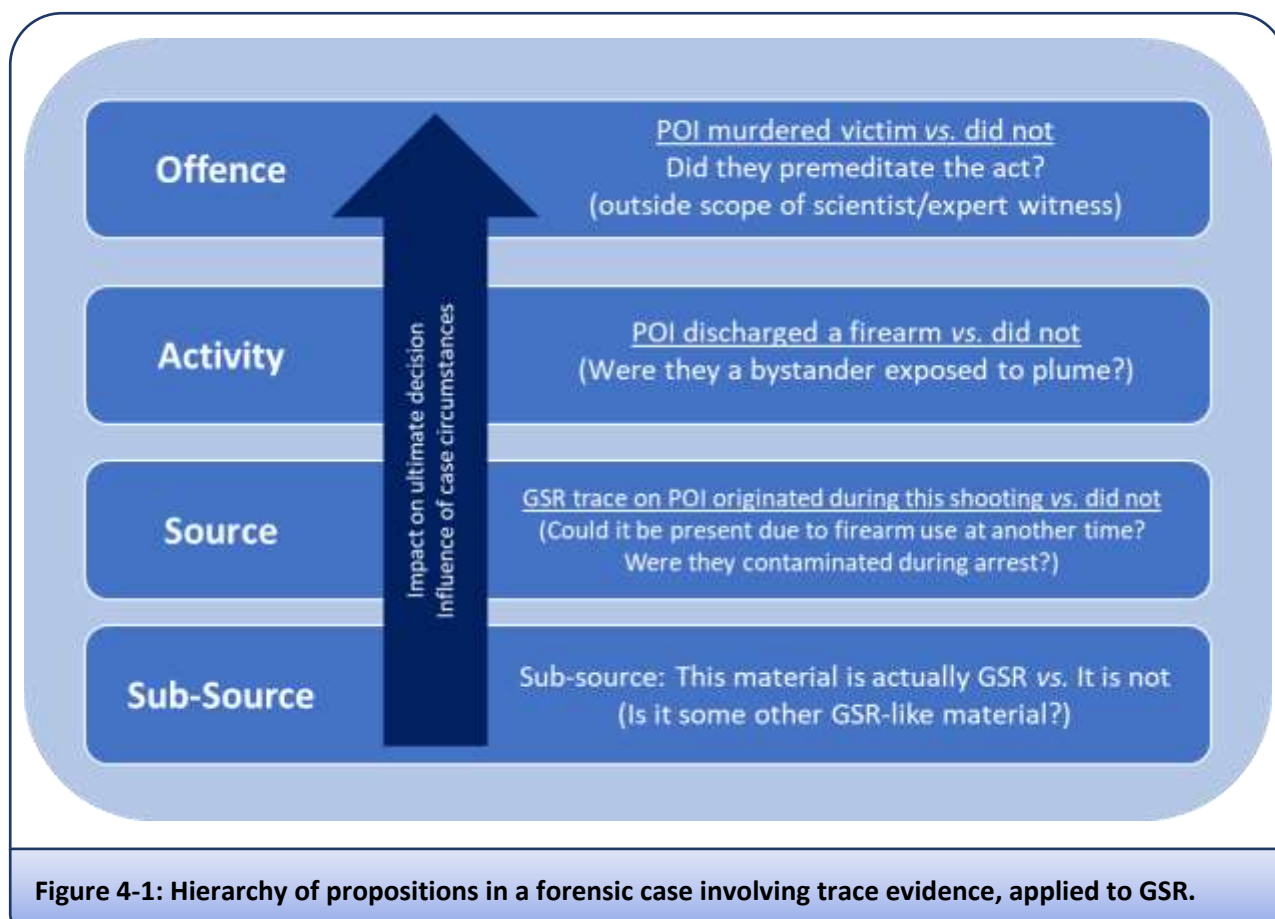
4.2.1 Evaluative Reporting

Each specific occurrence of GSR encountered during forensic investigations can be considered a *trace*. Traces are physical materials that have been deposited or transferred during some event, and knowledge about these traces can be used to support the narrative reconstruction of that same event. When forensic scientists provide reports or act as expert witnesses, their contributions can become *evidence* in a case. This distinction between traces and evidence is important—forensic scientists examine traces, but it is only when the forensic scientist's work is presented in court that it becomes evidence. It is also important to note that expert witnesses can only give evidence about traces, and not about the merits of the case itself. The *triers of fact*, whether jury or judges, are responsible for making the final decision by combining each piece of evidence comprising the whole of the case before them. While equally valid when reporting results to police officers during an ongoing investigation, for the sake of simplicity the following discussion will be oriented towards adversarial court systems.

The factors outlined above have led to two broad forms of reporting for results obtained during laboratory examination of traces. The simplest form is a technical report, where observations of the recovered traces are provided alongside some qualifying statements. At the time of writing this thesis, technical reporting is the most prevalent approach for GSR evidence [237]. A typical report might include the number of inorganic particles found matching certain criteria, or the types of organic compound detected, and their relevance to GSR. This style of reporting has the advantage of being the most neutral and objective, but places a greater onus of evaluation on the end-user. In particular, defence positions are likely to be given only cursory mention in accompanying material, with phrases such as “environmental sources cannot be completely excluded”. It may be difficult for triers of fact to assign relative weights to pieces of evidence reported from different scientific disciplines.

An alternative is evaluative reporting, also known as the “case-by-case” approach. When using this style of reporting, experts try to estimate the likelihood of observing the evidence given a set of mutually exclusive propositions [238, 239]. By convention these are often denoted as “prosecution” and “defence” hypotheses (H_p and H_d), although this is not strictly necessary so long as the propositions are mutually exclusive. Any type of trace can be forensically evaluated under a model called the *hierarchy of propositions*, first proposed by Cook *et al.* in 1998, depending upon the issues under dispute [240]. Application of the hierarchical model to GSR traces is shown in Figure 4-1. At the most basic level, analysts must evaluate whether laboratory observations (particles or compounds and associated spectra) are more likely to occur if the trace is GSR or some other GSR-like material. This is called a *sub-source* query, covering the majority of the work conducted by forensic GSR analysts at present. At the *source* level, the question addresses how likely it was for the GSR trace to

arise from the specific shooting in question. Even more rigorous investigation is required to evaluate *activity* level queries, about the actions taken by any involved parties to cause the observed traces. The defence hypothesis for each of these propositions might be explicitly stated, but may also be summarized as “any and all other circumstances” as the burden of proof falls to the prosecution in jurisdictions using an adversarial court system [241, 242]. Finally there is an *offence* level, which must only be evaluated by the triers of fact. The evaluative reporting style is thought to allow triers of fact to leverage greater amounts of scientists’ expertise to assist their decision making, compared to a technical report.



GSR evidence is not necessarily the dominant factor in the overall investigative effort when dealing with shooting incidents. However, it has been shown to influence the decisions made by both people under investigation and triers of fact. A study recently published by Charles & Jonckheere (2022) examined the effect that expert GSR evidence had on the eventual verdict of criminal investigations, in a jurisdiction using evaluative reporting [243]. They found that when the outcome of a GSR report was inconclusive, verdicts were approximately evenly split between conviction and acquittal ($n = 19$). When the evidence was found to support the prosecutions’ version of events, the proportion of cases resulting in conviction increased to 70% ($n=16$). The likelihood of POIs confessing to their charges also increased when GSR evidence was presented. The authors stated that:

“Of 34 cases that were argued in court, (The GSR evidence of) 28 in our opinion were correctly interpreted and used by the court in its judgement. There were still 6 cases where, in our opinion, the court probably misinterpreted or even misused the report; 4 were incriminating, 2 were exculpatory”.

In one example, a trace evaluated at the *source* level was used by the court as support for an *activity* level proposition. In another the court interpreted a single particle, which in the expert’s opinion had little probative value, as incriminating. The prosecutor’s fallacy, where an expert’s opinion on the traces is mistaken for an opinion on the probability of someone committing the offence, was identified in some judgements. The study stated that there was no risk of unsound verdicts in the wider context of these specific cases. The issues were raised as a matter of scholarly interest, showing that even evaluative reports prepared using best practice may be misinterpreted by end-users lacking technical expertise. Nevertheless, evaluative GSR reports were found to be correctly used by courts *“in the vast majority of cases”* ^[243].

4.2.2 Conditional Probability

When using an evaluative approach, forensic scientists must strictly adhere to the principle of considering **the evidence given the propositions, and not the propositions given the evidence**. Mathematically this principle is expressed with the notation $P(\text{evidence} \mid \text{proposition})$ and falls under the branch of statistics known as conditional probability. This requirement ensures the proper functioning of expert witnesses within judicial systems for several reasons. Firstly it helps to formalise any assumptions made by the scientist during their evaluation; if the assumptions are changed, then the evaluation of the trace may also change. Secondly, it acts as a reminder to only give evidence within the area of expertise. *Expertise* will generally comprise technical analysis of specific traces, and previous knowledge on the behaviour of similar traces in general. Expertise does not extend to the circumstances of the case at large, which are to be considered solely by the triers of fact.

Conditional probabilities can be used in the discipline of forensic science to produce likelihood ratios (LRs). These ratios are a numerical way of communicating the “strength” of evidence, or the degree to which it supports one or other of the competing propositions. LRs are also a mathematical tool to facilitate Bayesian reasoning. At its core, Bayesian reasoning is a system whereby an initial set of beliefs in the likelihood of an event can be revised by considering new data. This has been formalized under the eponymous Bayes’ Theorem, presented as its “odds form” in Equation 4-1.

Equation 4-1: Bayes’ Theorem, odds form

$$\text{Posterior odds} = \text{prior odds} \times \text{likelihood ratio derived from evidence}$$

In the context of a courtroom, the prior and posterior beliefs about the narrative of a case are held by the triers of fact, with each item of evidence influencing their overall opinion.

The likelihood is calculated by forensic scientists as the ratio between two probabilities, shown in Equation 4-2. If the LR = 1, the evidence is equally likely regardless of the proposed explanation, and it is therefore not particularly significant or useful to the triers of fact towards answering the question at hand. A LR trending towards 0 represents greater support for the defence explanation, while LRs trending toward infinity represent a greater degree of support for the prosecution’s version of events.

Equation 4-2: General LR Equation

$$\text{Likelihood Ratio} = \frac{\text{Probability of observations given the prosecution hypothesis}}{\text{Probability of observations given the defence hypothesis}}$$

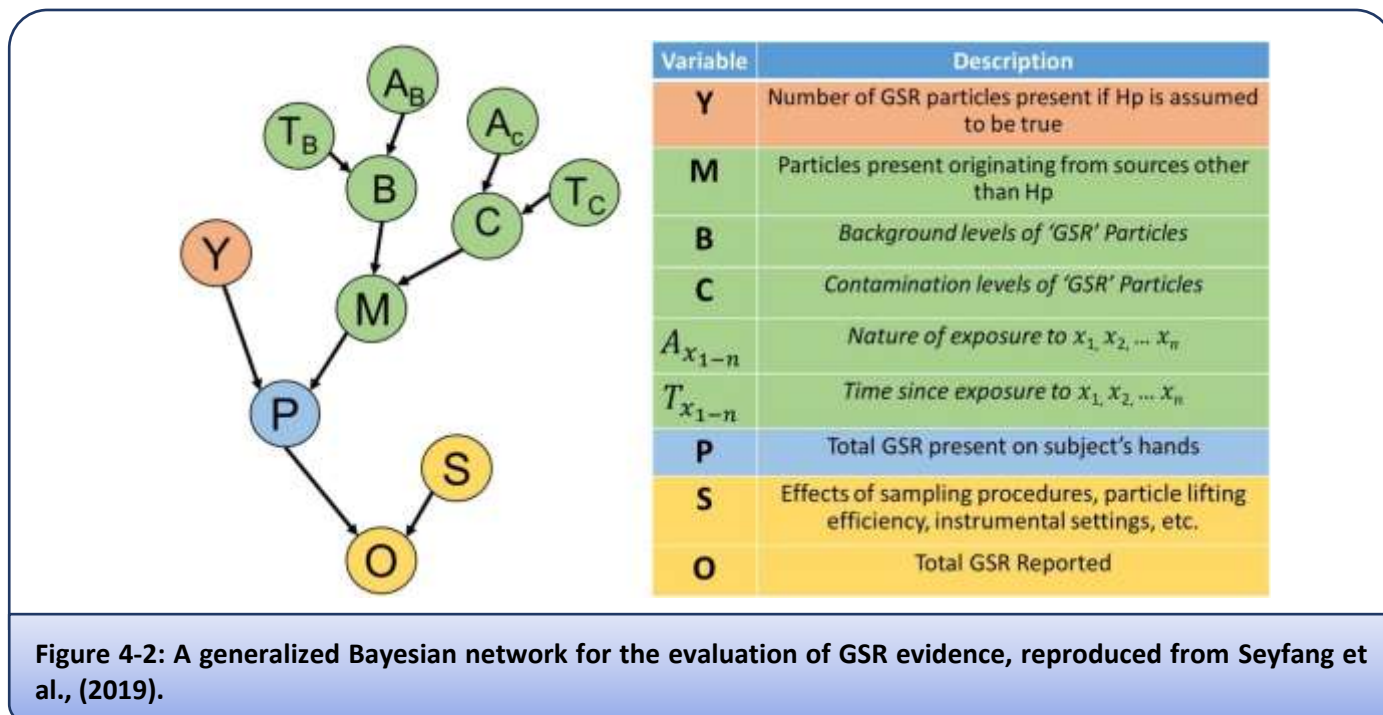
Having a numerical value for evidence strength is useful, as it provides a way for appropriately experienced scientists to combine or compare each item of evidence’s contribution to the case. To improve communication of results to those without any scientific or statistical training, verbal equivalence scales can be used to supplement likelihood ratios. These scales assign weightings to ranges of values. An example is provided in Table 4-1, adapted from the specific scale used by Martire *et al.* in a 2014 publication [244]. It should be noted that there are valid criticisms of verbal scales, such as those outlined by Morrison & Enzinger (2016) [245]. Further discussion on this topic has been provided by Maquis *et al.* (2016), among others [246].

Table 4-1: Verbal equivalent scale for numerical likelihood ratios. H_p = prosecution hypothesis, H_d = defence hypothesis		
Likelihood Ratio Range	Log₁₀ (LR) Range	Verbal Equivalent
0 - 0.000001	[< -6]	Extremely strong support for H _d
0.0001 - 0.000001	[-4, -6]	Very strong support for H _d
0.001 - 0.0001	[-4, -3]	Strong support for H _d
0.01 - 0.001	[-3, -2]	Moderately strong support for H _d
0.1 - 0.01	[-2, -1]	Moderate support for H _d
0.1 - 1	[-1, 0]	Weak or limited support for H _d
1	0	Evidence is neutral
1 - 10	[0, 1]	Weak or limited support for H _p
10 - 100	[1, 2]	Moderate support for H _p
100 - 1,000	[2, 3]	Moderately strong support for H _p
1,000 - 10,000	[3, 4]	Strong support for H _p
10,000 - 1,000,000	[4, 6]	Very strong support for H _p
>1,000,000	[> 6]	Extremely strong support for H _p

For more in-depth primers on applying conditional probability to forensic science, readers are directed to ANZPAA-NIFS' "An Introductory Guide to Evaluative Reporting" and "Fundamentals of Probability and Statistical Evidence in Criminal Proceedings" by Aitken, Roberts & Jackson [239, 247]. It is also relevant to acknowledge that the use of Bayesian probability theory in expert evidence has resulted in considerable controversy. Application of the above forms of LR for the presentation of evidence in a judicial setting has impassioned support from many authors in literature, especially those considering the issue from a theoretical perspective [248-251]. This has not necessarily resulted in widespread adoption by practitioners, including for GSR. Reluctance from forensic scientists has been attributed to practical concerns; often accurate evaluations cannot be made due to insufficient case-specific information or resources to obtain background data [237]. More fundamental opposition has been forthcoming from members of various legal communities, particularly through case law. Partially this may be due to misunderstanding the purpose and workings of the process itself, and high-profile misapplications during criminal trials [252, 253]. It is neither the intention nor within the scope of this work to address the legal arguments for or against the presentation of LRs in court. While ongoing, the discussion appears to be well outlined with thorough references to relevant cases by Fenton, Neil & Berger in their article "Bayes and the Law" (2016) [254]. Instead, Bayesian approaches are suggested as a useful lens through which to view presently obtained laboratory results.

4.2.3 Bayesian Networks for GSR evidence evaluation

There are many factors influencing the number of GSR particles that may be observed on a person of interest, spanning the hierarchy of propositions from the sub-source to activity levels. Starting with Biedermann, Bozza & Taroni in 2009, Bayesian networks have been constructed to signify the relationship between these variables for GSR evidence. Quoting from Taroni *et al.* (2004), Bayesian networks are graphical aids "... for representing relationships between characteristics of interest in situations of uncertainty, unpredictability or imprecision" [255]. BNs consist of interconnected nodes containing specific variables, with lines representing the flow of information through the system. Improved versions of Biedermann and colleagues' GSR network have been suggested in literature by Gauriot *et al.* in 2013, and Lucas and colleagues in 2018 [20, 256]. Figure 4-2, from Seyfang *et al.* (2019), illustrates an example of one such network constructed for the interpretation of GSR traces at the activity level [8]. There are nodes included for the detection of GSR due to actual recent firearm contact (Y), contamination during the collection procedure (C), and the background presence of GSR in the ambient environment (B).



4.2.4 Probability Distribution Functions

Probability distribution functions (PDFs) are mathematical models used to estimate how probabilities are allocated across a range of possible observations. They are often derived from empirical data, with analysts selecting two different data sets to represent the respective prosecution and defence hypotheses. The functions that best fit each set are calculated, and the ratio of the outputs from these functions at the value observed for the trace becomes the LR [257]. As the selection process is subjective and made given some conditions, Bayesian reasoning is also being followed to construct the LRs.

Several prior publications have suggested appropriate PDFs to apply to GSR evidence. In 2006 Cardinetti *et al.* proposed using Poisson distributions for both the numerator and denominator of a GSR LR [258]. This distribution specifically models discrete data such as the number of observed IGSR particles, and is known to often exhibit good fitting for rare events. Using data collected from two groups of police officers with dissimilar firearm-handling histories, the publication showed that observation of two or more GSR particles would produce positive LRs. Damary *et al.* (2016) agreed that the Poisson model seemed suitable for non-shooter models, but noted that proper validation would require a very large number of samples due to the rarity of observing GSR particles amongst this group [259]. Working with Cardinetti *et al.*'s data, these authors also demonstrated that a Negative Binomial model was more appropriate for modelling samples supplied by shooters, as the variance of these data were greater than accounted for under a Poisson model. Benzaquen *et al.* (2020) also used a mixture of Poisson and Negative Binomial functions, applying them to historical casework data. However they deliberately, although perhaps erroneously, used a single data set that included a mixture of shooters and non-shooters to develop both models [260].

Most recently, Maitre *et al.* (2022) demonstrated the application of probability density functions to model continuous data provided by LC-MS measurements of OGSR [261]. Samples were collected to represent competing propositions of traces arising from firearm use (H_p), and secondary OGSR traces occurring as contamination during an arrest (H_d). Three OGSR compounds' results were modelled independently using normal distributions based on their respective means and variances. The LRs broadly suggested support for a "contamination" hypothesis with low amounts of each OGSR compound, and increasing support for the "shooter" hypothesis with greater amounts of GSR. However, the precise LR values varied depending on which compound was being addressed, and whether a sample was collected from the dominant or nondominant hand.

A test case was provided by Maitre *et al.* using values close to the mean from the "contaminated" group to represent the observed trace [261]. Resultant LRs for the dominant hand were between 0.02-0.03; Using the verbal equivalent scale mentioned previously, this equates to moderate support for H_d , a seemingly fair assessment. Performing a similar calculation, but changing the simulated observed value, results in a very different outcome. If the mean value for DPA on a shooter's hand was observed, the LR is positive as expected. However the estimated magnitude is approximately 50^{58} . This is very extreme and probably not well-calibrated to a subjective understanding of the potential strength of this evidence. It is also presently unclear how this might compare to the values obtained from, for example, DNA evidence with the benefit of much larger databases through which to validate statistical analyses. These points were not explicitly stated by Maitre *et al.* but are apparent in Figure 6 of that publication displaying sensitivity analyses of the LRs to various peak-area inputs.

4.2.5 Multivariate Data: Machine Learning, Neural Networks, and Score-Based Approaches

When collecting multivariate measurements from traces, it is often feasible to create separate mathematical models and LRs for each variable. However as the dimensionality of the data grows, combining these models quickly becomes computationally complex. Difficulties can also arise when there are dependencies between the variables, or when some markers indicate support for one hypothesis, while others from the same trace support a conflicting hypothesis. Machine learning algorithms (MLAs) are increasingly employed as decision-making aids in tasks where rich data sets are available. This includes application to chemical analysis of traces, where the umbrella term *chemometrics* is applied [262].

Three general approaches can be seen in prior literature using MLAs on data from GSR traces. These include techniques based on decision trees, regression models or neural networks. All are examples of supervised learning, where the input data have already been associated with some form of categorisation prior to their introduction into the machine learning algorithm. Observations from samples collected under known conditions are fed into a program as training data, then the program incrementally adjusts weighting factors

until it can reliably assign samples into the chosen categories. The model should then be validated using previously unseen data, to detect over-fitting. Before discussing the specific techniques investigated in prior work, a distinction must be drawn between two different goals. Some authors have reported the use of machine learning to aid in evaluating whether a collection of signals represent a positive detection of GSR. Others instead perform comparative analyses of GSR traces to answer source-level queries i.e. matching GSR traces to each other or unfired ammunition. Preparing GSR data for comparative analyses with machine learning is more complex, as each pair-wise combination of samples in the database needs to be assigned a “similarity” score, rather than a single score per sample. While only the former is directly relevant to this thesis, literature on both are mentioned below.

MLA methods based on the concept of decision trees are probably the simplest to explain to laypeople of a jury. A decision tree is a flowchart-like structure with sequential binary decisions, leading to eventual categorisation of samples. As any single tree will likely perform poorly for new data beyond the training set, an extension of the concept called random forests may instead be used. Random forests use many decision trees each based on a random subset of explanatory variables, then average the results to make a final estimation of samples’ designations. Matzen *et al.* (2022) compared four MLA techniques and chose gradient-boosted tree classifiers as the basis for a model assigning scores to GSR stub samples based on match- (stubs collected from the same shooting incident) or nonmatch- (stubs collected from different incidents) probability [263]. However, these first-round scores did not produce inherently well-calibrated LRs, so Matzen chose to apply a logit transformation. This is equivalent to fitting a logistic regression model to the secondary scores, rather than the primary data. After calibration, LRs from the validation set fell between 10^{-3} and 10^4 with 0.04% of nonmatch samples falsely assigned $LRs > 1$, and 16% of matching samples falsely assigned $LRs < 1$. This bias towards the “non-match” condition is generally likely to benefit a defendant and as such is preferred for forensic applications. The magnitude of calculated LRs also correlated well with verbal scales and the empirically-expected frequency of “matches” between samples.

Regression algorithms seek to estimate the relationship between independent and dependent variables by applying weightings to each independent variable until the results for every sample fit a chosen parametric mathematical function. These models simplify complex data by assigning each sample a numerical score based upon raw analytical results, and then creating a single model from those scores. This two-stage process does entail a loss of information, but can empirically outperform univariate approaches given the difficulties inherent in modelling the original data [257]. It is important to understand that any LRs produced from scores refer to the likelihood of the scores, and not the specific features that produced those scores [264]. Logistic regression is a typical choice of function when the outcome of interest is binary, such as “GSR has/has not been detected”. This approach was investigated by Ott *et al.* (2020) for application to electrochemical data [156]. They found it was a workable classification method, with 97.3% of 350 non-shooter samples and 93.4%

of 395 shooter samples correctly identified by their algorithm. An alternative method is partial least squares-discriminant analysis (PLS-DA). This approach reduces dimensionality by projecting both independent and dependant variables to new vectors X and Y , then adjusting weighting factors to maximise covariance between the two [265]. PLS-DA is considered better than logistic regression for handling correlated variables, and data sets with low sample numbers compared to the number of predictor variables. Bueno & Lednev (2013) used PLS-DA when sorting samples collected from two different test ammunitions based on combined IR and Raman spectra [57]. They reported 100% accurate classification of 46 samples, although did not report the resultant distribution of LRs.

Artificial Neural Network (ANN) -based algorithms seek to classify samples into categories using parallel nodes that each apply weighting effects to input data, then iteratively pass the output to other nodes. Backpropagation steps are used to check that correct classification of training samples has been achieved. A benefit of such networks over simpler models is that they can more accurately map inputs to outputs when the variables exhibit complex interdependencies and/or produce nonlinear effects to the output. However for forensic settings, they have a distinct disadvantage that it is not necessarily intuitive to describe *how* each observation is affecting the final decision. A more thorough explanation of the concepts of ANNs as applied to chemometric applications was given by Marini (2009) [266]. In 2016 Bell *et al.* reported using ANNs as decision-making tools to evaluate ion-mobility spectroscopy (IMS) data, from a background population including known firearm users. The proportion of samples designated GSR-positive from the population by the algorithm was <5%, or <2% when LRs >10 were required [141]. Ott *et al.* (2020) also chose ANNs as their best performing MLA when compared against logistic regression and naïve Bayes classifiers. That study used electrochemical data as predictor variables, and ANN accurately classified 95.4% of 745 samples as either shooters or non-shooters [156]. There was a slight bias towards false negatives (6.58%) compared to false positives (2.67%). In Feeney *et al.* (2022), members of the same research group applied a ANN to LC-MS/MS data from 400 samples, with accuracies between 90-99% depending on the subpopulation's risk profile for GSR exposure [267]. This publication went further in assigning LRs, with samples from known shooters returning LRs around 10^{10} and non-shooter samples at "low risk" of contamination returning values of 10^{-10} .

Finally, Gallidabino *et al.* (2019) described a process they named "quantitative profile-profile relationship" modelling to use GC-MS data from the headspace of expended cartridges to predict the composition of unfired powders [268]. Fourteen different machine learning techniques were compared for their ability to predict the log-peak area of each compound in a smokeless powder sample based on a fired-cartridge headspace sample. A combination of models was eventually chosen, with a different ML method used to forecast each compound's peak in the predicted profile.

4.3 Aims

Firstly, this chapter aims to provide a quantifiable measure of the extent to which the forensic value of given GSR traces can be improved by considering OGSR and IGSR data in combination. This was addressed using a Bayesian updating model, focussing on the calculation of positive and negative predictive values following the process used in medical diagnostic testing.

Secondly, the chapter explores how the outputs obtained during instrumental analyses can be interpreted through statistical models. This approach would enable a more holistic assessment of various propositions that a forensic scientist may have to evaluate during casework, and is suggested prior to the implementation of evaluative reporting procedures. Initially, separate probability distribution functions were used to model each predictor variable. As these performed poorly, multivariate approaches were subsequently applied.

4.4 Calculations and Discussion

Empirical results detailed during the preceding chapter, specifically from a sampling-survey of the hands of shooters and non-shooters, have been used to build mathematical models and inform theoretical discussion. These samples were subjected to testing for the presence of organic and inorganic GSR using separate analytical instruments. Initially, dichotomous assessments of positive or negative are used, based on the qualitative criteria established in Chapter Three. Later, quantitative models are built on the amounts of GSR detected for each variable and subcategory of survey participants.

Throughout the chapter, there will be much discussion about competing hypotheses. These are modelled by samples collected from volunteers categorised as either “recent shooters” or “non-shooters”, and these names are retained. It is not intended to imply that all activity-level propositions have been modelled; for example GSR exposure to POIs as bystanders or during arrest have been comprehensively demonstrated in literature but are not addressed herein. Calculations of LRs to compare specific ammunition sources is also ignored, with all shooters considered equal regardless of ammunition/firearm combinations.

4.4.1 Predictive Power of Diagnostic Tests

The overall goal of this thesis was to investigate an integrated approach to analysing both the organic and inorganic portions of GSR traces. A multi-instrumental process using both SEM-EDS and HPLC-MS was proposed. Before the method could be further implemented, it was desirable to consider some criteria by which the efficacy of the testing processes can be measured. It was even more advantageous to consider the *change* in efficacy compared to existing methods. As integrating the results of two tests into a single outcome involves updating belief on the basis of further evidence, a Bayesian methodology is again appropriate.

4.4.1.1. Results of a Single Test per Trace

A simple way to assess the performance of diagnostic tests is to compare the sensitivity, selectivity, and rates of false positives/negatives. Detection rates achieved using the relevant instruments during the hand-sampling survey discussed in Chapter ThreeChapter 3: are expressed in Table 4-2; samples were initially designated “positive” when they met qualitative criteria only. The relative frequency of observing IGSR on a person, given that they were a recent shooter, was found to be equal to one (a certainty). The frequency of observing IGSR on a person, given that they were a non-shooter, was one-in-thirty or 0.03. The LR that would be estimated for a positive IGSR test result, using those values to populate Equation 4-2, should be $1.00/0.03$, or approximately 30. As this is >1 , it can be said that the evidence is useful for distinguishing between the two proposed explanations, and favours the prosecutor’s explanation of events. A similar calculation modelling a positive result from the OGSR test returns an indeterminate value, as no false positives were observed in the comparatively small sample set ($P(\text{OGSR+} | \text{non-shooter}) = 0, n=30$). This leaves a null value for the denominator in Equation 4-2. However for comparison purposes it could be assumed that a LR of >20 is achievable using the substitution $\text{LR}_{\text{OGSR+}} = (20/30) / (<1/30)$. The LR calculated for a positive result using either instrument then provides at least moderate support for the proposition that the sample belonged to a recent shooter.

Table 4-2: Observed Results for Each Test and Subgroup				
Measure of Performance		Bayesian Notation	Observation	Probability
SEM-EDS	True positive rate (sensitivity)	$P(\text{IGSR} + \text{Shooter}) =$	30/30	1.00
	False negative rate	$P(\text{IGSR} - \text{Shooter}) =$	0/30	0.00
	True negative rate (specificity)	$P(\text{IGSR} - \text{Non-shooter}) =$	29/30	0.96
	False positive rate	$P(\text{IGSR} + \text{Non-shooter}) =$	1/30	0.03
LC-MS	True positive rate (sensitivity)	$P(\text{OGSR} + \text{Shooter}) =$	20/30	0.66
	False negative rate	$P(\text{OGSR} - \text{Shooter}) =$	10/30	0.33
	True negative rate (specificity)	$P(\text{OGSR} - \text{Non-shooter}) =$	30/30	1.00
	False positive rate	$P(\text{OGSR} + \text{Non-shooter}) =$	0/30	0.00

Note that the conditional probabilities for positive and negative detection rates are expressed as $P(\text{evidence} | \text{propositions})$. This aligns with the conventions required of forensic scientists when presenting their findings to triers of fact. The point is reiterated because the transposed condition of $P(\text{proposition} | \text{evidence})$, termed the positive predictive value (PPV), is arguably the more useful number when considering the accuracy of a result provided to end-users [\[269\]](#). The PPV is commonly applied to clinical tests in a healthcare setting, although difficulties in correctly applying sensitivity, specificity and PPV to decision-making are shared between medical, forensic, and legal practitioners [\[269-273\]](#). That is not to say that the PPV itself should be included as part of a report, but rather that it is an appropriate measure when comparing different laboratory tests internally. It cannot be understated that $P(\text{evidence} | \text{propositions})$ and $P(\text{proposition} |$

evidence) are explicitly not equivalent. To state that they are is to commit the “prosecutors’ fallacy”, a well-documented courtroom phenomenon [274].

The intention of examining samples for GSR is to inform investigators as to whether an individual was involved in a shooting incident. Therefore, it is useful to know how likely a person is to actually be a shooter, given that they have returned a positive test result for GSR (or, $P(\text{shooter} \mid \text{GSR} +)$). The answer to this question is related to both the true and false positive rates of the test outlined in Table 4-2 above, but also the prior background distribution of the condition in question (*base rate* or *prevalence*). In the hand-sampling survey, the true status of each participant as a shooter/non-shooter is known in advance. Therefore, it is possible to calculate the PPV of each test directly from observation. It is also straightforward to calculate the negative predictive value (NPV), or the likelihood that any individual is a non-shooter given that they returned a negative test. The results of these calculations are summarized in Table 4-3.

Table 4-3: Predictive Values (Single Test)				
Measure of Performance		Bayesian Notation	Observation	Probability
SEM-EDS	Positive Predictive Value	$P(\text{Shooter} \mid \text{IGSR} +) =$	30/31	0.968
		$P(\text{Non-shooter} \mid \text{IGSR} +) =$	1/31	0.032
		$P(\text{Shooter} \mid \text{IGSR} -) =$	0/29	0.00
	Negative Predictive Value	$P(\text{Non-shooter} \mid \text{IGSR} -) =$	29/29	1.00
LC-MS	Positive Predictive Value	$P(\text{Shooter} \mid \text{OGSR} +) =$	20/20	1.00
		$P(\text{Non-shooter} \mid \text{OGSR} +) =$	0/20	0.00
		$P(\text{Shooter} \mid \text{OGSR} -) =$	10/40	0.25
	Negative Predictive Value	$P(\text{Non-shooter} \mid \text{OGSR} -) =$	30/40	0.75

The results suggest that LC-MS has a greater PPV than SEM-EDS, despite the latter’s much higher true positive rate, as no false positives were observed *via* LC-MS. *Ipsa facto*, if two randomly selected individuals each tested positive using a different test, the individual who was tested using LC-MS is very slightly more likely to be a shooter. On the other hand, LC-MS has a much poorer negative predictive value at $P(\text{Non-shooter} \mid \text{OGSR} -) = 0.75$. This would mean that at least one quarter of the individuals who return a negative result for GSR *via* the LC-MS test were in fact shooters. Note that the sample size of this experiment is much too small to expect this assessment of the two instruments to hold unconditionally; rather it is a limited data set to illustrate an appropriate use of PPV values.

4.4.1.2. Results of Sequential Testing on a Single Trace

Section 4.4.1.1 described the calculation of PPVs for two different qualitative GSR-detection tests individually. However, the proposed laboratory method allows for both tests to be applied to samples sequentially. It is reasonable to expect that more accurate results can be obtained, as false-positive and false-negative errors can be partially mitigated. Recall that Bayesian methods are used to revise prior beliefs by

incorporating additional data; consequently they provide a convenient framework for showing that the use of both SEM-EDS and LC-MS on fractions of the same trace can lead to increased confidence in inferences. This can be visualized using tree diagrams. Figure 4-3 depicts the process of calculating the PPV of a single test on a given GSR sample from the dataset obtained in Chapter Three, starting from first principles. Since all information about the status of test results and true status are known, the conditional probability equation (Equation 4-3) can be used. If limited information were available, it may instead be possible to use Bayes Theorem to reverse the direction of conditional probability (Equation 4-4). In the current context, the prevalence of shooters in the sample population is 0.5. This has the effect of being a known, unbiased prior value. The prior odds are updated using the results of the first test, for example SEM-EDS. This represents the current GSR-testing paradigm in many operation laboratories. The computed values can be cross-referenced with the summary in Table 4-3 above, as the calculated and observed values will match when an accurate prior probability is applied.

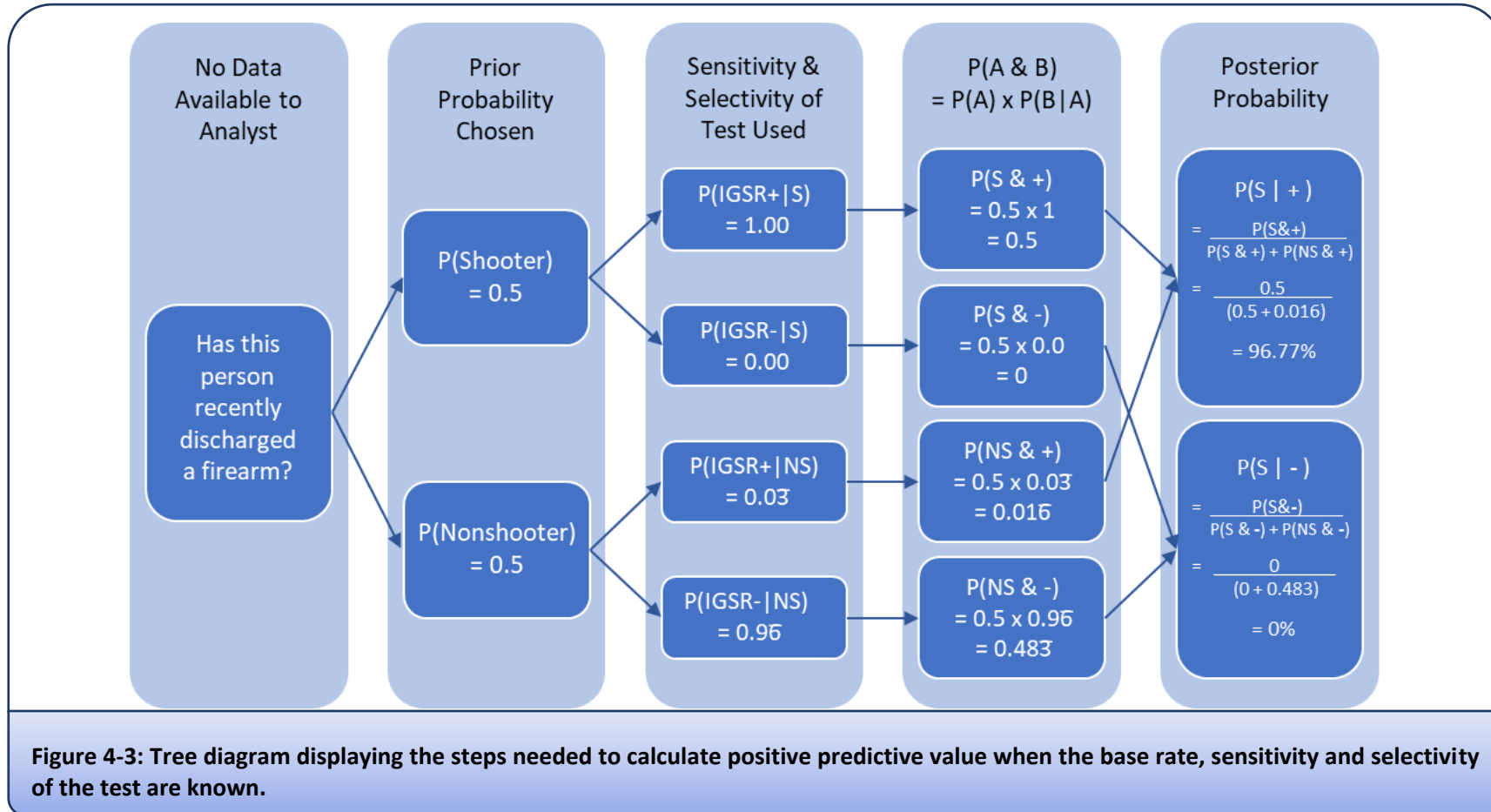
Equation 4-3: (PPV)

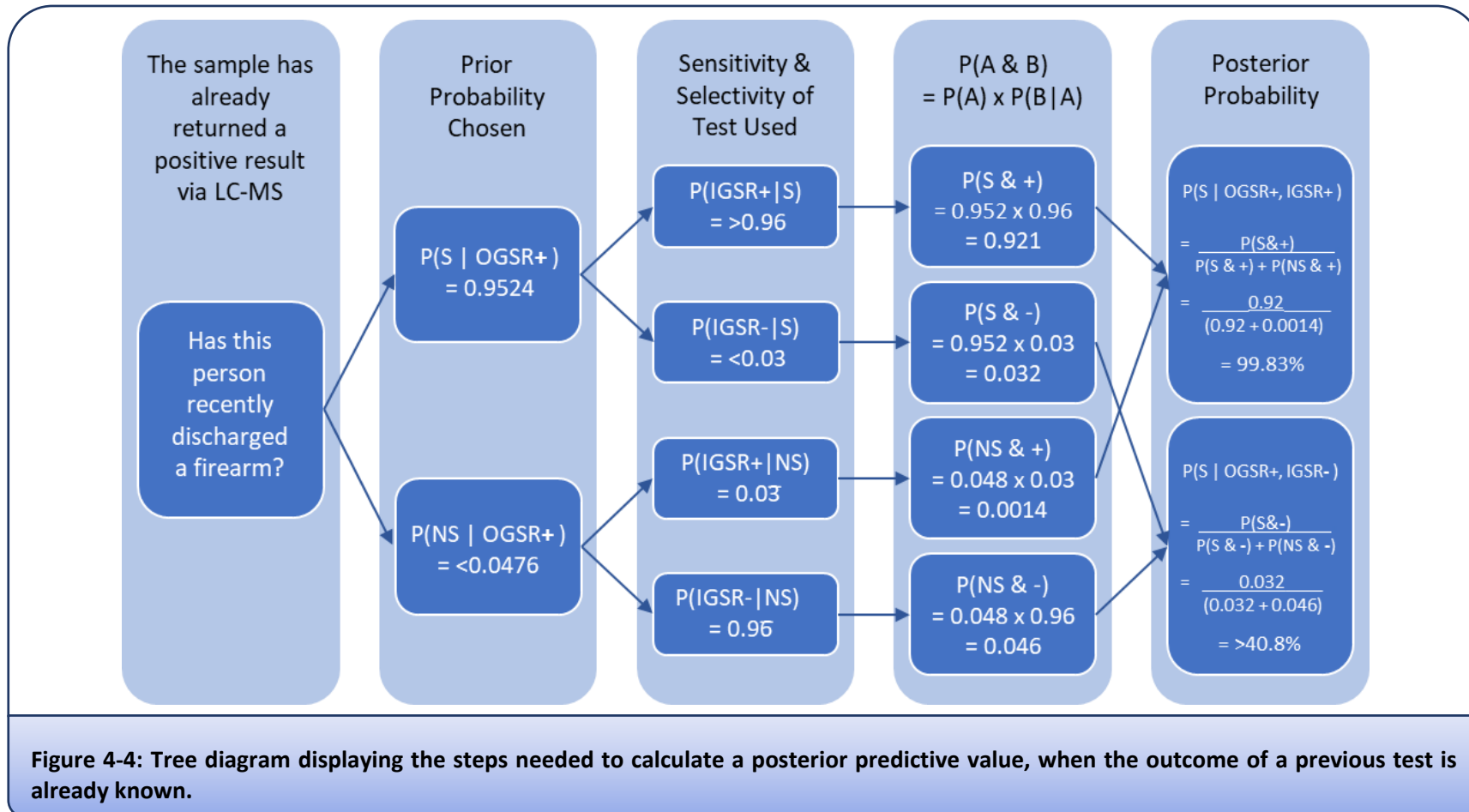
$$P(\text{Shooter} \mid \text{Positive Test Result}) = \frac{P(\text{Shooter} \ \& \ \text{Positive})}{P(\text{Positive Test})}$$

Equation 4-4: Bayes' Theorem, conditional probability form

$$P(\text{Shooter} \mid \text{Positive Test Result}) = \frac{P(\text{Positive Result} \mid \text{Shooter}) \times P(\text{Shooter})}{P(\text{Positive Test Result})}$$

When considering the diagnostic value of two separate tests performed sequentially, the PPV of one test is chosen as the prior probability. This value is then updated by the expectation of the result of a second test giving a true result [\[271\]](#). Since the LC-MS test for OGSR was performed first in the laboratory, it was selected as the prior value for Figure 4-4. However, the observed frequency for $P(\text{Shooter} \mid \text{OGSR+})$, $n=30$ was 20/20, or 1.00. As it is unlikely that no false positives would ever occur in an arbitrarily large sample set, the more conservative false-positive estimate of $P(\text{OGSR+} \mid \text{Non-shooter}) = (<1/30) = <0.033$ is substituted. A similar substitution was performed for the likelihood of a false negative *via* SEM-EDS. This can also be described as the likelihood that an individual really is a shooter after returning two positive readings, or $P(\text{Shooter} \mid \text{OGSR+}, \text{IGSR+})$. The findings of following a similar Bayesian revision process for each combination of positive and negative results for the respective tests is summarized in Table 4-4.





P(Shooter IGSR+) =	96.67%
P(Shooter IGSR-) =	<3.45 %
P(Shooter OGSR+) =	>95.24 %
P(Shooter OGSR-) =	25.00%
P(Shooter OGSR+ , IGSR+) =	>99.83 %
P(Shooter OGSR- , IGSR-) =	<1.18 %
P(Shooter OGSR+ , IGSR-) =	>40.82 %
P(Shooter OGSR- , IGSR+) =	>90.91 %

*note that discrepancies between Table 4-3 and Table 4-4 are due to making an assumption that the n+1 sample of each category may be incorrect, if that category otherwise returned a value indicating absolute certainty.

The findings in Table 4-4 display several measures of the combined testing regime’s performance on the examined dataset. The positive predictive values of either test alone are of similar magnitude, and suggest that for >95% of positive results, the person tested had in fact recently discharged a firearm. When an integrated testing regime was applied, the probability of someone being a shooter given that they returned two positive results rises to 99.83%. Therefore these findings indicate the additional test was beneficial, and offers improvement upon the state of the art. The difference seems even more stark when considering the corollary likelihood that a POI was actually a non-shooter, despite a finding of association with GSR. Instead of a 3.33% chance that the result(s) represent a false positive, there is now a <0.17% chance. Meanwhile the estimated likelihood of a shooter being incorrectly classified as a non-shooter by returning two sequential false negatives is <1.18%.

Additional understanding about the relative strength of each test is revealed by comparing the outcome when the two tests give conflicting information. For example, the PPV of a combined test where IGSR is observed and OGSR is not observed is >90%, because the observed false negative rate was high using LC-MS and very low using SEM-EDS. When only the LC-MS test suggests association with GSR, the probability that the participant was a shooter is somewhere >40%. This estimate is not very informative. It also cannot be substantiated by observation, as there was no data point that was simultaneously positive for OGSR and negative for IGSR. Taken together, it would seem that SEM-EDS is the more powerful of the two techniques for predictive value.

Again, it is crucial to avoid the temptation of making the prosecutor’s fallacy. It is accurate to state that $P(\text{Non-shooter} | \text{OGSR+ , IGSR+}) < 0.17\%$ within the context of the experiment, as a measure of test efficacy. However it is neither appropriate or accurate to infer a probability of innocence of 0.17% for a POI who returned the same test results while under investigation for a shooting. These results are only valid because the true status of each participant, and their distribution in the sample set, are known in advance. The same results cannot be presented in court as indicators of evidential strength for two key reasons. Firstly in a real case, the distribution of shooters in the population is not one-in-two, and the true value may not be known

with any degree of certainty. As background prevalence of the tested condition drops, the relative impact of the false-positive rate (which does not vary across test populations) becomes much stronger. Secondly the calculations above are made on the basis of only two pieces of information – the results of the two tests. During a criminal trial, the triers of fact may (and almost always will be) in possession of further pieces of information that they must take into consideration.

4.4.2 Independence of Diagnostic Results

There is another piece of information that can be determined using the binary categorisation of OGSR and IGSR test outcomes. These are ostensibly two independent tests, as they assess different physical material originating in separate components of the original ammunition. However, are the results independent in the statistical sense? If they are, the probability of observing each can simply be multiplied to form a combined LR, which has the potential to provide much stronger evidence ^[247]. If instead the conclusions are dependant, then knowing the outcome of one test can tell an observer something about the range of possibilities that may occur in the other test. In that case, the nature of the interdependency/relationship needs to be accounted for when attempting to combine results mathematically. Two simple tests for statistical dependency are shown in Equation 4-5 and Equation 4-6.

Equation 4-5:

If $P(A|B) = P(A)$, then results are independent

$$P(\text{IGSR} + | \text{no further info}) = 0.5$$

$$P(\text{IGSR} + | \text{OGSR} +) = 1.00$$

$$0.5 < 1.00$$

∴ Variables are dependent

Equation 4-6:

If $P(A \& B) = P(A) \times P(B)$, then results are independent

$$P(\text{IGSR} + | \text{no further info}) = 0.5$$

$$P(\text{OGSR} + | \text{no further info}) = 0.33$$

$$P(A) \times P(B) = 0.16$$

$$P(\text{IGSR} + \& \text{OGSR} +) = 0.33$$

$$0.1667 < 0.3333$$

∴ Variables are dependent

Using either equation, results from the two instruments used for the experiment were shown to be statistically dependent. This agrees with a common-sense assessment; a person with OGSR on them will be more likely to also have IGSR compared to some other randomly selected individual. While the tests

themselves are orthogonal, their results can be linked through origins in the same trace. However, this proposal may not hold under some defence propositions; innocent sources of IGSR-like contamination do not necessarily produce OGSR compounds, and *vice versa*.

As the HPLC-MS approach to GSR detection requires significantly less time, labour and resources compared to SEM-EDS, it has potential as a triaging tool prior to microscopy. This is only possible if the results are dependent in some way. In this study the frequency of observing GSR particles by SEM-EDS was increased if OGSR compounds had already been detected using LC-MS, compared to having no prior indication. If OGSR compounds were not found to be present, the likelihood of later observing particles was decreased. However, under the modelled extraction method there remains a one-in-four chance that a sample returning no chromatographic peaks for OGSR compounds will later be found to contain IGSR particles. This is one reason amongst several why it is recommended that SEM-EDS should remain the preferred technique. Extraction for LC-MS should be considered to better target investigative resources and to provide complimentary analytical information.

4.4.3 Summary of Qualitative Results

Bayesian analyses were applied to simplified categorical outcomes generated using LC-MS and SEM-EDS testing for the presence of GSR on 60 samples evenly divided between shooters and non-shooters. This was explicitly for the purpose of evaluating the potential benefit of combining testing techniques, not assigning likelihood ratios to the participants. SEM-EDS alone did not fail to detect any of the shooters, but resulted in a single false positive. LC-MS alone did not return any false positives, but missed 10 of the 30 shooters. Each instrument individually had similar positive predictive values at >95%. When the tests were combined sequentially, this rose to >99.83%. Therefore the findings support using sequential, orthogonal testing to improve the correct recognition of samples' shooter status. Prior knowledge of the OGSR status of a sample was found to be informative towards the subsequent frequency of finding IGSR. This is an indicator of statistical dependency between the two results. Again the use of an integrated testing regime is endorsed by observation, in order to prioritise stubs with a high likelihood of success using the current best-practice test.

To the best of the authors knowledge, this is the first study to distinctly model the outcome of combining separate organic and inorganic GSR test results in a detection role. This is despite three previous approaches:

1. Only one of the two components of a GSR trace is considered (typically IGSR).
2. Independent analysis of the OGSR and IGSR portions of the same trace is demonstrated. Chemical information from each test is used to bolster a qualitative inference that GSR has been detected.
3. Elements of both components are tested using a single technique. New criteria for what may constitute unambiguous identification are proposed *ad hoc*. No particular importance is placed on elucidating the effects of different parts of the trace on the final designation.

Consequently, comparisons between PPV values are suggested for consideration to assess the improvement offered by any pair (or greater number) of sequential analytical methods applied to subsamples of a single trace. They can also be a useful addition to reporting false-positive and false-negative rates to allow comparison between studies. Nevertheless, the present report does have two weaknesses that should be addressed with further research. A small convenience sample (n=60) was investigated, due to limitations on SEM access. While some generalizations can be made, more accurate data could be collected by monitoring method performance across much larger sample populations.

Also limiting generalization of inferences onto casework is the fact that binary designation of samples to either “positive” or “negative” categories was applied. In particular, a single particle caused the IGSR false-positive under the formalized, prescriptive approach used for assigning specimens. This is not likely to be presented without qualifying comments in any real case, and in some jurisdictions would be considered an insufficient amount of material to be considered “positive” for GSR. Additionally, eight of ten false-negatives assigned using LC-MS were caused by disregarding samples that only returned a reading above LOD for one compound; including these as positive results would drastically alter calculated likelihoods. Further nuance was lost by not considering the magnitude of each GSR trace (counts and/or concentration). The use of quantitative measurements of IGSR to calculate LRs has a solid basis in literature, although differing models have been suggested [20, 258-260, 275]. Quantitative calculations also allow better evaluative reporting at the activity level, and modelling of effects of transfer or persistence over time. Now that data are available to support integrated testing as both informative and statistically dependent, further work investigating the probative combination of quantitative results can be attempted.

4.5 Univariate, Quantitative Models of GSR Evidence

When examining samples for GSR, it is currently considered best-practice to compare the chemical composition and morphology of recovered traces against formal written criteria as described above. In some cases, scientists may also perform statistical calculations to support evaluative reporting, using only *characteristic* IGSR as inputs. This approach discards potentially useful information from the magnitude of other components in recovered traces. Quantitative measurements can be used to better distinguish between support for competing hypotheses, especially as the issues at hand move up the hierarchy of propositions. Therefore, there is interest in examining whether the compounds representing OGSR can be modelled using probability distribution functions (PDFs) in a similar fashion to characteristic IGSR particles.

The experimental results obtained in Chapter Three were divided into 16 data sets: eight GSR markers for each shooter or non-shooter sample. However, no non-shooter sample returned an analytical measurement above the LOD for organic compounds. This made them unsuitable for PDF modelling, a known problem when trying to capture rare events using small data sets [259]. Furthermore, few to no instances of detectable

dinitrodiphenylamine or methyl centralite were observed amongst the shooter subpopulations. Following Maitre *et al.* (2022), the remaining 7 sets (IGSR for both shooters/non-shooters, and 5 OGSR markers for shooters only) were fitted against many different parametric PDFs, and metrics for goodness-of-fit were calculated [261]. These represent potential distributions to model H_p for LR calculation. All instances below the respective LODs were substituted with the arbitrarily chosen 10^{-2} , to avoid algebraic errors for functions that are undefined at $x=0$. The automatic distribution fitting tool of Addinsoft Corporation's XLStat Life Science package was first used to estimate p-values for each distribution using Sturge's Rule and the Kolmogorov-Smirnov test, shown in Table 4-5 [276]. Higher p -values are an indication of greater suitability of the proposed distribution. If the p -value exceeds an alpha threshold of $\alpha = 0.05$, then the hypothesis that a data set fits a particular distribution cannot be rejected.

Table 4-5: p - values calculated for the data under each parametric PDF							
	S IGSR	EC	Ak	DPA	NO.DPA	NO ₂ .DPA	NS IGSR
Log-normal	0.629	0.255	0.123	<0.001	<0.001	<0.001	<0.001
Gamma	0.246	0.749	0.042	<0.001	<0.001	<0.001	<0.001
Beta	0.101	<0.001	<0.001	0.011	<0.001	<0.001	<0.001
Negative binomial	0.101	<0.001	<0.001	<0.001	<0.001	<0.001	<0.001
Exponential	0.095	0.002	<0.001	<0.001	<0.001	<0.001	<0.001
Logistic	0.048	0.004	<0.001	0.002	0.005	<0.001	<0.001
Normal	0.024	0.002	<0.001	0.002	0.010	<0.001	<0.001
Chi-square	<0.001	0.001	<0.001	<0.001	<0.001	<0.001	<0.001
Student	<0.001	<0.001	<0.001	<0.001	<0.001	<0.001	<0.001

Using the present sample set, diphenylamine and its derivatives were not fit well by any common parametric distributions. Based on the results from IGSR particles, ethyl centralite and akardite, two PDFs were selected for further testing to represent H_p . The p -values suggested that these data were best fit by the Log-Normal and/or Gamma functions. Those functions have a high degree of positive skewness, a consequence of some fundamental observations about the underlying traces. While the concentration of any single OGSR compound in each sample is likely to be small, occasional observation of larger concentrations is not unexpected. The expected likelihood decreases as the concentration increases. The functions and their parameters are shown in Figure 4-5, overlaid onto histograms displaying the observed data for each GSR marker. The Gamma function specifically is an equivalent to the Poisson PDF used by other authors for modelling counts of IGSR particles, noting that the former is appropriate for continuous data while the latter is restricted to discrete data. It should also be noted that while PDFs have been calculated for all variables, those shown in Figure 4-5 (d-f) should be rejected based on their p values (they poorly fit the data).

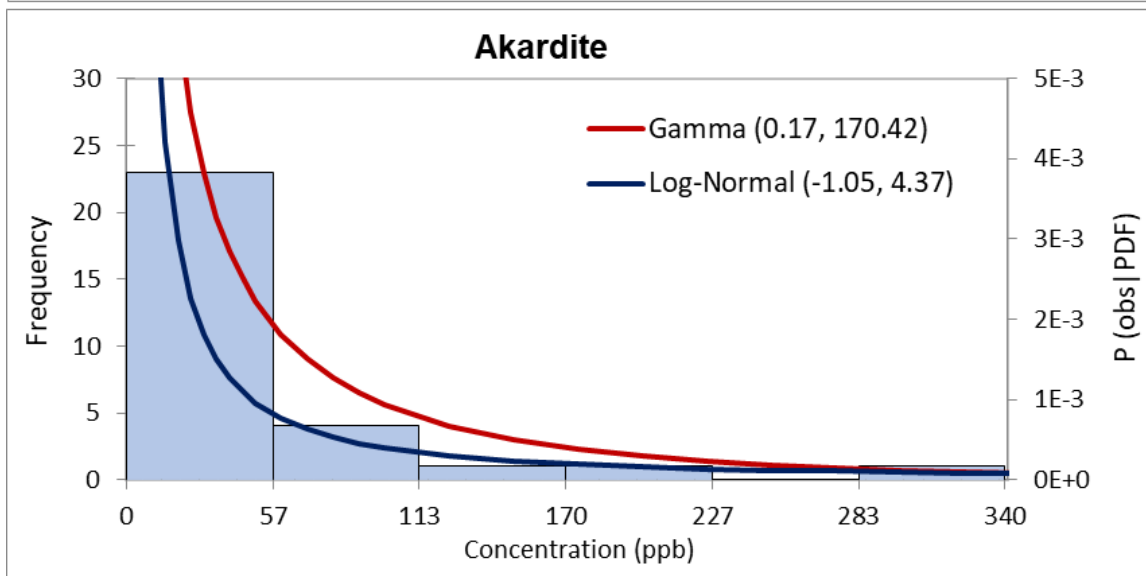
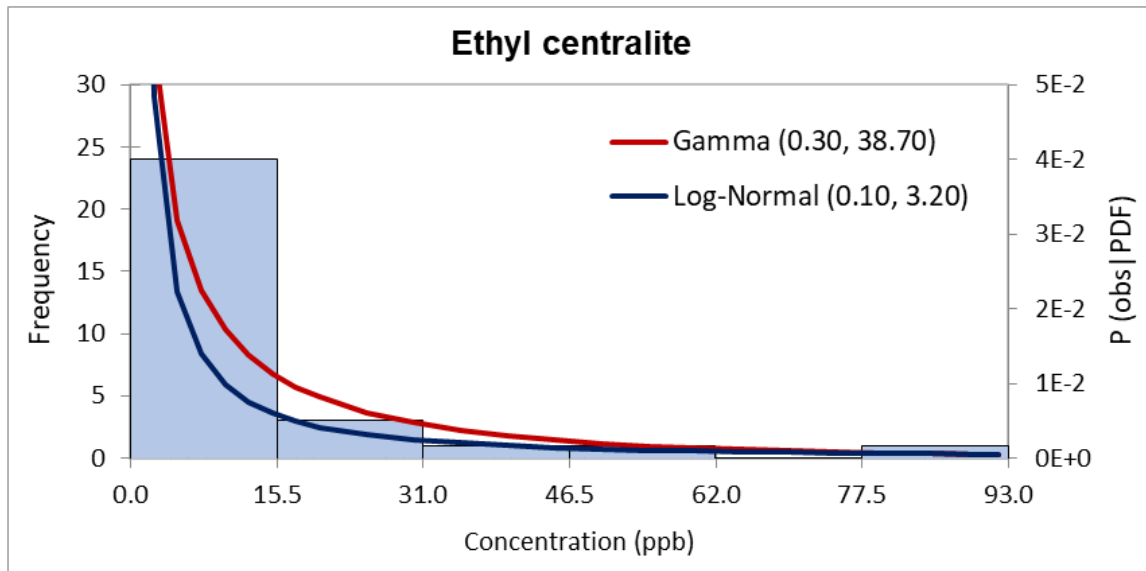
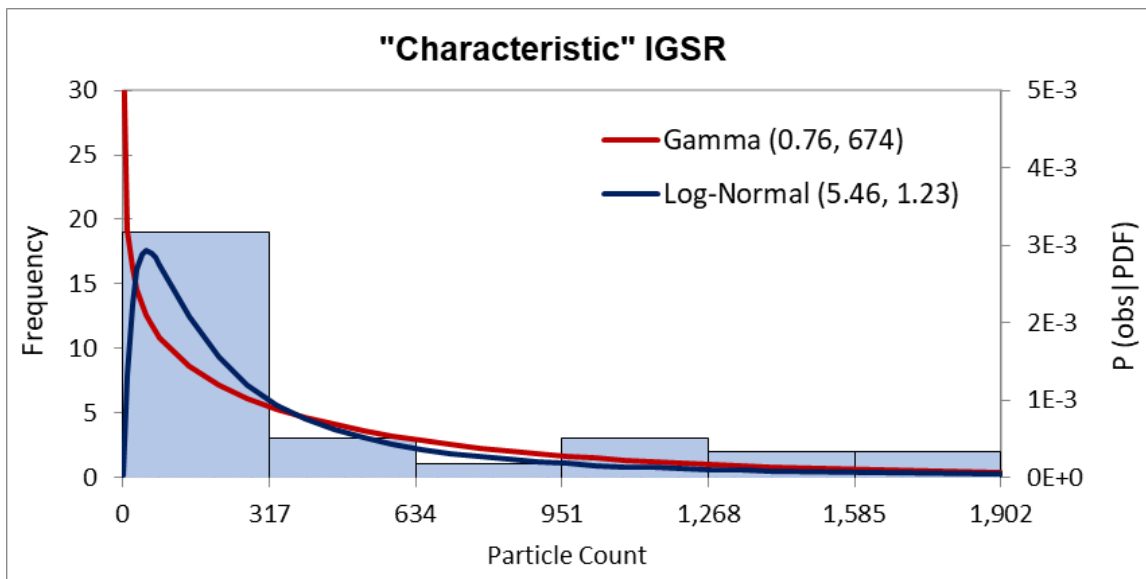


Figure 4-5 a-c: Quantized observations of GSR loading, and calculated PDFs

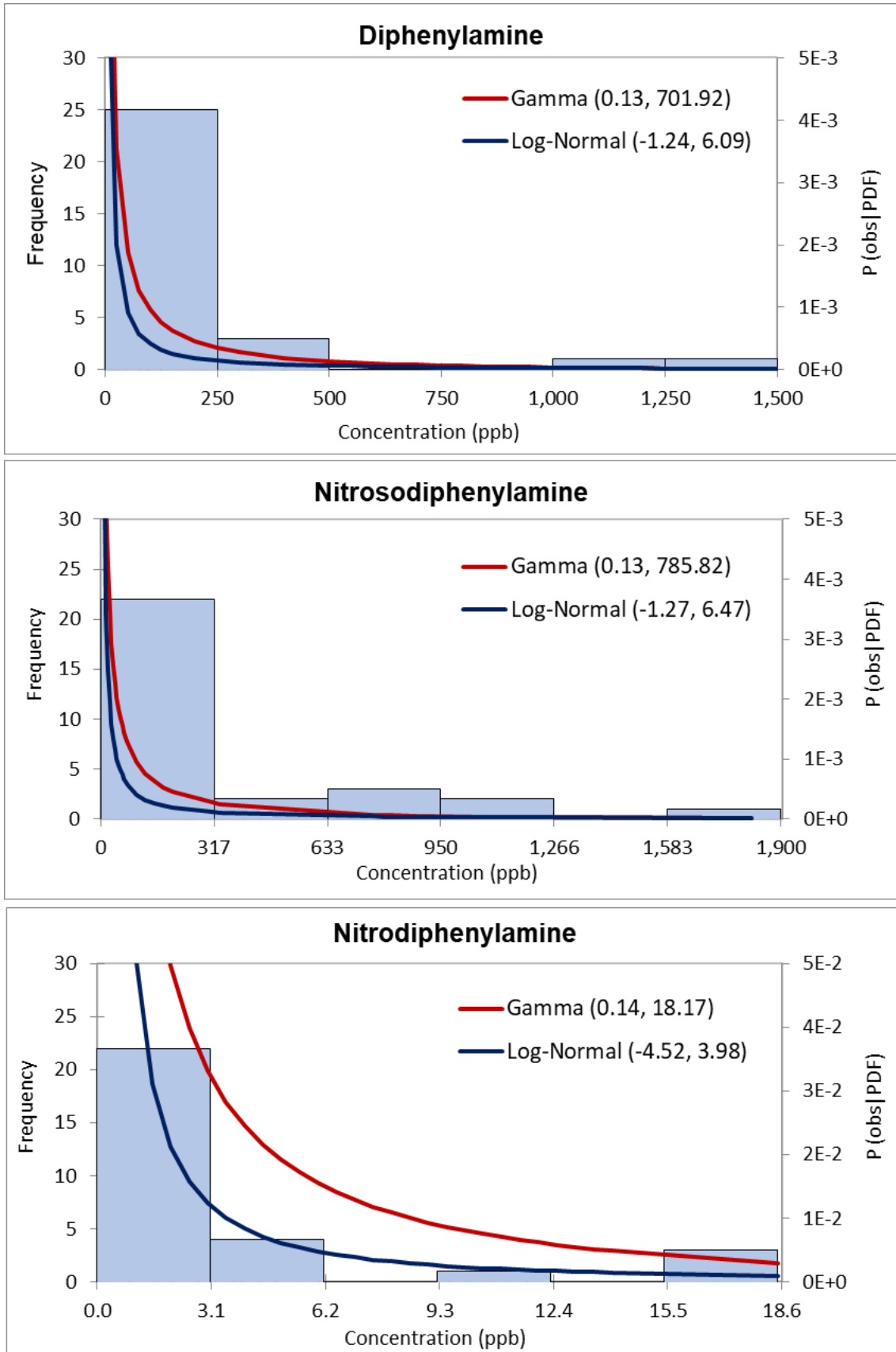


Figure 4-5 d-f: Quantized observations of GSR loading, and calculated PDFs.

A single characteristic IGSR particle was detected amongst the non-shooter samples. This allowed the set to be modelled using a Poisson function in the same manner used by Cardinetti in 2006 and Damary in 2016 [258, 259]. In turn, LRs could be calculated over a range of observed particle numbers to compare the following competing hypotheses:

H_p: The sample originated from a person that recently fired a gun

H_d: The sample originated from a person that has no recent involvement with firearms

Table 4-6 shows the LRs obtained using a Poisson distribution to represent H_d, and each of the two PDFs taken from Figure 4-5(a) for H_p. While the shapes of the PDFs approximately track one another for larger particle counts, there are important differences for smaller observed counts. Firstly, the LR for zero characteristic particles is 0.03 under the Gamma model, but 10^{-6} using the Log-Normal model. These equate to “moderate” and “extremely strong” support for H_d, respectively [244]. None of the participant shooters were actually free from GSR, suggesting the Log-Normal model is a better representation of these data. However it may not be accurate to generalize the model to broader POI data sets, as in practice there are many reasonable explanations why a recent shooter may not produce any IGSR when sampled [9, 24]. Each model also crosses the threshold from supporting H_d to H_p at a different number of particles (two vs. three particles). Once six or more particles are observed, the numerical LRs continue to rise beyond the upper limit of the verbal equivalence scale.

Observed Particles	Gamma Model		Log-Normal Model	
	Numerical LR	Verbal Equivalent	Numerical LR	Verbal Equivalent
0	0.03	Moderate support for H _d	<math><<1 \times 10^{-7}</math>	Extremely strong support for H _d
1	0.2	Weak or limited support for H _d	5×10^{-4}	Moderately strong support for H _d
2	9	Weak or limited support for H _p	0.2	Weak or limited support for H _d
3	7×10^2	Moderately strong support for H _p	33	Moderate support for H _p
4	8×10^4	Very strong support for H _p	6×10^3	Strong support for H _p
5	1×10^7	Extremely strong support for H _p	1×10^6	Very strong support for H _p
6	2×10^9	Extremely strong support for H _p	3×10^8	Extremely strong support for H _p

Unfortunately, it was not possible to create a justifiable PDF to model H_d for organic GSR markers using the present sample set, as no instances of detection occurred. Models using normal distributions based on the raw signal of non-shooter samples resulted in excessively high LRs at all concentrations above the LOD; the LOD having been set three standard deviations above the mean blank for precisely this reason. If an evaluation was to be conducted using the case-specific approach, further samples could be collected to reflect H_d and then obtain respective LRs. However, a conservative approach using values such as the risk of

contamination during arrest may be more appropriate. This should favour defendants more strongly, as greater frequencies of GSR-exposure have been observed in experiments modelling transfer compared to random background sampling (e.g. [\[34, 37\]](#) and [\[23, 26\]](#)). It is also theoretically possible to combine PDFs from different studies into LR calculations; however differences in analytical methods between existing studies are currently a barrier.

There is another issue when using separate PDFs to produce LRs for each variable in multivariate tests. For LRS that are statistically independent, combining each measured variable into a posterior likelihood (posterior for the forensic scientist, not the finders of fact) can be achieved through simple multiplication. In practice this can lead to unreasonably high or low ratios for data sets with large dimensionality; consider that the upper bounds of a common verbal scale were easily exceeded using a single variable above. If the necessary data were available to create LRs for the other variables, multiplication would only compound the problem. Additionally, it is often not possible to observe simultaneous occurrence of many independent, rare events within a single specimen chosen from a realistically achievable sample size. Therefore while all LRs are estimates based upon available information, consolidating higher-dimensional data can require substantial extrapolation with no means of cross-referencing. Furthermore, it is not rational to assume that GSR data are in fact independent. This was shown above using categorical measurements, but becomes even more important with quantitative data. Extreme LRs can occur when dependencies between the variables are not accounted for, because in essence the same support provided to the hypotheses is counted multiple times. It may be possible to map these dependencies using Bayesian Networks; this was demonstrated by Biedermann & Taroni in 2006 for the joint evaluation of GSR and toolmark evidence [\[277\]](#). However this again requires a larger amount of data collection and becomes more complex as the number of variables increases [\[278\]](#). Therefore multivariate methods of data analysis are explored below.

4.6 Multivariate Models of GSR Evidence

4.6.1 Pre-processing and Exploratory Analysis

Due to the issues described above when considering each category of GSR as separate pieces of evidence, the performance of multivariate approaches were also investigated. These are mathematical procedures that account for all observations prior to the calculation of a single likelihood ratio for each sample. The methods were judged on their ability to aid in decision making by classifying samples into shooter/non-shooter categories based on analytical measurements. The power of each model to communicate a degree of support for competing hypotheses was also assessed. Again, Addinsoft's XLStat Life Sciences package was used to facilitate computations [\[279\]](#).

Initial pre-processing and exploratory analyses were conducted, to narrow down the list of chemometric or machine learning techniques in common use to only the most applicable to the current data. The LC-MS/MS

peak areas for each compound were converted into concentration values using an external calibration curve, and all values below the instrumental LOD were assigned the arbitrary value of 10^{-2} as previously described. Methyl centralite and dinitrodiphenylamine were removed from the list of variables, due to their infrequent occurrence in both the shooter and non-shooter sample subsets. Quantitative data consisting of operator-verified particle counts were collected for ten categories of IGSR, representing both “characteristic” and “consistent” designations under the relevant ASTM standard [112]. Data for all sixty samples were then normalized between the minimum and maximum values for each variable following the example of Feeney *et al.* (2022) [267]. This helps to avoid models being overly influenced by compounds with higher concentrations at the expense of lower-concentration compounds that still have a statistically significant effect on the output. It also helped to ensure that concentrations of OGSR compounds and counts of IGSR compounds were assessed on a common scale.

Statistical tests were performed to check for multicollinearity between measured variables in the model. A Pearson correlation coefficient matrix with associated p -values was generated (Table 4-7). The absolute values of each coefficient represent the strength of pair-wise linear relationships, while the p -values estimate whether the relationships are statistically significant. As expected, strong and statistically significant relationships were found between the concentrations of diphenylamine and its nitric oxide derivatives. Correlations were also found between every pair-wise combination of OGSR markers, with the concentration of akardite being more strongly correlated to other variables than ethyl centralite. Statistically significant multicollinearity also occurred between OGSR compounds and particles identified as PbSbBa, PbSb and SbBa composition. Finally it was found that linear correlation between “consistent” particles such as Sr or BaAl, and either OGSR or “characteristic” particles, was more frequently statistically insignificant.

Variance inflation factors (VIFs) were also used as a measure of dependency between variables. Rather than directly measuring the strength of correlations, this statistic instead measures the effect on variance of regression coefficients. For example, a VIF of two indicates, all else being equal, that the variance of a particular variable’s regression coefficient will be twice as large than if it had been completely independent of all other variables in the model. Increased variance implies lesser precision of both the individually estimated coefficient and any subsequently calculated models. Several rules-of-thumb for acceptable VIFs such as <4 and <10 have been suggested, although all are essentially arbitrary [280]. The data examined here frequently had much larger VIFs than any of the commonly used cut-offs, with $VIF_{\text{diphenylamine}} \sim 20$ and $VIF_{\text{akardite}} >25$. Both the Pearson and VIF findings suggest that machine-learning techniques with underlying assumptions of independence between variables, such as logistic regression or Naïve Bayes classifiers, are not appropriate to data from these samples. Therefore two MLAs previously applied by others to GSR data, that are also able to contend with correlations between observations, were investigated further. These were partial least squares discriminant analysis (PLS-DA) and artificial neural networks (ANN).

Table 4-7: Correlation matrix between indicators of GSR exposure collected from the samples in Chapter 3:. Pearson coefficients are displayed above the diagonal, with associated *p* values below the diagonal.

Variables	Diphenyl-amine	Nitroso diphenyl-amine	Nitro diphenyl-amine	Akardite	Ethyl Centralite	Pb Sb Ba	Pb Ba Ca Si Sn	Sb Ba	Pb Sb	Pb Ba	Pb Ba Ca Si	Ba Ca Si	Ba Al	Ti Zn Sn	Sr
Diphenyl-amine		0.88	0.78	0.96	0.41	0.62	-0.06	0.72	0.41	-0.02	-0.03	-0.03	0.08	-0.07	-0.04
Nitroso diphenyl-amine	<0.01		0.74	0.85	0.57	0.62	-0.07	0.65	0.47	0.18	0.07	-0.04	0.14	-0.08	-0.05
Nitro diphenyl-amine	<0.01	<0.01		0.71	0.31	0.54	-0.07	0.56	0.39	0.02	0.13	0.05	0.38	-0.06	-0.05
Akardite	<0.01	<0.01	<0.01		0.39	0.66	-0.05	0.77	0.45	-0.07	-0.09	-0.04	0.02	-0.07	-0.02
Ethyl Centralite	<0.01	<0.01	0.02	<0.01		0.35	-0.03	0.44	0.42	0.55	0.01	0.08	0.34	-0.08	-0.04
Pb Sb Ba	<0.01	<0.01	<0.01	<0.01	<0.01		-0.02	0.79	0.70	0.02	-0.06	-0.03	0.06	-0.09	0.00
Pb Ba Ca Si Sn	0.66	0.58	0.62	0.69	0.82	0.89		0.06	0.26	0.37	0.84	0.76	0.32	0.54	0.70
Sb Ba	<0.01	<0.01	<0.01	<0.01	<0.01	<0.01	0.65		0.56	-0.01	0.04	0.12	0.25	0.01	0.11
Pb Sb	<0.01	<0.01	<0.01	<0.01	<0.01	<0.01	0.05	<0.01		0.33	0.26	0.29	0.31	0.06	0.20
Pb Ba	0.84	0.08	0.69	0.84	<0.01	0.63	0.31	0.72	0.02		0.21	0.17	0.17	0.04	0.12
Pb Ba Ca Si	0.81	0.59	0.31	0.50	0.94	0.63	<0.01	0.78	0.05	<0.01		0.73	0.54	0.43	0.59
Ba Ca Si	0.82	0.78	0.70	0.74	0.54	0.81	<0.01	0.36	0.02	<0.01	<0.01		0.68	0.68	0.83
Ba Al	0.55	0.29	<0.01	0.89	<0.01	0.63	0.01	0.05	0.02	0.03	<0.01	<0.01		0.26	0.33
Ti Zn Sn	0.59	0.52	0.66	0.60	0.55	0.52	<0.01	0.92	0.62	0.04	<0.01	<0.01	0.05		0.79
Sr	0.79	0.72	0.70	0.86	0.75	0.97	<0.01	0.40	0.12	<0.01	<0.01	<0.01	0.01	<0.01	

*Values in **bold** are different from 0 with a significance level $\alpha = 0.05$

VIFs	19.83	11.00	56.00	6.13	26.51	4.99	5.85	10.10	6.49	3.13	3.32	11.00	17.37	10.23	2.91
------	-------	-------	-------	------	-------	------	------	-------	------	------	------	-------	-------	-------	------

4.6.2 Partial least squares discriminant analysis (PLS-DA)

PLS-DA algorithms reduce the dimensionality of data by combining and projecting original measurements onto new axes, generating latent variables that give the strongest possible relationship between X and Y in the process. The procedure is in effect a supervised equivalent of principle-components analysis (PCA), with the difference being that the samples' classifications are known in advance, rather than being driven purely by observation. Compared to other regression models, it is particularly suited to data sets with collinearity between variables, or with more variables than samples. In the current work, a PLS-DA model with two latent variables was built using Addinsoft's XLSTAT software and the scaled data described in the preceding section. Due to the small sample size ($n=60$), a random number generator was used to withhold 10% of samples for validation, evenly split between shooter/non-shooter classes. For these samples, the model was not given any prior information on the sample's class. The remaining 90% were used for training the model. A leave-one-out cross-validation requirement was applied, such that each sample was removed from the model as its score was calculated, to reduce over-fitting.

The first score vector (t_1) of the model was found to explain 44% of variation in sample classification, increasing to 56% when the second score vector (t_2) was added. A plot correlating the initial variables and the score vectors is provided in Figure 4-6. As expected, all were positively correlated with the "shooter" category along the t_1 axis. The scattering of projections can also help to identify trends in the underlying variables; it was noteworthy to see that the model generally clustered OGSR and *characteristic* IGSR together, separate from categories of particle classified as only *consistent with* GSR. These delineations were not specified at any point when training the algorithm, but have been identified from the data nonetheless.

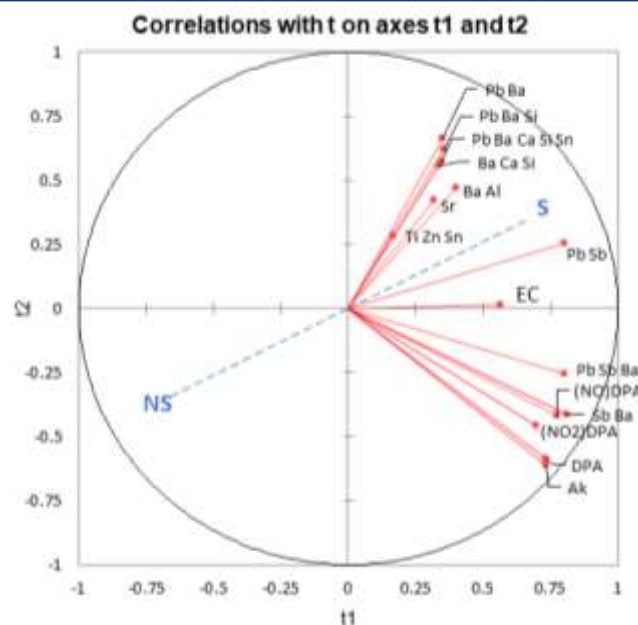


Figure 4-6: Partial least squares discriminant analysis (PLS-DA) plot of GSR survey data

As the t_1 latent variable provided sufficient information for discrimination between the two sample classes, t_2 was not used for the remainder of the analyses. A plot of t_1 scores for each sample is included as Figure 4-7, showing the distribution of the scores assigned to each subset. The non-shooters' samples can be found to the left of the plot. The raw data for these samples were very similar, due to them having the same concentrations of OGSR compounds (nil) and low numbers of "consistent" IGSR particles only. Therefore, the model performs as expected by assigning similar scores to all non-shooters' samples. On the other hand, there was greater variation between both the underlying analytical results and the assigned scores for shooters' samples shown to the right. It is also possible to see that the scores can be separated fully using a threshold cut-off approach, estimated visually by the dashed line.

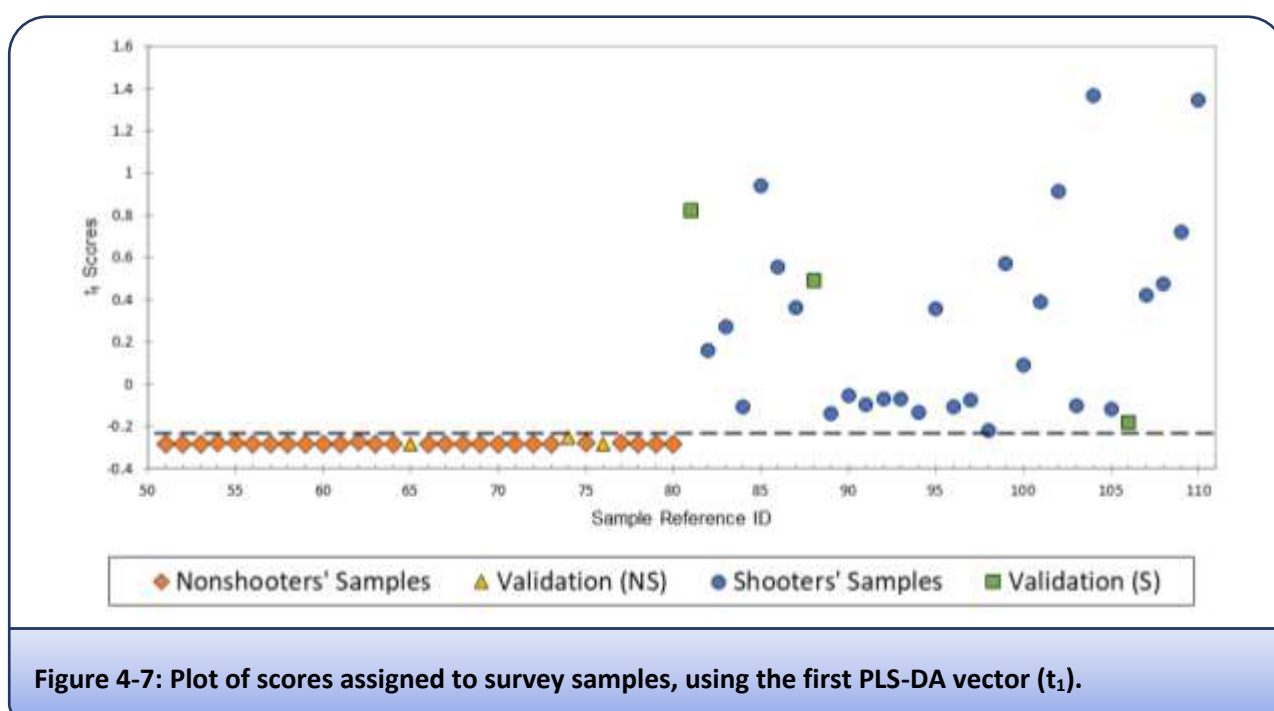


Figure 4-7: Plot of scores assigned to survey samples, using the first PLS-DA vector (t_1).

Sensitivity and specificity values were plotted against potential decision thresholds (Figure 4-8) to graphically display the discriminating power that this PLS model achieved with the available data. These plots chart the cumulative categorisation of samples into the groups of interest and allow for a better visualisation of the decision-making process. Figure 4-8 shows that it is possible to select a cut-off threshold that results in 100% accurate classification of samples from both the training and validation subsets. However there is only a narrow window ($-0.25 < t_{crit} < -0.22$) where this is achieved, suggesting that the model may not be robust to any future samples that exhibit scores between the presently observed ranges. It is not difficult to imagine scenarios that would result in such scores, such as the contamination and transfer scenarios investigated by others [26, 30, 40]. Evaluation of these scenarios would require collection of further samples, and rebuilding statistical models. In practice a more conservative threshold might be chosen, with some false-negatives accepted as a trade-off to ensure the lowest practical rate of false-positives.

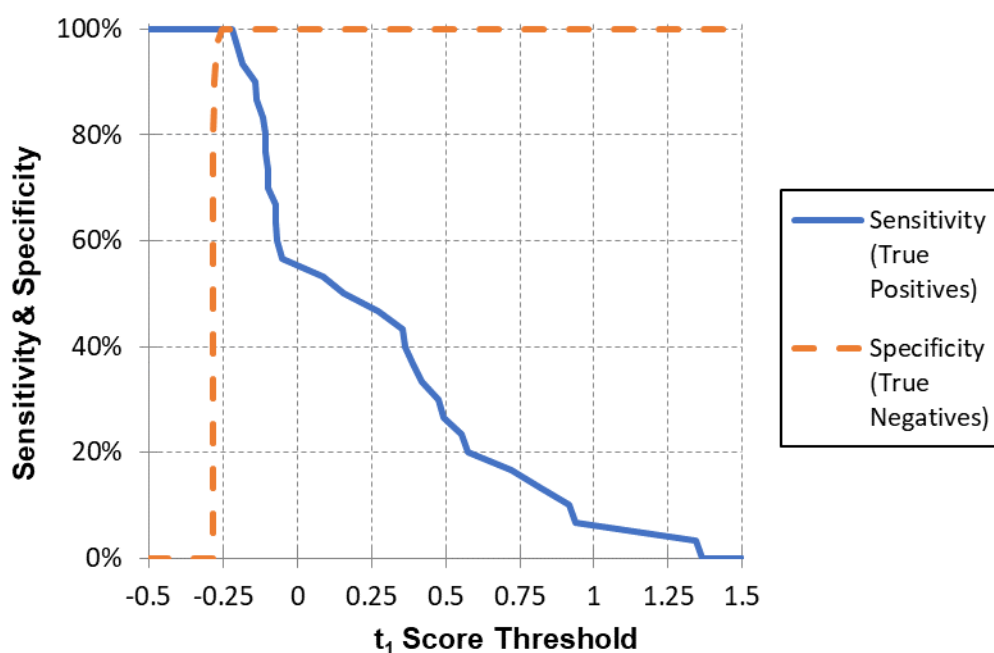


Figure 4-8: Sensitivity and specificity of decision thresholds applied to PLS-DA scores

PDFs were also separately fitted to the univariate scores produced by the PLS-DA algorithm for the shooter and non-shooter data subsets. This allows estimation of the strength of evidence provided by each sample, in addition to binary classification rates of the system. Of the common parametric functions, both were best fit by log-normal distributions. While the fit was statistically significant for the shooters' sample scores ($p = 0.31$, $\alpha = 0.05$), this was not the case for non-shooters' scores ($p = 0.005$, $\alpha = 0.05$). LRs were calculated for each sample and have been summarized by order of magnitude in Figure 4-9 according to the verbal equivalency system referenced throughout this chapter. Using the PLS-DA and log-normal model, LRs assigned to the samples varied across twelve orders of magnitude. Most samples trended towards the extreme ends of the verbal equivalency scale. In general the LRs supported correct classifications; there was however one instance of *weak support for H_p* provided by a sample that in fact belonged to a non-shooter. This sample contained five PbSb particles, greater than any of the other non-shooters' samples. As higher counts of particles with this composition are particularly closely correlated with classification as a shooter (see Figure 4-6), the underlying mechanism driving the false positive is apparent.

Compared to the process of generating individual LRs for every observed variable, the PLS-DA regression algorithm allows samples to be compared using a single coherent value. This value simultaneously represents inter- and intra- group variation, while accounting for dependencies between variables. However a misclassification and tendency towards extremes of support for either H_d or H_p suggest that this system is not well-calibrated to a subjective interpretation of the information that these samples provide.

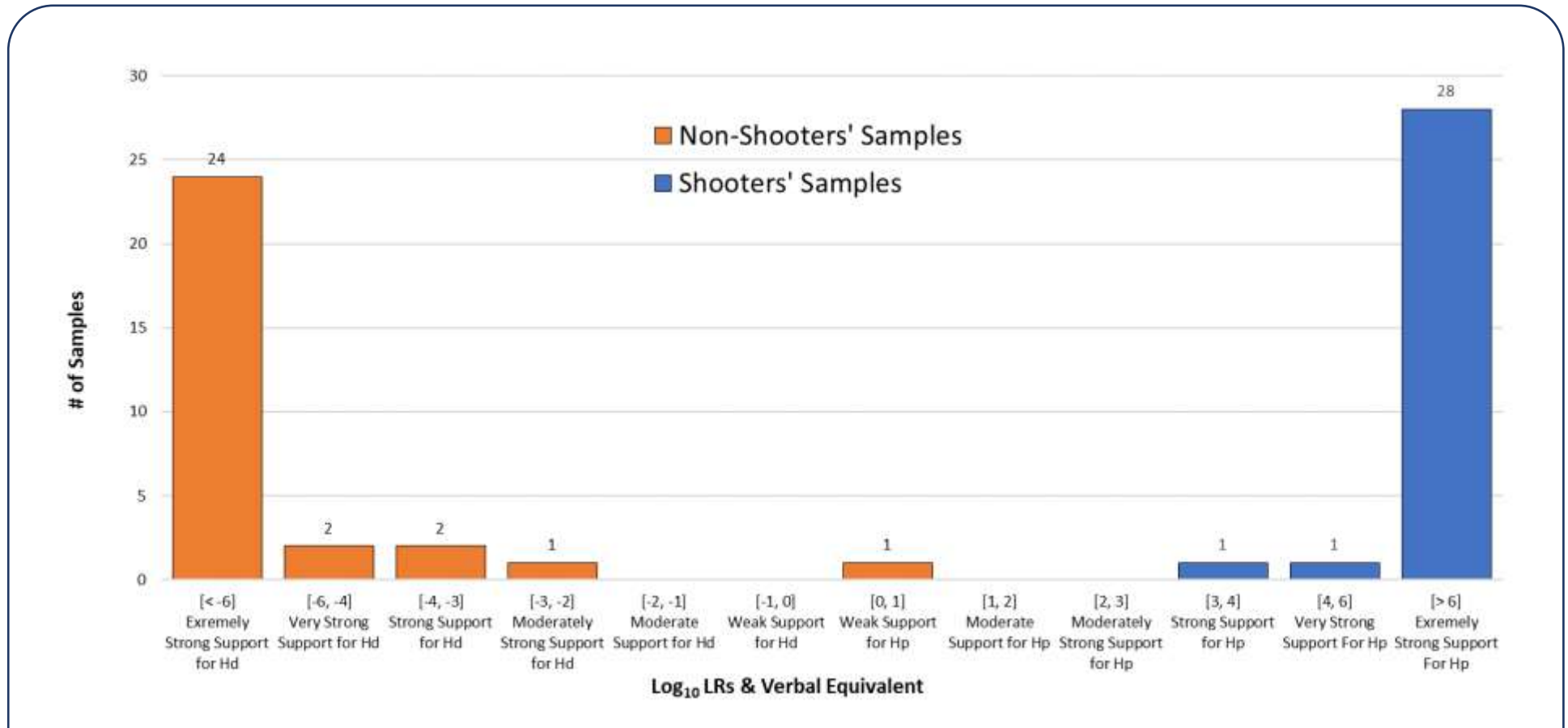


Figure 4-9: Likelihood ratios assigned to survey samples using PLS-DA modelling

4.6.3 Artificial Neural Networks

An artificial neural network (ANN) was constructed using the scaled OGSR and IGSR data described in section 4.6.1. The same 10% of samples that were withheld for validation of the PLS-DA model were again removed for the ANN model. A single hidden layer consisting of three nodes was applied to the 90% of samples used for training, with three repetitions of back-propagation and 10^5 adjustment iterations each. Outputs included weightings between each node, binary estimation of sample class, and probabilistic scores for each sample. A general overview of the model's structure can be found in Figure 4-10, with specific weightings shown in Table 4-8.

The ANN model was able to successfully classify all 54 training samples as originating from either a shooter or non-shooter's hands. This indicates complete separation between the classes i.e. no shooters produced data similar to non-shooter samples and *vice versa*, agreeing with manual examination of the data. It also correctly sorted the six validation samples based on weighting LC-MS/MS and IGSR particle observations. While less thorough than *k*-fold or leave-one-out cross validation (features not available in the specific software accessible at the time), the 10% validation at least to some degree suggests that the model can be generalized to previously unseen samples. Since all samples were correctly sorted, the ANN achieved sensitivity, selectivity, positive predictive and negative predictive values all = 1.00. A sensitivity/selectivity plot was also generated to graphically display the discriminating power that this ANN model achieved with the available data. As the network model uses a logistic, rather than linear, combination of latent variables to drive the algorithm, a much wider separation between the classes' scores is produced. In theory, a broader choice of threshold scores could conceivably result in accurate classification and this is evident when comparing Figure 4-8 and Figure 4-11.

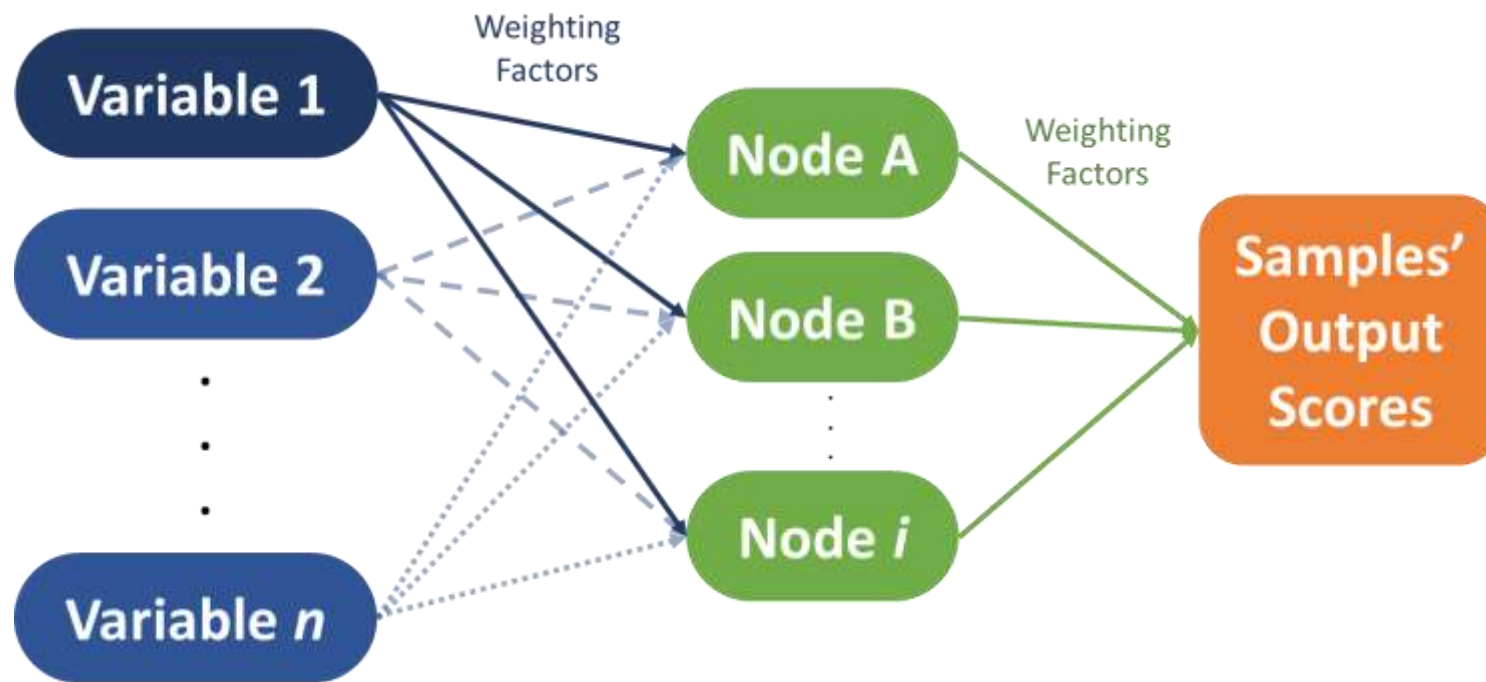


Figure 4-10: General form of an artificial neural network. The modelling program will apply prospective weightings to the measurements taken from each sample iteratively, until the training data can be correctly categorized based upon their output scores. Weightings calculated for this experiments' data set can be found in Table 4-8.

Table 4-8: ANN Weightings using GSR Survey Training Data					
Variable → A	Weighting	Variable → B	Weighting	Variable → C	Weighting
Conc. Diphenylamine to Node A	4.413	Conc. Diphenylamine to Node B	5.958	Conc. Diphenylamine to Node C	-6.421
Conc. Nitrosodiphenylamine to Node A	6.334	Conc. Nitrosodiphenylamine to Node B	5.931	Conc. Nitrosodiphenylamine to Node C	-7.277
Conc. Nitrodiphenylamine to Node A	7.143	Conc. Nitrodiphenylamine to Node B	5.984	Conc. Nitrodiphenylamine to Node C	-5.573
Conc. Akardite to Node A	7.500	Conc. Akardite to Node B	5.271	Conc. Akardite to Node C	-5.612
Conc. Ethyl Centralite to Node A	6.679	Conc. Ethyl Centralite to Node B	4.303	Conc. Ethyl Centralite to Node C	-4.822
# Pb/Sb/Ba particles to Node A	6.330	# Pb/Sb/Ba particles to Node B	6.499	# Pb/Sb/Ba particles to Node C	-7.288
# Pb/Ba/Ca/Si/Sn particles to Node A	8.761	# Pb/Ba/Ca/Si/Sn particles to Node B	7.499	# Pb/Ba/Ca/Si/Sn particles to Node C	-4.723
# Sb/Ba particles to Node A	6.110	# Sb/Ba particles to Node B	5.232	# Sb/Ba particles to Node C	-6.848
# Pb/Sb particles to Node A	8.230	# Pb/Sb particles to Node B	6.527	# Pb/Sb particles to Node C	-7.045
# Pb/Ba particles to Node A	7.427	# Pb/Ba particles to Node B	6.471	# Pb/Ba particles to Node C	-6.377
# Pb/Ba/Si/Ca particles to Node A	6.234	# Pb/Ba/Si/Ca particles to Node B	7.789	# Pb/Ba/Si/Ca particles to Node C	-7.024
# Ba/Ca/Si particles to Node A	-2.200	# Ba/Ca/Si particles to Node B	0.309	# Ba/Ca/Si particles to Node C	-0.887
# Ba/Al particles to Node A	6.693	# Ba/Al particles to Node B	7.193	# Ba/Al particles to Node C	-6.971
# Ti/Zn/Zn particles to Node A	0.240	# Ti/Zn/Zn particles to Node B	0.281	# Ti/Zn/Zn particles to Node C	-0.608
# Sr particles to Node A	0.081	# Sr particles to Node B	0.781	# Sr particles to Node C	-0.162
Intercept to Node A	-1.089	Intercept to Node B	-0.842	Intercept to Node C	1.072
Node A to Shooter Status	7.206	Node B to Shooter Status	5.531	Node C to Shooter Status	-7.437
Intercept to Shooter Status:			-1.642		

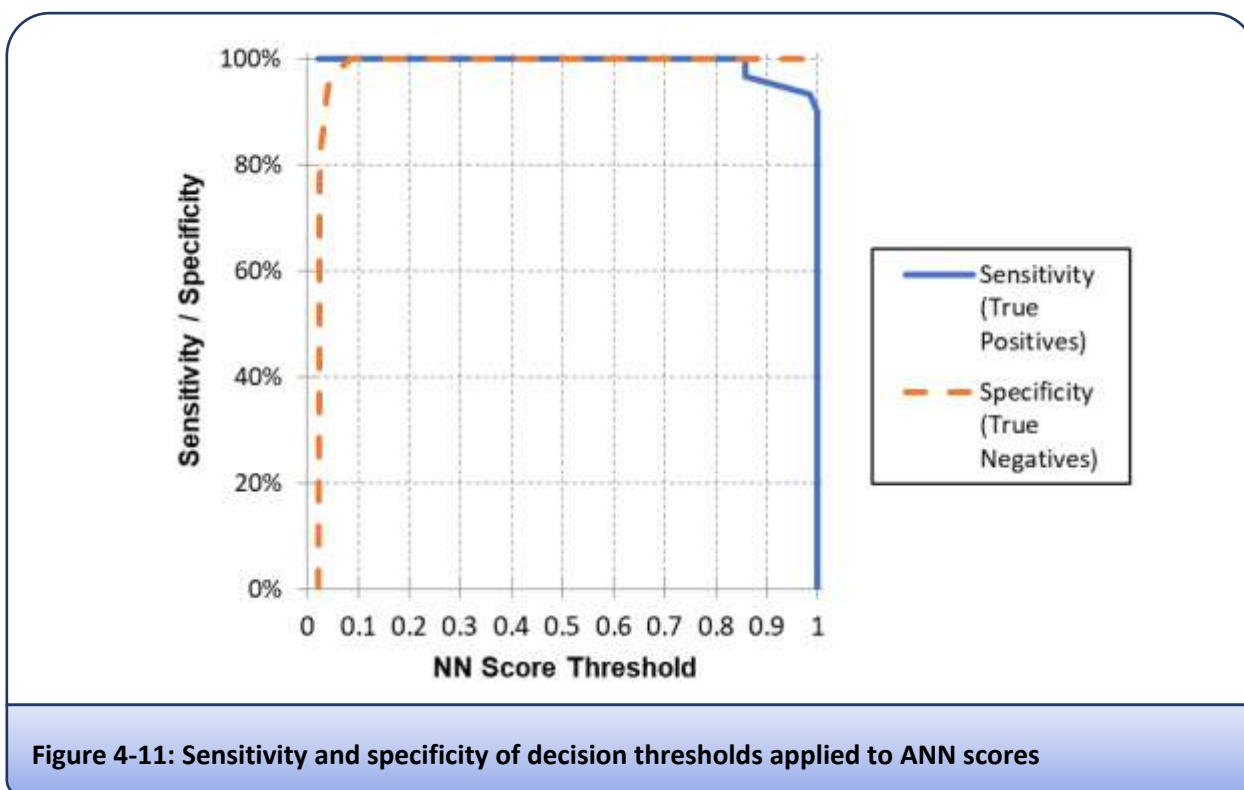
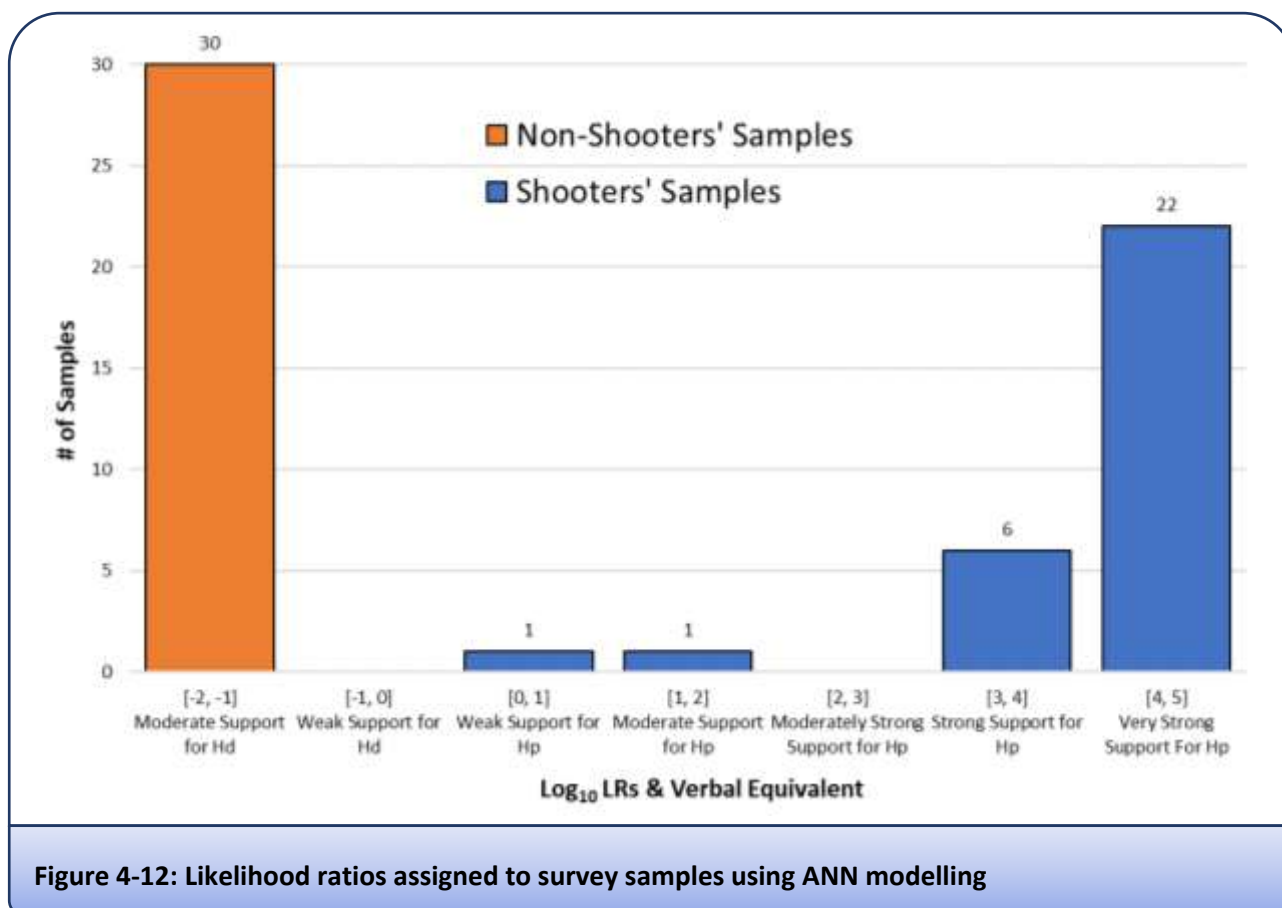


Figure 4-11: Sensitivity and specificity of decision thresholds applied to ANN scores

The ANN model was also able to give a more nuanced assessment of how well each sample supported H_p or H_d through a probabilistic output. LRs were calculated for each sample and have been summarized by order of magnitude in Figure 4-12. Observed ratios varied across seven orders of magnitude, with all non-shooter samples estimated to provide *moderate support for H_d* . As with the PLS-DA model, there was greater variation between scores for the shooters' samples. Of these, a majority (22/30) were estimated to provide *very strong support to H_p* . These samples could typically be described as having several OGSR compounds and a large number of IGSR particles detected. This model seems to more accurately reflect a subjective understanding of the evidence; samples were collected from the hands of known shooters soon after firing several shots, were found to contain relatively large amounts of GSR compared to what is observed during case work, and were notably dissimilar from non-shooters' samples.

Of interest were two samples estimated to provide "weak" and "moderate" support for H_p respectively. The sample providing *weak* support was found to have no LC-MS/MS peaks above LODs, 102 characteristic IGSR particles, and comparatively few consistent particles compared to other samples originating from shooters' hands. The sample providing *moderate* support for H_p had an OGSR peak for akardite at just above the LOD, 74 characteristic IGSR particles, and again a lower-than-typical amount of supporting particles. While either of these samples could possibly provide *strong support for H_p* judged upon characteristic IGSR alone, the NN model has "learned" that OGSR is a feature of samples originating from shooters. When the OGSR features are not present, the model still correctly classifies the samples based on IGSR but assigns a lower degree of belief to the classifications.



4.7 Conclusions

The first aim of this chapter was to quantify the increase in diagnostic accuracy that could be achieved by testing samples for the presence of GSR using two laboratory instruments sequentially. Positive predictive values (PPVs), in addition to false positive or negative rates, were chosen as appropriate measures of testing accuracy. This method applies the Bayesian approach to the testing process, rather than to individual samples, with $PPV = P(\text{shooter} \mid \text{observations})$. It is reiterated that this statistic is not interchangeable with the numerator in the LR equation used in presentation of evidence to court, as it embodies the prosecutor's fallacy and can only be used when the underlying prevalence of shooters in the sample population are known with certainty.

Initially samples were categorically determined to be either positive or negative for GSR based upon the standardized, qualitative procedures in current widespread use. Specifically, ASTM Standard E1588-20 was used to assess SEM-EDS data for inorganic GSR particles, while the proposed Standard WK72856 was used to assess LC-MS/MS data for organic GSR compounds [93, 112]. Using these standards and the available data (n=60), the individual PPVs of SEM-EDS and LC-MS/MS were estimated at 96.67% and 95.24% respectively. When combined sequentially, the PPV rises to 99.83%. The impact of such an improvement is best illustrated by considering the inverse inference. It was estimated that there was only a 0.17% probability that any

sample testing positive for GSR using both instruments could actually belong to someone who had not recently used a firearm. Therefore the diagnostic accuracy, at least for this sample set, has demonstrably improved with more comprehensive testing of the traces.

The two instruments used to potentially detect GSR operate on different principles and target different aspects of the sample, making the tests nominally orthogonal. However, the sample originates from the same trace. Using only qualitative assessments, it was demonstrated that OGSR and IGSR detection are statistically correlated. This allows the possibility of triaging more operationally demanding analyses such as SEM-EDS scanning, with faster and less intensive LC-MS analysis.

The second major aim of the chapter was to investigate the best use of multivariate, quantitative data collected from GSR samples when providing actionable information to end-users. Evaluative reporting, based upon the framework of Bayesian reasoning and likelihood ratios, was used as a lens for comparing different data-modelling strategies. Attempting to fit individual parametric PDFs to each variable in the data resulted in generally poor outcomes, with insufficient instances of detection in the non-shooter subset to build models. Collection of larger data sets through surveys, while potentially burdensome, may address this shortcoming. Few measured variables amongst the shooter subset were found to match parametric functions to a statistically significant level ($p > 0.05$). Evaluation of more specific scenarios representing H_p might produce data that better fit parametric functions, although the magnitude of GSR deposition is known to be variable and unpredictable. However, Pearson coefficients and variance inflation factors were used to demonstrate linear dependencies between measured variables; even if individual PDFs were sound models for the data, combining them rationally would be challenging.

Two machine-learning algorithms (PLS-DA and ANN) were used to combine observations for each sample into a single numerical output. As the underlying data were well-separated, it was possible to choose thresholds that allowed for 100% accurate classification of samples using either method. However, the separation between the highest-scoring non-shooter and lowest-scoring shooter was much wider using ANN compared to PLS-DA. Likelihood ratios were also calculated as estimates of the evidential strength provided by each sample, in addition to simple binary classification. Of most concern, PLS-DA produced one false-positive with a non-shooter's sample estimated to provide *weak support for* the shooter hypothesis. Values for the remaining samples were largely clustered at opposite extremes of a verbal-equivalence scale depending on their class. Between the narrow score-based window available for setting threshold scores, and tendency towards more extreme ratios, it is the author's opinion that the PLS-DA model was probably not well-calibrated to expectations for informative evaluative reporting.

The ANN model also reduces multivariate data to a single output for each sample, while seeking to maximise the information that can be used from a recovered trace. The scores for each class were well-separated, and

the resultant LRs appear to reflect the original data more appropriately. Therefore, of all the prospective models applied to this data set, ANNs appeared to offer the most potential as reporting aids for scientific experts. The drawback of this technique for forensic applications is the difficulty in describing to triers of fact the weighting process between inputs and outputs, which may appear to be a statistical “black box” to laypeople.

The major limitation of this chapter was that for many variables, no false positives were observed. A minimum value of $< 1/30$ was imposed to enable calculations when assessing samples using categorical criteria. This gives the greatest possible benefit to any potential defendants based upon the small data set. If an arbitrarily larger data set was collected, eventually a small but measurable false-positive rate could be determined. This will almost certainly be much less than $1/30$, but the magnitude is unknown. Unless a hitherto undiscovered source of pervasive OGSR contamination/interference is found, it is expected that LRs based upon larger data sets will trend towards providing stronger evidence than is currently estimated in this chapter.

Finally, it is important to remember that there is no true likelihood ratio or Bayes factor that each statistical model is trying to approximate. It is up to each analyst to select the model that they feel most accurately reflects the available data, to codify their subjective degree of belief in the strength of the evidence. However, subjectivity in this context does not mean that the expert has been arbitrary or capricious when making their assessment. The evaluative approach instead seeks to improve transparency and consistency, by formalising any assumptions made during the process of translating observations of a trace into expert evidence.

Chapter 5:
GSR in Vehicles

5.1 Background

Vehicles are often closely associated with incidents of gun crime. There is even a specific type of violent act that combines the two; the *modus operandi* of drive-by shootings. Vehicles are also used to flee scenes of shootings after the act. As such, forensic investigators are commonly required to search suspect vehicles for traces of gunshot residue. The events that could cause a positive result during examination can be sorted into four broad categories:

1. Occupants of a vehicle have discharged a firearm towards an external target.
2. An external assailant has fired into a vehicle.
3. An individual or item previously exposed to GSR has entered the vehicle, causing subsequent deposition. The initial exposure could result from either legitimate or criminal actions.
4. A non-firearm source has caused physical traces not readily distinguishable from GSR (false positives).

Evaluation and communication of GSR evidence in light of the competing propositions outlined above can also fall to forensic experts. These may be considered formally under the likelihood ratio (LR) framework given in [Equation 5-1](#), where scenarios are chosen to represent the respective prosecution and defence propositions.

Equation 5-1:

$$\text{Likelihood Ratio} = \frac{\text{Probability of observations given the prosecution hypothesis (H}_p\text{)}}{\text{Probability of observations given the defence hypothesis (H}_d\text{)}}$$

The potential for analytical false positives falls under so-called “sub-source” issues (point 4 above). Existing publications, reviewed and discussed in Section 5.2, have largely focussed within this domain when considering GSR in vehicles. The remaining scenarios listed above represent activity-level propositions, where the events leading to the deposition of a GSR trace may be more important to a judicial proceeding than the identification of the trace as GSR. There have been fewer fundamental studies on how this issue may affect GSR examination for vehicles. This is despite the fact that activity-level issues can be expected to feature frequently in criminal cases; a relevant example can be found in Ground 1c(ii) of the appeal decision in *Nicolaides vs The State of Western Australia* (2007, WASCA 203) [\[281\]](#):

“It was contended that the learned trial judge should have told the jury that the fact that gunshot residue particles were found in the hire car may have had nothing whatever to do with the robbery, particularly as there was no evidence of the provenance of the hire car before the appellant took possession of it.” - Buss, Miller & Murray, 2007 [\[281\]](#)

Some published surveys have covered specific sub-populations of vehicles, such as those operated by law enforcement personnel and recreational shooters. However, these omit coverage of key defence propositions for reasons outlined in Section 5.3. Summaries of further publications offering specific case-studies on GSR found in vehicles are given in Section 5.4.

5.2 Vehicles as a potential source of “GSR-like” material:

Several vehicle components have been specifically identified as potential sources of GSR-like material – traces that have similar chemical composition or morphology to the residues produced by firearms. Of particular interest are airbags containing energetic materials to facilitate rapid deployment, and brake-pads containing lead (Pb), barium (Ba) and antimony (Sb). Tyre rubber has also been suggested as a potential source of environmental pollution containing diphenylamine. If these sources do indeed generate traces indistinguishable from actual GSR, then the significance of this type of evidence for shooting investigations would be greatly diminished. This can be measured as a decrease to the LR by increasing the denominator of Equation 5-1, as the ubiquity of environmental particles would exceed the occurrence of traces generated by firearms.

5.2.1 Brake Pads:

A common brake configuration for passenger vehicles is the disc brake, wherein flat brake pads are pressed against a rotating metal disc to create friction and thus slow the vehicle. This friction results in heating and abrasion of the brake pads' surface. Under these conditions fine particles are produced - studies have shown that the proportion of brake dust measuring <10 microns can be between 65-98% by mass [282]. Kukutschová *et al.* (2011) showed that as brake temperature increases (towards 300° C under the specific conditions studied) the fraction of particles measuring <100 nm increases. This was attributed to a process of evaporation/condensation with subsequent aggregation of primary nanoparticles having greater influence than purely abrasive particle generation, mirroring the formation process of GSR [283]. These size fractions are directly relevant to GSR. The individual elements comprising *characteristic* IGSR are also associated with brake pads. Although the use of Pb in all consumer products has been decreased, concentrations up to 12% by weight have previously been measured in brake pads and these products may still be in circulation [284]. Antimony in the form of Stibnite (Sb₂S₃) can be used at 1-5 %/w as a solid lubricant [282]. Iijima *et al.* (2007) found a much lower amount of Sb (0.7-1.6%) in brake pads sourced in Japan, but also report Ba between 7.3-13.2% [285].

Taken in summation, the above measurements seem to suggest that the conditions required to produce GSR-like particles may exist under heavy braking, at least in theory. Indeed, three studies from approximately the same time period show evidence of particles containing Pb, Ba and/or Sb produced by brake pads. Garofano

et al. (1999) collected 175 samples from vehicles, vehicle parts and automotive workers. They found many two-component particles of irregular “lithic” morphology, but three-component particles were only found in association with workers who had used cartridge-activated nail guns [81]. Torre *et al.* (2002) directly sampled brake pads and wheel rims, again finding many particles that separately had the three elements of major interest. They did not report Pb/Ba/Sb within the same particle unless said particle also had major contributions of other elements. The presence of either sulfur or magnesium as a major contributor to the spectrum of a particle were specifically noted as disqualifying, as was a “rough or dusty” morphology [82]. The opinion expressed in Cardinetti *et al.* (2004) differs from the preceding two publications, in that they argue gross morphology is not sufficiently discriminatory between environmental- and firearm- derived aggregates. They instead recommend the use of elemental mapping under SEM-EDX to examine the distribution of elements within questionable particles. True GSR particles were found to be somewhat homogenous, either with all elements evenly distributed or Pb existing as discrete nodules. Environmental particles were more likely to present as a patchwork of discrete regions each dominated by a particular element [94].

Tucker *et al.* (2017) suggested that the findings presented by the aforementioned authors may have had a disproportionate effect on the confidence in GSR evidence as understood by non-experts. They examined 75 brake pads sourced from Australian automotive repairers and found no particles meeting the requirements for classification as *characteristic*, few Pb-only particles, but many particles containing both Ba and Sb [95]. The decrease in observed Pb was attributed to changing manufacturing trends. The traces did not exhibit the spherical morphology typical of GSR, were present alongside an abundance of Fe and BaS particles, and contained higher levels of elements such as K, S, Si, Mg, Al, Ti, Cu and Zn. The authors emphasized the importance of evaluating a sample based on the entire population of recovered particles as a whole, rather than the value of each singular particle. As such they determined that a properly informed examiner would not falsely reach the conclusion that a brake sample originated from a firearm.

5.2.2 Airbags:

While there are a variety of different airbag designs in vehicles, many use pyrotechnic devices either as their primary gas-generating component or as initiators. A tendency to form solid by-products is explicitly viewed as an advantage in these designs, as particulates can be filtered from cabin air more easily than gasses or vapours [286]. Several metal-oxidiser systems that have been used in airbags are listed as follows [287]:

- Sodium azide with potassium nitrate and silicon dioxide
- Zirconium/potassium perchlorate (ZPP)
- Boron/potassium nitrate (BPN)
- Basic copper nitrate/ guanidine nitrate (BCN/GN)
- Hexamine/cobalt (III) trinitrate (HACN) with copper (III) trihydroxynitrate
- Aluminium powder/ hexahydrotrinitrotriazine (Al/RDX)
- Strontium nitrate/ ammonium nitrate

Many other metal oxides and hydrides can be used in pyrotechnic blends and have been named in patents for airbag inflators – including B, Mg, Al, Si, Ti, Mn, Zn, Fe, Zr and mixtures thereof [288, 289].

In a two-part study (both 2009), Berk used a modified GSR SEM-EDS protocol to detect and classify airbag residue particles as potential trace evidence for the investigation of automobile accidents. Many of these had no chemical similarities to IGSR [287]. However, it was found that a very small fraction of the particle population (0.02-0.46%) could contain Pb, Ba and Sb [236]. Some of these individual particles included major contributions of zircon, aluminium, potassium or cobalt, indicating a non-firearm source. Others did not, or the disqualifying elements were present only at trace quantities that could potentially be overlooked. Nevertheless, the majority of detected particles contained disqualifying elements rather than the *consistent* and *commonly associated* particle types expected of GSR, along with many iron-rich particles. Similar to Tucker *et al.* (2017), Berk stressed the importance of considering the entire particle population when determining the significance of the small number of otherwise *characteristic* particles [95, 236]. Another marker of airbag residue was the presence of microfibrils and melted, glassy spheres containing aluminium, silicon, and sometimes calcium. Aluminosilicate filters within the airbag are a likely source of this additional material [287].

Following the results reported by Berk, Denis *et al.* (2018) collected 53 airbag specimens from 28 vehicle models available in Canada spanning 1993-2011 [235]. Only two were found to produce Pb, Ba and Sb – both were from side curtain airbags. A sample from a 2003 Chevrolet Silverado yielded 37,621 particles, of which 18 were “GSR-similar” but also contained F which is not typical of GSR. The remainder had signature compositions of Zr and Cu. A sample from a 2007 Honda Civic yielded 23,508 particles, of which 15 were GSR-similar but also contained Co. The remainder had signature compositions of Cu, Co, Zr and Ca. All the particles containing Pb, Ba and Sb from these two vehicles also exhibited elevated levels of K and Mg which are unusual to GSR, although particles containing trace levels of either are included as GSR in the ASTM definition [112]. Samples collected from separate vehicles of each model, in relevant manufacture years, did not contain any GSR-like particles.

5.2.3 Tyre Rubber:

Some of the compounds used as stabilisers in propellant are also used for similar reasons in the manufacture of polymers for vehicle tyres. Diphenylamine (DPA) is added to smokeless powders for the purpose of inhibiting autocatalytic degradation caused by the release of nitric-oxide radicals from nitrocellulose. The presence of DPA is therefore considered indicative of gunshot residue, while derivatives such as nitrosodiphenylamine (NODPA) and nitrodiphenylamine (2- or 4- NO₂DPA) may provide even stronger signs of association. This same compound has previously been noted to provide resistance to both thermal

degradation and flex-cracking for rubber products in addition to its role as a chemical antioxidant [97, 290]. Whilst para-amine-substituted DPAs such as N-isopropyl-N'-phenyl-p-phenylenediamine (IPPD) and N-(1,3-dimethylbutyl)-N'-phenyl-p-phenylenediamine (6PPD) (see Figure 5-1) reputedly represent a greater market share of tyre rubber additives, there have been some reports of nascent OGSR markers being detected in vehicle tyres [290]. Gadd & Kennedy (2003) detected NODPA and DPA (reported collectively) in three of six tyre specimens representative of the New Zealand market at concentrations of 18, 34, and 60 mg/kg respectively [291]. During the process of driving, vehicle tyres produce particulate pollution as the tread surface is abraded by the road. This is a significant source of material; estimates based on typical annual mileage suggest that Australia may produce 20 thousand tonnes of tyre particulates per annum, with a worldwide figure of nearly 6 million tonnes [292]. The material is then dispersed as dust *via* wind and water runoff [293, 294].

Recycled rubber products such as outdoor paving and playground flooring have been identified as secondary sources of dust containing DPA derivatives. Working in China, Liu *et al.* (2019) collected thirty samples of dust from different outdoor playgrounds featuring rubber base material, and also collected a further thirty samples of dust from inside residential housing (results presented in Table 5-1) [295]. All samples were found to contain DPA, up to 129 ng/g. Furthermore measurable amounts of NO₂DPA were found in >90% of indoor dust samples, with the greatest concentration noted at 188 ng/g. NODPA was reported less frequently, but was still in 20% of samples. While there are some accounts of direct application of DPA's nitric-oxide derivatives to elastomer products, the contribution arising from environmental reactions with DPA is unclear [296]. If occurrences of DPA and derivatives in Chinese residential dust are assumed to have originated from tyre rubber, either through road-wear or *via* secondary products using tyres as an input, then low-level detection of these compounds in dusty vehicles interiors would also seem likely.

Compound	Outdoor Dust			Indoor Dust		
	% Samples	Concentration Range (ng/g)	Mean Concentration (ng/g)	% Samples	Concentration Range (ng/g)	Mean Concentration (ng/g)
DPA	100	2.33-32.6	8.02	100	8.71-129	25.5
NO.DPA	10	<LOQ-10.5	1.29	20	<LOQ-12.0	1.58
2-NO ₂ .DPA	73	<LOQ-5.80	0.69	93	<LOQ-51.7	7.12
4-NO ₂ .DPA	93	<LOQ-16.3	4.19	90	<LOQ-188	17.1

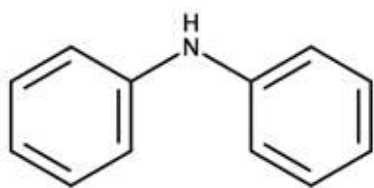
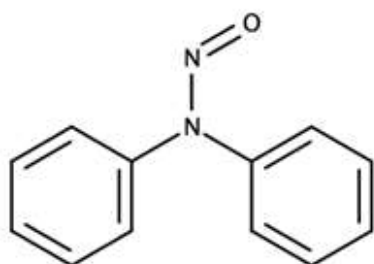
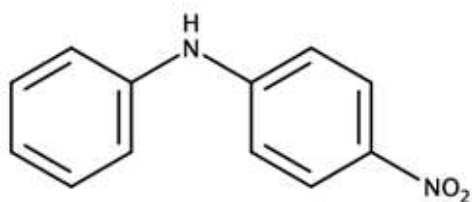
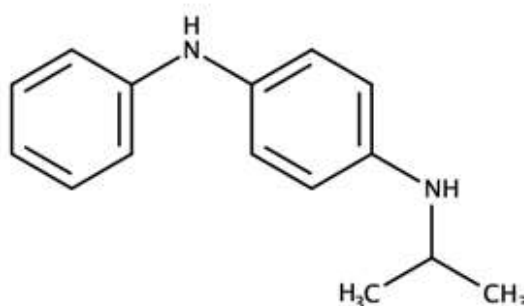
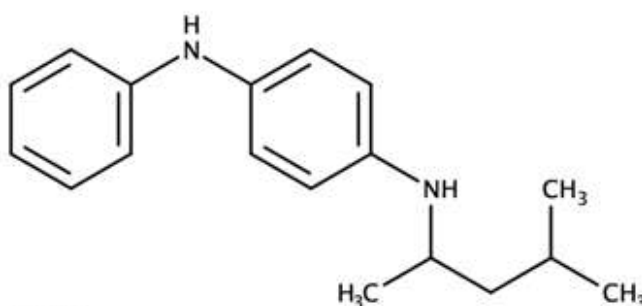
**Diphenylamine**Molecular weight: 169.23 g mol⁻¹Formula: C₁₂H₁₁N**Nitrosodiphenylamine**Molecular weight: 198.23 g mol⁻¹Formula: C₁₂H₁₀N₂O**4-nitrodiphenylamine**Molecular weight: 214.22 g mol⁻¹Formula: C₁₂H₁₀N₂O₂**IPPD**Molecular weight: 226.32 g mol⁻¹Formula: C₁₅H₁₈N₂**6PPD**Molecular weight: 268.40 g mol⁻¹Formula: C₁₈H₂₄N₂

Figure 5-1: Diphenylamine (DPA) and related compounds with known or suspected association with tyre-rubber.

5.3 Background surveys of vehicles for GSR traces

In addition to sources of GSR-like material originating from vehicles themselves, it is also possible that the distribution of actual GSR in vehicles is non-zero. This does not inevitably imply criminality. GSR could easily be transferred to vehicles after someone has handled a firearm for employment or sporting purposes, and vehicles are used to transport legal firearms directly. Consequently, GSR detected in a vehicle needs to be interpreted in light of the circumstances of the particular case at hand. Significance may be left up to triers of fact in court (with varying levels of verbal guidance from expert witnesses) or else it could be explicitly stated in a likelihood ratio (Equation 5-1) with the following propositions:

H_1 : vehicle was exposed to GSR during the commission of this crime

H_2 : vehicle was exposed to GSR by any other pathway

Surveys with a broader scope than those reviewed in Section 5.2 can be used to model the values for H_2 . Unfortunately, existing studies are not well suited to such a task. Much of the survey work in current literature has focussed on examining vehicles operated by law enforcement personnel (Table 5-2), many of whom carry a duty firearm and transport this with them in their work vehicle. This stems from the view that there is a risk of POIs being contaminated pre-examination if they are detained and transported in police vehicles already polluted with GSR. While important for the interpretation of GSR traces located on a POIs' person, such surveys are not an accurate reflection of the pool of questioned samples collected from vehicles suspected of use in criminal activity.

Table 5-2: Summary of studies reporting on GSR detected in <u>police</u> vehicles			
Study	Technique	Vehicle Samples Collected	Key Findings
Berk <i>et al.</i> 2007 (U.S.A.) [38]	SEM-EDX	81	Two <i>characteristic</i> particles found in separate tactical cars. Significant but unspecified numbers of <i>consistent</i> particles.
Gerard <i>et al.</i> 2012 (Canada) [231]	SEM-EDX	18	Two <i>characteristic</i> particles found in separate police vehicles.
Ali <i>et al.</i> 2016 (U.S.A.) [39]	SEM-EDX & LC-MS	32	One <i>consistent</i> IGSR particle, and two separate incidences of EC, were found on the hands of volunteers who spent 10 minutes handcuffed in the back of a police vehicle.
Gassner & Weyermann 2020 [297]	LC-MS	64	Many drivers' seats (20) and rear passenger seats (26) returned positive readings. Between 1-6 of 7 targeted compounds were found in any single positive sample. The frequency of specimens decreased as the number of compounds detected simultaneously increased.

Thus far there has only been one reported SEM-EDX study on the distribution of GSR in vehicles belonging to recreational shooters. Blakey *et al.* (2019) collected 24 samples from each of seven recreational shooters' cars [298]. Each motorist had discharged firearms within the preceding week but had only transported them (rifle or shotgun inside a carry-bag) in the rear of the vehicle on the day of sampling. The total number of *characteristic* GSR particles seen in each vehicle varied from 51 to 876. The distribution of these particles throughout the vehicles was also assessed. The greatest number were found in the rear storage compartment, where the firearms were placed for transport. Large numbers were also observed on the passenger seats, thought to be less affected by losses due to contact. Lower amounts were observed on frequently handled surfaces, especially the outer door handles.

A separate study on the presence of Pb, Ba and Sb in personal vehicles was published by Comanescu *et al.* (2019) using Graphite-Furnace Atomic Absorption Spectrometry as the detection technique. As this is a bulk technique, it has several limitations for the indisputable detection of GSR. Five samples were collected from each of ten vehicles [110]. Eleven of these (22%) returned readings for the three elements above their respective instrumental limits of quantification (**LOQs: Pb: 0.06 ug Ba: 0.052 ug Sb: 0.013 ug**). However, the authors state that their in-house method requires each specimen to exceed the apparently arbitrary threshold values of “0.04 ug for antimony, and values of at least 0.10 ug of barium and lead” to be considered positive [110]. Therefore according to the criteria set by that study, none of the 50 samples were deemed GSR-positive.

In 2021, Stamouli *et al.* published the results of a Eurocentric interlaboratory study assessing 1,343 SEM stubs taken from the hands of volunteers categorized into various GSR-exposure risk groups [34]. Car mechanics represented 11% (n = 153) of participants, and as such were assigned their own risk category due to the aforementioned concerns. While no samples were collected from vehicles directly, the potential for frequent transfer events to automotive workers (if any traces of interest were present) also make this study relevant. None of these individuals' samples were reported by the contributing laboratories as positive for three-component Pb-Ba-Sb particles, although the compiling authors noted that a distinction could not be made between non-occurrence of such particles or that some GSR-like particles were disqualified due to distinguishing features. Further statistical evaluation found that this sub-population could not be reasonably distinguished from the broader (non-mechanic, non-shooter) survey population by their propensity to carry GSR or GSR-like material.

5.4 Published case studies featuring specific GSR/Vehicle interactions:

5.4.1 Discharge of a Pistol Out a Car Window with the Breech Within the Interior of the Car: Analysis of Gunshot Residue on a Car's Interior Surfaces (2017), Burnett & Lebiedzki [299].

The driver of a 1997 Honda Civic allegedly extended their arm over the front passenger seat and fired a single shot from a handgun through the open window. The muzzle of the firearm remained within the car. The vehicle was impounded 2 weeks after the shooting, and a box containing 0.380 ACP cartridges was found. No pistol, spent casing or projectile was recovered. The vehicle was then stored outside for approximately six months with the “skylight and windows open”, exposing the interior to wind and rain while allowing a thick layer of dust to accumulate on horizontal surfaces such as the dashboard. The only surfaces suitable for adhesive sampling after the delay were the vertical pillar and upper liner forming the periphery of the passenger window frame; two and zero *characteristic* Pb/Ba/Sb particles were located respectively.

A 2005 Honda Civic and a fitting box of 0.38 ammunition were sourced for comparative purposes, then a single shot was fired in the configuration alleged above. Control specimens showed no *characteristic* particles prior to shooting. Adhesive stubs were used to sample the following locations within the vehicle, with associated numbers of *characteristic* particles: Front passenger window headliner (15), front passenger window vertical pillar (3), front passenger seat (1), dashboard (12), rear seat (2).

Burnett & Lebieczik concluded that the low number of GSR particles observed in the suspect vehicle were consistent with the results seen during the test scenario. However, they noted the susceptibility of the area around the front passenger window to pollution by GSR from an external source if a recent shooter placed their hands in these locations when entering the vehicle. An assumption was made that the GSR loading on the dashboard of the test vehicle would not be replicated *via* secondary transfer, and could only occur by deposition of airborne GSR. While unstated in the original article, the authors appear to imply that poor storage conditions precluded collecting the samples necessary to provide an informed opinion on the activities that caused the presence of GSR particles in the original case.

5.4.2 A case of alleged discharge of a firearm within a vehicle (2018), Burnett [\[300\]](#).

During a “road-rage” incident, the driver of vehicle 1 (D1) was alleged to have fired two shots from within their vehicle, over the heads of the occupants of vehicle 2 (V2). The driver of V2 (D2), a police officer, returned fire with a 0.45 calibre bullet which penetrated the windshield and dashboard before coming to rest inside V1’s instrument panel. This second event was not in dispute. D1 immediately fled the scene and later denied having fired at V2. D1’s hands and neck were sampled for GSR 12 hours after the incident. Several locations within the vehicle were also sampled and D1’s clothing was secured (but not sampled).

The author of the publication became involved in the case as an expert witness at a later stage in the trial, not being a part of the initial investigating law enforcement agency. Only a partial copy of the original GSR evidence report was made available. Additional samples were collected by Burnett from within V1 and from D1’s clothing 16 months after the incident. The list of samples reviewed by Burnett are given in Table 5-3. D1 stated that they had visited recreational shooting ranges at least three times prior to the incident.

Table 5-3: GSR samples reported in the case			
Sampling Location:	Sample Analysed By:	Results	
		Characteristic	Consistent
D1's hands (L&R combined)	crime lab	0	5
D1's neck (L&R side combined)	crime lab	0	4
V1 interior: headliner	crime lab	1	unspecified
V1 interior: driver's seat and headrest (combined)	crime lab	>3, "numerous"	"numerous"
V1 interior: driver's door & window panel (combined)	crime lab	5	unspecified
V1 interior: steering wheel & dash (combined)	crime lab	1	unspecified
D1's shirt, seized by crime lab	expert witness	1	9
V1 interior of instrument panel assembly	expert witness	105	178
V1 Dashboard left, near bullet hole	expert witness	0	2
V1 Dashboard, centre	expert witness	0	8
V1 Dashboard, right	expert witness	0	2

Burnett was critical of the original GSR examination for several reasons:

1. Results from separate GSR stubs were combined improperly in the report
2. Excessive significance was attributed to low numbers of *characteristic* particles
3. Sources of GSR other than the prosecution's alleged series of events were not considered

Burnett concluded that a lack of *characteristic* GSR particles on D1's hands, neck and clothing was more likely to be observed if D1 had not recently discharged a firearm, assuming they had not showered and washed their clothing. The lack of *characteristic* GSR particles on the outer surface of the dashboard was also not likely to be observed if a firearm had been discharged within the vehicle.

Burnett further concluded that the small number of *characteristic* particles observed in V1 (driver's seat, door, steering wheel + dash) were more likely to occur because of residue trailing D2's bullet, or else secondary transfer following previous recreational shooting. The largest number of particles were in fact recovered from inside the vehicle's instrument panel, along the path of the bullet fired by D2.

5.4.3 Gunshot residue and airbags: Part II. A case study (2019), Denis & Hearn ^[301].

During an alleged attempted carjacking, two vehicles collided. The intended victim, a truck driver, stated that they were confronted by two assailants in a separate car. The truck driver rammed the aggressors' vehicle in order to escape, causing the smaller vehicle's airbags to deploy. Shots were then fired towards the fleeing truck driver. When police attended the scene, they found the damaged car abandoned, with three separate airbags deployed. A short time later a person of interest was located and sampled for GSR using four standard adhesive stubs (hands and face). The origin of any particulates found in these samples could be subject to doubt; did they result from the airbags, or a firearm?

All three airbags were recovered at the scene and sent for examination. Separate stub samples were collected from the interior and exterior of each, with three distinct populations of particles identified. The first population included particles containing the characteristic elements of Pb/Ba/Sb along with supporting particles. These were found on the suspect (10 *characteristic*) and exterior of the airbags (1, 5 and 52 *characteristic*), but no *characteristic* or *consistent* particles were located within the airbags' interiors. The PbBaSb particles recovered from the exterior of the airbags reportedly incorporated a similar element profile to those found on the suspect stubs, including contributions from Al, Cu, Zn, Fe, Si and K.

The second two populations of particles had markedly different chemical compositions. The sample taken from the interior of the steering-wheel airbag was dominated by particles containing Fe, or high K & Zr, or with high K, Zn & P; varying amounts of Al, Cu, Mg and Cl were also observed. Material consistent with this composition was also detected on the suspect, supporting the conclusion that they were present in the vehicle as the airbag deployed. The residues from inside both curtain airbags were each dominated by particles containing Ti, K, Cl & Zr, or else high K, Cl, Zn & P with Fe. Particles containing titanium specifically were not detected either on the suspect or the interior of the steering-wheel airbag.

Denis & Hearn were able to show, at least within the context of a specific case, that it is possible to discriminate GSR and airbag residues using SEM-EDX. They were further able to infer links between suspect, airbags and firearms resulting from two-way transfer by comparing stubs taken from specific areas within the vehicle.

5.5 Aims

Thus far, the background population of vehicles most likely to be presented to examining experts in GSR cases has not been surveyed in a wide-ranging manner. Vehicles randomly selected from the community inside which a POI resides will form the best sample set to accurately inform key issues of criminal shooting investigations. Therefore, a survey consisting of both physical sample collection from private vehicles and a written questionnaire was carried out. The study also examined IGSR and OGSR in unison, differing from the majority of previous surveys.

Examination of a sample set of this type will provide data on the combined prevalence of both GSR-like environmental material and background dispersal of traces from legitimate firearms use. The prevalence or rate of specimens designated as positive will reflect a typical urban/suburban environment in Australia.

5.6 Methods

5.6.1 Positive Control Scenario

An initial trial was conducted to provide a set of known positive specimens against which survey samples could be compared. A volunteer attended an indoor recreational shooting range and discharged approximately 30 rounds of 0.22 cal ammunition from a revolver. A spent cartridge from one of the fired rounds was placed into a small resealable bag and agitated to release any residue contained within. This provided a comparison sample, as the range prohibited removal of spent cartridges. The premises were also likely to be highly polluted with GSR traces from diverse ammunition/firearm combinations, which could be transferred to the participant. This shooter then left the range without washing their hands, entered their personal vehicle (automatic sedan), and drove for approximately 30 minutes to another location. At this location, samples were collected from the driver's hands and clothing using adhesive stubs. After another 30 minutes had elapsed, during which time the vehicle was left parked, the steering wheel, handbrake and gear lever, driver's seat, dashboard and rear storage compartment were also sampled (7 samples total). The bag containing cartridge residues was cut open and the internal surfaces sampled.

5.6.2 Survey

Samples representing the general motoring public were sought from volunteers following ethical research approval (Flinders University Social and Behavioural Research Ethics Committee application #6870). Participants were asked to use adhesive stubs to collect material from their own hands and four locations within their personal vehicle. While all participants were provided with identical written and pictographic instructions for adhesive sampling (Appendix 5-1), the sampling process itself was not supervised and inter-donor variability may have occurred. Volunteers were asked to disclose any prior use of firearms for either recreation or business, particularly if this involved transport of a gun within their vehicle. They were also asked to report contact with any of several likely sources of GSR-like pollution. No identifying personal information was recorded. The final composition of the survey group included seven shooters disclosing visits to recreational ranges with variable frequency and recency; and fifteen "non-shooters" asserting no previous contact with firearms. Each individual provided 5 sample stubs (n=110).

The adhesive stubs were returned for examination, which involved extraction and analysis following the protocol outlined in Chapter Two. Briefly, each stub was extracted with 100 μ L of acetonitrile using a pipette. Liquid extracts were analysed *via* a Thermo Scientific (Massachusetts, USA) Vanquish liquid chromatography system interfaced to a Velos Pro linear ion trap mass spectrometer operating in multi-channel SIM mode. Stubs were allowed to air-dry, and were then carbon-coated and scanned using an Oxford Instruments (Tubney, UK) electron microscope. The microscope was operated with an accelerating voltage of 25 kV, 3 nA probe current, and a magnification of 869-fold. The GSR particle search was performed following the

methodology detailed in the relevant ASTM standard (ASTM E1588) ^[112]. The Aztec 5.1 particle-search function was limited to 4 hours per sample and 5 minutes per field unless otherwise noted. Results from chemical analyses were obtained prior to comparison with written survey findings.

5.7 Results and Discussion:

5.7.1 Positive Control Scenario

5.7.1.1. OGSR:

The extract prepared from a spent cartridge during the positive control scenario was found to contain the stabilisers DPA, nitroso-DPA, nitro-DPA, and ethyl centralite (EC). These four compounds were found together in extracts from the driver's hands and jacket, as well as the vehicle's steering wheel, following 30 minutes of driving. Additionally, the stub used to sample the handbrake and gear lever (combined) did exhibit peaks for nitro-DPA and EC. Chromatographic peak areas for some samples were greater than the upper standard of the calibration curve, (6 points used per compound, upper concentration = DPA: 400 ppb, nitroso-DPA:150 ppb, nitro-DPA: 200 ppb, EC: 10 ppb) so calculated concentrations were extrapolated and listed as approximate only. These results, displayed in Table 5-4, suggest a pattern of decrease in recoverable OGSR traces as a chain of transfer events occur.

Table 5-4: Approximate concentrations of each smokeless powder stabiliser in extracts recovered <i>via</i> adhesive stub, separated by location.								
Conc (ppb)	Cartridge Debris	Driver's Hands	Driver's Jacket	Steering Wheel	Handbrake & Gear Lever	Driver's Seat	Dash	Rear Storage
DPA	1,500	1,400	1,050	600	Nil	Nil	Nil	Nil
NO.DPA	900	300	200	100	Nil	Nil	Nil	Nil
NO ₂ .DPA	240	140	70	30	10	Nil	Nil	Nil
EC	40	470	20	20	2	Nil	Nil	1

The greatest concentrations of OGSR were found in samples from the driver's hands, in immediate contact with the firearm. A notable amount was also detected on the jacket worn by the driver while shooting, but located further from the breach and muzzle. The steering wheel sample bore lesser amounts than the driver's person, as transfer events were required to deposit material to this surface. However the steering wheel is the most intensely handled component when driving, and so this surface out of all others in the vehicle's interior gave the greatest recovered concentration of each compound. The handbrake and gear lever showed possible but inconclusive signs of exposure to OGSR. As the vehicle in question was right-hand drive and had an automatic transmission, these surfaces were handled only briefly with the non-dominant hand when starting and parking. Lastly, surfaces not directly handled by the participant did not indicate any exposure to OGSR. Another potentially noteworthy result can be seen when comparing the various specimens' concentration of EC, as the cartridge extract has a noticeably lower concentration than the other positive

specimens. This may be an artefact of variation in extraction efficiency coupled with the lack of replicate samples obtained throughout the test scenario. However, the potential occurrence of weapon-memory effects from previous ammunition or intensive pollution of the indoor shooting site with EC offer alternative explanations.

5.7.1.2. IGSR:

Each of the stubs that produced a positive detection for OGSR also contained IGSR traces. For simplicity, only the values for *characteristic* three component Pb/Ba/Sb particles will be discussed here. A summary of observations is presented in Table 5-5. Approximately 15,000 *characteristic* particles were identified by the automated search procedure on the specimen collected from the driver's hands, and a further ~600 were located from the driver's clothing. The EDS spectra from several dozen particles from each stub were manually reviewed to verify their composition and to confirm that an abundance of *characteristic* particles were indeed present. The search function was then arbitrarily limited to 50 *characteristic* particles for the stubs collected inside the vehicle to reduce analysis time. This value was quickly reached on the stub taken from the steering wheel (SEM scans for 1% of search fields were required to reach 50 Pb/Ba/Sb particles), and also on the stub taken from the handbrake and gear lever (7% of fields searched). These results generally provide corroboration of the observed organic GSR extracted from the same stubs, recorded above in Table 5-4.

There were three remaining stubs that had not shown any indication of GSR when analysed *via* extraction for LC-MS. These were collected from the driver's seat, front dashboard, and rear storage compartment (boot/trunk). The stub from the seat was found to bear 52 *characteristic* particles across 36% of search fields. This may offer some indication of the relative sensitivity of the proposed analytical process to different types of GSR – inorganic particles were detected on this stub, but there was no analytically significant signal present to signify compounds relevant to smokeless powder. There is also weak evidence to suggest that a lesser amount of inorganic GSR may have been transferred to the driver's seat compared with the steering wheel or control levers, as a greater portion of the stub's surface was mapped before reaching the requisite limit of 50 particles. However this assumes that the respective stubs were equally efficient at collecting GSR from different locations (of dissimilar size and construction) and also that any material was evenly distributed across the stub's surface. A single particle on the stub collected from the car's dash was identified to potentially contain Pb/Ba/Sb, after 100% of the surface was scanned. This was assigned low significance compared to other samples containing many particles.

An unexpected result was obtained from the stub collected from within the rear storage compartment. As the vehicle was a sedan, the storage compartment was isolated from the rest of the vehicle. This sample

reached the 50-particle cut-off after 7% of search fields were scanned by SEM, approximately equalling the result obtained from the combined handbrake/gear lever sample. This was not anticipated as the rear storage compartment was not accessed during implementation of the test scenario. However, this area of the vehicle (and only this area) had previously been used to transport items associated with firearms use, such as perforated targets, away from firing ranges. Tertiary transfers from firearm -> target -> vehicle may explain this observation. A very minor chromatographic peak representing nitro-diphenylamine, observed above the blank but below the validated limit of detection, was also associated with this stub. No other organic GSR markers were observed.

	Hands	Clothing	Steering Wheel	Handbrake + Gear Lever	Driver's Seat	Rear Storage	Dashboard
Characteristic	14,958	619	53	50	52	50	1
Consistent	15,288	328	51	108	107	117	121
Total (including no association with firearms)	37,162	1,060	142	285	484	263	4478
Fields Searched	56%	14%	1%	7%	36%	7%	100%

In addition to Pb/Ba/Sb, some of the particles designated as *characteristic* were observed to contain contributions from Si, Al, Mg, Na, K, Ca, Cl, Cu, and/or Zn. Copper and zinc are commonly associated with GSR as they are components of brass (cartridge casings) and are used as a wash over projectile surfaces to reduce fouling and lead exposure. The other elements are less frequently associated with some types of ammunition, but are specifically linked to 0.22 calibre rimfire primers that produce IGSR with a glassy component. High-resolution elemental mapping of particles recovered from the cartridge debris revealed GSR comparable to results reported by Collins *et al.* (2003) and Seyfang *et al.* (2019) (shown in Figure 5-2) [\[69, 71\]](#). On the basis of the observed data, it is postulated that the ammunition used in this specific test may have contained soda-lime glass in its primer, although no unfired specimen was available for comparative analysis.

These data reflect the casework experience of GSR analysts, namely that *characteristic* IGSR particles can be transferred from a shooter into a vehicle occupied by that shooter. To the best of the author's knowledge, this scenario has not previously been explicitly documented in scientific literature under controlled conditions. This is despite publication of pollution rates for vehicles associated with firearm users in a more general sense [\[38, 298\]](#), or records of similar scenarios investigated under forensic casework conditions where the "ground-truth" is not knowable by the GSR expert. These observations were used to inform survey design and act as a "baseline" for comparison.

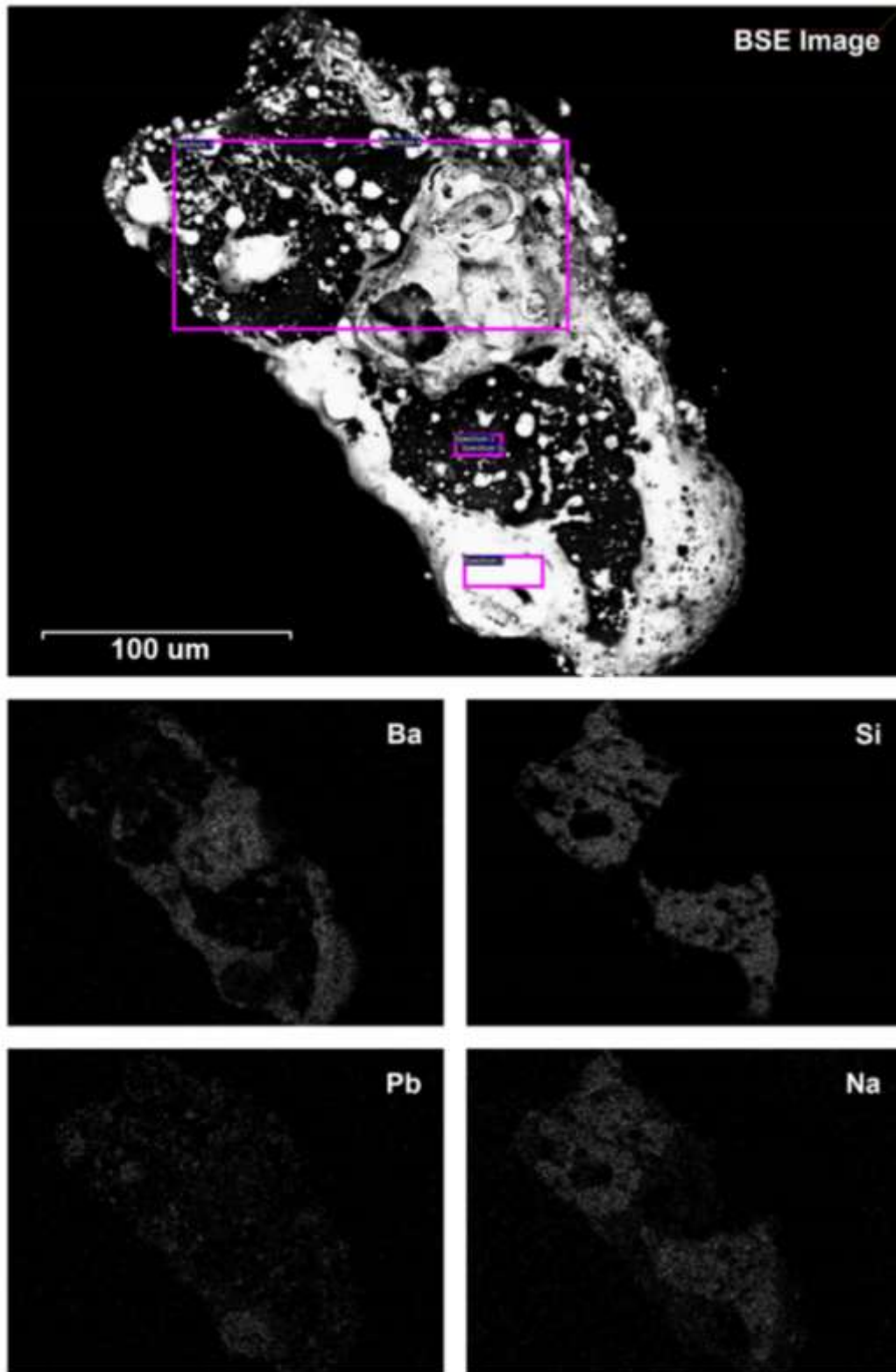


Figure 5-2: An arbitrarily selected particle recovered from cartridge debris shown in back-scatter and selected elemental maps reconstructed from EDX spectra. This particle appears to consist of a glassy core partially encapsulated by a Ba/Pb shell. Further analogous particles were also observed.

5.7.2 Survey of privately-owned vehicles

Observations about trends within the sample populations are provided here, with some illustrative examples from specific samples or participants highlighted. A full record of observations from each sample can be found in Appendix 5-2.

5.7.2.1. Vehicles owned by Shooters

Of the 22 vehicles covered by respondents to the survey, 7 were regularly driven by people declaring an association with firearms (n=35). Within this group, two further subgroups were identified on the basis of the written questionnaire: high-activity and low-activity firearm users. Three individuals stated that they typically attended sports shooting matches three times per week, and had last discharged a firearm 1.5 hrs, 2 hrs, and 2 days prior to sample collection respectively. Each regularly transported their firearms (within a case or bag) to local ranges using the vehicle in question, either in the rear storage compartment or in one instance on the front passenger seat. These were designated as high activity shooters. Using SEM-EDX, large numbers of particles designated as *characteristic of* and *consistent with* IGSR were detected on each of the four sampling locations of every vehicle of this group. Despite each declaring that they had washed their hands since the most recent contact with firearms, the subgroups' hands were also heavily loaded with *characteristic* IGSR (\bar{x} =128, s =76 particles). One participant's hands were also found to contain traces of akardite (0.8 ppb) and ethyl centralite (1.0 ppb).

The distribution of particles throughout each vehicle is represented by Figure 5-3. The drivers of vehicles designated V41 and V43 stated that they regularly transport firearms and ammunition in the rear of the vehicle, while the driver of V42 places a bag on the front passenger seat. The effect on the distribution is clear, as the cabin area of V42 has a much greater proportion of the total compared to the others. Each dashboard was also observed to yield traces of IGSR exposure despite no clear mechanism of transfer; guns had not been fired from within the vehicles and the dash surface is not typically contacted by the hands when driving. Similar results were reported by Blakey *et al.* (2019) [\[298\]](#). It is hypothesised that particulates from contaminated surfaces entering the car (the shooter, their gun bags) may dislodge through normal activity and then be distributed *via* airflow, only to later settle on horizontal surfaces.

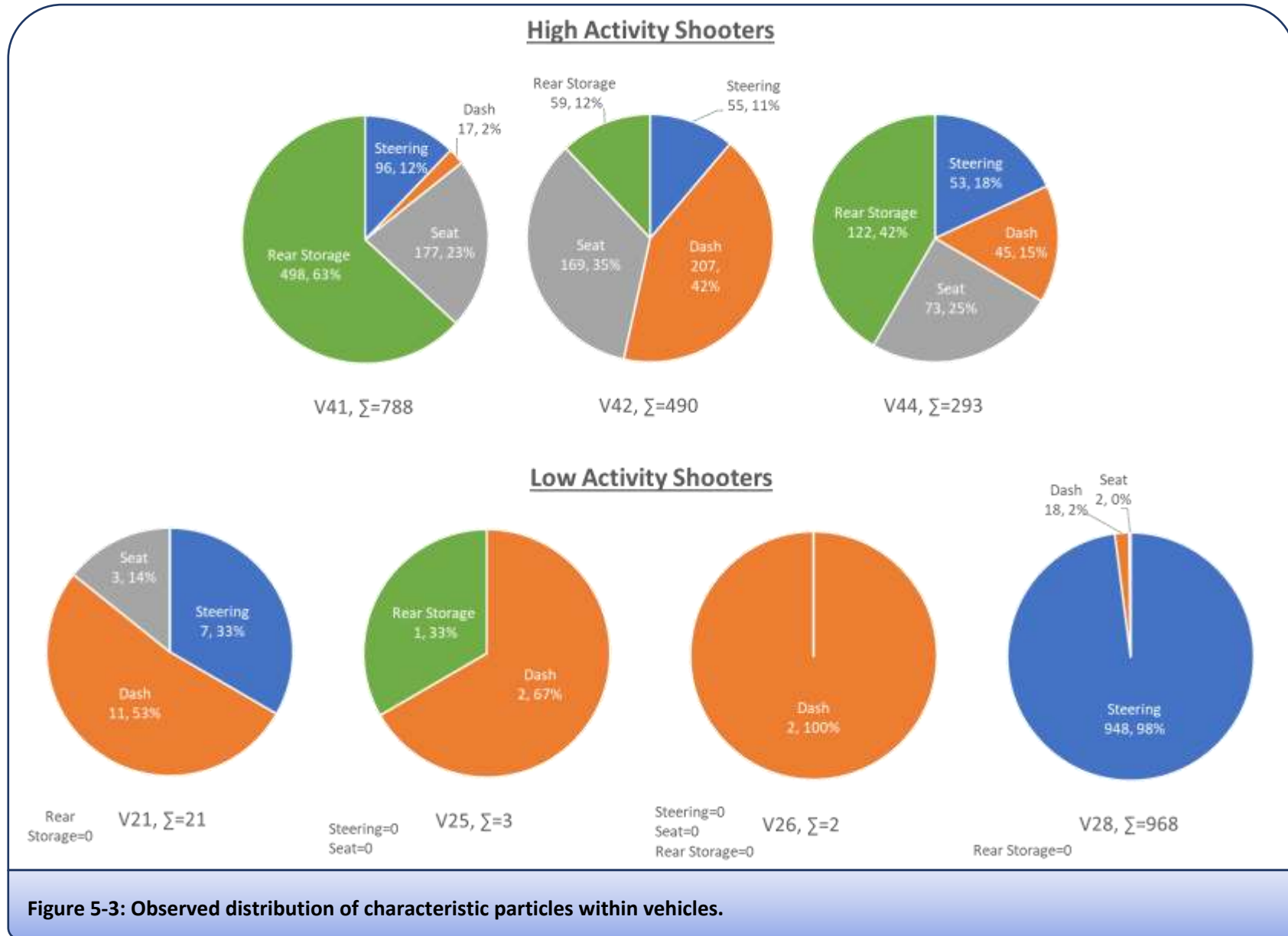


Figure 5-3: Observed distribution of characteristic particles within vehicles.

Two of the three high-activity vehicles (V41 & V43) were found to contain designated OGSR marker compounds >LODs in the rear storage compartment samples, with 5 compounds simultaneously detected by UHPLC-MS/MS in each. V43 also had 3 compounds present in the driver's seat sample. The estimated concentrations, determined by external calibration curve, are given in Table 5-6. These three samples meet the requirements to be considered *characteristic* of OGSR under the 2020 ASTM working standard [93].

Conc (ppb)	DPA	NO.DPA	(NO ₂).DPA	(NO ₂) ₂ .DPA	Ak	MC	EC
V41, Rear Storage Stub	40	1,700	3	28	Nil	Nil	5
V43, Rear Storage Stub	60	310	4	Nil	Nil	Nil	Nil
V43, Driver's Seat Stub	100	550	9	14	Nil	Nil	5

The second subgroup represented contributors who might participate in shooting activities every few weeks and had not attended their local range for ~1 month prior to sample collection due to a temporary closure (low activity shooters). Some members of this group had transported firearm paraphernalia in their vehicle previously while others had not. Of these participants none had *characteristic* IGSR particles on their hands. A noticeably smaller amount of IGSR was detected in this subgroup compared to the more active shooters – the absolute number of particles for three vehicles was in the range 2-21, with a higher proportion of these located on the dashboard. V26 yielded measurable amounts of akardite from two locations (Dashboard 5 ppb and Rear Storage 2 ppb) and thus these samples could be considered *inconclusive* for OGSR under the OSAC guidelines [93]. This result should however be considered in light of the fact that 2 *characteristic* IGSR particles were co-located on the dashboard stub.

The steering wheel sample from V28 initially appeared to be an outlier, as the automated SEM search function flagged 968 *characteristic* GSR particles. Upon manual review it was found that the majority of these were located in nine discrete clusters on some underlying low BSE brightness features, each containing dozens to hundreds of *characteristic* particles. This sample was also the only one of the low-activity shooters to return a *characteristic* designation for OGSR, with LC-MS/MS peaks matching methyl centralite (<1 ppb) and ethyl centralite (5 ppb). One potential explanation could be that larger pieces of debris, bearing both propellant and primer residues, were transferred to the steering wheel and not dislodged by later actions until adhering to the sampling stub.

Overall observations from the “shooter” group agree with the control scenario and previous studies like that of Blakey *et al.* (2019) [298]. The personal vehicles of recreational shooters are very likely to contain numerous traces of IGSR, correlated with the frequency and recency of shooting activities. The “high-activity” group had both more locations return reportable positive results and greater raw numbers of particles than the

“low-activity” shooters. *Characteristic* combinations of OGSR were also observed intermittently amongst this set of vehicles. These traces were only detected in locations expected to undergo the most intensive contact with GSR-contaminated items, such as firearms and associated paraphernalia being transported in the rear of a vehicle.

Some locations within the vehicles driven by low-activity shooters did not return any indication of GSR exposure. This may be because less material had initially been transferred into the vehicle, or because enough time and activity has occurred between shooting and sampling to reduce the recoverable GSR loading.

5.7.2.2. Vehicles owned by Non-Shooters

Of the 22 vehicles covered by respondents to the survey, 15 were regularly driven by people declaring NO association with firearms, resulting in 75 samples. Approximately half of these produced an analytical result indicating no contact with GSR whatsoever (*characteristic* or *consistent*, OGSR or IGSR). A single particle *characteristic* of IGSR was detected in this population subgroup, on a dashboard (1.3% samples positive, or 6.6% of vehicles). SEM images and an EDX spectrum collected from this particle are presented in Figure 5-4. The spectrum contained peaks for Ba, Pb, and Sb, along with Si, Al, Cu and Fe in decreasing intensity. In particular there were nodular regions enriched in Pb and Al, while the bulk of the particle appeared to consist of all listed elements comingled amorphously. While the morphology was not clearly spherical, the author was satisfied that the particle met requirements to be classified as GSR. This opinion was later confirmed by a qualified and experienced GSR expert. Therefore this particle was determined to be sufficiently GSR-like to meet the ASTM definition of *characteristic* ^[112]. There was a noted absence of any supporting population of *consistent* or *commonly associated* particles for this sample, nor were any diagnostic OGSR compounds observed. Consequently, such a sample would likely be interpreted very conservatively and in accordance with any further case-specific information known to the analyst. However the particle is noteworthy because, in agreement with studies conducted on human hands, it shows that there is a background prevalence of GSR or indistinguishable-from-GSR particles that must be accounted for when interpreting laboratory findings.

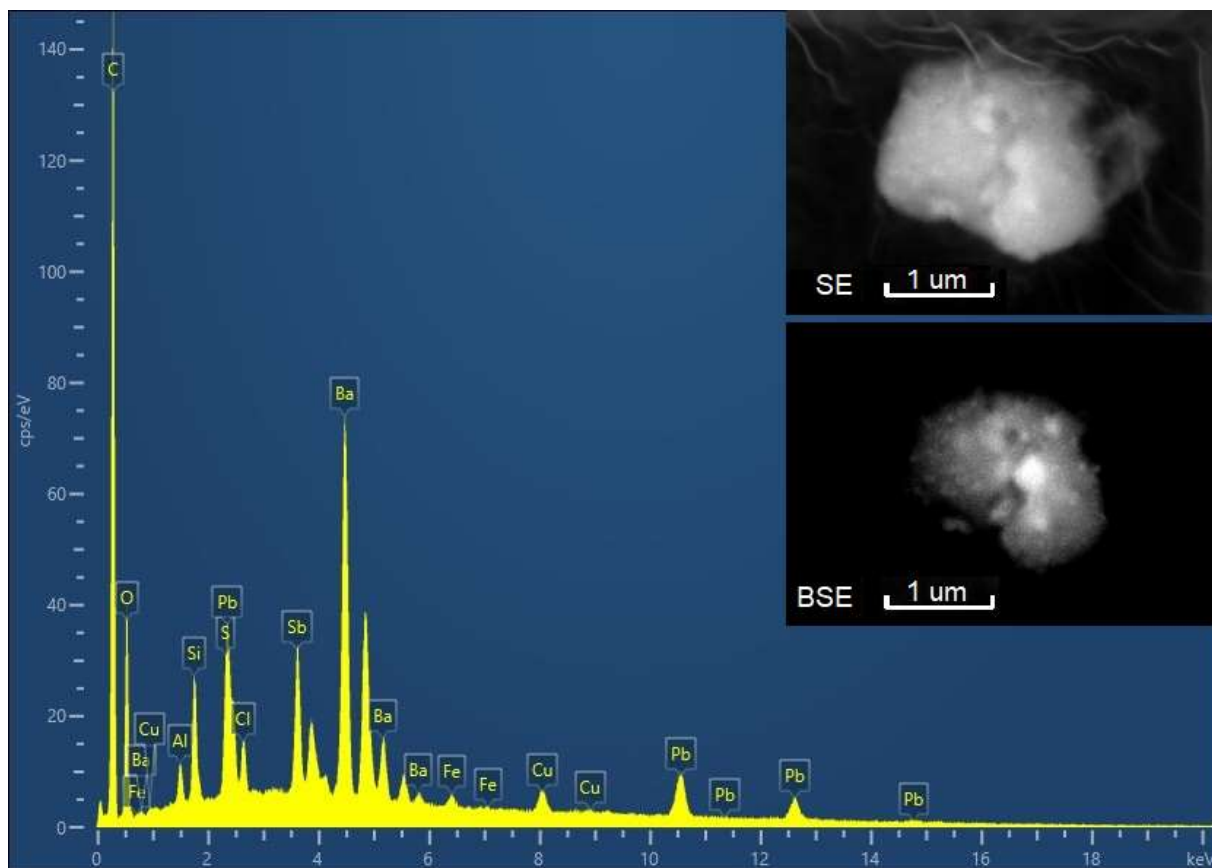


Figure 5-4: EDX Spectrum and SEM imaging for characteristic GSR particle located in a vehicle belonging to a survey respondent stating that they had never had contact with firearms.

As expected, it was comparatively more common to have samples containing particles meeting the ASTM definition of *consistent with* IGSR, with 26 samples (35%). Most had only 1-3 particles, largely of BaAl, Sr, or PbSb type. No trend was found in the distribution of these particles throughout the vehicle. One sample from a non-shooting driver's hands contained 21 PbSb particles; a potential explanation was found *via* the written survey wherein this individual declared recent or frequent contact with welding equipment.

Of the 75 samples, 12 (16%) were found to have a peak indicative of a single OGSR marker above their respective LODs. This was most frequently akardite ($n=10$, range 1-8 ppb) although nitrodiphenylamine was also detected ($n=3$, range 2-90 ppb). While one sample (V33D in Appendix 5-1

Information and instructions provided to participants in survey and sample collection



Sampling Instructions

Dear Volunteer,

Thank you for agreeing to take part in this research. In this kit you should have received a short survey and five adhesive stubs in plastic holders. We ask that you use one of these stubs to collect residues from your hands and use the remaining stubs to collect residues from four surfaces within your car as indicated below. The purpose of doing this is to see if residues from your hands or your car may give a positive result if tested for gunshot residue. This could occur because you have used a firearm for legitimate reasons, have come into contact someone else who has, or there is an unrelated substance causing a false positive.



In order to collect each sample of residue, you will need to unscrew the plastic cap and dab the adhesive against the relevant surface approximately 50 times or until it is no longer sticky. This shouldn't leave any noticeable residue behind. Please try to dab the stub straight up and down onto the surface it is sampling and press the stub flat as dragging the adhesive may cause it to tear or separate from its' aluminum backing. Once each sample has been collected, replace the plastic screw caps to avoid further contamination and put all samples together in the return envelope.

For samples collected from your hands, please use a single stub for both hands and focus on the webbing between thumb and forefinger as indicated in the pictures below.





If you are providing residues from your vehicle, there are four target areas that we request you sample:

- A) control surfaces – steering wheel, handbrake & gear levers using the same stub.
- B) front dashboard.
- C) driver's seat and seat-back.
- D) rear storage.

A visual guide is included below. On textile surfaces and the dashboard the sampling stub is likely to lose its stickiness quite rapidly. Therefore, in order to ensure maximum coverage of the large areas in B), C) and D), we suggest that you widely space your dabs across each surface.

Once the samples have been collected, double check that all five stubs are placed in the envelope alongside the completed questionnaire. Posting the kit for return will conclude your direct participation in the research, as your samples will be separated from any identifying information before analysis.

Once again, we thank you for your valuable contribution of time to this project.



Appendix 5-) was notable for having a greater concentration of NO₂DPA than any returned by a shooter, each of these are only classified as *inconclusive* under the proposed schedule. Sample V36D appeared to contain very low amounts of both akardite (7 ppb) and NO₂DPA (2 ppb), reaching the definition of *consistent* with OGSR. This represented 1.3% of non-shooter samples. No non-shooter sample met the requirements for designation as *characteristic* of OGSR under the ASTM's working standard [\[93\]](#).

5.7.3 Evaluating and Assigning Weight to Analytical Observations

Under the likelihood ratio framework, the extent to which observation of GSR traces helps to differentiate between hypotheses depends on the separate likelihoods of making those observations under each set of assumptions. If the LR = 1, the evidence is equally likely regardless of the proposed explanation, and it is therefore unlikely to be either significant or useful in answering the question at hand. A LR trending towards either 0 or infinity represents a greater degree of significance and support for one of the two competing propositions. The following discussion uses this framework to explore combining the data collected from the various subpopulations within the survey group, and how they might influence the assessment of a given forensic case.

5.7.3.1. Formal or Qualitative Assessment

The empirical data set detailed in section 5.7.2 categorized samples on the basis of prior activity, and can therefore be used to assign likelihood ratios to activity-level inquiries. Samples were designated "positive" for GSR if they contained *characteristic* material under the relevant definitions set by the ATSM [\[93, 112\]](#). These may or may not have also contained corresponding *consistent* material. The second category was samples containing some *consistent* traces only, expected by definition to offer a lower level of support to a prosecution hypothesis. The final category consists of samples entirely devoid of reportable GSR markers. The distribution of formal designations within each of the sample populations is shown in Figure 5-5.

In order to use these data to examine the outcomes that may be achieved using an evaluative approach, a typical set of hypotheses that could be set by the prosecution and defence are presented:

H₃: vehicle belongs to an individual who recently committed a criminal shooting

H₄: vehicle belongs to someone claiming no association with firearms

In this example, the high-activity shooter group was chosen as the most appropriate population for *H₃*, while *H₄* is best represented by the non-shooter group. If a questioned sample in this case was found to contain traces *characteristic* of GSR, the individual probabilities taken from Figure 5-5 are:

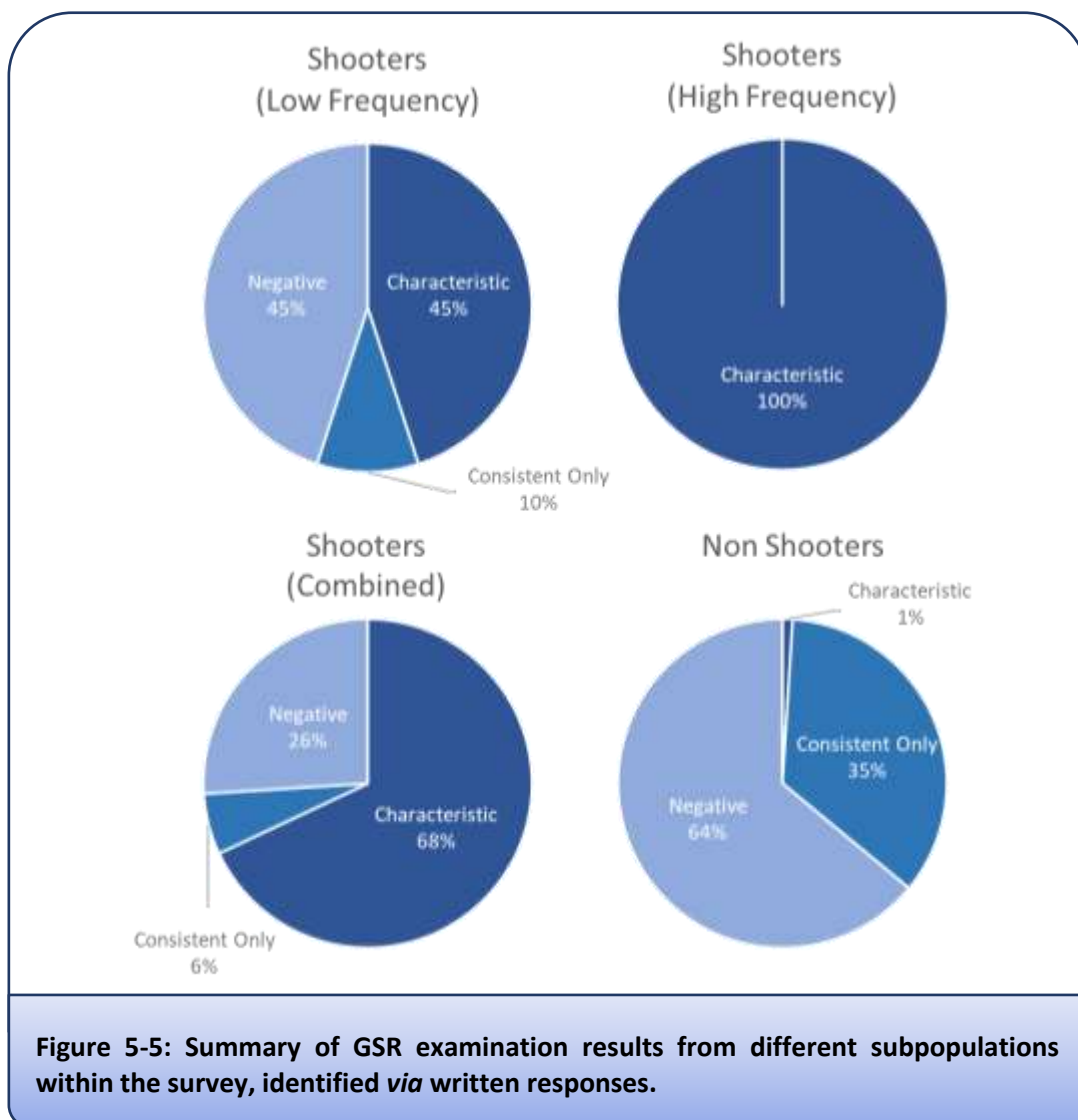
$$P(\text{Characteristic GSR} \mid \text{Car belongs to high-activity shooter}) = 15/15 = 1.00$$

$$P(\text{Characteristic GSR} \mid \text{Car belongs to non-shooter}) = 1/75 = 0.013$$

$$LR_1 = 1.00/0.013$$

$$= 75$$

Or stated in text, “It is 75 times more likely to observe *characteristic* GSR in a sample taken from a shooter’s car, than from a non-shooter’s car”. For reasons outlined in Chapter Four this is not the same as saying that a car containing GSR is 75 times more likely to belong to the criminal shooter, as the background rate of shooters amongst the motoring public is neither accounted for nor accurately modelled by the survey’s design. However using the verbal equivalent scale published by Martire *et al.* (2014), the evidence confers “moderate support for” H_p [244].



The result can be contrasted by using H_3 and the same data as the prosecution scenario, but instead substituting a different defence hypothesis. This alternate defence is presented as H_5 , with an accompanying change of model population:

H_5 : vehicle belongs to a recreational shooter

$$P(\text{Characteristic GSR} \mid \text{Car belongs to high-activity shooter}) = 15/15 = 1$$

$$P(\text{Characteristic GSR} \mid \text{Car belongs to recreational shooter (any activity level)}) = 24/35 = 0.686$$

$$LR_2 = 1/0.686$$

$$= 1.46$$

Under these conditions, the likelihood ratio is close to 1, and thus an observable GSR trace does not provide particularly meaningful support towards either of the propositions. This shows an empirical reflection of the instinctive notion that GSR traces found in the vehicle of a recreational shooter provide lesser potential as forensic evidence than when found associated with someone claiming no prior association with firearms.

For a final example, LR_1 from above is revisited. However in this case the combined shooter group is used to model H_p (perhaps the interval between shooting incident and sample collection is unknown). The non-shooter group is again used to model H_d . Finally, the hypothetical laboratory result is that no *characteristic* GSR markers are present (the presence of *consistent* traces is indeterminate). Under this scenario the $LR = 0.32$, offering weak support for H_d . This asymmetry in LRs calculated for GSR evidence, where the range of possible strength is biased towards the prosecution, has been noted previously [\[259\]](#). It is a consequence of the common situation wherein it is not possible to recover any physical trace of GSR after a shooting, due to losses such as natural transference or deliberate cleaning.

$$P(\text{No Characteristic GSR} \mid \text{Car belongs to Shooter}) = 11/35 = 0.314$$

$$P(\text{No Characteristic GSR} \mid \text{Car belongs to Non-Shooter}) = 74/75 = 0.987$$

$$LR_3 = 0.314/0.987$$

$$= 0.32$$

5.7.3.2. Quantitative Modelling

The preceding estimates of LR under various propositions relied solely on a binary designation for each sample; either it contained some unspecified amount of *characteristic* GSR, or it did not. Consequently samples containing only a single particle were given equal weighting with those containing hundreds of particles. It can be readily assumed that this assumption does not accurately reflect real-world conditions. A greater degree of evidential strength can be gained by considering the magnitude of each GSR trace, measured by a broader range of potential LR values.

Due to insufficient instances of OGSR in the survey group, inputs were based solely on *characteristic* IGSR particles, forming two univariate sets of discrete data (shooter and non-shooter). Furthermore the count of particles on sample V28A was revised down to 9 (see discussion in 5.7.2.1 above). A mixed-model methodology estimating the LR was undertaken, following prior work described by Damary *et al.* (2016) [\[259\]](#).

This approach assumes that observing small numbers of particles is the norm, and that the likelihood of occurrence is inversely correlated to the number of particles. A Poisson distribution was used to model non-shooter samples, as the empirical mean and variance were equal for that set. A negative binomial distribution was used to model the shooter group, as the sample variance was much greater than the sample mean for these data. Equation 5-2 and Equation 5-3 describe the Poisson and negative binomial functions respectively, while Figure 5-6 shows the result of modelling the survey data. The LR for a given number of particles is then calculated as the ratio of the two probability distribution functions (PDFs). In contrast to Damary *et al.*, who worked on data collected by Cardinetti *et al.* (2006), the models herein did not account for time-since-shooting [258, 259]. Nonetheless they do serve to demonstrate the advantages of quantitative LR modelling and indicate an approach that might be applied to more comprehensive empirical surveys.

Equation 5-2:

Poisson distribution describing the expected probability of observing a given number of IGSR particles, where \bar{x} = mean number of particles across the samples and x = number of particles observed in a specific sample.

$$P(x|\bar{x}) = e^{-\bar{x}} \left(\frac{\bar{x}^x}{x!} \right)$$

$$\bar{x}_{\text{non-shooter}} = 0.013 \quad \sigma^2_{\text{non-shooter}} = 0.013$$

Equation 5-3:

Negative binomial distribution describing the expected probability of observing a given number of IGSR particles, where \bar{x} = mean number of particles across the samples, x = number of particles observed in a specific sample, and r = the dispersion parameter. r was derived using the maximum likelihood estimator method; $r = \bar{x}^2 / (\sigma^2 - \bar{x})$.

$$P(x|\bar{x}, r) = \left(\frac{\Gamma(x+r)}{\Gamma(r)x!} \right) \left(\frac{r}{r+\bar{x}} \right)^r \left(\frac{\bar{x}}{r+\bar{x}} \right)^x$$

$$\bar{x}_{\text{shooter}} = 57.46 \quad \sigma^2_{\text{shooter}} = 9,935 \quad r_{\text{shooter}} = 0.334$$

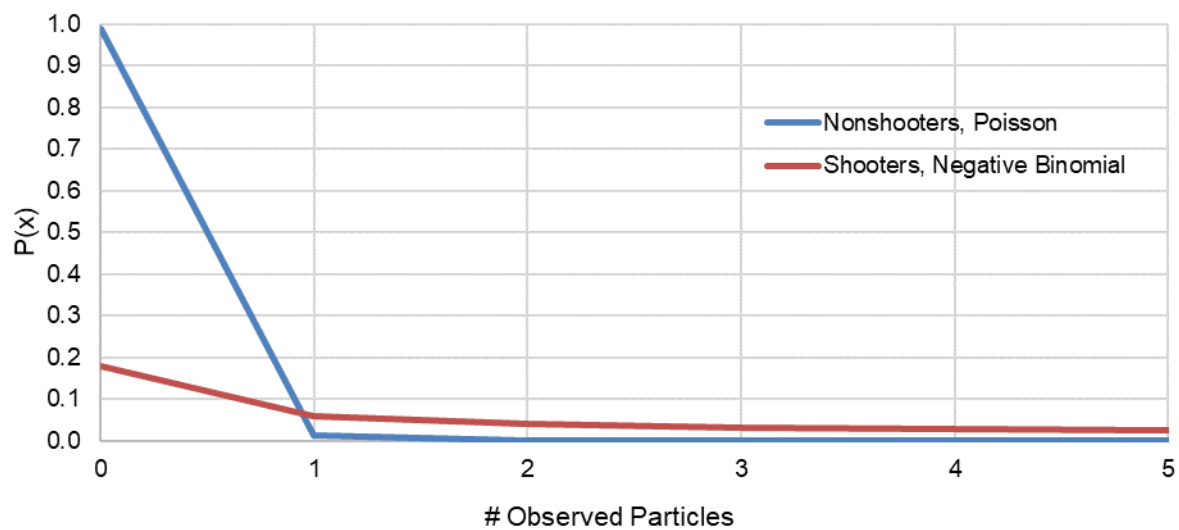


Figure 5-6: Probability distribution functions describing the estimated probability of observing a given number of characteristic particles, in samples taken from different subpopulations

Using the mixed-PDF calculation, finding no particles results in $LR_4 = 0.18$, offering weak support to H_d . Observing a single particle shifts support towards favouring the H_p proposition, albeit also weakly. As there is little overlap in the distribution of particles between the two population subgroups, the likelihood ratios quickly reach unwieldy proportions as shown in Table 5-7. The adjusted mean value for particles observed when combining both shooter-group sets was 57. Even though this value is comparatively conservative when considering the number of particles that may be observed after a criminal shooting, LRs in excess of 1×10^{181} are generated. Considering the modelled probability of observing 57 particles in a sample from the shooter group is only ~ 0.03 , this suggests poor modelling by the right-side tail of the Poisson distribution for the non-shooter group. Finding GSR traces in non-shooters' cars is certainly rare, and so more accurate modelling might require an unacceptably large amount of field survey samples. Instead, minimum probability values could be set empirically by the expected rate of gross errors (mislabelling, contamination during collection etc.), or else derived from first principles based statistically on the number of samples collected in the survey used to generate PDFs. However overly large numerical LRs may in some respects be mitigated by well-calibrated verbal scales, as all values above 1×10^6 become equivalent under the description "extreme support".

Table 5-7: Likelihood ratios estimated under mixed-PDF model				
Observed Count	P(x NS, Poisson)	P(x S, Neg Binom.)	LR	Verbal Equivalent
0	0.987	0.179	0.18	Offers weak support to H_d
1	0.013	0.059	4.51	Offers weak support to H_p

2	9×10^{-5}	0.039	449	Offers moderately strong support for Hp
3	4×10^{-7}	0.030	78,143	Offers very strong support for Hp
4	1×10^{-9}	0.025	$1.9 \times 10^{+7}$	Offers extreme support for Hp
5	3×10^{-12}	0.022	$6.3 \times 10^{+9}$	
10	5×10^{-26}	0.013	$2.8 \times 10^{+23}$	
57*	3×10^{-184}	0.003	$1.0 \times 10^{+181}$	

5.8 Conclusions:

The purpose of the work outlined in this chapter was to investigate the potential prevalence of GSR in vehicles **not** connected with criminal shootings. This is important as a contrast to observations made about suspect vehicles, so that the possible weight of evidence provided by analytical findings can be appropriately communicated to police investigators or the judicial system. Trials conducted under controlled circumstances, and survey samples collected from recreational shooters, showed that detectable traces of both OGSR and IGSR are transferred into vehicles from shooting events that occur separate from the vehicle. This is both intuitive and in agreement with previous studies [\[297, 298\]](#). The magnitude of these traces was highly variable but commonly correlated to the intensity and recency of drivers' previous firearm use.

The background prevalence of GSR in vehicles having no known association with firearms was also examined. While the rate of occurrence was very low, a non-zero amount of GSR or indistinguishable GSR-like material was observed. Notably a single "three-component" particle, meeting the requirements to be formally identified as *characteristic* GSR, was found on the dashboard of a non-shooter's vehicle. There was also more widespread, but formally *inconclusive*, observation of compounds indicative of OGSR. The outcomes of the present study are generally in line with equivalent surveys of individuals' hands, but is among the first to target vehicles [\[206\]](#). These results may serve to inform the "maximum" evidential strength that can be assigned to GSR detected within questioned samples.

The examples given in section 5.7.3 above show that the selection of statistical model can strongly influence the numerical estimation of evidential strength that is eventually calculated, while using the same underlying

data. They also illustrate the importance of collecting data to represent the potential range of hypotheses that may be advanced by both prosecution and defence. Some of these have not been addressed in previous literature on the subject, which has tended to focus on either police vehicles or recreational shooters' vehicles, while omitting non-shooter's vehicles. A set of 22 specimen vehicles is clearly an inadequately small sample size with which to capture the true prevalence of GSR or GSR-like material in Australian motorists' vehicles. The work herein suggests that there is a need for larger, inter-laboratory studies of vehicles such as the one exemplified by Stamouli *et al.* (2021) for POIs' hands [\[34\]](#). Such a study would allow for further refinement of statistical models and hence a stronger foundation for numerical evaluation of case findings.

Chapter 6:

Analysis of OGSR by Ambient Mass Spectrometry

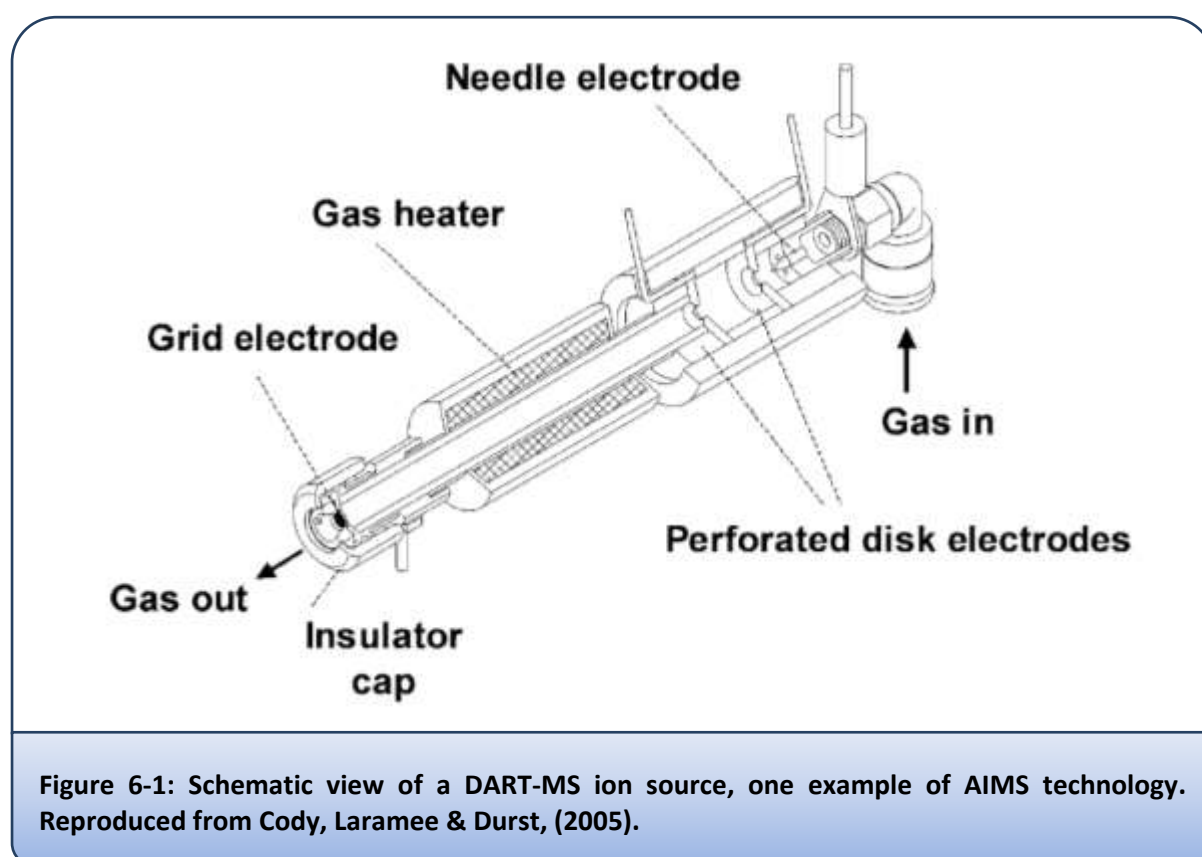
6.1 Background

At the outset of this project, there was neither a published standard nor settled practitioner consensus on the method most appropriate for analysing organic gunshot residues (OGSR). During the intervening period, hyphenated chromatography-mass spectrometry systems have, as in so many other sub-disciplines of forensic science, gained traction as the primary technology in this regard. A provisional standard based upon this foundation has since been distributed by The Organization of Scientific Area Committees for Forensic Science [\[93\]](#). Pending any radical innovations, it would seem reasonable to expect that further inter-laboratory harmonisation will develop along related lines. Accordingly, much of the experimental work outlined in the preceding chapters made use of ultra-high performance liquid chromatography and tandem mass spectrometry (UHPLC-MS/MS) for data collection.

However, an alternative technology was explored prior to the aforementioned developments. Promising initial results by Morelato and colleagues, and especially Cody and colleagues, suggested that ambient-ionization mass spectrometry (AIMS) may be fit for purpose [\[188, 202\]](#). AIMS describes the family of instruments capable of desorbing and ionizing material from an ambient state, such as on a surface or in solution, and determining chemical composition solely *via* mass spectrometry. This can be achieved by forming a flow of reagent species such as charged vapour droplets, plasma or metastable gaseous species. The reagent stream is typically heated before it is directed towards potential analytes, in order to better stimulate them into a gas phase, where they can be ionised and dawn into a mass spectrometer for detection. If the sample type is amenable, such an approach offers many potential benefits including speed, sensitivity, and versatility. As originally conceptualized, it was thought that it may be possible to detect OGSR traces directly from the carbon adhesive tabs used for both inorganic GSR collection and mounting of samples for electron microscopy. This would circumvent requirements for either a separate GSR sampling platform or an extraction process, while allowing for significantly faster provision of preliminary results than the prevailing state of the art.

Two instruments featuring AIMS capabilities were accessible for use during the project. Both operated by inducing electronically excited reagent species into a flow of gas with high-voltage electrodes, and thus offer AIMS through Penning and atmospheric-pressure chemical-ionization (APCI) mechanisms. The first was a Perkin-Elmer AxION® Direct Sample Analysis (DSA™) system with an associated time-of-flight mass spectrometer (ToF-MS). The second was a Jeol USA Direct Analysis in Real Time (DART®) system, interfaced to a Thermo Fisher Scientific Velos Pro linear ion trap spectrometer. An example schematic is provided in Figure 6-1. The utility of the DSA system towards analysis of smokeless powders was assessed, as an intermediary towards more challenging residue trace samples. The

results of this study were published in the Journal of the American Society for Mass Spectrometry under the title “*Armed with the Facts: A Method for the Analysis of Smokeless Powders by Ambient Mass Spectrometry*” in 2020 (Bonnar et. al., 2020, Journal of the American Society for Mass Spectrometry, DOI: <https://doi.org/10.1021/jasms.0c00193>.)^[302]. The full text of this article has been reproduced in section 6.2, with minor changes to formatting to maintain consistency. The introduction of this publication provides a background on both previous instrumental approaches to OGSR analysis, and also the operating principles and potential benefits of AIMS instruments in general. Similar fundamental studies on the performance of the DART for compounds relevant to OGSR are detailed in section 6.3, along with comparisons to the DSA as appropriate. Concluding remarks can then be found in section 6.4.



6.2 Armed with the Facts: A Method for the Analysis of Smokeless Powders by Ambient Mass Spectrometry.

6.2.1 Abstract

The work presented here follows several others in investigating what capabilities, if any, ambient mass spectrometry might have towards the analysis of compounds commonly associated with smokeless propellant powders. This family of instrumental techniques has attracted curiosity from the field of forensic science due to desirable properties such as rapid collection of information-rich data, combined with minimal requirements for sample mass and preparation. Experiments were conducted with a “Direct Sample Analysis” ion-source integrated with a time-of-flight mass spectrometer. The ionization behaviours of nitroglycerin, methyl- & ethyl- centralite, akardite, diphenylamine, nitrosodiphenylamine and nitrated diphenylamine derivatives were investigated specifically, with accurate-mass data presented for each. Diphenylamine standards were used to demonstrate the performance of this instrument, which exhibited good response linearity across one order of magnitude and sub-nanogram detection limits.

Thirty smokeless powder extracts, recovered from ammunition potentially in circulation within Australia, were analysed to determine whether the technique is appropriate for rapid analysis of smokeless powder particles. Results demonstrated that the technique might be applied to compare individual particles with each other or to a database. Such a capability may be of value in the examination of explosive devices containing smokeless powder, post-blast residues therefrom or muzzle discharge from a close-range shooting. However, when efforts were made to detect residues from the hands of a volunteer shooter, only some returned positive results, and a high background signal from the sample collection stub indicate that detection using this instrument is thus far insufficiently reliable.

6.2.2 Introduction

“Smokeless powder” (SP) is an energetic material based on nitrocellulose, often also containing nitroglycerin and a variety of additives such as plasticisers, burn-rate modifiers and stabilisers [\[303\]](#). It is among the more readily available energetic materials [\[303, 304\]](#), being present in firearm cartridges as a propellant and also available for purchase as a bulk product in some jurisdictions. As such, the analysis of SP can be of interest in criminal investigations due to its misappropriation for use in improvised explosive devices (IEDs) [\[304, 305\]](#). In addition, the analysis of SP can be important in the investigation of shootings. This is because the plume of ‘smoke’ ejected during discharge of a firearm contains traces of SP (referred to as organic gunshot residue or OGSR) as well as traces derived from

the ammunition primer, cartridge case and projectile (referred to as inorganic gunshot residue, or IGSR). The two types of gunshot residue (GSR) settle on nearby surfaces, including the shooter (especially their hands) and the victim in the case of a close-range shooting, and may be collected for analysis [9]. The detection and analysis of intact SP kernels, post-blast traces and GSR by forensic scientists can provide valuable information by establishing links between persons of interest, explosive devices, firearms/ammunition, victim(s) and crime scene.

The composition of SPs and the residues they produce when ignited or detonated have been extensively studied [224]. OGSRs may additionally incorporate material originating from the ammunition's primer, gun oils, projectile and gun barrel [9]. While up to 136 compounds have been associated with ignited SP [84], many of these are likely to be encountered as generic chemical products from the combustion or pyrolysis of organic matter and are therefore not solely indicative of a SP source. Goudsmits *et al.* (2016) shortlisted 20 compounds considered to have significant forensic value (see Table 6-1) [85]. Their selection criteria included known origins, strong association with SP and minimal non-propellant applications. The resulting targets largely are molecules that are present in the original SP formulation that remain unchanged during combustion or explosion. Particularly strong attention in literature has been placed on nitroglycerin (NG), methyl- and ethyl- centralite (MC and EC), diphenylamine (DPA) and nitrated or nitrosylated derivatives of DPA formed during propellant degradation. It is envisaged that these compounds, especially in combination with one another, may eventually be codified as "characteristic of" or "consistent with" a sample truly originating from propellant. The Gunshot Residue discipline-specific Subcommittee under the auspices of the National Institute of Standards and Technology (NIST) Organization of Scientific Area Committees (OSACs) has already made movements in this direction with regard to OGSR specifically [93], which if adopted would bring OGSR analysis in line with the current interpretative and reporting frameworks used for IGSR, for example ASTM E1588-17 [112].

Beyond the initial determination of whether a specimen contains SP or SP-residues, further information can be extracted from the combination of additives linked to individual product formulations [134]. This can potentially be exploited to discriminate between SP sources; either by inclusion/exclusion when compared to other case-specific samples, or else statistical methods may be used to evaluate the relative strength of associations within reference libraries [59-62]. A robust discussion of some of the factors affecting the value of these associations was given by Dennis *et al.* (2016) [62]. Supporting activity-level narratives with SP trace evidence with regards to OGSR examination requires more cautious interpretation, as many factors may affect the observed traces aside from the act of shooting itself. These factors include background distribution of material from

lawful firearm use, subsequent transfers between surfaces, pollution from law enforcement equipment and the actions taken by individuals between incident and evidence collection [12, 20, 157, 208].

Table 6-1: Goudsmits *et al.*'s proposed hierarchical classification of compounds associated with propellant [85]

Proposed Classification	Compound Name	Purpose in Smokeless Powder
1. Compounds that are very strongly associated with GSRs with very restricted applications unrelated to GSR.	Ethyl centralite	Stabiliser
	Methyl centralite	Stabiliser
	Nitroglycerin	Explosive
	Nitroguanidine	Explosive
2. Compounds that are strongly associated with GSRs, but which have more applications unrelated to GSR.	2,4-Dinitrotoluene	Flash suppressor
	Akardite II	Stabiliser
	2-Nitrodiphenylamine	Stabiliser
	4-Nitrodiphenylamine	Stabiliser
	Diphenylamine + nitrated derivatives	Stabiliser
3. Compounds that are associated with GSR, but which are detected less frequently and have more applications unrelated to GSR.	Nitrocellulose	Explosive
	Other nitrotoluenes	Sensitizer
	Other Diphenylamine Derivatives	Stabilisers
	Triacetin	Plasticiser

In a forensic context, SP residues can be recovered using several different methods, such as swabs, wipes, adhesive lifts, solvent washes, or headspace absorption. These were reviewed comprehensively by Goudsmits *et al.* in 2015 [84] and more recently by Feeney *et al.* (2020) [224]. Some technologies, such as portable ion-mobility spectrometry, can also provide compositional information directly without a “collection” step [306]. While swabbing remains popular for explosion debris [165], adhesive-based collection techniques have been shown to most efficiently recover SP residues from the hands after firearm discharge [18, 53]. This is convenient, as current standard practice for the detection of GSR is to sample surfaces using conductive carbon-adhesive stubs, then analyse the stubs with scanning electron microscopy coupled with energy dispersive spectroscopy (SEM-EDS). This approach specifically targets inorganic GSR (IGSR) that condenses from an ammunition’s primer after firing [112] and it also detects metallic particles arising from the gun, projectile and cartridge case. Black *et al.* (2017) [202] demonstrated that sufficient SP material could be extracted from the surface of such a stub with a droplet of organic solvent to enable analysis of OGSR compounds by Direct Analysis in Real-Time Mass Spectrometry.

Further evaluation of this stub-and-droplet extraction approach has shown successful detection of SP residues on the hands of a recent shooter using hyphenated liquid chromatography and mass

spectrometry, without disruption to particles of IGSR present on the stub surface [223]. While OGSR examination is unlikely to fully replace the prevailing method of choice for shooting investigations (i.e., IGSR examination), there are potentially many benefits to carrying out the analysis of OGSR traces in addition to the analysis of IGSR. When compared to assessing IGSR alone, OGSR may increase the total mass of crime-related trace for detection, provide a greater amount of orthogonal chemical information, and may help analysts discriminate between types of ammunition and non-firearm sources of GSR-like material [123, 125].

Many analytical techniques have been applied to characterisation of SPs and the detection of their trace remnants after combustion or detonation. It should be noted that these are distinctly different challenges as traces are expected to consist of micrograms or nanograms of mass, be distributed over an unknown area, and be present on a variety of surfaces [9, 165, 305]. Approaches explored in literature are wide-ranging and include colour tests, infrared & Raman spectrometry, electrochemistry, electrophoresis, ion mobility spectrometry, and hyphenated chromatography-mass spectrometry. These have been reviewed by authors such as Meng & Caddy (1997), Dalby & Butler (2010), Goudsmits *et al.* (2015), Brozek-Mucha (2017) and Klapac *et al.* (2020) [9, 84, 105, 160, 307]. In particular, the application of many forms of mass spectrometry to OGSR was reviewed by Taudte *et al.* in 2014 [104]. Publications are now emerging that utilise HPLC-MS to answer further questions about the forensic implications of the detection of OGSR and the factors impacting upon it, such as sampling effectiveness, transfer or persistence [18, 23, 208] and therefore LC-based techniques may be emerging as the preferred analytical system moving forward. A note on limits of detection (LODs) reported using liquid-chromatography techniques is provided for context; Tables compiled by authors such as Taudte *et al.* (2014) and Maitre *et al.* (2017) indicate that LODs for individual compounds are in the low-nanogram to high-picogram range [104, 157]. However this will typically represent the on-column amount of sample, which indicates that the actual sample mass *in vitro* (e.g., the OGSR present in the entire trace collected from a person of interest) may need to be somewhat higher, to account for sample manipulation and injection requirements.

In contrast, there is another family of evolving analytical techniques that are of great interest to the field of forensic science, and which may be uniquely suited to the task of SP residue detection as a result of several benefits described below. These are the techniques based on instruments capable of desorbing and ionising material from an ambient state for analysis by mass spectrometry. The seminal works introducing ambient-desorption/ionization mass spectrometry (henceforth abbreviated as AIMS) were released by Takats *et al.* (2004) and Cody *et al.* (2005), although dozens of instruments have been developed in the intervening time and the field has been regularly reviewed [177, 179-182, 193,

[308](#). Broadly speaking, AIMS instruments operate by forming ionising reagent species such as plasma, metastable excited molecules or charged droplets in a heated gas or liquid spray. The reagent stream is then directed towards a sample surface in the open environment where the desired analytes are first desorbed and then ionised in the gas or vapour phase. These methods are expected to provide a relatively gentle ionization environment compared to spectrometers operating *via* principles such as electron ionization in a vacuum, leaving a greater proportion of intact molecular ions (likely in a protonated or otherwise adducted form). In the absence of a chromatogram, identification of specific compounds must be achieved through accurate-mass measurement. This is nonselective between isomeric compounds. If the mass spectrometer has the capability, multiple reaction monitoring (MRM) can then be used to produce characteristic fragmentation patterns from selected parent ions, to aid in structural confirmation and potentially discriminate between isobaric interferences.

AIMS has been proposed as a strategy to rapidly analyse many different sample types relevant to forensic science – indeed the two have been described as a “*perfect couple, destined for a happy marriage*” (Correa *et al.* 2016) [178](#). AIMS would appear to offer several strengths over pre-existing hyphenated mass spectrometry workflows in the forensic context. The first is the potential for markedly reduced sample preparation time; analytes can often be detected directly from any matrix or surface that does not itself ionize strongly or cause undue ion suppression. This is useful for decreasing laboratory workload, improving turnaround times for reporting and for enabling the rapid analysis of unstable, time-sensitive analytes. Secondly, as AIMS is highly sensitive and minimally destructive, little mass is required and sample integrity can be largely preserved for further analyses. The ever-increasing number of proof-of-concept studies also suggests that AIMS is robust and universal enough to find applications spanning counter-terrorism, chemical warfare, food adulteration, counterfeiting, illicit drug detection and toxicology [177](#), [185](#), [309-311](#).

There is a growing body of literature specifically relating to the application of these techniques to SPs and OGSR, as apparent in the review “Recent advances in ambient mass spectrometry of trace explosives” by Forbes & Sisco in 2018 [312](#). Zhao *et al.* (2008) reported the detection of MC and EC from a variety of surfaces using a bespoke desorption electrospray ionization (DESI) source in positive ionization mode, including directly from volunteers’ hands at a limit of detection (LOD) as low as 8 pg cm⁻² [98](#). This group then used their instrument to correctly sort a group of 20 participants into shooter and non-shooter categories. In 2012 Morelato *et al.* attempted to apply DESI-MS to the adhesive stubs commonly used to sample suspects for GSR, with the aim to provide a comprehensive sampling strategy including IGSR analysis by SEM-EDS [188](#). Their method was successful in expanding the list of target analytes to include DPA and its nitrated derivatives, and in detecting these from a glass surface.

However, they reported high limits of detection for EC on the stub sampling surface and DPA could not be reliably detected. Perez *et al.* (2016) analysed SP residues from the surface of sectioned small-arm ammunition casings using Laser Electrospray Mass Spectrometry (LEMS), which introduces the possibility of chemical imaging [59]. An alternative sampling medium was proposed by Fedick & Bain (2017) who used medical swabs constructed with an aluminium handle and rayon absorbent tip to sample shooters' hands. Solvent was then applied to the tip while a high voltage was applied to the handle to induce spray ionization, thus making the sampling media integral to the ionization process. Limits of detection by an Orbitrap mass spectrometer were reported as 50 ng [190].

Plasma-based AIMS has also been described several times for application to SP and OGSR analysis, almost entirely using Direct Analysis in Real Time (DART) MS instrumentation. Li *et al.* (2016) explored the use of sorbent-coated wire mesh to concentrate dynamic headspace samples from above 5 mg of SP, to represent post IED-blast traces [200]. The wire was then desorbed by DART-MS to detect NG in negative-ionization mode and DPA, nitrosodiphenylamine (NNODPA), Akardite (AK), EC and dibutyl phthalate in positive-ionization mode. Williamson *et al.* (2018) instead described a different dynamic headspace-sampling technique called capillary microextraction of volatiles (CMV) to pre-concentrate vapours emitted from standards of SP compounds [201]. When 15 ng deposits of standard were vaporized and diluted with 2.5 L of air, between 1-6 ng was recovered on the CMV and this was shown to be enough for both qualitative screening by DART-MS and confirmatory analysis by GC-MS from the same sample. In 2017 Black *et al.* presented a feasibility study on a novel trace evidence source – polymers incorporated into OGSR from 3D printing material used to self-manufacture firearms [202]. Glass capillary tubes were used to scrape the bullet and cartridge cases and then the tube was placed in the DART ionization path, where various polymers corresponding to the printing materials were readily detected. SP compounds more traditionally associated with OGSR were also detected in this manner, and from methanol extracts of GSR stubs used to sample a cotton target. Lennert & Bridge (2018) took the DART-MS approach further, comparing the data it produces to GC-MS outputs for the purpose of classifying and discriminating between 34 different SP products. They found that comparable results were obtained for individual powders on each instrument, with the exception that NNODPA was observed by DART only. Spectra obtained *via* either source were found to fit into 11 categories (based on powder composition) by hierarchical cluster analysis, although the distribution of those categories varied depending on the source of data. The same authors have also explored using an independent thermal desorption device to improve analyte desorption, with improved reproducibility on propellant additives but with the trade-off that thermally sensitive NG was not detected [61].

This manuscript aims to add to the aforementioned studies by investigating three different aspects relevant to applying a specific type of ambient mass spectrometry instrument, the Perkin Elmer Direct Sample Analysis-Time of Flight mass spectrometer (DSA-ToF-MS), to the analysis of SP samples:

1. The specific ionic species formed from probative SP compounds under a given set of DSA-ToF analysis conditions were examined
2. Analytical figures of merit for the DSA-ToF were collected, to understand its performance
3. Results from simulated, real world-relevant samples that may be encountered during forensic case work were demonstrated.

For the third aspect of this study, the simple and rapid extraction process reported by Black *et al.* [202] was used as it offered the greatest potential for simple integration into current forensic operations and does not interfere with IGSR deposits [223]. The authors explicitly recognise that there are additional considerations regarding analysis of OGSR recovered from hands such as sampling efficiency, persistence, transfer and interferences that affect the forensic interpretation of OGSR evidence for legal purposes. These are not explored in the current work, in favour of focussing on the performance of the instrument itself.

6.2.3 Experimental

6.2.3.1. Ionization Source and Mass Spectrometry

The instrument used for this work was a Perkin Elmer AxION 2 ToF-MS equipped with the DSA ionization source. The application of DSA mass spectrometry to gunshot residues has not previously been the subject of detailed reports in scientific literature. However, promotional material by the manufacturer indicates that two key compounds, nitroglycerin and ethyl centralite, can be analysed using this technology. The DSA ion source utilises a high-voltage corona needle to generate initial reagent species from a flow of heated nitrogen gas. The energy from some of these species may be directly transferred to the analyte, but it has been observed that a larger contribution occurs *via* a series of intermediary charge transfers involving protonated water clusters [313, 314]. As such, the DSA provides AIMS capability through an atmospheric pressure chemical ionization (APCI) mechanism. The ionization behaviour of several key OGSR compounds under the conditions provided by this instrument were explored. Analytical selectivity and several key figures of merit of use in instrument validation were determined, to present an indication of likely performance in an operational setting. This was applied to a variety of extracts prepared from unfired smokeless powders and from hand samples collected after shooting tests.

APCI-TOF Tuning mix (G1969-85010, Supelco/Agilent Technologies) diluted 1:10 in ultra-pure milliQ water (18.2 M Ω .cm) was continuously nebulised alongside the nitrogen flow to enable accurate m/z calibration. No further reagents were added to promote adduct formation. All sample solutions were analysed by pipetting 10 μ L onto stainless steel mesh wells (PerkinElmer Waltham, MA, USA), typically with three replicates for smokeless powder extracts and five replicates for studying fragmentation patterns.

Negative ionization mode was used for the detection of nitroglycerin and nitro-derivatives of propellant stabilizers (e.g., nitrodiphenylamines) under the following settings: Heater Temp: 150°C, Corona Current: 4 μ A, Endplate: 200 V, Capillary Entrance: 800 V, Capillary Exit: -100 V, Spectra Acquisition Rate: 1 Hz. Positive ionization mode was used for the detection of additive compounds and their reference standards under the following settings: Heater Temp: 250°C, Corona Current: 4 μ A, Endplate: -100 V, Capillary Entrance: 800 V, Capillary Exit: 100 V, Spectra Acquisition Rate: 1 Hz. Spectra were analysed in the "ToF MS Driver" software (Perkin Elmer, version 8.1) by averaging \sim 5 spectra per sample and calculating the accurate mass-to-charge ratio to +0.00005 Da. This value was then averaged over the 3 or more repeated solution injections. The measured m/z was then compared to the calculated accurate mass for the relevant ions, with discrepancies reported in ppm.

6.2.3.2. Materials:

Reference Standards: Trinitroglycerin (1,000 μ g mL⁻¹) in acetonitrile and a mixed GSR surveillance standard containing dimethylphthalate (200 μ g mL⁻¹), diphenylamine (200 μ g mL⁻¹), n-nitrosodiphenylamine (75 μ g mL⁻¹), two isomers of nitrodiphenylamine (50 μ g mL⁻¹ each) and four isomers of dinitrodiphenylamine (50 μ g mL⁻¹ each) in acetonitrile were purchased from Cerilliant, *via* Sigma Aldrich, Sydney, Australia. Single standards of diphenylamine and nitrosodiphenylamine were also purchased from Sigma Aldrich, and their deuterated analogues (*d*6) were purchased from CDN Isotopes *via* SciVac Vacuum Components, Sydney. Methyl- and ethyl- centralite standards (1.0 mg mL⁻¹) were purchased from Accustandard, *via* Novachem, Melbourne, Australia. Acetonitrile, acetone, methanol, and dichloromethane were used as solvents in this work. All were listed as chromatography grade \geq 99.9% and purchased from Sigma-Aldrich.

Smokeless powders and ammunition: A selection of 30 smokeless powders removed from live ammunition were made available to the researchers from an Australian state police reference collection. These powders were selected to broadly represent ammunition available in Australia, past and present, and as such includes a greater proportion of 0.22 calibre rimfire ammunitions than might be circulating in the global market.

6.2.3.3. Evaluation and Figures of Merit:

An evaluation was conducted to assess the analytical performance of the instrument in isolation, distinct from the evaluation of a broader method including the additional steps of sampling, instrumental analysis, and interpretation. This process was informed by the document “General Accreditation Guidance: Validation and Verification of Quantitative and Qualitative Test Methods” produced by the National Association of Testing Authorities, Australia (NATA) [\[315\]](#). Diphenylamine was chosen as a representative compound for OGSR due to its simple and consistent ionization behaviour and availability of an isotopologue. A set of DPA calibration solutions ($n=7$) were made with deuterated d_6 -DPA as an internal standard at $0.1 \text{ ng } \mu\text{L}^{-1}$ in acetonitrile. The concentration of DPA varied between 0.025 to $0.25 \text{ ng } \mu\text{L}^{-1}$, with $10 \text{ } \mu\text{L}$ aliquots deposited on the sampling mesh. Consequently, the mass deposited for the lowest standard was $\sim 0.25 \text{ ng}$, although the efficiency of transfer *via* desorption/ionization between sampling mesh and the ToF-MS detector is unknown. Each position on the mesh holder was passed through the plasma stream for approximately 10 seconds prior to addition of samples for analysis, to ensure that no volatile contamination was present. Although the mesh holder is designed to take 13 samples arranged side-by-side, samples were applied and analysed individually before deposition of the next standard in order to avoid loss of volatile material from adjacent mesh wells that might unintentionally be heated by the plasma. Each sample solution was analysed three times consecutively ($<5 \text{ min}$ intervals), followed by a fourth analysis at the end of the working day for a total of $n=28$ data points. This regime was used to capture a measure of intra-day instrument drift within the calibration.

The spectra resulting from these acquisitions were used to assess system performance for accuracy, precision and selectivity using the m/z ('x') axis, as well as sensitivity, linearity, and limits of detection on the 'y' axis. While the evaluation process was thorough, there are at least two further aspects that should be addressed for the proposed method to be considered more rigorously validated for routine use. Firstly, measures of robustness recommended by NATA, such as minor deliberate variations to the instruments' settings or comparing analyses between different operators, were not investigated categorically. More importantly, instrument performance pertaining to only a single compound (DPA) was evaluated in depth, rather than the full suite of valuable SP compounds explored in other parts of the work. The scope of this expansion to other compounds is deliberately left undefined, until consensus on the most probative SP compounds is reached amongst the forensic science community and isotopologues of these compounds become available.

6.2.3.4. Powder Extractions:

SP samples were extracted following a procedure similar to that published by the National Centre for Forensic Science, University of Central Florida [209]. Subsamples of dry powder (10 mg) were extracted in 300 μL dichloromethane, containing 0.5 mg mL^{-1} *d6*-DPA internal standard, for 3 hours at room temperature. Supernatant (200 μL) was removed by pipette, from which an aliquot was diluted 1:100 in acetonitrile for analysis by DSA-ToFMS.

6.2.3.5. Stub Extractions:

Samples were collected from the hands of a volunteer shooter using SEM stubs equipped with a circle of double-sided adhesive carbon tape (Tri-Tech Forensics Inc. North Carolina, USA). First, the volunteer thoroughly washed their hands, and a blank sample was collected using a single stub to sample from both of the volunteer's hands. Then six rounds of 0.40 S&W Federal Premium Law Enforcement ammunition (Batch No. V42Z458) were discharged from a 0.40 calibre Smith and Wesson M&P (Military and Police) semi-automatic pistol into a bullet recovery tank. Immediately following, the hands of the volunteer shooter were sampled using GSR stubs, first from the right hand, then the left. Two stubs were used for each hand, with particular attention being placed upon collection of traces from the back of the hand and the webbing between fingers and thumbs. This process was then repeated two more times, totalling 18 rounds of ammunition discharged and 12 samples collected.

The shooter then thoroughly washed and dried their hands before a second blank sample was collected. The sampling protocol and replicate procedure was then repeated as above until 18 rounds of ammunition had been discharged and 12 samples collected.

A solvent mixture of methanol, acetone and acetonitrile was mixed, in 2:2:1 ratio, in accordance with Ali *et al.* [39]. Following the method presented by Black *et al.* [202], an aliquot of this solvent (50 μL) was added to cover the surface of the SEM stub, and allowed to interact with the surface for approximately 30 seconds. The solvent was collected from the surface by tilting the stub and pipetting the solvent that gravitated to the lowest edge of the stub. Of the 50 μL added to the surface, only approximately 15 μL was able to be recovered, owing to the nature of the solvent removal technique and the volatility of the solvent mix itself. Any solvent unable to be recovered from the surface of the stub was allowed to evaporate to dryness before the stubs were resealed. Samples were stored at 4°C until analysis and were analysed within two hours of extraction, with analysis consuming all extract and no further storage being required.

6.2.4 Results and Discussion

6.2.4.1. Ionization behaviour

The ions that can be observed in a given mass spectrum are dependent upon both the chemical properties of the analyte in question and the mechanism by which the instrument ionises them. During previous AIMS studies^[104], positive charge ionization has been used to detect SP additives as many stabilisers contain an amino moiety that readily accepts a proton. In contrast, negative ionization is used to detect nitrate esters in propellant and explosives as the nitrate groups are strongly electrophilic. It is also useful to understand where, if at all, fragmentation of analytes will occur. The observed ionization behaviour of the target compounds is detailed below, and accurate mass data are summarized in Table 6-2.

Table 6-2: Charged species representing targeted analytes as observed when using DSA-ToF-MS					
Compound	Formula	Observed Peaks (<i>m/z</i>)		Assigned Identity	Δ ppm
		-ve mode	+ve mode		
Trinitroglycerin	C ₅ H ₃ N ₃ O ₉	261.9708 288.9926 488.9724		[M+Cl] ⁻ [M+NO ₃] ⁻ [2M+Cl] ⁻	+2.11 -7.70 +3.22
Methyl Centralite	C ₁₅ H ₁₆ N ₂ O		241.1345 134.0594 106.0658	C ₇ H ₈ N ⁺ [(C ₆ H ₅)NCH ₃ NC=O] ⁺ C ₇ H ₈ N ⁺	+1.57 -4.31 +0.52
Ethyl Centralite	C ₁₇ H ₂₀ N ₂ O		269.1658 148.0763 120.0449	[M+H] ⁺ [(C ₆ H ₅)NCH ₂ CH ₃ NC=O] ⁺ [(C ₆ H ₅)-N=C=O+H] ⁺	+1.4 +4.13 +4.17
Diphenylamine	C ₁₂ H ₁₁ N		170.0970 211.1243	[M+H] ⁺ [M+AcCN+H] ⁺	+0.59 +3.79
N-Nitrosodiphenylamine	C ₁₂ H ₁₀ N ₂ O		199.0859 169.0890	[M+H] ⁺ [(C ₆ H ₅) ₂ NH] ⁺	-3.72 +2.25
Nitrodiphenylamine	C ₁₂ H ₁₀ N ₂ O ₂	213.0665 249.0422		[M-H] ⁻ [M+Cl] ⁻ [M+H] ⁺	+0.62 -3.45 +2.32
Dinitrodiphenylamine	C ₁₂ H ₉ N ₃ O ₄	258.0511 294.0275		[M-H] ⁻ [M+Cl] ⁻ [M+H] ⁺	-1.5 -2.47 0.00
			260.0671		

Nitroglycerin (NG): Mono-, di- and tri- nitroglycerin from separate standards could all be detected using the same instrument settings in negative ionization mode (information for tri-nitroglycerin, the compound most relevant for the analysis of SP samples, is presented). Other authors using AIMS instrumentation have previously reported that the species typically observed is a $[M+NO_3]^-$ adduct with a theoretical m/z of 288.9904 [61, 202, 316]. Abundant nitrate reagent ions are formed from plasma-excited ambient air according to mechanisms described by Sekimoto & Takayama (2008) and others; these ions are stable for up to ~ 10 s in air, compared to fractions of a second for intermediary species ([317-319]). A peak corresponding to $[NG+NO_3]^-$ was indeed observed using the DSA-ToFMS ($n=4$, meas. m/z : 288.9926, Δ ppm: +7.70).

However, much more intense twin peaks corresponding to the two isotopic $[NG+Cl]^-$ adducts at m/z 261.9714 and 263.9684 ($n=4$, meas. m/z : 261.9708 & 263.9688, Δ ppm: -2.12 & +1.45 respectively) were observed here. A dimer peak with calculated m/z 488.9740 ($n=4$, meas. m/z : 488.9724, Δ ppm: -3.22) corresponding to $[2M+Cl]^-$ was also present. It is a common APCI strategy to control adduct behaviour through the deliberate addition of reactive species [197, 312]; this was demonstrated for nitroglycerin in promotional literature provided by Perkin Elmer for the instrument used in these studies by adding 2% DCM to the m/z calibrant solution [320]. Surprisingly, the results shown in Figure 6-2 were achieved without the deliberate introduction of additional reagents containing chlorine. It was first thought that chloride ions were originating from residual dichloromethane (DCM) used as a solvent for either extraction of SP samples or as a dilution solvent for the nitroglycerin reference standard. That would have been consistent with behaviour seen by Nilles *et al.* (2010) who used a DART source with an open container of DCM near the sample desorption region [321]. Kozole *et al.* (2012) have previously calculated that the ion-molecule binding energy of $[NG+Cl]^-$ (117 kJ mol⁻¹) is greater than that of $[NG+NO_3]^-$ (96 kJ mol⁻¹), and therefore formation of the chlorine adduct is favoured when both species are present [132]. However, when standards and extracts were prepared with acetonitrile to which no additional chlorine-containing solvents or salts were added, the chloride adducts were still detected undiminished. Additionally Lennert & Bridge (2018) report only the nitrate adduct when using dichloromethane in their extraction procedure [61]. Therefore it is presently unknown whether chloride adduction is in some way promoted by the ionization settings and technical design of the DSA-ToFMS instrument, whether it is peculiar to some level of adventitious ambient chloride present in our laboratory environment, or whether carry-over of chloride from previous analyses is responsible.

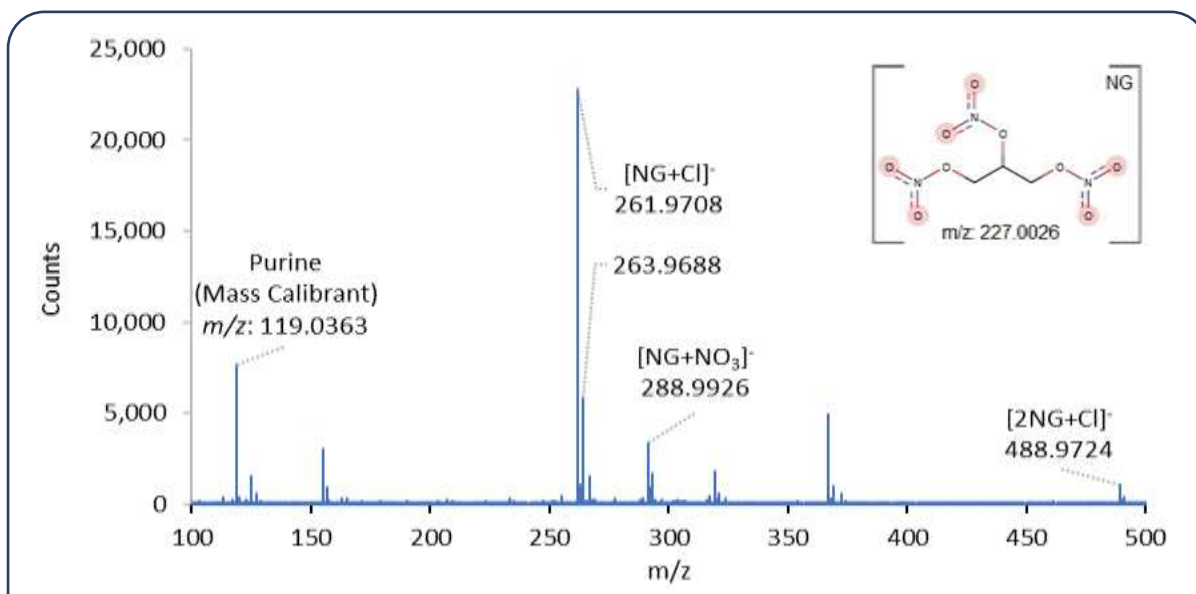
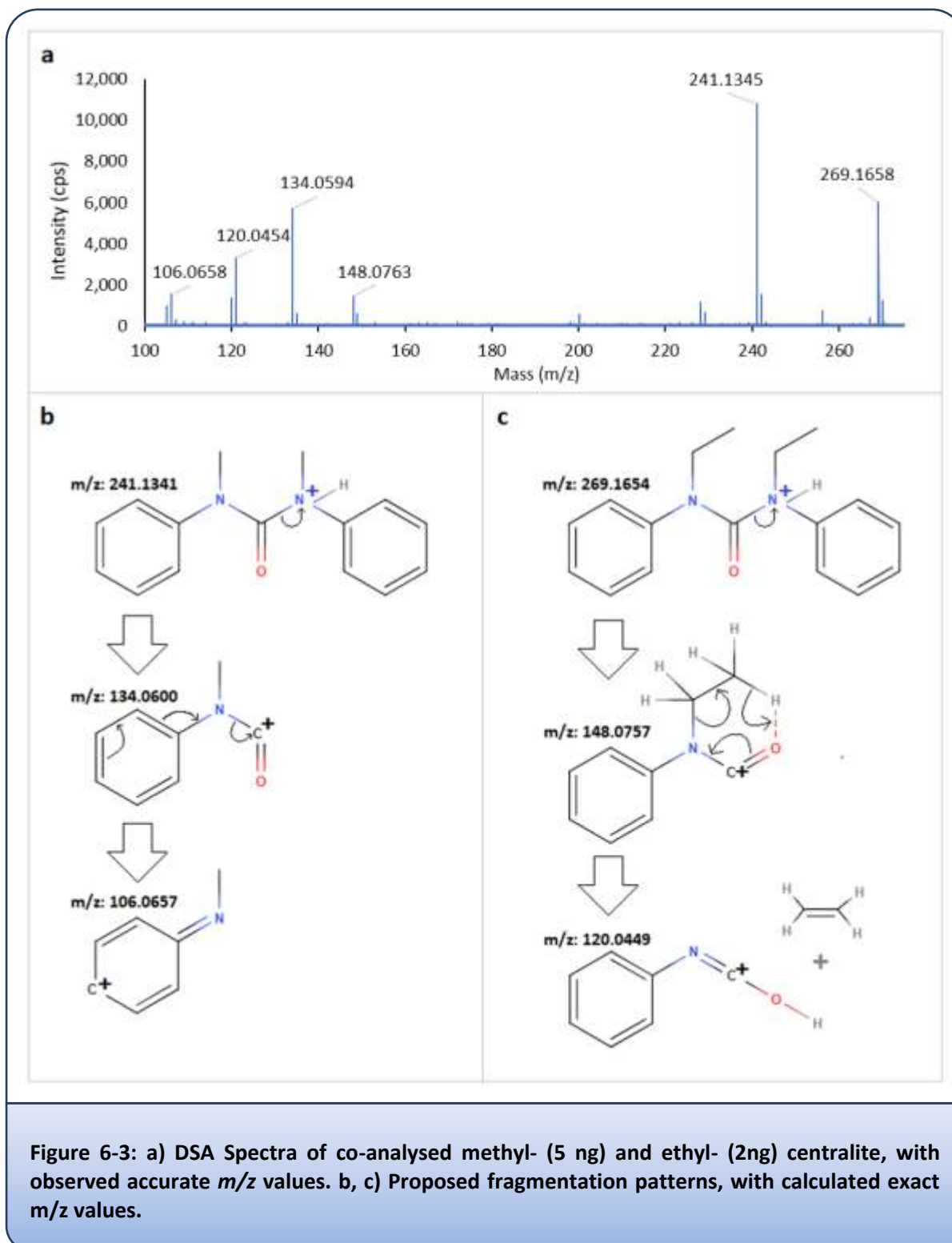


Figure 6-2: Negative-ion DSA-ToF-MS Spectrum for the analysis of trinitrolycerin

Centralites: Methyl- and ethyl- centralite were reliably observed as their protonated molecular ions in positive-ion mode (**MC** calc. m/z : 241.1341, meas. m/z : 241.1345, $n=9$, Δ ppm: +1.57 and **EC** calc. m/z : 269.1654, meas. m/z : 269.1658, $n=9$, Δ ppm: +1.40). Peaks representing an accurate mass consistent with $[2M+H]^+$ clusters were observed infrequently (data not shown). Each also yielded two fragments, with the first arising from cleavage of the C-N bond in the urea moiety. This is largely consistent with the results seen by Zhao *et al.* (2008) and Scherperel & Smith (2009) using electrospray mass spectrometry [98, 170]. For the second fragment, an ion with the average accurate mass value of m/z 120.0454 ($n=9$) was observed in the solution containing ethyl centralite. At first glance it appears to be the equivalent of the methyl-centralite fragment $[C_7H_8N]^+$ at m/z 106.0657 ($n=9$, meas. mass: 106.0658, Δ ppm: +0.52), with an additional 14 mass units from the longer alkyl chain [170]. However, comparison using the calculated accurate mass (m/z 120.0813) resulted in a much larger Δ ppm value (-299 ppm) for the EC fragment. The molecular formula back-calculated from the measured mass is a much closer match (+4.17 ppm) to protonated phenyl isocyanate (calc. m/z : 120.0449), which presumably arises *via* a McLafferty rearrangement. The spectra and proposed fragmentation mechanisms are shown in Figure 6-3 (a-c).



Diphenylamine: Mass spectra of diphenylamine are commonly reported in literature (calc. m/z : 170.0969) [163, 184, 288]. Using the DSA-ToF, DPA exhibited simple ionization behaviour in positive-ion mode, with a single peak for the protonated molecular ion very much dominating the spectra (meas. m/z : 170.0970, $n=5$, Δppm : +0.57). DPA is also known to produce a fragment ion at $m/z \sim 92$, assigned to $[\text{C}_6\text{H}_5\text{NH}]^+$, resulting from the loss of a benzyl moiety from the protonated parent. However, in this study the mass spectrometer was set with a lower m/z cut-off at 100 to reduce spectral noise from atmospheric gasses. While it is likely the fragment is being formed, it will not be recorded under these settings.

Acetonitrile was routinely used as a solvent to dilute DPA standards and to transfer them to the sampling mesh. If the sample spot was exposed to the ionising gas flow before all the acetonitrile had evaporated and cleared the sampling enclosure, it was possible to observe peaks consistent with protonated solvent-analyte adducts $[(\text{C}_6\text{H}_5)_2\text{NH} + \text{CH}_3\text{CN}]^+$ (calc. m/z : 211.1235, meas. m/z 211.1248, $n=1$, Δppm : +3.79). It is suggested that this adduct is forming in the gas phase, as it was not observed when the sample spot was allowed to fully dry (2-3 minutes).

N-Nitroso-Diphenylamine: It is widely acknowledged that detection of NNODPA is difficult to achieve *via* gas chromatography-MS, as the nitroso- compound readily decomposes to DPA when exposed to high temperatures at the column inlet [288]. NNODPA has a N–N bond dissociation energy of only 96 kJ mol^{-1} [322] and upon cleavage of this bond very stable nitric oxide and diphenylamidogen free radicals are formed. This is of particular relevance when attempting to analyse SPs, as the relative amounts of DPA and NNODPA are dependent upon the age of the material or its thermal history and this information is lost when GC analysis is carried out. NNODPA has previously been differentiated from DPA using mass spectrometry because NNODPA produces protonated diphenylamidogen radical cations during ionization [288], which give a signal at m/z 169.0891. DPA, which has a neutral exact mass also at 169.0891 Da, is detected as its protonated cation at m/z 170.0969.

NNODPA has been a noticeable omission from other studies on the ambient ionization of forensic samples, for example Black *et al.* (2017) and Gonzalez-Mendez & Mayhew (2019) [202, 323]. Lennert & Bridge (2018) did report detection of the diphenylamidogen radical cation fragment by DART-MS, but when applying principal components analysis they found this peak had little impact for their purpose of classifying SPs within the sample population [61]. In contrast to results presented by many authors but in agreement with Li *et al.* (2016) [200], simultaneous detection of both the NNODPA protonated molecular ion (calc. m/z : 199.0866, meas. m/z 199.0859, $n=5$, Δppm : -3.72) and the more commonly described diphenylamidogen radical cation (calc. m/z : 169.0886, meas. m/z 169.0890, $n=5$, Δppm : +2.25) were achieved in the current study. Examples can be seen in spectra obtained from SP samples shown in Figure 6-5. This was attributed to the comparatively gentle ionization conditions. During

routine analysis of a mixed GSR surveillance standard the peak at $m/z \sim 169$ is generally more intense than the peak at $m/z \sim 199$.

Nitro- and Dinitro- Diphenylamine: The compounds nitro- and dinitro- DPA differed from other compounds targeted in this study, in that they were evident in both positive and negative ionization mode. Summarized accurate mass observations are presented in Table 6-2, while example spectra of SP containing nitro-derivatives of DPA are shown in Figure 6-5. In either ionization mode, the molecular ion predominated. However the $[M+Cl]^-$ adducts of each were also present in very low abundance in negative ionization mode – less than 10% of the intensity for nitro-DPA and less than 1% for dinitro-DPA.

6.2.4.2. Summary of Observations:

Overall, the spectra obtained using DSA-ToF-MS for key OGSR compounds are largely consistent with, or more definitive than, those reported by other authors. Detection of NNODPA, previously recognised as a problematic analyte, was reliable. While the diphenylamidogen radical cation fragment predominates, the additional detection of the protonated molecular ion offers increased confidence. The more surprising result was observing nitroglycerin as a chloride adduct, as opposed to the more widely reported nitrate adduct. While the exact cause has not been determined, this does not impact on the utility of the result. The simultaneous presence of multiple ionization products from the one analyte will result in more complicated spectra. Whilst this compromises analytical sensitivity (i.e. the signal intensity for a single analyte is spread across multiple m/z values) it also aids in identification in the absence of an in-built orthogonal confirmation such as the retention time of a hyphenated chromatography-spectrometry instrument.

6.2.4.3. Evaluation and Figures of Merit:

The initial experiments detailed above established that the DSA-ToFMS system was capable of ionising compounds relevant to SP, and how spectra containing these compounds were likely to appear. In order to assess how this type of instrument may perform when detecting SP traces in forensic casework, evaluation tests were performed. The key metrics of interest were the reliability for accurately measuring compound mass-to-charge ratio (needed for identification), and the sensitivity towards low amounts of analyte.

Accurate Mass Measurement: The capability for accurate mass measurement is critically important in enabling ambient mass spectrometry techniques to achieve appropriate selectivity for application in fields such as forensic science. Mass accuracy is defined as the difference between the theoretically calculated mass-to-charge ratio of a compound, and its experimentally measured value ^[324]. This

cannot be corroborated by retention time from a known standard as in a hyphenated instrument, so it is important the mass accuracy is sufficient to distinguish between different compounds with the same notional or integer m/z . Results are often presented in the form of the part-per-million (ppm) error, calculated as follows:

$$\Delta \text{Mass (ppm)} = 10^6 \times \left(\frac{\text{Measured } m/z - \text{Calculated } m/z}{\text{Calculated } m/z} \right) \quad (1)$$

What can be considered an acceptable mass error for unequivocal identification is strongly influenced by the mass of the compound under analysis, with a smaller field of candidates fitting a lower measured mass. For the purpose of propellant component identification, the list of “targeted” compounds is known and their calculated mass-to-charge ratios are generally <300 Da. In order to evaluate whether the DSA-ToF-MS instrument is fit-for-purpose towards qualitative forensic analysis, 28 repeat measurements of both DPA and *d6*-DPA were used to calculate the accuracy, precision and mass resolution of the instrument under the applied conditions. Representative figures of these criteria are listed in Table 6-3, with further data presented in Appendix 6-1.

Mass Values		DPA	<i>d6</i> -DPA
Accuracy (n=9)	Calculated Exact m/z (M+H) ⁺	170.0969 Da	176.1346 Da
	Mean Measured m/z	170.0960 Da	176.1341 Da
	Mean $\Delta m/z$ from Calculated	-0.0009 Da	-0.0005 Da
	Mean Δ ppm from Calculated	-5.25 ppm	-3.02 ppm
Precision (n=28)	Standard Deviation (m/z)	0.0010 Da	0.0015 Da
	Standard Deviation (Δ ppm)	5.71 ppm	8.38 ppm
Resolution (n=28)	Peak width at Half Height (Da)	0.0162 Da	0.0202 Da
	Peak width at Half Height (ppm)	95.08 ppm	114.65 ppm

These data imply that the measured m/z is underestimating the true mass-to-charge ratio by a comparatively small margin. For DPA the mean measured delta falls at -5.25 ppm, while for *d6*-DPA this value is approximately -3 ppm. However for protonated DPA's calculated exact mass value of m/z 170.0969, the next nearest candidate has the formula $C_9H_{14}O_3$ ($m/z = 170.0943$) for a ppm error of -15.32. In practice this means the observed mass accuracy was deemed sufficient for compounds in the relevant mass range.

Another factor to consider is the precision of the measurements. The standard deviation for this set of measurements was 5.71 ppm for DPA and 8.38 ppm for *d6*-DPA. The calculated exact m/z falls within one standard deviation of the measured values. Two strategies are recommended to minimise the impact of this spread during casework. The first is using a deuterated internal standard, as minor

deviations in m/z calibration are expected to effect both isotopologues similarly, allowing for correction. The second is to perform repeat injections of the same sample solution, so that the final measured mass is calculated as an average rather than a single measurement. Overall m/z accuracy was considered appropriate to proceed with further development of the technique, however a cautious interpretation is suggested.

Potential for Quantitative Analysis: It is well-accepted that the amount of trace evidence present for forensic exploitation is highly variable, even using tightly controlled simulations of crime items or activities carried out by persons of interest. Therefore it would not be typical to report the amount of SP residue recovered from a crime-related trace [305]. Indeed, the standard proposed as a working document (at the time of publication) by NIST's Gunshot Residue Subcommittee on OGSR requires only that certain combinations of compound classes are detected in association with one another, not that any particular compound is quantified above some specified minimum amount [93]. However, some quantitative investigation into AIMS is appropriate to understand the instrument's performance in a binary "detected/not detected" screening role. To calculate the limits of detection and linearity of this system, an extracted ion desorption profile (analogous to an extracted ion chromatogram in GC-MS or LC-MS) was generated for DPA. This necessitates the use of an isotopically labelled internal standard (*d6*-DPA) to correct for variance in ionization efficiency, as raw signal intensities can vary significantly shot-to-shot due to the relatively unconstrained sample desorption process. Fig 3 a shows the observed peak area when solutions of DPA (at levels of 0.25, 0.5, 0.75, 1.0, 1.5, 2.0 and 2.5 ng of analyte) spiked with *d6*-DPA (1.0 ng) were analysed (n=4 per DPA level). There is significant variation in the replicates of each solution (e.g., analyses #25-28). A calibration curve constructed by plotting the DPA m/z analysed versus the average observed DPA signal corrected for variability in ionization efficiency using the average observed signal for *d6*-DPA as shown in Figure 6-4 (b). Good linearity observed over the single order of magnitude tested. The LOD (0.105 ng) and LOQ (0.347 ng) for DPA were then calculated taking 3 and 10 times the standard deviation of regression (S) respectively, rather than the more common method of 3 time the standard deviation of the blank, as allowed by section 3.5.1.3 of the NATA's method-accreditation guidance [315]. Further metrics of method validation can be found in Appendix 6-2.

The limit of detection for DPA calculated from these measurements (0.10 ng) compare favourably to those listed by Taudte *et al.*'s 2014 review that described a variety of MS techniques for detection [104]. Results from mixed DPA and *d6*-DPA solutions suggest that DSA-ToF-MS is equally sensitive towards other compounds in positive-ion mode (data not shown) and will likely have comparable LoD values. These were not explicitly calculated, as deuterated standards for compounds such as ethyl centralite

were not accessible to the authors at the time of analysis. Attempts to use DPA as an internal standard for NNODPA with the same peak-ratio approach resulted in such poor inter-spectra repeatability that any calculated figures of merit could not be considered valuable. This suggests that the current method might not be suitable for use in the manner described by Lennert & Bridge (2018) to compare SPs containing the same compounds by the relative amounts of each component [61]. However, it can be used to indicate the likely components of a sample, for further confirmatory analyses or to exclude potential sources.

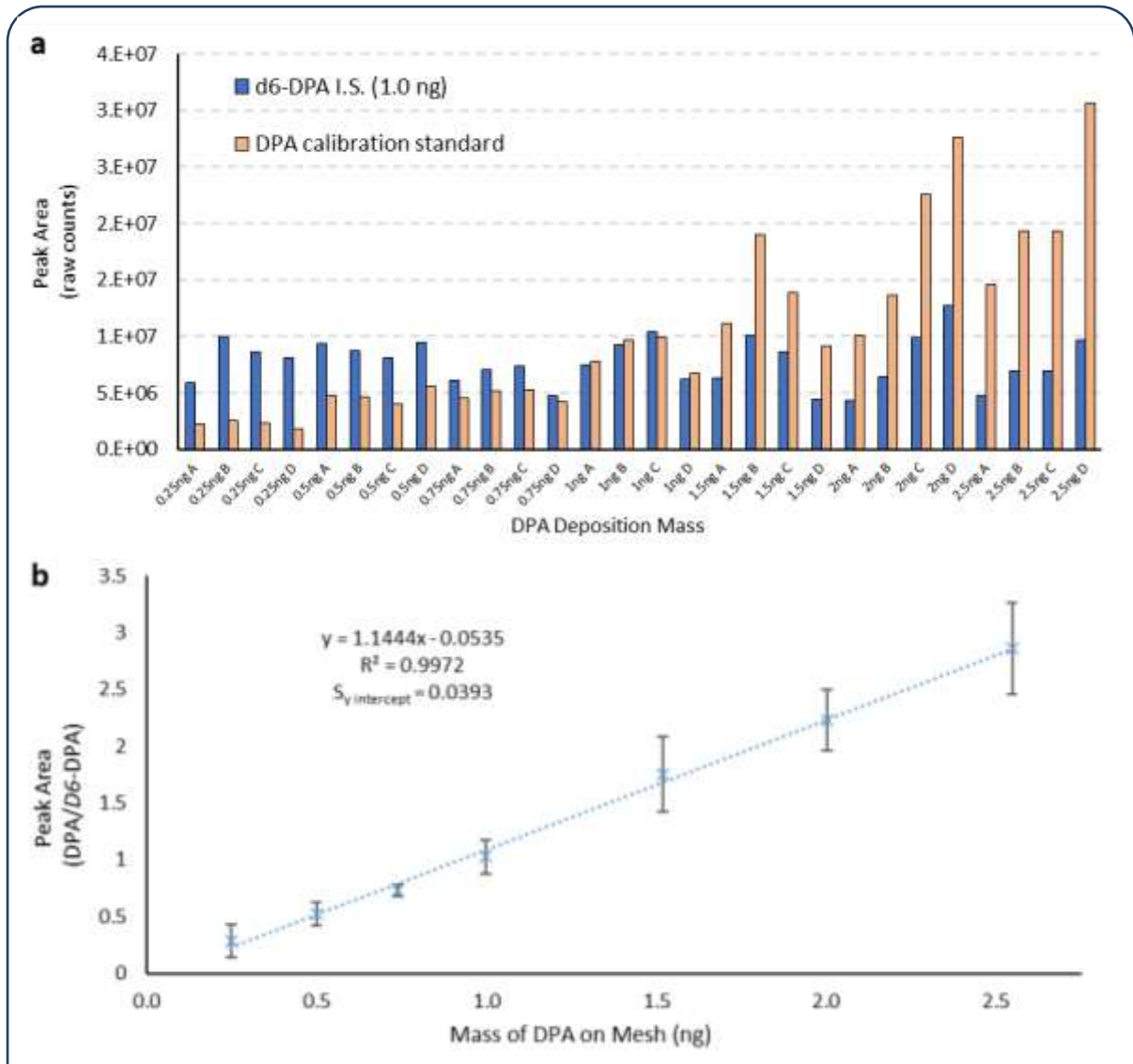


Figure 6-4: a) Plot of the raw peak areas obtained for deposits of both the d6-DPA internal standard (1.0 ng) and DPA calibration (0.25, 0.5, 0.75, 1.0, 1.5, 2.0 and 2.5 ng, 4 replicates of each). b) Mean corrected peak area plotted against DPA mass deposited to mesh. Error bars represent three standard deviations (n=4).

6.2.4.4. Exemplar Specimens

Powder Extracts: A selection of 30 SPs, recovered from live ammunition, were extracted in DCM and analysed without further separation or clean-up. This was used to qualitatively identify their components, shown in Table 6-4. Individual spectra from several samples are also shown for illustrative purposes in Figure 6-5. In addition to the compounds targeted during evaluation studies, several other compounds were tentatively identified by comparing their accurate mass and fragmentation patterns to compounds known to be associated with SP. In the absence of a retention time or reference standard, these compounds are recommended onwards for further research before data relating to them could be relied upon for court purposes. However, this indicates that the presented method does exhibit a level of versatility towards unanticipated, but nonetheless potentially informative, compounds within the sample.

The spectra suggest that the majority of these powders are classified as double-base, as they contained nitroglycerin. Black *et al.* (2017) have reported detection of pyrolytic saccharide fragments originating from nitrocellulose, with peaks in the low m/z region of the spectra (m/z 97, 113, and 159) [202]; the latter two ions were not seen in the present study and m/z 97 is below the 'x' axis cut-off used. These ions are also formed by other polysaccharide polymers such as cotton, so their forensic value in the absence of more characteristic SP compounds is likely low. Most samples contained DPA and all samples containing DPA also had signals for NNODPA and nitroDPA, while very few contained dinitroDPA. This suggests that some amount of aging has occurred, but most powders have not degraded to an extreme degree. Of the samples which did not give a signal for DPA, centralite seemed to be the next most common stabiliser choice. Four samples gave peaks at m/z ~227 consistent with the compound 1-methyl-3,3-diphenylurea, also known as akardite (AK). This was confirmed with repeat measurements of an additional certified reference standard (calc. m/z : 227.1184, meas. m/z 227.1183, $n=4$, Δ ppm: +0.55). Many powders apparently contained a phthalate plasticiser, typically dibutyl phthalate, but peaks at m/z 319.0972 and m/z 225.0548 ($n=3$) consistent with diphenyl phthalate (DPP) were also observed. Finally, there were indications that some samples contained nitrated toluenes (di- and/or tri- nitrotoluene) which are frequently associated with SP. However, there were minor discrepancies in the measured accurate mass values, and therefore further testing with known standards is required to confirm that this technique is suitable for those compounds.

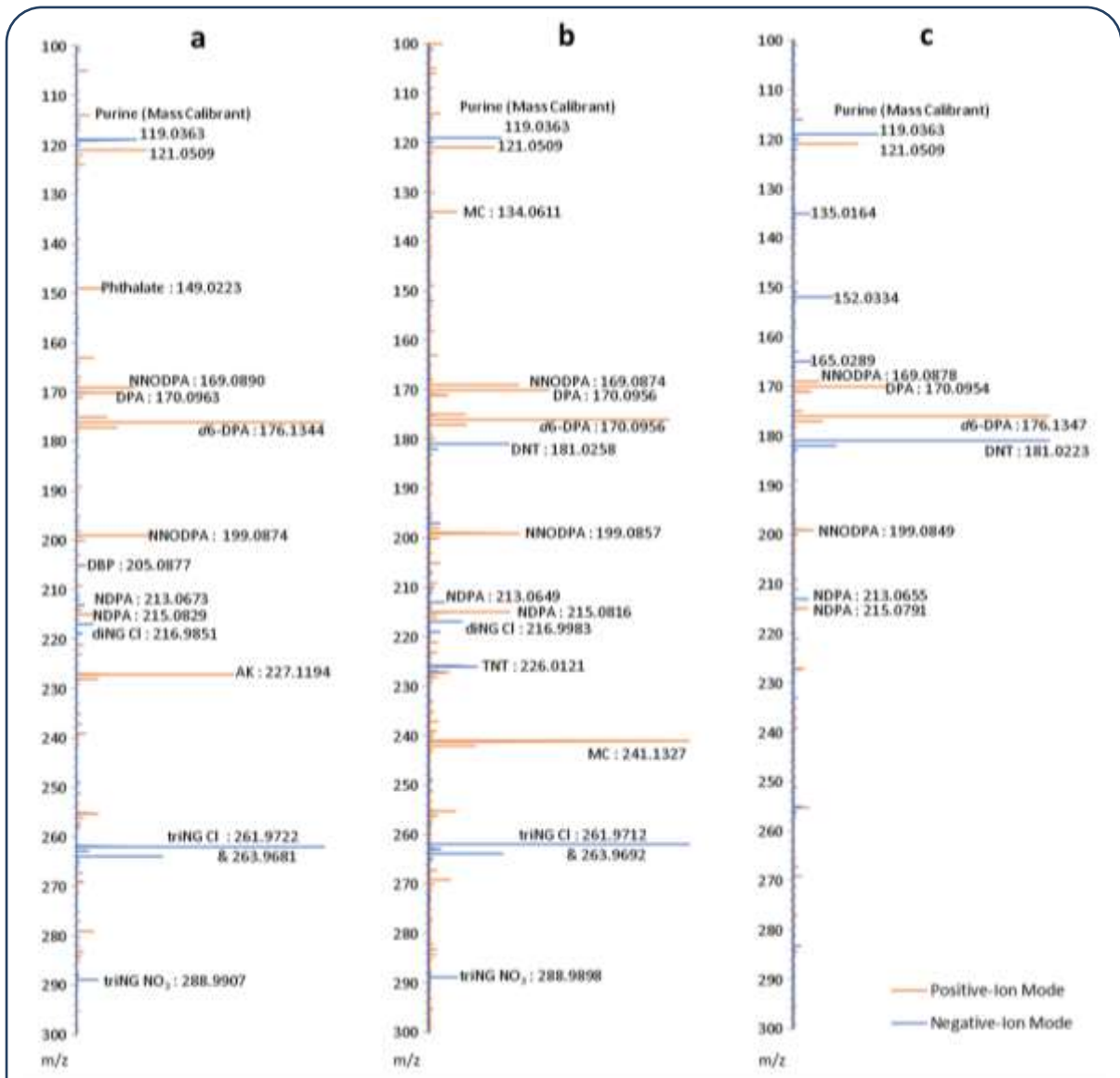


Figure 6-5: Powder sample extracts #3 (a), #22 (b) and #26 (c), analysed in both positive- and negative- ion modes. Spectra are normalised to the most abundant peak in each.

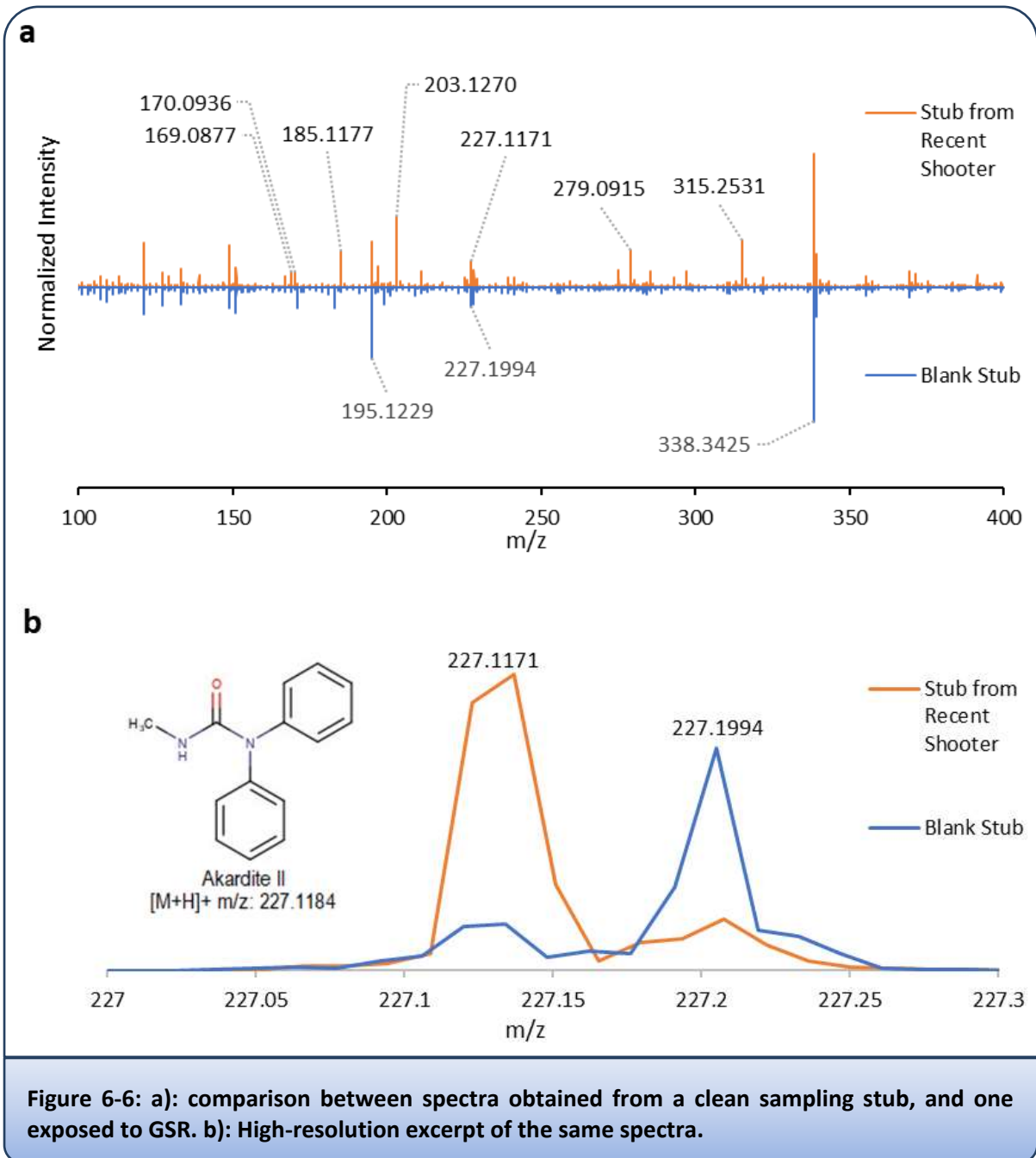
Table 6-4: Observed composition of 30 smokeless powders, representing past and present products accessible in Australia

Sample ID	triNG	diNG	DPA	(NO) DPA	(NO ₂) DPA	(NO ₂) ₂ DPA	MC	EC	Ak	Phthalates	Nitro-toluenes
1. Remington - Subsonic, LR (USA)	√	√	√	√	√	√	x	x	x	x	x
2. Canadian Industries Limited - Pistol Match, LR (Canada)	√	x	√	√	√	√	x	x	x	DBP	x
3. Federal - Champion, LR (USA)	√	√	√	√	√	x	x	x	√	DBP	x
4. Sellier Bellot (Czechoslovakia)	√	√	√	√	√	x	√	√	x	x	√
5. CCI - Target, Standard velocity, LR (USA)	√	√	√	√	√	x	x	x	√	DBP	x
6. Aguilla - SE Super Extra, LR (Mexico)	√	√	√	√	√	√	x	x	x	DBP	x
7. Eley - Club, LR (UK)	x	x	√	√	√	√	x	x	x	x	x
8. RWS - Subsonic (Germany)	√	√	√	√	√	x	x	√	x	DBP	x
9. Browning - HP, LR (Australia)	√	√	√	√	√	√	x	x	x	DBP&DPP	√
10. Stirling - High Impact, LR (Philippines)	√	√	√	√	√	√	x	√	x	DBP	x
11. Winchester - XTR pistol, LR (Australia)	√	√	√	√	√	x	x	√	x	DBP	x
12. PMC - Zapper, LR (Korea)	√	√	√	√	√	x	x	x	x	x	x
13. Lapua - Midas, LR (Finland)	x	x	√	√	√	x	x	x	x	x	x
14. Mauser - KK80, LR (Germany)	√	√	√	√	√	x	x	x	x	DBP	√
15. Fiocchi - Maxac, LR (Italy)	√	√	x	x	x	x	x	√	x	DBP	x
16. Nitron - Naboje, LR (Poland)	x	x	√	√	√	√	x	x	x	x	x
17. Swartklip - LR (South Africa)	√	√	√	√	√	√	x	x	x	DBP	x
18. Imperial - CIC HP, LR (Australia)	√	√	x	x	x	x	√	√	x	x	x
19. CBC - Super Velox, LR (Brazil)	√	√	x	x	x	x	√	√	x	x	x
20. Gevelot - LR (France)	√	√	√	√	√	√	x	x	x	x	x
21. Nicorro - hp, LR (Germany)	x	x	√	√	√	√	x	√	x	x	x
22. Vostok - Target, LR (Russia)	√	√	√	√	√	x	√	√	x	x	√
23. Dominion - LR (Canada)	√	√	x	x	x	x	x	√	x	x	x
24. Valor - Ultrasonic, LR (Yugoslavia)	√	√	√	√	√	x	x	√	x	x	x
25. Hornady - 30GR VMAX, 22WMR (USA)	√	√	√	√	√	x	x	√	x	DBP	x
26. Unspecified Powder - Batch A (Australia)	x	x	√	√	√	x	x	x	x	x	√
27. Unspecified Powder - Batch B (Australia)	x	x	√	√	√	x	x	x	x	DBP	x
28. Unspecified Powder - Batch B, Artificially Aged (Australia)	x	x	√	√	√	x	x	x	x	DBP	x
29. Hilti - Nail Gun Cartridge, Yellow (Australia)	√	√	√	√	√	x	x	√	√	DBP	x
30. Hilti - Nail Gun Cartridge, Red (Australia)	√	√	√	√	√	x	x	√	√	x	x

Residue Hand Samples: OGSR traces were collected from the hands of a volunteer shooter using carbon-filled adhesive tape on SEM stubs using the typical procedure used for forensic examination. Material present on the adhesive was then extracted by pipetting 50 μL of solvent onto the surface, and the recovering the solution after 30 seconds (i.e., the method described by Black *et al.* [\[202\]](#)). These extracts were analysed using the same DSA-ToF-MS procedures described above. However, it was not possible to distinguish between a blank stub sample and many of the extracts from stubs exposed to GSR. The most prominent peaks were consistent with dimethyl phthalate ($m/z \sim 195$) and erucamide (m/z 338.3425, Δ 0.62 ppm), likely components of the stub's carbon adhesive polymer. The stub background also had a peak at m/z 227.1994, a potential interference (Δ -357 ppm) with the SP compound Akardite (m/z 227.1184). It is possible that the signal from OGSR was suppressed by the stub matrix as the more abundant adhesive molecules outcompeted the analytes for available charged reagent species. This indicates that further work is required to integrate the sampling process with DSA-TOF for reliable residue analysis.

One sample taken from the volunteer's right hand after firing a 0.40 calibre semi-automatic handgun did provide a spectrum that showed evidence of OGSR exposure (Figure 6-6 a). Small peaks were present at m/z 169.0874, 170.0936, and 227.1171 corresponding to DPA (-5.72 Δppm), NNODPA (-19.84 Δppm) and AK (+1.77 Δppm), respectively. These compounds were later confirmed to be present in the ammunition used for the test. This demonstrates the strength of accurate mass identification, as lower-resolution mass spectrometers would not distinguish between Akardite and the unidentified compound from a clean stub both with a nominal m/z of 227 (Figure 6-6 b).

The difficulties of using DSA-ToF-MS instrumentation for detection of SP residue from an adhesive stub appears to agree with the outcomes reported by Morelato *et al.* (2012) [\[188\]](#) and Perez *et al.* (2016) [\[59\]](#) using DESI-MS and LEMS respectively. Both publications describe poorer outcomes when SP material is associated with adhesive rather than non-porous substrates. This contrasts with the promising preliminary results presented by Black *et al.* (2017) [\[202\]](#) who used a similar recovery procedure with DART-MS. Further investigation of whether the combination of stub brand (and thus, potentially, adhesive composition) and solvent or instrument design (DSA- versus DART- MS) may form the basis of further studies on this topic.



6.2.5 Conclusions

The results provided above suggest that ambient ionization mass spectrometry, using DSA-ToF-MS instrumentation, has some scope for the laboratory analysis of the components within SPs. Many compounds previously associated with SPs and OGSR in literature were observed in some form during this work, with ionization behaviour mostly following that seen by others using DART- or DESI- MS. Compounds including nitroglycerin, methyl- & ethyl- centralite, akardite, diphenylamine, nitrosodiphenylamine and nitrated diphenylamine derivatives were tested specifically, with accurate m/z data collected for each. In the case of ethyl centralite a previously undescribed fragmentation differing from that of methyl centralite, was detected and a mechanism proposed. Diphenylamine was chosen to evaluate the performance of the DSA-ToF using validation guidelines for forensic methods provided by Australia's National Association of Testing Authorities. Spectra obtained while using an isotopically labelled internal standard allowed measures of m/z accuracy, precision, resolution, sensitivity, linearity, and limit of detection to be calculated.

The method described above was used to analyse and compare 30 samples of SP, representing ammunitions available in the Australian context. This could be applied to rapidly screen large numbers of potential samples to prioritise confirmatory analyses, or to quickly compare whether two samples can be distinguished to rule out a common source in an investigative context. DSA-ToF analysis was also applied to samples collected from a volunteer shooter's hands using a simple stubbing and extraction approach, with only minor success. Before the integration of DSA-ToF analysis with stub extraction approaches can be considered reliable in a hand-residue detection role, further work will have to be done comparing different types of adhesive for sample collection to reduce matrix effects. If that interference can be overcome, the DSA-ToF may offer the benefits of speed and specificity that other ambient mass spectrometry techniques avail to OGSR analysts.

6.2.6 Acknowledgments

The authors wish to thank Jason Young for his valuable advice and technical support at Flinders Analytical during the collection of the reported data. We are also grateful for the support provided to this research by the Ross Vining Memorial Research Fund (administered by Forensic Science SA) and by the South Australia Police, in particular Brevet Sergeant Andrew Plummer, PhD. We acknowledge the preparation and instrumental analysis performed by our colleague Eliza Moule on the post-firing OGSR hand samples used to produce Figure 6-6, and her input on the related discussion points. This research was supported by an Australian Government Research Training Program (RTP) Scholarship

6.3 Direct Analysis in Real-Time (DART)

6.3.1 Introduction:

DART was one of the first commercially available AIMS ion sources, and its potential for application to forensic analyses were immediately apparent. These applications were recently reviewed by Pavlovich *et al.* (2016) and Sisco & Forbes (2021) [309, 325]. Specifically, previous work published by Black *et al.* (2017) suggested that DART-MS could be suitable for the analysis of OGSR traces recovered from targets using adhesive carbon SEM stubs [202]. Whilst Perkin Elmer's DSA and IonSense's DART ion sources operate based upon similar principles, there are some engineering differences in implementation that had consequences for the data they produced. The most fundamental of these is that the DSA used nitrogen as its feed gas, whereas DART could use either nitrogen or helium. This is noteworthy because of the difference in ionisation potential between the respective reactive species. The DSA also featured an enclosed housing that encapsulated the sample support mesh and the path from the ion source towards the spectrometer inlet. This housing provided a more regulated ionisation environment, at the cost of decreased versatility for analyses taken from the native surface of samples. These differences are illustrated in Figure 6-7. Finally, the specific DSA available for this research was purchased as part of a system already integrated with a ToF spectrometer by the same manufacturer. On the other hand, a DART ion source was fitted as an aftermarket accessory to a linear ion-trap spectrometer produced separately. The experiments recorded below sought to extend the evaluation outlined in Section 6.2 to also assess DART instrumentation.

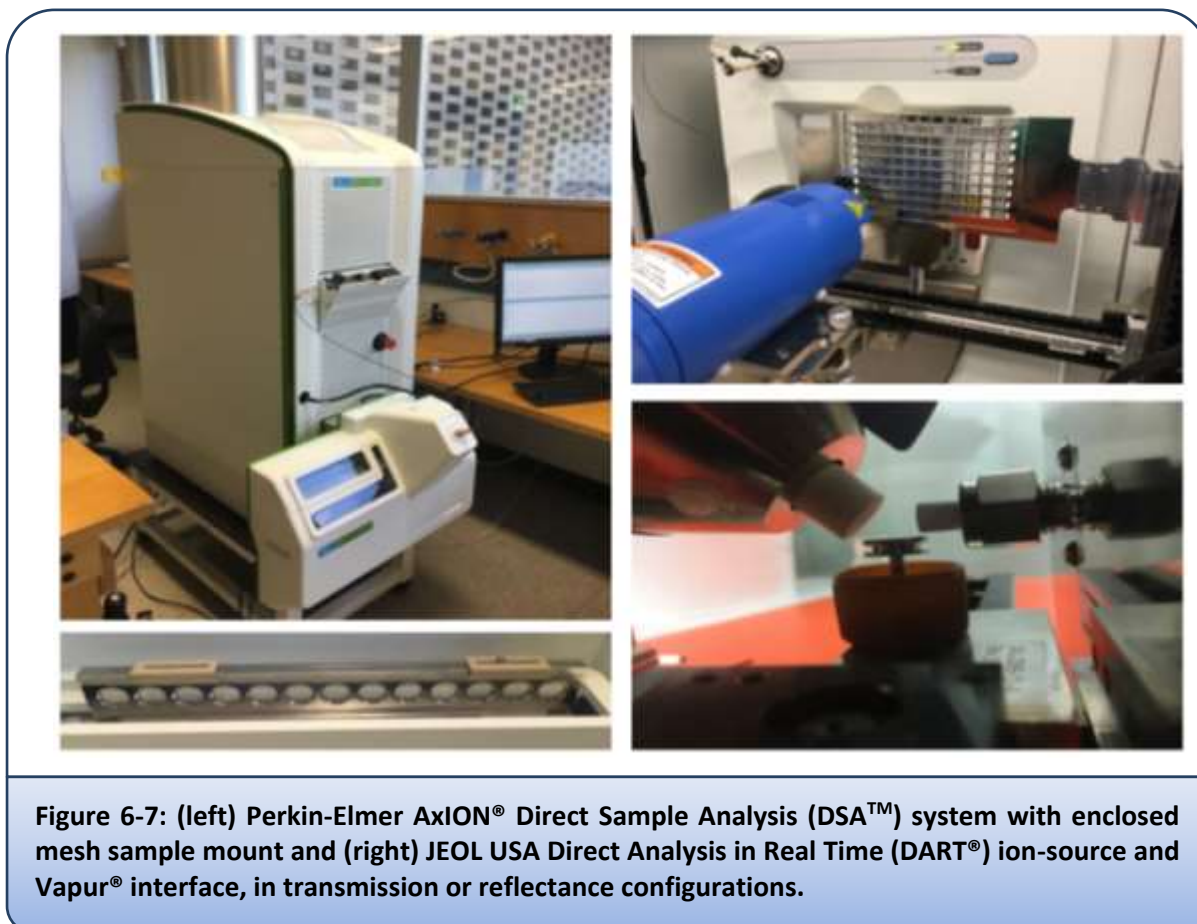


Figure 6-7: (left) Perkin-Elmer AxION® Direct Sample Analysis (DSA™) system with enclosed mesh sample mount and (right) JEOL USA Direct Analysis in Real Time (DART®) ion-source and Vapur® interface, in transmission or reflectance configurations.

6.3.2 Experimental:

6.3.2.1. Ionization Source and Mass Spectrometry:

The instrument used for this work was a Thermo Fisher Scientific Velos Pro linear ion trap mass spectrometer. It was fitted with a Direct Analysis in Real Time (DART-SVP) ion source interfaced *via* a Vapur® interface, both from IonSense Inc., Saugus, MA. This interface consists of an enclosure connected to a roughing pump to create a low-pressure region immediately prior to the inlet of the mass spectrometer. A ceramic tube draws analytes into the spectrometer, while atmospheric gases that may otherwise interfere are reduced. In positive-ionization mode the DART grid voltage was set to 400 V; in negative mode it was 350 V. The Velos Pro was operated in “full-scan” mode i.e. the range of m/z values for the particular experiment was scanned fully. No ion-trap fragmentation (MS/MS or MSⁿ) or selected-ion monitoring (SIM) scans were used with the DART source attached. Output data included mass spectra and time-dependant plasmagrams (analogous to chromatograms, but without column separation). These data were viewed and evaluated using Xcalibur Qual. Browser software. The process of measuring spectra from samples was as follows: The Vapur® interface pump was activated and the DART ion-source was preheated. Although the pump did not give a direct readout of flow, it was capable of a maximum flow rate of $2.3 \text{ m}^3 \text{ hr}^{-1}$ and was not varied. Samples were spotted

onto the support mesh at the desired concentration and allowed to dry for a few moments. Shortly before analysis, the DART source was activated and then run to stabilise temperature and gas flow. The mass spectrometer was set to acquire data. The instrument was then directed to move the sampling mesh through the reagent stream at a pre-determined speed using the DART control software. Using a speed of 1mm sec^{-1} , each sample position was analysed for approximately 5 seconds. After all desired sample locations had passed the inlet, the spectrometer was stopped and would generate the relevant digital data files.

6.3.2.2. Evaluation:

An initial period of method development was conducted using the same set of pure reference compounds described in section 6.2.3.2. Three parameters were varied to optimise the DART-Velos Pro system's performance. These were ion-source heating temperature, MS scan settings, and reagent gas (He or N_2). After the most effective settings were selected, two sets of sample extracts were tested. These represented examples of both intact smokeless powders and extracts prepared from GSR traces collected from shooters' hands' using adhesive SEM stubs.

6.3.3 Results and Discussion

6.3.3.1. Instrumental Method Development

Control software provided with the DART source allows the operator to set heating temperature and choose reagent gas supply. MS Scan settings could be controlled using Thermo Fisher Scientific's Xcalibur Instrument Setup program. Desorption temperature was investigated first, as it was important to establish that samples were effectively desorbed from the support mesh while minimising thermal degradation. Deposits containing 20 ng each of nitrosodiphenylamine (NODPA) and its *d6* isotopologue were used, as this compound was already known to be particularly sensitive to the effects of heating [\[164\]](#). Four temperatures were applied to three replicate mesh positions ($n=12$). Ions representing both the parent molecule and a thermal degradation product were observed in spectra at each temperature, so two response variables were measured. The first was the sum of the MS peak heights for these two ions to represent total desorbed analyte, and the second was the ratio between the ions to represent the degree of degradation. The results are shown in Figure 6-8. There was a negative correlation between desorption temperature and total analyte signal, and also a negative correlation with the proportion of analyte observed as the (protonated) intact parent molecule. While the greatest amount of signal was observed with the DART set to 100°C , all following experiments were conducted using 150°C gas flow to quickly dry and desorb any aqueous components that may be present in more realistic specimens. Additionally, this allowed for more direct comparison with the DSA source, also set to 150°C .

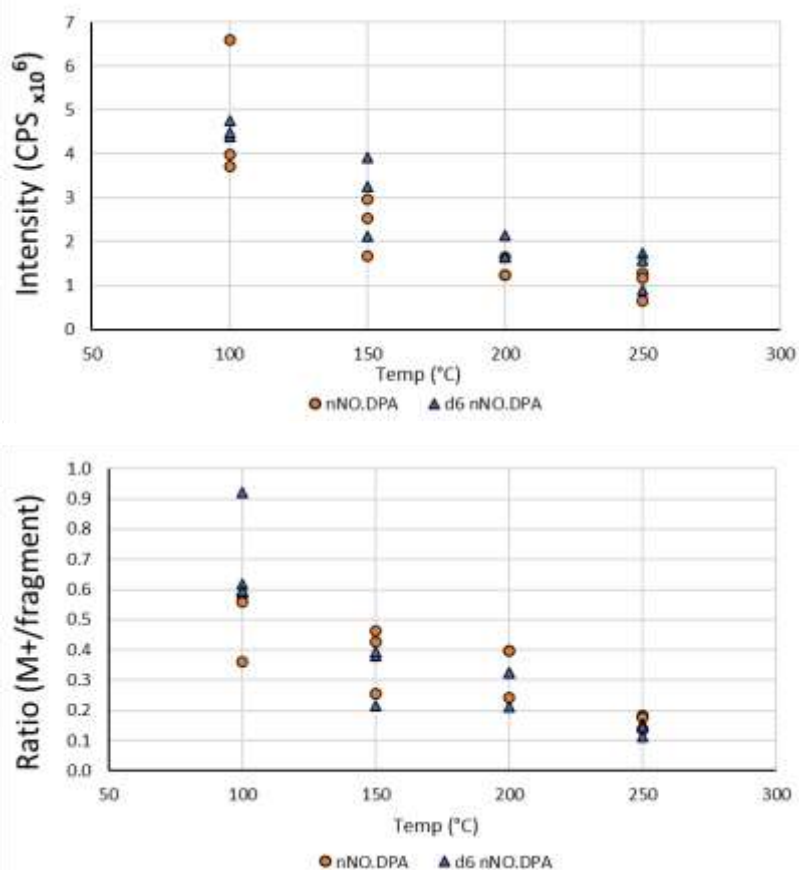
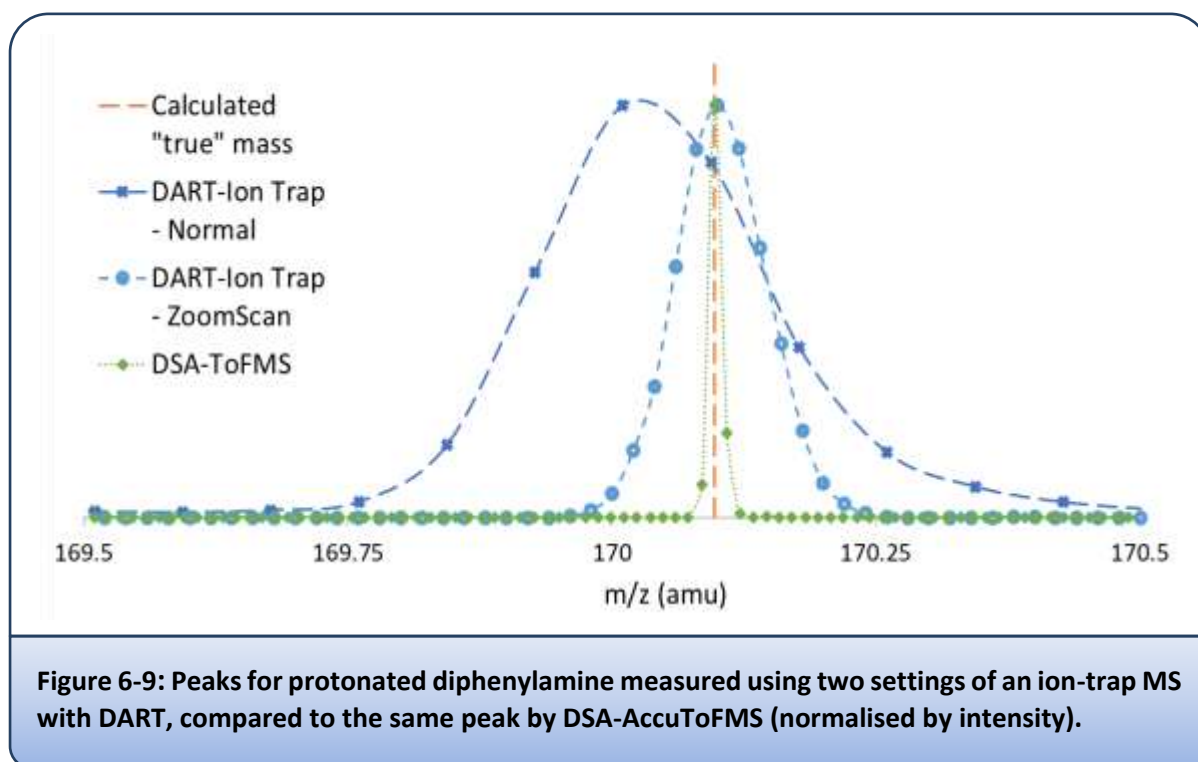


Figure 6-8: (Top) Sum of parent and product ions for each analyte plotted by desorption temperature. (Bottom): Ratio of parent ion to product ion with increasing desorption temperature.

The second aspect of the system to be examined was the m/z resolution that could be achieved using the Velos Pro spectrometer. Resolution is vitally important to ambient mass spectrometry, as the preferred method of confirming analytes' identities is through accurate mass measurements (see discussion in section 6.2.4.3). However, a trade-off between resolution and acquisition speed must occur. Speed is also important in AIMS as the limited amount of sample must be captured and recorded by the instrument as it desorbs from a substrate surface. The instrument control software contains a selection of pre-set modes allowing operators to tailor the system to their needs. Performing scans across the m/z range between 50-550 amu, two of these modes were tested: "Normal" mode, the default balance between speed and selectivity, and "ZoomScan" mode, favouring resolution. Measurements were made using three replicate 10 μL spots of an OGSR reference standard containing DPA, nNODPA, EC and dimethyl phthalate (DMP). The average peak width at half maximum (FWHM, amu) observed for the protonated molecular ion of each, is noted in Table 6-5. Using the ZoomScan setting, peak widths of approximately 0.1 amu were achieved for each compound. While exceeding the performance values quoted in the operating manual provided with the instrument

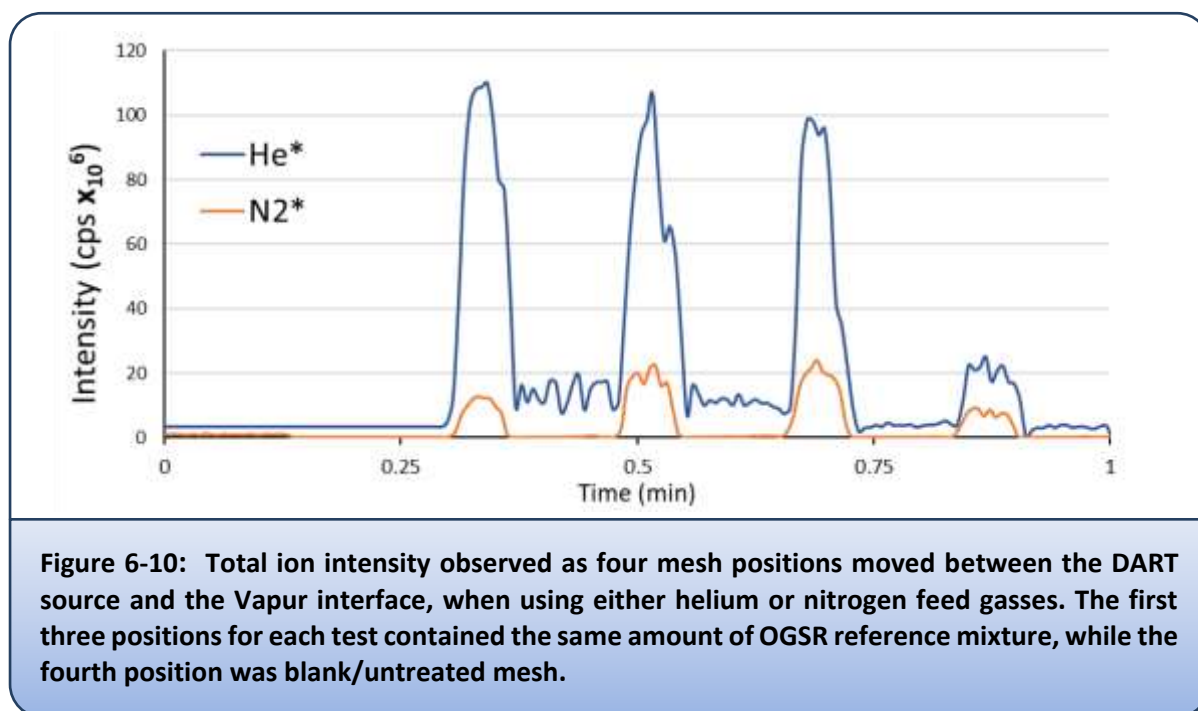
(≤ 0.25 amu), this is approximately five-fold greater than the equivalent value achieved using the DSA's ToFMS. The effect of these three conditions on the MS peak shape of DPA reference standards is shown in Figure 6-9. ZoomScan mode was selected for the remainder of the experimental work using the Velos Pro spectrometer.

Table 6-5: Mass-resolution (FWHM, amu) of OGSR reference compounds using two Velos Pro operating modes		
	Normal	ZoomScan
DPA	0.251	0.102
nNODPA	0.241	0.110
EC	0.239	0.116
DMP	0.252	0.128

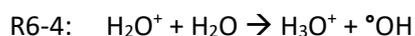
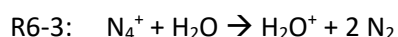
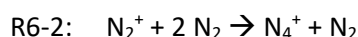


Lastly, the effect of changing reagent gas from helium to nitrogen was tested due to the cost of the former. It was found that this caused a 80-90% reduction in signal when measured *via* total ion intensity (Figure 6-10), or when observing peak heights for individual analytes in mass spectra. This was not unexpected, due to the difference in potential ionisation energy (IE) between the species thought to be responsible for energy-transference. In DART-MS, gaseous helium is excited to the metastable neutral $\text{He}^* 2^3\text{S}_1$, with a very long predicted lifetime ($\sim 8,000$ s) and carrying 19.8 eV of energy [326]. This efficiently ionises water (requires IE > 12.6 eV) to produce the H_3O^+ ions responsible for eventual protonation of analyte molecules to their $[\text{M}+\text{H}]^+$ equivalent [180]. On the other hand, Song *et al.* (2018) estimated that neutral N_2 reagent streams contain excited states with energies in the

range of 9.8 – 12.3 eV, with much shorter lifespans [327]. They found that N_2^* most efficiently ionised compounds requiring <10.2 eV of IE, and thus it should theoretically be suitable for most organic molecules. However water vapour and atmospheric gasses such as oxygen (IE = 12.1 eV) may be responsible for quenching the reaction and hence the lack of sensitivity observed when comparing the two reagent gasses, as displayed in Figure 6-10. Therefore helium was subsequently used as the DART's feed gas.



Superficially these observations appeared to contradict the results seen when the DSA source produced sensitive and stable ionisation using nitrogen as the reagent gas [302]. However the DART source is configured to screen charged particles from the exiting reagent stream, leaving only electronically or vibrationally excited metastable species. The DSA works on an opposing principle, described for atmospheric-pressure chemical ionisation (APCI) since the 1970s [328]. In this case it is the metastables that are screened, with N_2^+ (IE = 15.6 eV, greater than water) being the initiating species (Reactions R6-1 to R6-5).



6.3.3.2. Ionization Behaviour of Standards

As shown above, the ion-trap MS had a lower resolution than the ToF MS. Therefore it was not possible to replicate the more detailed studies performed with the DSA for representative OGSR molecules. However a panel of reference standards was used to confirm that analytes of interest were mostly observed as protonated ions in positive ionisation mode, and as deprotonated ions in negative mode. Details are provided in Table 6-6, which also shows that the mass-accuracy of the ion trap was typically worse than the ToF MS, with Δ ppm values in the range of -2.56 to +165 ppm. The lack of a co-ionised mass calibration solution may have contributed. Lesser mass accuracy and mass resolution combine to increase the likelihood of false-positive identification from ions having similar molecular masses if used in a screening role. This may be addressed in future work by taking advantage of MS/MS fragmentation capabilities. However when comparing smokeless powders, a fingerprinting approach considering the mix of stabilisers may be sufficient, rather than unambiguous identification of each stabiliser compound itself [\[61, 62, 199, 329\]](#).

DPA, Ak, MC and EC were all observed as protonated molecular ions. NODPA was again observed as two peaks, with the de-nitrosylated fragment having greater intensity than the protonated molecule. Mass peaks for nitrated diphenylamine isomers were of low intensity in positive-ionisation mode, and were generally unsuitable for the identification of these molecules. However, this group of compounds was identifiable from their deprotonated ions in negative-ionisation mode. They were also observed to produce ions with 15 amu greater mass than the parent compound; it is speculated that this effect may be caused by ionisation with an incoming OH⁻ ion, followed by loss of molecular hydrogen. Nitroglycerin was observed using negative ionisation mode as an adduct with NO₃⁻, along with an abundance of NO₃⁻ at m/z 62 amu not seen in the background spectra.

Table 6-6: Accurate-mass measurement of OGSR molecules by DART-MS					
Compound	+ve/-ve	Ionic Species	Accurate (calculated) m/z	Average measured m/z (n ≥ 3)	Δ ppm
DPA	Pos	[M+H] ⁺	170.0970	170.1068	57.61
NODPA	Pos	[M+H] ⁺	199.0859	199.1030	85.89
	Pos	[M-NO] ⁺	169.0890	169.1040	88.71
(NO ₂)DPA	Pos	[M+H] ⁺	215.0820	215.1175	165.05
	Neg	[M-H] ⁻	213.0665	213.1009	161.30
	Neg	[M+O-H] ⁻	229.0613	229.0942	143.48
(NO ₂) ₂ DPA	Pos	[M+H] ⁺	260.0671	260.0965	113.05
	Neg	[M-H] ⁻	258.0511	258.0799	111.61
	Neg	[M+O-H] ⁻	274.0464	274.0714	91.10
tri-NG	Neg	[M+NO ₃] ⁻	288.9926	289.0008	28.49
		[M+OH] ⁻	244.0053	244.0246	79.10
DMP	Pos	[M+H] ⁺	195.0652	195.0647	-2.56
		[M-CH ₃ O] ⁺	163.0390	163.0497	65.63
AK	Pos	[M+H] ⁺	227.1184	227.1261	33.90
MC	Pos	[M+H] ⁺	241.1345	241.1390	18.66
EC	Pos	[M+H] ⁺	269.1658	269.1866	77.28

6.3.3.3. Extracts Prepared from Intact Smokeless Powders

Following criminal incidents such as shootings or explosions, residues and/or fragments of partially burned propellant powders may be recovered. The chemical composition of these traces can provide useful investigative information, by narrowing down the list of potential propellant products involved. This may also allow investigators to infer links between individuals and the incident if a POI is found to be in possession of smokeless powders that cannot be excluded as a source of the trace. Of course, the strength of these links is dependent upon the rarity of a given compositional “profile” within the smokeless powder market accessible to the relevant populace.

The same 30 smokeless powder extracts reported in 6.2.4.4 were analysed in triplicate, this time using the DART – Ion Trap system, approximately six months after the extracts’ initial preparation. Fresh extracts were not prepared, as doing so would have required interstate transport of smokeless powders. Comparable results were seen using either ion source, with 22 powders determined to be double-base (containing nitroglycerin propellant) using the DART. All 26 powders found to contain DPA and NODPA by DSA had equivalent mass peaks when using DART. The stabilisers ethyl centralite and akardite were also detected equally well using either ion source (12 and 4 powder specimens, respectively). The most notable difference in observed composition occurred for nitrated DPA derivatives, with mass peaks for NO_2DPA found in 13 samples (vs. 26) and mass peaks for $(\text{NO}_2)_2\text{DPA}$ found in only two samples (vs. 10). Therefore DART may be a less appropriate tool for assessing the extent of powder degradation/aging *via* stabiliser by-products than DSA. Two figures are provided to allow for a visual comparison between the results from each AIMS configuration. Spectra obtained by DART-MS from three smokeless powder samples are provided in Figure 6-11; these are the same three specimens used for Figure 6-5 above. Table 6-7 summarizes the components relevant to OGSR identified in each powder by DART-MS, and is equivalent to Table 6-4 showing the same powders analysed by DSA-MS. Lennert & Bridge (2018) used mass spectrometry for a similar application to the one described above [\[61\]](#). They analysed 34 smokeless powders for the presence of nitroglycerin, dinitrotoluene, diphenylamine, ethyl centralite and dibutylphthalate using both DART-MS and GC-MS instrumentation. The compositional profiles were then used as input data for chemometric classification methods, including principal components analysis (PCA) and hierarchical cluster analysis (HCA). HCA produced 11 groupings using either of the instruments, although the arrangement of groupings varied slightly. Although there was no powder specimen in common between the two research groups’ experiments, the present observations were generally in agreement with that of Lennert & Bridge both by visual comparison of spectra, and approximate characteristics of the powder collections.

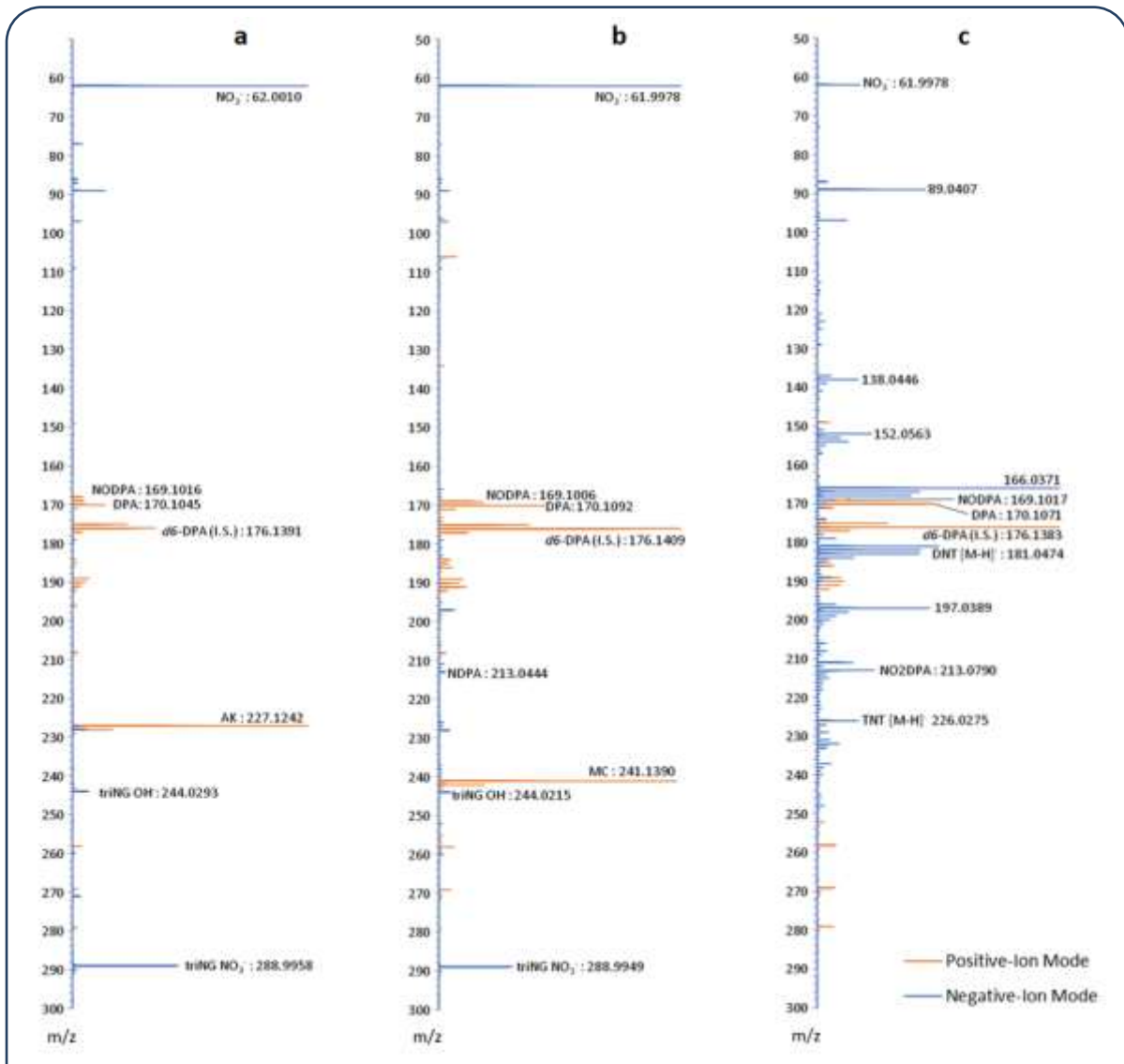


Figure 6-11: Spectra from powder extracts #3 (a), #22 (b), and #26 (c) in Table 6-7. Each was analysed in both positive- and negative- ion modes. Spectra are normalized to the most abundant peak.

Table 6-7: Observed composition of 30 smokeless powders using DART-MS								
Sample ID	NG	DPA	(NO) DPA	(NO ₂) DPA	(NO ₂) ₂ DPA	MC	EC	Ak
1. Remington - Subsonic, LR (USA)	√	√	√	√	x	x	x	x
2. Canadian Industries Limited - Pistol Match, LR (Canada)	√	√	√	√	x	x	x	x
*3. Federal - Champion, LR (USA)	√	√	√	x	x	x	x	√
4. Sellier Bellot (Czechoslovakia)	√	√	√	√	x	√	√	x
5. CCI - Target, Standard velocity, LR (USA)	√	√	√	x	x	x	x	√
6. Aguilla - SE Super Extra, LR (Mexico)	√	√	√	x	x	x	x	x
7. Eley - Club, LR (UK)	x	√	√	√	√	x	x	x
8. RWS - Subsonic (Germany)	√	√	√	x	x	x	√	x
9. Browning - HP, LR (Australia)	√	√	√	x	x	x	x	x
10. Stirling - High Impact, LR (Phillipines)	√	√	√	√	x	x	√	x
11. Winchester - XTR pistol, LR (Australia)	√	√	√	√	x	x	√	x
12. PMC - Zapper, LR (Korea)	√	√	√	x	x	x	x	x
13. Lapua - Midas, LR (Finland)	x	√	√	√	x	x	x	x
14. Mauser - KK80, LR (Germany)	√	√	√	√	x	x	x	x
15. Fiocchi - Maxac, LR (Italy)	√	x	x	x	x	x	√	x
16. Nitron - Naboje, LR (Poland)	x	√	√	√	x	x	x	x
17. Swartklip - LR (South Africa)	√	√	√	x	x	x	x	x
18. Imperial - CIC HP, LR (Australia)	√	x	x	x	x	x	√	x
19. CBC - Super Velox, LR (Brazil)	√	x	x	x	x	x	√	x
20. Gevelot - LR (France)	x	√	√	√	x	x	x	x
21. Nicorro - hp, LR (Germany)	x	√	√	√	√	x	√	x
*22. Vostok - Target, LR (Russia)	√	√	√	x	x	√	√	x
23. Dominion - LR (Canada)	√	x	x	x	x	x	√	x
24. Valor - Ultrasonic, LR (Yugoslavia)	√	√	√	x	x	x	√	x
25. Hornady - 30GR VMAX, 22WMR (USA)	√	√	√	x	x	x	√	x
*26. Unspecified Powder - Batch A (Australia)	x	√	√	x	x	x	x	x
27. Unspecified Powder - Batch B (Australia)	x	√	√	√	x	x	x	x
28. Unspecified Powder - Batch B, Artificially Aged (Australia)	x	√	√	√	x	x	x	x
29. Hilti - Nail Gun Cartridge, Yellow (Australia)	√	√	√	√	x	x	√	√
30. Hilti - Nail Gun Cartridge, Red (Australia)	√	√	√	x	x	x	x	√

6.3.3.4. Stub-derived OGSR hand samples

In order to expand from specimens of smokeless powder towards other forensically relevant traces, attempts were made to detect post-shooting residues on the hands of volunteers. To this end 24 samples were collected from the hands of students who attended an “open day” style event at a recreational shooting club. The students used handguns in a variety of designs and calibres. Samples were collected from the volunteers using conductive carbon adhesive stubs, following the common procedure used for IGSR recovery. Each sample was accompanied by a stub collected from the same individual’s hands pre-shooting, to establish a baseline for comparison. The stubs were extracted with 100 µL of acetonitrile, with three replicate 10 µL aliquots applied to the DART’s sample support mesh for analysis.

Each of the prepared extracts resulted in rich spectral information; however there was little difference between the extracts collected pre- or post- shooting. There was also a noticeable difference between stubs from different suppliers. Two examples are supplied in Figure 6-12, with equivalent results observed for the remaining samples. This represents a similar outcome to that achieved using DSA-MS and suggests that the adhesive stubs contain compounds that either suppress or mask the desired analytes [\[302\]](#). As AIMS analyses do not inherently feature a separation procedure, all components of each sample are subject to competitive ionisation processes occurring simultaneously. If the solution contains compounds that are either: a) significantly more susceptible to ionisation, due to their ionisation energy or proton affinity, or b) in such abundance that they are involved in most gas-phase collisions with the reagent species, then the critical analytes are not likely to be observed in spectra above the background signal. DART-MS has been used previously by Mess *et al.* (2011) to measure the composition of tackifier resins in pressure-sensitive adhesives [\[330\]](#). While none of the mass-peaks reported by those authors were also observed in the present study, their work does at least suggest that such adhesives do indeed contain material that can be ionised under conditions produced during DART-MS.

The inability to detect OGSR from adhesive stubs using DART contrasted with observations made by others using AIMS techniques. Morelato *et al.* (2012) reported detection of EC but not DPA directly from post-shooting hand-stubs using DESI-MS, although the “experiments conducted on stubs generated weak and unstable signals” [\[188\]](#). Black *et al.* (2017) claimed better success using a similar pairing of liquid extracts and DART-MS. Those authors reported that they “readily detected ethyl centralite, methyl centralite and diphenylamine, commonly found in firearm propellants ... in the solvent wash of the GSR stub”, with mass peaks consistent with nitro-glycerine also shown [\[202\]](#).

Three major differences were noted between the procedures described herein and those used by Black *et al.*, which may have contributed to the discrepancy in outcomes. Firstly, during the sample preparation process, acetonitrile was used as the extraction solvent rather than methanol. Secondly, a different brand of stubs was used, potentially affecting signal suppression through competitive ionisation processes. Thirdly, the spectrometers providing detection post-ionisation were different. Black *et al.* used a JEOL AccuToFTM spectrometer with the DART unit being an integral component. On the other hand, a Velos Pro ion-trap was used for the current work. To account for the difference in equipment available to each laboratory, a small selection of post-shooting hand stubs were sent to one of the co-authors of that study with a request for analysis. Results are shown in Figure 6-13 a) and b). While the pre-shooting stub also resulted in spectra with many mass peaks, blank-subtracted spectra from shooter-samples did show mass peaks consistent with ethyl centralite. This compound is considered characteristic of GSR, suggesting that DART-MS may still have future applications in GSR detection.

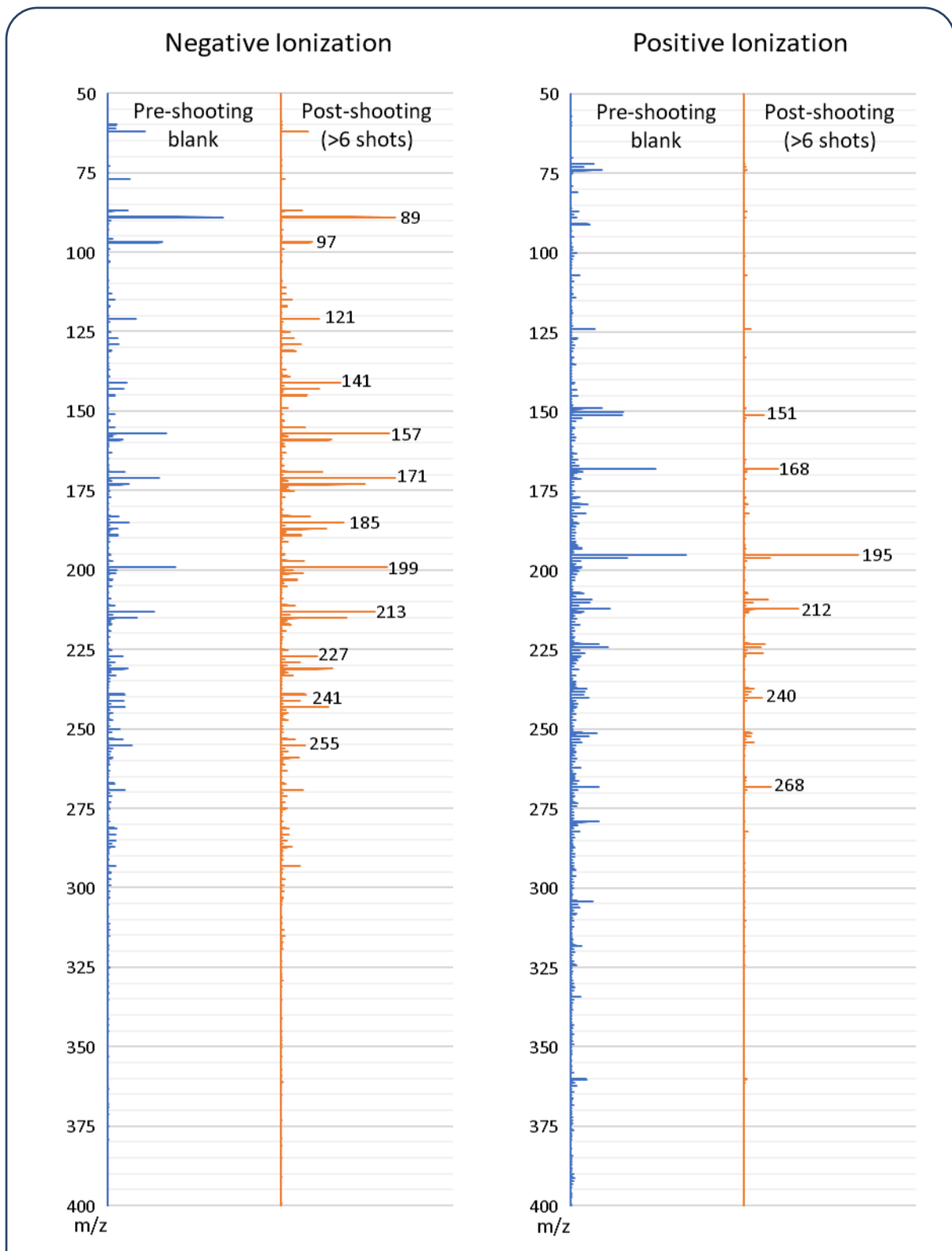


Figure 6-12: a) Comparison of pre-shooting and post-shooting DART-MS spectra from hand samples collected with adhesive stubs supplied by Pelco. No differences signifying detection of OGSR were observed.

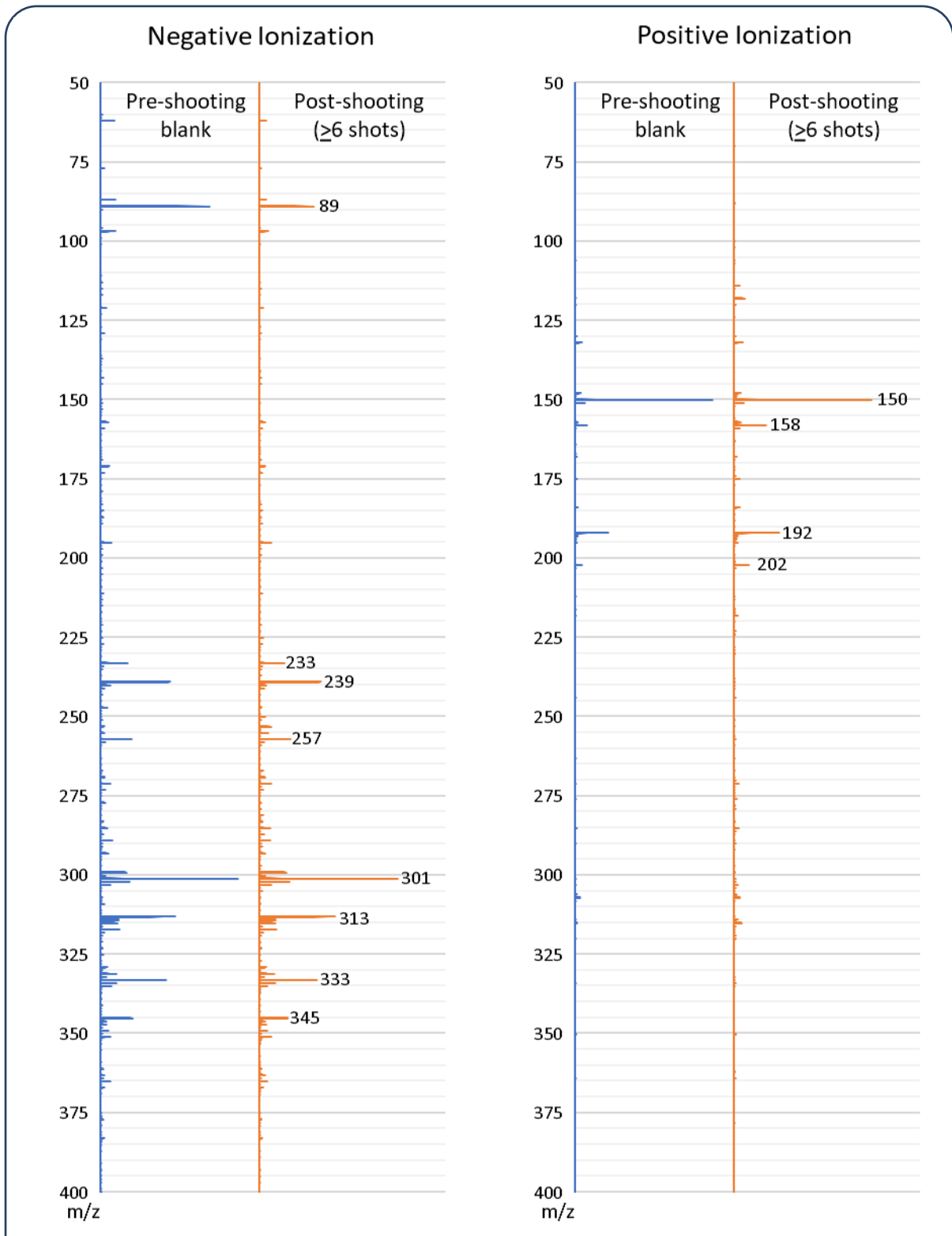


Figure 6-12 b) Comparison of pre-shooting and post-shooting DART-MS spectra from hand samples collected with adhesive stubs supplied by ChemCentre. No differences signifying detection of OGSR were observed.

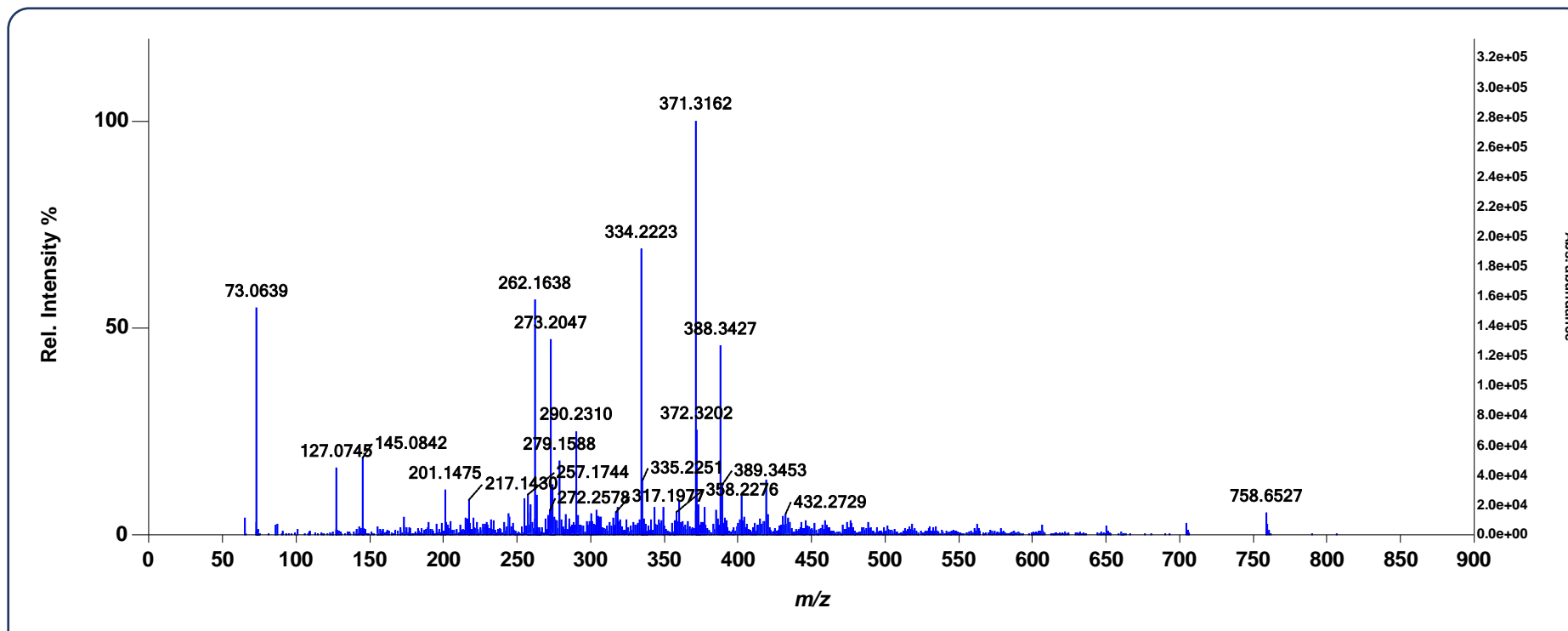


Figure 6-13: a) Spectra collected from extracted post-shooting hand-samples using DART-AccuToFTM MS. Spectrum A from blank stub, supplied by Ted Pella. The author would like to thank Dr. R. Cody and colleagues for their valuable contribution of these data (R. Cody, personal communications, February 2020).

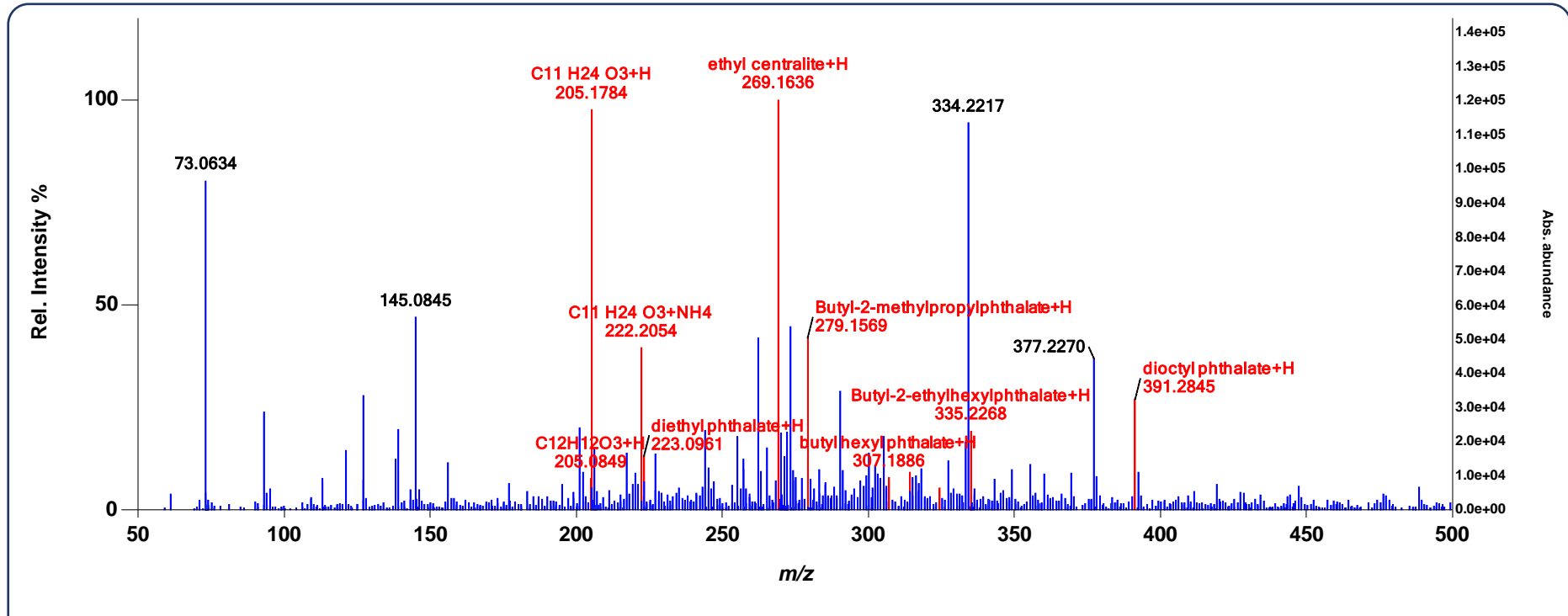


Figure 6-13: b) Spectra collected from extracted post-shooting hand-stubs using DART-AccuToFMS. Blank-subtracted spectrum from sample provided by volunteer after discharging one round from a Glock G17 9mm handgun. The author would like to thank Dr. R. Cody and colleagues for their valuable contribution of these data (R. Cody, personal communications, February 2020).

6.3.4 Conclusions

A system consisting of a DART ion-source and linear ion-trap mass spectrometer was evaluated for potential use as an OGSR detection and comparison tool. The effect of varying several user defined settings including temperature, input gas and scan speed/resolution were investigated. It was found that once optimized, the system was capable of ionising relevant organic compounds and recording their mass spectra in a few minutes or less per sample. m/z accuracy and resolution were not sufficient to apply accurate mass calculations for the confirmation of structural formula. However adequate information was available for use in a screening role pending further confirmation. While not explored further here, the spectrometer was also capable of controlled fragmentation (“MS/MS” or “M/S”) functionality. If implemented this capability may improve such a systems’ discriminating power so that it is fit-for-purpose.

Extracts prepared from whole smokeless powders produced spectra with considerable compositional information. It was possible to identify smokeless powders as such on the basis of that information, and to perform limited discrimination between various products/ammunitions by visual or categorical comparison. Samples of smokeless powder residue collected from the hands of recent shooters using adhesive stubs were also analysed. However, it was not possible to distinguish these samples from pre-shooting blank stubs by their respective mass spectra.

6.4 Conclusions

Two separate spectrometers featuring ambient-ionisation capability were assessed for possible use in detecting GSR. AIMS can potentially provide analytical results within seconds to minutes, much faster than either hyphenated chromatography instruments or especially traditional SEM-EDS scanning. Both the DSA and DART sources were found to be capable of desorbing and ionising relevant OGSR compounds. Of the two, the DSA’s spectrometer gave greater confidence in analyte identity due to its better mass accuracy and resolution; the technique of comparison between observed and calculated accurate mass could be used. On the other hand, the DART was more versatile towards introducing physical samples rather than only liquid extracts.

Either instrument was suitable for analysing, detecting, and potentially discriminating between smokeless powders. These capabilities may be useful for forensic cases involving recovered ammunition, improvised explosive devices, or post-blast debris when large amounts of partially unburned propellant are present. However, the outcomes for GSR samples collected using adhesive stubs were mixed to poor for both instruments. While mass peaks consistent with OGSR markers were occasionally observed, it was much more likely to observe no difference between the spectra from blank or GSR-laden stubs. This was due to a significant background signal arising from the adhesive in the stubs themselves. Any future efforts to incorporate AIMS into a GSR detection procedure should therefore focus on sample collection or isolation.

Chapter 7: General Conclusions

7.1 Themes

Both the organic and inorganic portions of gunshot residue originate from the same act of discharging a firearm. However, OGSR has been largely ignored by forensic scientists in recent history. If organic analyses were conducted, the results have been considered as distinct and separate pieces of information. The overall theme of the research underpinning this thesis was the investigation of more holistic approaches towards these traces. An integrated approach to collection, analysis and interpretation of GSR traces can potentially provide analysts with more chemical information, upon which their expert opinion must be based.

A review of prior academic literature showed that many competing techniques have been proposed for the laboratory analysis of OGSR, although these appear to be used rarely if at all during routine forensic casework. Fewer publications have addressed the integration of these techniques with SEM-EDS, the analytical instrument representing the current state-of-the-art for GSR detection and characterisation. Due to the lack of combined analyses, there was also a scarcity of knowledge about the evaluation of investigative propositions using data from both OGSR and IGSR.

In this thesis original contributions to knowledge were made in three general areas, building upon one another successively. These were:

- a) Laboratory method development
- b) Collection of data using samples representing real-world conditions
- c) Exploration of approaches for the forensic evaluation of these data

The research process and key findings for each of these areas are summarized individually, as follows. The relevance and potential impact of those findings are then discussed. Lastly, potential directions for future work on the subject matter are suggested.

7.2 Technical method development

The purpose of the method development presented in Chapter Two was to demonstrate that concurrent analysis of both organic and inorganic portions of the same GSR trace is technically feasible, and should be within the capabilities of most modern analytical chemistry laboratories. SEM-EDS and LC-MS/MS are considered the leading techniques for analysis of IGSR and OGSR respectively. This work represents one of the first procedures that uses both instruments in tandem for the same trace sample.

Parallel subsamples were produced by extracting OGSR from the surface of adhesive stubs using an organic solvent, while leaving insoluble particulate IGSR behind. This solvent was applied and then recovered using a disposable pipette tip, with care taken to avoid contact with the surface. The procedure is simple, rapid, and aims to minimize handling of the sample. While similar approaches had been suggested in prior literature, the full implementation has not been demonstrated comprehensively until now. A key design

consideration was to retain the use of conductive, adhesive sampling stubs, to avoid any alteration of current sample collection procedures. There were two reasons for this decision. Firstly, these stubs have previously been shown to be the most efficient option for collecting GSR traces from surfaces. Secondly, laboratory analysts will not necessarily be responsible for collecting samples from POIs. As sample collection procedures are currently in place, for example by police officers, minimising disruption to other participants in the chain between crime scenes and laboratories was also considered important.

Electron microscopy was used to map the position of IGSR particles on several stub samples, pre- and post-extraction. The differences between the maps were minor, within the expected margins for re-analysis of samples containing $<1\ \mu\text{m}$ particles. This offered confidence that particles were not necessarily stripped from the surface by the extraction procedure. Undeniably, there is still some potential for particle loss. In an operational setting, risk assessments would need to be made to determine whether additional information from OGSR is worth the potential disruption to IGSR particles. These decisions will be influenced by the type of questions raised during specific cases.

A laboratory method for analysis of OGSR extracts by UHPLC-MS/MS was also developed, building on work published by others. Instrumental LODs were calculated for seven compounds associated with GSR, with all falling in the low-ppb range. Recoveries were then tested using standard reference solutions, with results varying between approximately 50-100%. It is important to consider that this only estimates the recovery of true OGSR, which is likely to exist as discrete pieces of partially burned propellant rather than as a homogenous film. Actual GSR is not typically used when assessing recovery, due to extreme variation in the quantities that may be initially deposited.

Real-world GSR samples were collected from the hands of volunteers after discharging firearms including semi-automatic pistols, revolvers, pump-action shotguns, and bolt-action rifles. These represent a cross-section of guns available to civilians in Australia. Specific figures on detection rates are discussed in Chapter 3: and section 7.3. However, in general terms the combination of solvent extraction and LC-MS/MS was sufficiently sensitive to detect OGSR from as few as one shot(s). In some instances, this may provide the necessary information sought by police or judiciary. The data also provided additional information about the composition of ammunition used in a shooting; in three separate experiments the post-shooting OGSR extracts were confirmed to qualitatively match their unfired smokeless powders. Some ability to triage samples for SEM-EDS analysis is also offered, as LC-MS is much faster than scanning electron microscopy.

Where reasonable, efforts were made to test the proposed method against increasingly difficult samples. Detection of OGSR from close-range targets including both textiles and dirtied surfaces was shown, as was

detection from immobile surfaces up to 24 hours post-shooting. While preliminary, the results of these tests suggest that OGSR detection and recovery is affected by the same general principles as IGSR.

Additional data were collected on the use of ambient-ionisation mass spectrometry for potential use in GSR detection. AIMS has the potential to collect mass spectra very quickly (<1 minute) without any preparation of the questioned samples. It was hoped that spectra for OGSRs could be detected directly from SEM stubs, avoiding any meaningful disruption of collected traces. Two ion-sources offering AIMS capability were tested: "Direct Analysis in Real Time" by Jeol USA and "Direct Sample Analysis" by Perkin Elmer. Both proved capable of ionising standard OGSR reference compounds, and producing spectra that could be used for the qualitative comparison of smokeless powders. Of the two, the DSA gave better performance for the selective identification of organic compounds. This was credited to the greater mass accuracy attainable by the time-of-flight mass spectrometer interfaced with that source, compared to the DART source paired with an ion-trap design.

Unfortunately, success with AIMS for smokeless powders did not lead to similar outcomes for OGSR traces recovered post-shooting. A very intense background signal was produced by the stubs themselves, and little to no difference was observable in spectra after stubs were collected from recent shooters' hands. As ambient ionisation is a competitive process, it is suggested that components of the adhesive were preferentially ionised and effectively masked the presence of OGSR. Separation or pre-concentration may have overcome these difficulties. This approach was not explored further, as the introduction of preparatory steps was deemed antithetical to the advantages offered by ambient mass spectrometry.

7.3 Collecting representative data from real GSR traces

While necessary, validation of laboratory techniques to be used on specific samples in isolation does not fully meet the requirements for forensic applications. It is also important to collect data on the range of results that will be encountered during real-world testing. These data can then be used when communicating the implications of individual laboratory findings to end users. Regarding GSR, knowledge is required about the traces found in relation to known shooting events, and also traces found/not found on persons unrelated to firearm crimes. Existing surveys have been conducted to model the amount of IGSR and OGSR found (separately) for shooters. The background prevalence of IGSR has been surveyed previously, particularly within the contexts of the U.S.A. and Europe. Fewer studies have considered the prevalence of OGSR and OGSR-like background material. Since the existing knowledge base appeared to cover only part of the overall situation regarding GSR traces, survey samples were collected from Australian shooters, non-shooters, and their personal vehicles.

7.3.1 Samples Collected from Hands

Many post-shooting samples were analysed for both IGSR and OGSR throughout this research. At least 30 were deliberately collected from shooters' hands following "natural" behaviours, rather than scenarios directed by researchers. These can be summarized as eventuating after competition shooting or safety training courses, by individuals familiar with firearms but not forensic procedures. Often there were delays of approximately 15-30 minutes between the cessation of shooting and collection of stub samples, during which the participants packed away their firearms, manipulated door handles and scoring paperwork *etc.* Unsurprisingly, all these individuals' samples were found to contain numerous IGSR particles meeting the ASTM's definitions for both "characteristic" and "consistent" classifications. The mean number of characteristic particles was 483, with the variation of counts across the samples best fit by a log-normal distribution. These particles were found despite any losses to due physical activity using the hands, and also despite any losses incurred due to the solvent extraction process.

Additionally, 28 of the 30 samples were found to contain at least one of the stabiliser compounds selected to represent OGSR. Even when applying stricter criteria requiring ≥ 2 compounds, 20 could still be deemed "positive" for OGSR. These findings support the assertion that additional chemical information can be obtained from traces collected using existing practices. This additional information has two potential benefits. Firstly it allows better recognition of GSR, particularly if large numbers of characteristic particles happened to be absent. Secondly, it is currently difficult to discriminate between ammunition sources based on IGSR, as many products use similar "Sintox" formulations in their primers. A more thorough characterisation of the trace using OGSR could allow analysts to classify GSRs according to the presence of individual stabiliser compounds.

A further 30 samples were collected from the hands of individuals declaring that they had no recent contact with firearms, nor exposure to potential sources of contamination provided in a questionnaire. In general, this group could be described as students and administrative workers. None of their samples were found to contain stabiliser compounds linked to OGSR. While it is unwise to draw broad conclusions from such a limited survey, these data at least suggest low background prevalence of the compounds in Australia. This includes cross-contamination from actual shooters, and sources of these compounds in applications unrelated to firearms. It is suggested that these results be interpreted as a pilot study demonstrating the soundness of the technique for surveys with a greater number of participants.

Conversely, a single particle meeting the requirements to be classified as "characteristic" under ASTM standard E1588-17 was found on the hands of one volunteer in this subset i.e. the background prevalence is estimated at one-in-thirty. Similar findings of low but relevant numbers of particles have been made during

other surveys in Australia (and elsewhere). Policies on the minimum number of particles required for a “positive” result differ between jurisdictions, but single particles have previously been used as evidence of contact with firearms. In this instance the inclination is to believe the participant when they stated they had not recently handled any firearms, as they had no incentive to offer a false statement. Therefore, if the result was used as evidence to support a prosecution case, it could mislead the finders of fact to the defendants’ detriment. Within the context of this study, it is particularly interesting to note that the IGSR findings were not supported by the concurrent presence of OGSR. In samples collected from known shooters, most (28 of 30) instances of IGSR-detection were associated with at least one stabiliser compound.

7.3.2 Samples collected from Vehicles

Vehicles are frequently used by offenders when committing or fleeing crimes involving firearms. Consequently, it is often necessary to forensically examine the interior of vehicles for the presence of GSR. However, specific vehicle components have previously been identified as potential sources of material that is poorly distinguishable from IGSR. Prior surveys have focussed on these components, such as airbags or brake pads. Several case studies examining the presence of actual GSR in vehicles were identified in literature; however to the best of the author’s knowledge this work is the first to report a broad survey for GSR in vehicles not linked to known shootings. These data are necessary for evaluative approaches. Samples were collected from vehicles belonging to seven individuals declaring an association with sports shooting, and fifteen individuals with no prior association with firearms. Adhesive stubs were used to collect samples from four interior locations, plus the drivers’ hands ($n_{\text{total}} = 110$).

Unsurprisingly, vehicles belonging to recreational shooters were found to contain IGSR traces. A distinction could be seen between vehicles belonging to frequent shooters (more observed particles) and infrequent shooters (fewer observed particles). For individuals who habitually transported firearm bags in the rear of their vehicles, this region was heavily loaded with particles. Steering wheels and drivers’ seats were also heavily loaded.

Notably, as many as 207 particles were also seen on the dashboards of some cars. Among the infrequent shooters, the dashboard was likely to be the most heavily loaded region, although overall numbers were lower. As all participants declared that no shots had been fired from the immediate vicinity of their vehicles, and the dashboard is not typically touched during driving, these findings suggest that airborne redistribution of IGSR may be occurring. If true, this could have ramifications when the location of GSR within a vehicle is a pertinent issue.

Of the 75 samples collected from vehicles having no declared association with firearms, there were several noteworthy findings. Most importantly, a single characteristic IGSR particle was located on the dashboard of

one vehicle. This represents a background positive rate of 1.3% from all samples, or from 6.6% of non-shooters' vehicles. There is presently no indication of whether this particle is truly GSR and has been deposited following some transfer event, or if it is some other material indistinguishable from GSR. While similar findings have been made when sampling volunteers' hands, this is the first reported discovery when specifically considering vehicles. When tested for stabiliser compounds using HPLC-MS/MS, 10 samples were found to produce chromatographic peaks consistent with akardite. Concentrations in these samples were estimated between 1-8 ppb by external calibration. This result was surprising, as akardite (N-Methyl-N',N'-diphenylurea) is not generally reported to have uses outside smokeless powders. However the observed concentrations were very low compared to authentic shooter samples and chromatographic peaks were near to the instrumental LOD. Therefore, further surveys for akardite are recommended before estimation of its' prevalence in vehicles can be made. Greater confidence was assigned to a single instance of detection for nitrodiphenylamine with an estimated concentration of 90 ppb, having a clearer chromatographic peak and mass spectrum. Again, this observation represented 1.3% of non-shooter vehicle samples. As the simultaneous observation of many stabiliser compounds did not occur, the sample population could be summarized as "negative" or "inconclusive" for OGSR under the standard proposed by The Organization of Scientific Area Committees for Forensic Science (OSAC) and ASTM.

There was no simultaneous detection of material consistent with O & I GSR on non-shooters or their vehicles.

These findings are very important because they represent the first published instances of GSR background in vehicles. Therefore, further investigation is recommended for any jurisdictions that may sample vehicles when investigating shooting events. Additional data should be gathered to both reflect relevant populations (geographically or demographically), and to build defensible evaluative models.

7.4 Investigating how these new data could be interpreted

7.4.1 Technical Interpretation of GSR Evidence

Since the publication of pioneering work in the 1970s, recovered IGSR traces have been assigned evidential weight based upon the distinctiveness of their chemical composition. While specific classifications have evolved over time, ASTM standard E1588 currently recognises three qualitative levels of support for inferences as to whether specific inorganic particles are GSR. These are, in order of decreasing significance, characteristic of-, consistent with-, and commonly associated with- GSR. This published standard represents the normative approach taken by forensic laboratories in Australia and many other jurisdictions. Results are generally reported as numbers of identified particles along with general qualifying statements, although these can be supplemented with case-specific opinions if analysts are asked to testify as expert witnesses. This is an example of technical reporting. Technical reporting styles generally use predefined thresholds and

narrow criteria to transmit information from forensic laboratories to end users. This promotes standardisation and objectivity, while reducing complex laboratory data to an easily understood output. However technical reports can only make use of quantitative and multivariate data to the extent that it has already been incorporated into an assessment framework.

On the other hand, it was found that no equivalent document existed to support the evaluation or communication of laboratory data generated from OGSR traces. There was at least one academically-published attempt to list and prioritize organic compounds relevant to GSR, while other research authors have preferred to set criteria for detection “positives” on a study-by-study basis. In May of 2020, a working document entitled “*Standard Practice for the Collection, Preservation, and Analysis of Organic Gunshot Residues*” (WK72856) was circulated for comment by the OSAC Subcommittee for Ignitable Liquids, Explosive, and Gunshot Residue. Section 10.2 of this document contained a two-tiered classification scheme for OGSR compounds, with accompanying minimum criteria for reporting detection. While these criteria were applied in preceding chapters of this thesis, they appear to have been discarded from later documents released by the Subcommittee.

The present work was the first to explicitly examine whether holistic assessments of samples, incorporating data from both the organic and inorganic portions, was better able to discriminate between GSR and non-GSR traces than current single-test regimes. The results supported an affirmative position. Samples were collected from 60 volunteers, evenly split between known shooters and known non-shooters. Tests using LC-MS and SEM-EDS were performed on all samples, and the results were initially assigned as either positive or negative for GSR using separate assessment criteria. For the first time in GSR research, a Bayesian updating approach was used to show that the use of parallel testing improves diagnostic accuracy. Predictive values were used in addition to false positive or negative rates to measure this improvement. Notably, the probability that a sample in fact belonged to a shooter, given that they were found to have at least one IGSR particle (Positive Predictive Value) was 0.9667. When GSR was detected by both SEM-EDS and LC-MS, the probability of the sample belonging to a shooter was found to be 0.9983. This represented an approximately twenty-fold reduction in the likelihood of falsely concluding a non-shooter’s sample belonged to a shooter.

Qualitative criteria were also used to prove that while the testing of OGSR and IGSR are conducted orthogonally using independent instruments, the results obtained are not *statistically* independent. That is, knowing the results of one test will affect the expected result in the other test. This mutual dependency arises because the laboratory subsamples originate from the same trace when actual GSR is present. It will be important for GSR experts to consider that both results are linked, if using two separate technical reports to communicate results to stakeholders in future.

7.4.2 Evaluative Interpretations of Quantitative and Multivariate GSR Data

During an evaluative process, forensic scientists formally consider the likelihood of their observations given two or more mutually exclusive propositions. The extent to which the evidence supports either proposition can then be calculated numerically in the form of a likelihood ratio. This contrasts with technical reporting, which generally discards some amount of case-specific perspective. The evaluative approach seeks to improve transparency and consistency, by formalising any assumptions made by the expert. It also allows forensic scientists to share expert knowledge on queries spanning a greater range of the hierarchy of propositions. In practice, this means that an opinion can be made on *how* a GSR trace has come to be found, rather than just *if* a trace sample contains GSR. If suitably robust statistical models can be developed, likelihood ratios can also be a powerful way to reduce the complexity of multivariate data without discarding any underlying information from the final output.

Prior to the original work in this thesis, several frameworks that applied likelihood ratios and evaluative reporting to GSR evidence have been published. This previous research has been largely focussed on discriminating between shooters and contaminated non-shooters, and on the strength of evidence that can be achieved at different time points since an alleged incident. Likelihood ratios can be strongly influenced by the choice of equations or algorithms used to statistically model laboratory results, even when underlying data are kept consistent. However, most of the underlying models reported in literature have been based on only a single variable (counts of characteristic particles). All other data collected about each trace have typically been omitted from the evaluative process. Gaussian, Poisson, and Negative Binomial equations have been popular choices for univariate models. Research on interpretation of GSR traces from multivariate perspectives was comparatively sparse, because additional OGSR data were not previously collected. Therefore potential for further investigation into evaluative methods was identified.

In this work, two machine learning algorithms (Partial Least-Squares Discriminant Analysis (PLS-DA) and Artificial Neural Networks (ANNs)) were identified as promising tools. These are both capable of combining multivariate observations into a single numerical output for each sample, even when multi-collinearity is observed within the data. Using either method, it was possible to choose thresholds that allowed for 100% accurate classification of shooter and non-shooter samples. However, the separation between scores generated for each group was much wider using an ANN compared to the PLS-DA approach. In addition to this simple binary classification, likelihood ratios were calculated as estimates of the evidential strength provided by each sample. ANNs appeared to produce a better-calibrated range of likelihood ratios. Therefore, these results suggest that ANNs may be the more appropriate tool for helping forensic scientists to calculate rational likelihood ratios from multivariate GSR data. However, the use of machine learning in a forensic process might risk confusing laypeople if it is not made clear that likelihood ratios are only a means

of supporting the expert witnesses' opinion. There is no universally true likelihood ratio that forensic scientists are trying to approximate when using statistical models; It is up to each analyst to select the model(s) that they feel most accurately reflect the available data. They can then use the likelihood ratio to communicate their opinions in a transparent and standardized manner.

7.5 Further Research Directions and Future Prospects

The work presented in this thesis showed that the combined analysis of gunshot residues is within the capability of contemporary analytical laboratories. Portions of the same GSR traces were analysed by commercially available instruments representing the state of the art for inorganic and organic residues respectively. However, there is still much work to be done before practicing forensic scientists can gain the full benefits of this approach. Firstly, practitioners should be made aware of these opportunities to generate additional chemical data from the same trace samples that are already being collected and submitted to laboratories. Secondly, a true understanding of the case circumstances most likely to benefit from integrated analysis can only arise through application and experience, rather than purely academic research.

This can be developed through the establishment of a broad consensus, and eventually published standards, to support the reporting of OGSR findings. While classifications for the relative discriminating power of IGSR particles are familiar to the discipline, no standardized categories exist for organic compounds connected with GSR. This has already been identified as an objective by the Organization of Scientific Area Committees for Forensic Science. Specifically, more comprehensive surveys into the background prevalence of compounds suspected of providing probative value are required. A small-scale study presented above suggested that the prevalence of OGSR stabilisers is likely to be low, at least in urban Australia. On the other hand, experience with classifying IGSR has shown that chemical compositions thought to be "unique" to GSR have subsequently been downgraded as new non-firearm sources are identified. Indeed, results shown above indicated that sporadic background detection of compounds in OGSR may occur from vehicles. Further research would support better understanding of any pre-existing background material and expand models into international contexts. New detection targets may also be discovered through the careful characterisation of smokeless powder products and the residues they produce.

While a classification system for OGSR compounds is viewed as essential, it is the author's opinion that broader issues should be considered during the development of any forensic OGSR standard. If established, how might a scientist report the findings of both inorganic and organic analyses in the same case? Would the reports be presented separately, or as a unified whole? It is also interesting to consider whether the presence of OGSR can elevate the importance of an otherwise ambiguous population of consistent IGSR particles.

This leads to another area where further research is suggested. Results included in Chapter Four supported the use of multivariate models to underpin evaluative reporting. However, only very simplistic scenarios were chosen for investigation. These did not cover even the most common propositions that forensic scientists may need to evaluate for GSR casework. It is suggested that pairs of propositions, previously used by academics to generate likelihood ratios from univariate experimental data, might be revisited for multivariate analysis in a more rigorous way than was used in this thesis.

Chapter 8: Bibliography and Appendices

8.1 Reproduced Figures

Figure 1-5 was reproduced from *Forensic Chemistry*, 2018, vol 8, p146-156. *Fast identification of inorganic and organic gunshot residues by LIBS and electrochemical methods*, by T Trejos, C. Vander Pyl, K. Menkong-Hoggatt, A. Alvarado & L. Arroyo, with permission from Elsevier.

Figure 1-6 was reproduced from *Forensic Science International*, 2018, vol 292, p167-175. *Real-time detection of GSR particles from crime scene: A comparative study of SEM/EDX and portable LIBS system*, by A. Doña-Fernández, I. Andres-Gimeno, P. Santiago-Toribio, E. Valtuille-Fernández, F. Aller-Sanchez & A. Heras-González with permission from Elsevier.

Figure 1-7 was reproduced from *Analyst*, 2012, vol 137, p3265-3270. *Simultaneous electrochemical measurement of metal and organic propellant constituents of gunshot residues*, by M. Vuki, K.K. Shiu, M. Galik, A. O'Mahoney & J. Wang with permission from the Royal Society of Chemistry

Figure 1-8 was reproduced from *Science*, 2006, vol 311, p1566-1570. *Ambient Mass Spectrometry*, by R. Cooks, Z. Ouyang, Z. Takats & J. Wiseman with permission from the American Association for the Advancement of Science.

Figure 4-2 was reproduced from *Forensic Science International*, 2019, vol 298, p284-297. *Glass-containing gunshot residues and particles of industrial and occupational origins: Considerations for evaluating GSR traces*, by K. Seyfang, N. Lucas, K. Redman, R. Popelka-Filcoff, H. Kobus & K.P. Kirkbride with permission from Elsevier.

Figure 6-1 was reproduced from *Analytical Chemistry*, 2005, vol 77, p297-2302. *Versatile New Ion Source for the Analysis of Materials in Open Air under Ambient Conditions*, by R. Cody, J. Laramée, & H. Durst with permission from the American Chemical Society.

8.2 Bibliography

1. Chapman, S., et al., *Australia's 1996 gun law reforms: faster falls in firearm deaths, firearm suicides, and a decade without mass shootings*. Injury prevention, 2006. **12**(6): p. 365-372.
2. Chapman, S., et al., *Fatal firearm incidents before and after Australia's 1996 national firearms agreement banning semiautomatic rifles*. Annals of internal medicine, 2018. **169**(1): p. 62-64.
3. Alpers, P., M. Lovell, and M. Picard, *Guns in Australia: Total Number of Gun Deaths*. 2022, Sydney School of Public Health, The University of Sydney.
4. ABS, *Use of weapon in commission of offence by selected offences, 2010–2019*, in *Recorded Crime - Victims*. 2020, Australia Bureau of Statistics: <https://www.abs.gov.au>. Released online 09/07/2020.
5. Kegler, S.R., et al., *Vital Signs: Changes in Firearm Homicide and Suicide Rates - United States, 2019-2020*. Morbidity and Mortality Weekly Report, 2022. **71**(19): p. 656-663.
6. FBI, *Crime in the United States, Expanded Offense Data 2016*, in *Uniform Crime Report*. 2017, Federal Bureau of Investigation, U.S. Department of Justice.
7. Duquet, N. and D.V. Auweele, *Project Target: Targeting gun violence and trafficking in Europe*. 2021: Flemish Peace Institute, Brussels.
8. Office for National Statistics (UK). *Appendix Table 17: Offence recorded by the police in which a firearm has been discharged, by barrel type, year ending March 2020*, in *Offences involving the Use of Weapons: data tables*. 2020: United Kingdom.
9. Dalby, O., D. Butler, and J.W. Birkett, *Analysis of Gunshot Residue and Associated Materials: A Review*. Journal of Forensic Sciences, 2010. **55**(4): p. 924-943.
10. K. Pitts and C. Bonnar, *Gunshot Residue*, in *Encyclopedia of Forensic Sciences (Third Edition)*, M. Houck, Editor. 2023, Elsevier Science. p. 63-74.
11. Kirkbride, et al., *Chapter 87: "Gunshot Residues" in Expert Evidence*. 2016, North Ryde, NSW, Australia: Freckleton and Selby: Law Book Company Limited.
12. Blakey, L.S., et al., *Fate and Behavior of Gunshot Residue: A Review*. Journal of Forensic Sciences, 2018. **63**: p. 9-19.
13. Bendrihem, S.A., R. Pyle, and J. Allison, *The Analysis of Gun-Cleaning Oil as Long-Distance Gunshot Residue and Its Implications for Chemical Tags on Bullets*. Journal of Forensic Sciences, 2013. **58**(1): p. 142-145.
14. Wingfors, H., et al., *Emission factors for gases and particle bound substances produced by firing lead-free small caliber ammunition*. Journal of Occupational and Environmental Hygiene, 2013.
15. Ditrich, H., *Distribution of gunshot residues - The influence of weapon type*. Forensic Science International, 2012. **220**(1-3): p. 85-90.
16. French, J. and R. Morgan, *An experimental investigation of the indirect transfer and deposition of gunshot residue: Further studies carried out with SEM-EDX analysis*. Forensic Science International, 2015. **247**: p. 14-17.
17. Fojtasek, L., et al., *Distribution of GSR particles in the surroundings of shooting pistol*. Forensic Science International, 2003. **132**(2): p. 99-105.
18. Gassner, A.L., et al., *Organic gunshot residues: Observations about sampling and transfer mechanisms*. Forensic Science International, 2016. **266**: p. 369-378.
19. French, J., R. Morgan, and J. Davy, *The secondary transfer of gunshot residue: an experimental investigation carried out with SEM-EDX analysis*. X-ray spectrometry, 2013. **43**(1): p. 56-61.
20. Gauriot, R., et al., *Statistical Challenges in the Quantification of Gunshot Residue Evidence*. Journal of Forensic Sciences, 2013. **58**(5): p. 1149-1155.
21. Moran, J.W. and S. Bell, *Skin permeation of organic gunshot residue: implications for sampling and analysis*. Analytical Chemistry, 2014. **86**(12): p. 6071.
22. Taudte, R., et al., *The development and comparison of collection techniques for inorganic and organic gunshot residues*. Analytical and Bioanalytical Chemistry, 2016. **408**(10): p. 2567-2576.
23. Hofstetter, C., et al., *A study of transfer and prevalence of organic gunshot residues*. Forensic Science International, 2017. **277**: p. 241-251.

24. Lucas, N., et al., *Quantifying gunshot residues in cases of suicide: Implications for evaluation of suicides and criminal shootings*. Forensic Science International, 2016. **266**: p. 289-298.
25. Mistek, E., et al., *Toward Locard's Exchange Principle: Recent Developments in Forensic Trace Evidence Analysis*. Analytical Chemistry, 2019. **91**(1): p. 637-654.
26. Gassner, A.-L., et al., *Secondary transfer of organic gunshot residues: Empirical data to assist the evaluation of three scenarios*. Science & Justice, 2019.
27. Brožek-Mucha, Z., *Chemical and Morphological Study of Gunshot Residue Persisting on the Shooter by Means of Scanning Electron Microscopy and Energy Dispersive X-Ray Spectrometry*. Microscopy & Microanalysis, 2011. **17**(6): p. 972-982.
28. Moran, J. and S. Bell, *Analysis of organic gunshot residue permeation through a model skin membrane using ion mobility spectrometry*. International Journal for Ion Mobility Spectrometry, 2013. **16**(4): p. 247-258.
29. Gallidabino, M., F.S. Romolo, and C. Weyermann, *Time since discharge of 9 mm cartridges by headspace analysis, part 2: Ageing study and estimation of the time since discharge using multivariate regression*. Forensic Science International, 2017. **272**: p. 171-183.
30. Maitre, M., et al., *An investigation on the secondary transfer of organic gunshot residues*. Science & Justice, 2019. **59**(3): p. 248-255.
31. Maitre, M., et al., *A forensic investigation on the persistence of organic gunshot residues*. Forensic Science International, 2018. **292**: p. 1-10.
32. Andrasko, J. and S. Ståhling, *Time since Discharge of Spent Cartridges*. Journal of Forensic Sciences, 1999. **44**(3): p. 487-495.
33. Chang, K.H., C.H. Yew, and A.F.L. Abdullah, *Study of the Behaviors of Gunshot Residues from Spent Cartridges by Headspace Solid-Phase Microextraction–Gas Chromatographic Techniques*. Journal of Forensic Sciences, 2015. **60**(4): p. 869-877.
34. Stamouli, A., et al., *Survey of gunshot residue prevalence on the hands of individuals from various population groups in and outside Europe*. Forensic Chemistry, 2021. **23**: p. 100308.
35. Brozek-Mucha, *On the prevalence of gunshot residue in selected populations - An empirical study performed with SEM-EDX analysis*. Forensic Science International, 2014. **237**: p. 46-52.
36. Margot, P., *Lecture: DNA is not the magic bullet*, in *Challenging Forensic Science: How Science Should Speak to Court*. 2020, <https://www.coursera.org>. Last accessed online 07/20/2020.
37. Charles, S. and N. Geusens, *A study of the potential risk of gunshot residue transfer from special units of the police to arrested suspects*. Forensic Science International, 2012. **216**(1-3): p. 78-81.
38. Berk, R.E., et al., *Gunshot Residue in Chicago Police Vehicles and Facilities: An Empirical Study*. Journal of Forensic Sciences, 2007. **52**(4): p. 838-841.
39. Ali, L., et al., *A Study of the Presence of Gunshot Residue in Pittsburgh Police Stations using SEM/EDS and LC-MS/MS*. Journal of Forensic Sciences, 2016. **61**(4): p. 928-938.
40. Cook, M., *Gunshot residue contamination of the hands of police officers following start-of-shift handling of their firearm*. Forensic Science International, 2016. **269**: p. 56-62.
41. Lucas, N., et al., *Gunshot residue background on police officers: Considerations for secondary transfer in GSR evidence evaluation*. Forensic Science International, 2019. **297**: p. 293-301.
42. Hearn, N.G.R., D.N. Laflèche, and M.L. Sandercock, *Preparation of a Ytterbium-tagged Gunshot Residue Standard for Quality Control in the Forensic Analysis of GSR*. Journal of Forensic Sciences, 2015. **60**(3): p. 737-742.
43. Donghi, M., et al., *A new ammunition for forensic needs: FIOCCHI-RIS*. Forensic Chemistry, 2019. **13**: p. 100159.
44. Lucena, M.A.M., et al., *Investigation of the use of luminescent markers as gunshot residue indicators*. Forensic Science International, 2017. **280**: p. 95-102.
45. Rosengarten, H., O. Israelsohn, and Z. Pasternak, *The risk of inter-stub contamination during SEM/EDS analysis of gunshot residue particles Comment*. Forensic Science International, 2021. **323**.
46. Bricknell, S., *Criminal use of handguns in Australia*. Trends & Issues in Crime and Criminal Justice, 2008(361): p. 1-6.

47. Bricknell, S., *Firearm trafficking and serious and organised crime gangs*. Research and Public Policy Series, Australian Institute of Criminology, 2012. **no. 116**: p. 59.
48. Knowles, L., *Gun theft doubled since 2007 as gun control lobby calls for regulation overhaul*, in *ABC Investigations*. 2018, ABC News Australia: Australia.
49. Richards, C., *Cartridge Reloading in the Twenty-First Century*. 2013, U.S.A.: Skyhorse Publishing.
50. Charles, S., B. Nys, and N. Geusens, *Primer composition and memory effect of weapons: Some trends from a systematic approach in casework*. *Forensic Science International*, 2011. **212**(1): p. 22-26.
51. Andrasko, J., *Characterization of Smokeless Powder Flakes from Fired Cartridge Cases and from Discharge Patterns on Clothing*. *Journal of Forensic Science*, 1992.
52. Lopez-Lopez, M., J.J. Delgado, and C. Garcia-Ruiz, *Ammunition identification by means of the organic analysis of gunshot residues using Raman spectroscopy*. *Analytical Chemistry*, 2012. **84**(8): p. 3581.
53. Gassner, A.L. and C. Weyermann, *LC-MS method development and comparison of sampling materials for the analysis of organic gunshot residues*. *Forensic Science International*, 2016. **264**: p. 47-55.
54. Reardon, M.R., W.A. MacCrehan, and W.F. Rowe, *Comparing the additive composition of smokeless gunpowder and its handgun-fired residues*. *Journal of Forensic Science*, 2000. **45**(6): p. 1232-1238.
55. Brozek-Mucha and Jankowicz, *Evaluation of the possibility of differentiation between various types of ammunition by means of GSR examination with SEM-EDX method*. *Forensic Science International*, 2001. **123**(1): p. 39-47.
56. Steffen, S., et al., *Chemometric classification of gunshot residues based on energy dispersive X-ray microanalysis and inductively coupled plasma analysis with mass-spectrometric detection*. *Spectrochimica Acta Part B: Atomic Spectroscopy*, 2007. **62**(9): p. 1028-1036.
57. Bueno, J. and I. Lednev, *Advanced statistical analysis and discrimination of gunshot residue implementing combined Raman and FT-IR data*. *Analytical Methods*, 2013. **5**(22): p. 6292-6296.
58. Bueno, J. and I. Lednev, *Raman microspectroscopic chemical mapping and chemometric classification for the identification of gunshot residue on adhesive tape*. *Analytical and Bioanalytical Chemistry*, 2014. **406**(19): p. 4595-4599.
59. Perez, J.J., D.A. Watson, and R.J. Levis, *Classification of gunshot residue using laser electrospray mass spectrometry and offline multivariate statistical analysis.(Report)*. *Analytical Chemistry*, 2016. **88**(23): p. 11390.
60. Reese, K.L., A.D. Jones, and R.W. Smith, *Characterization of smokeless powders using multiplexed collision-induced dissociation mass spectrometry and chemometric procedures*. *Forensic Science International*, 2017. **272**: p. 16-27.
61. Lennert, E. and C. Bridge, *Analysis and classification of smokeless powders by GC-MS and DART-TOFMS*. *Forensic Science International* 2018. **292**: p. 11-22.
62. Dennis, D.-M.K., M.R. Williams, and M.E. Sigman, *Assessing the evidentiary value of smokeless powder comparisons*. *Forensic Science International*, 2016. **259**: p. 179-187.
63. Rijnders, M.R., A. Stamouli, and A. Bolck, *Comparison of GSR Composition Occurring at Different Locations Around the Firing Position*. *Journal of Forensic Sciences*, 2010. **55**(3): p. 616-623.
64. Israelsohn-Azulay, O., Y. Zidon, and T. Tsach, *A mixed composition particle highlights the formation mechanism of the weapon memory effect phenomenon*. *Forensic Science International*, 2018. **286**: p. 18-22.
65. Zeichner, A., et al., *Application of lead isotope analysis in shooting incident investigations*. *Forensic Science International*, 2006. **158**(1): p. 52-64.
66. Basu, S., *Formation of Gunshot Residues*. *Journal of Forensic Science*, 1982. **27**(1): p. 72-91.
67. Rathsburg, H. and E.v. Herz, *Verfahren zur Herstellung von Zuendsaetzen*, Reichspatentamt, Editor. 1928: Germany.
68. Brede, U., et al., *Primer Compositions in the Course of Time: From black powder and SINOXID to SINTOX compositions and SINCO booster*. *Propellants, Explosives, Pyrotechnics*, 1996. **21**(3): p. 113-117.
69. Collins, P., et al., *Glass-containing gunshot residue particles: a new type of highly characteristic particle?* *Journal of Forensic Science*, 2003. **48**(3): p. 538-53.

70. Seyfang, K.E., et al., *Analysis of elemental and isotopic variation in glass frictionators from 0.22 rimfire primers*. Forensic Science International, 2018. **293**.
71. Seyfang, K.E., et al., *Glass-containing gunshot residues and particles of industrial and occupational origins: Considerations for evaluating GSR traces*. Forensic Science International, 2019. **298**: p. 284-297.
72. Cameron, E.J., *Comparative Analysis of Airborne Chemical Exposure to Air Force Small Arms Range Instructors*, in *Air Force Institute of Technology, USAF*. 2006: U.S.A.
73. Laidlaw, M., et al., *Lead exposure at firing ranges - a review*. Environmental Health, 2017. **16**(1): p. 34-34.
74. Oommen, Z. and S.M. Pierce, *Lead-Free Primer Residues: A Qualitative Characterization of Winchester WinClean, Remington/UMC LeadLess, Federal BallistiClean, and Speer Lawman CleanFire Handgun Ammunition*. Journal of Forensic Sciences, 2006. **51**(3): p. 509.
75. Snow, J. *Everything You Never Knew About Primers, and the New Technology That's Revolutionizing Them*. 2021; Available from: <https://www.outdoorlife.com>. Accessed online 23/08/2022.
76. Wallace, J., *Chemical Analysis of Firearms, Ammunition, and Gunshot Residue 2nd Ed*. 2018, Boca Raton: CRC Press.
77. Wolten, G., et al., *Final Report on Particle Analysis for Gunshot Residue Detection (Report ATR-77)*. 1977, The Aerospace Corp: Segundo, CA.
78. Wolten, G., et al., *Particle analysis for the detection of gunshot residue I: scanning electron microscopy/energy dispersive x-ray characterization of hand deposits from firing*. Journal of Forensic Science, 1979. **24**(2): p. 409-422.
79. Wolten, G., et al., *Particle Analysis for the Detection of Gunshot Residue 2: Occupational and Environmental Particles*. Journal of Forensic Science, 1979. **24**(2): p. 423-430.
80. Wallace, J.S. and J. McQuillan, *Discharge Residues from Cartridge-operated Industrial Tools*. Journal of the Forensic Science Society, 1984. **24**(5): p. 495-508.
81. Garofano, L., et al., *Gunshot residue: Further studies on particles of environmental and occupational origin*. Forensic Science International, 1999. **103**(1): p. 1-21.
82. Torre, C., et al., *Brake linings: a source of non-GSR particles containing lead, barium, and antimony*. Journal of Forensic Science, 2002. **47**(3): p. 494-504.
83. ASTM, *ASTM E1588-94 Standard Practice for Gunshot Residue Analysis by Scanning Electron Microscopy/Energy Dispersive X-Ray Spectrometry*. 1994: West Conshohocken, PA.
84. Goudsmits, E., G.P. Sharples, and J.W. Birkett, *Recent trends in organic gunshot residue analysis*. Trends in Analytical Chemistry, 2015. **74**: p. 46-57.
85. Goudsmits, E., G.P. Sharples, and J.W. Birkett, *Preliminary classification of characteristic organic gunshot residue compounds*. Science & Justice, 2016. **56**(6): p. 421-425.
86. Schroeder, M.A., et al., *Condensed-phase processes during combustion of solid gun propellants. I. Nitrate ester propellants*. Combustion and Flame, 2001. **126**(1): p. 1569-1576.
87. De la Ossa, M.A., et al., *Analytical techniques in the study of highly-nitrated nitrocellulose*. Trends in Analytical Chemistry, 2011. **30**(11): p. 1740.
88. Murray, S.G., *Explosives (Military)*. 2nd ed. Encyclopedia of Forensic Sciences, ed. Siegel and Suakko. 2013, Boston MA: Elsevier Ltd. 92-97.
89. Makashir, P.S., R.R. Mahajan, and J.P. Agrawal, *Studies on kinetics and mechanism of initial thermal decomposition of nitrocellulose*. Journal of Thermal Analysis, 1995. **45**(3): p. 501-509.
90. Chin, A., et al., *Investigation of the Decomposition Mechanism and Thermal Stability of Nitrocellulose/Nitroglycerine Based Propellants by Electron Spin Resonance*. Propellants, Explosives, Pyrotechnics, 2007. **32**(2): p. 117-126.
91. Trache, D. and A. Tarchoun, *Stabilizers for nitrate ester-based energetic materials and their mechanism of action: a state-of-the-art review*. Journal of Materials Science Letters, 2018. **53**(1): p. 100-123.

92. Stevens, B., S. Bell, and K. Adams, *Initial evaluation of inlet thermal desorption GC-MS analysis for organic gunshot residue collected from the hands of known shooters*. *Forensic Chemistry*, 2016. **2**: p. 55-62.
93. ASTM, *WK72856 Standard Practice for the Collection, Preservation, and Analysis of Organic Gunshot Residues*. 2020, American Society for Testing and Materials: West Conshohocken, PA.
94. Cardinetti, B., et al., *X-ray mapping technique: a preliminary study in discriminating gunshot residue particles from aggregates of environmental occupational origin*. *Forensic Science International*, 2004. **143**(1): p. 1-19.
95. Tucker, W., et al., *Gunshot residue and brakepads: Compositional and morphological considerations for forensic casework*. *Forensic Science International*, 2017. **270**: p. 76-82.
96. Crowson, C., et al., *A Survey of High Explosives Traces in Public Places*. *Journal of Forensic Science*, 1996. **41**(6): p. 980-989.
97. Drzyzga, O., *Diphenylamine and derivatives in the environment: a review*. *Chemosphere*, 2003. **53**(8): p. 809-818.
98. Zhao, M.X., et al., *Desorption electrospray tandem MS (DESI-MSMS) analysis of methyl centralite and ethyl centralite as gunshot residues on skin and other surfaces*. *Journal of Forensic Science*, 2008. **53**(4): p. 807-811.
99. Harrison, H.C. and R. Gilroy, *Firearms discharge residues*. *Journal of Forensic Science*, 1959. **4**(2): p. 184-199.
100. Bartsch, M., H. Kobus, and K. Wainright, *An Update on the Use of the Sodium Rhodizonate Test for the Detection of Lead Originating from Firearm Discharges*. *Journal of Forensic Science*, 1996. **41**(6): p. 1046-1051.
101. Cowan, M.E. and P.L. Purdon, *A study of the "paraffin test"*. *Journal of Forensic Science*, 1967. **12**(1): p. 19-36.
102. Turkel, H.W. and J. Lipman, *Unreliability of Dermal Nitrate Test for Gunpower*. *Journal of Criminal Law, Criminology & Police Science*, 1955. **46**(2): p. 281-284.
103. ENSFI, *Best Practice Manual for Chemographic Methods in Gunshot Residue Analysis*. 2015, European Network of Forensic Science Institutes: European Union. p. 1-15.
104. Taudte, R.V., et al., *Detection of gunshot residues using mass spectrometry*. *BioMed Research International*, 2014.
105. Brozek-Mucha, *Trends in analysis of gunshot residue for forensic purposes*. *Analytical and Bioanalytical Chemistry*, 2017. **409**(25): p. 5803-5811.
106. Charles, S., et al., *Interpol review of gunshot residue 2016–2019*. *Forensic Science International: Synergy*, 2020. **2**: p. 416-428.
107. Pitts, K.M. and S.W. Lewis, *Forensic Sciences: Gunshot Residues*, in *Encyclopedia of Analytical Science (Third Edition)*, P. Worsfold, et al., Editors. 2019, Academic Press: Oxford. p. 48-55.
108. Turillazzi, E., et al., *Analytical and quantitative concentration of gunshot residues (Pb, Sb, Ba) to estimate entrance hole and shooting-distance using confocal laser microscopy and inductively coupled plasma atomic emission spectrometer analysis: An experimental study*. *Forensic Science International*, 2013. **231**(1): p. 142-149.
109. Merli, D., et al., *Comparison of Different Swabs for Sampling Inorganic Gunshot Residue from Gunshot Wounds: Applicability and Reliability for the Determination of Firing Distance*. *Journal of Forensic Sciences*, 2018. **64**(2): p. 558-564.
110. Comanescu, M.A., T.J. Millett, and T.A. Kubic, *A Study of Background Levels of Antimony, Barium, and Lead on Vehicle Surface Samples by Graphite Furnace Atomic Absorption*. *Journal of Forensic Sciences*, 2019. **64**.
111. ENSFI, *Best Practice Manual in the Forensic Examination of Gunshot Residues* 2003. p. 1-34.
112. ASTM, *ASTM E1588 - 20 Standard Practice for Gunshot Residue Analysis by Scanning Electron Microscopy/Energy Dispersive X-Ray Spectrometry*. 2020: West Conshohocken, PA.

113. Coumbaros, J., et al., *Characterisation of 0.22 caliber rimfire gunshot residues by time-of-flight secondary ion mass spectrometry (TOF-SIMS): a preliminary study*. Forensic Science International, 2001. **119**(1): p. 72-81.
114. Bykowicz, J., *FBI lab scraps gunfire residue*, in *The Baltimore Sun*. 2006: U.S.A.
115. Orellana, F.A. and C.G. Galvez, *Applications of laser-ablation-inductively-coupled plasma-mass spectrometry in chemical analysis of forensic evidence*. Trends in Analytical Chemistry, 2013. **42**: p. 1.
116. Jantzi, S.C. and J.R. Almirall, *Elemental Analysis of Soils Using Laser Ablation Inductively Coupled Plasma Mass Spectrometry (LA-ICP-MS) and Laser-Induced Breakdown Spectroscopy (LIBS) with Multivariate Discrimination: Tape Mounting as an Alternative to Pellets for Small Forensic Transfer Specimens*. Applied Spectroscopy, 2014. **68**(9): p. 963-974.
117. Trejos, T. and J.R. Almirall, *Laser Ablation Inductively Coupled Plasma Mass Spectrometry in Forensic Science*, in *Encyclopedia of Analytical Chemistry*, R.A. Meyers, Editor. 2010.
118. Hark, R. and L. East, *Forensic applications of LIBS*. Springer Series in Optical Sciences, 2014. **182**: p. 377-420.
119. Vander Pyl, C., et al., *Analysis of primer gunshot residue particles by laser induced breakdown spectroscopy and laser ablation inductively coupled plasma mass spectrometry*. Analyst (London), 2021. **146**(17): p. 5389-542.
120. Dockery, C.R. and S.R. Goode, *Laser-induced breakdown spectroscopy for the detection of gunshot residues on the hands of a shooter*. Applied Optics, 2003. **42**(30): p. 6153-6158.
121. Rosenberg, M.B. and C.R. Dockery, *Determining the Lifetime of Detectable Amounts of Gunshot Residue on the Hands of a Shooter Using Laser-Induced Breakdown Spectroscopy*. Applied Spectroscopy, 2008. **62**(11): p. 1238-1241.
122. Silva, M.J., et al., *Gunshot residues: Screening analysis by laser-induced breakdown spectroscopy*. Journal of the Brazilian Chemical Society, 2009. **20**(10): p. 1887-1894.
123. Tarifa, A. and J.R. Almirall, *Fast detection and characterization of organic and inorganic gunshot residues on the hands of suspects by CMV-GCMS and LIBS*. Science & Justice, 2015. **55**(3): p. 168-175.
124. Fambro, L.A., et al., *Laser-Induced Breakdown Spectroscopy for the Rapid Characterization of Lead-Free Gunshot Residues*. Applied Spectroscopy, 2017. **71**(4): p. 699-708.
125. Trejos, T., et al., *Fast identification of inorganic and organic gunshot residues by LIBS and electrochemical methods*. Forensic Chemistry, 2018. **8**: p. 146-156.
126. Menking-Hoggatt, K., et al., *Novel LIBS method for micro-spatial chemical analysis of inorganic gunshot residues*. Journal of Chemometrics, 2019. **35**(1): p. n/a.
127. Doña-Fernández, A., et al., *Real-time detection of GSR particles from crime scene: A comparative study of SEM/EDX and portable LIBS system*. Forensic Science International, 2018. **292**: p. 167-175.
128. Abrego, Z., et al., *Unambiguous Characterization of Gunshot Residue Particles Using Scanning Laser Ablation and Inductively Coupled Plasma-Mass Spectrometry*. Analytical Chemistry, 2012. **84**(5): p. 2402-2409.
129. Benito, S., et al., *Characterization of organic gunshot residues in lead-free ammunition using a new sample collection device for liquid chromatography-quadrupole time-of-flight mass spectrometry*. Forensic Science International, 2015. **246**: p. 79-85.
130. Pluháček, T., et al., *Laser ablation inductively coupled plasma mass spectrometry imaging: A personal identification based on a gunshot residue analysis on latent fingerprints*. Analytica Chimica Acta, 2018. **1030**: p. 25-32.
131. Ferreira, I.M.d.S., et al., *Gunshot residue and gunshot residue-like material analysis using laser ablation inductively coupled plasma mass spectrometry imaging*. Spectrochimica Acta. Part B: Atomic Spectroscopy, 2021. **177**: p. 106087.
132. Kozole, J., et al., *Gas phase ion chemistry of an ion mobility spectrometry based explosive trace detector elucidated by tandem mass spectrometry*. Talanta, 2015. **140**: p. 10-19.
133. Zolotov, Y.A., *Ion mobility spectrometry.(Editorial)*. Journal of Analytical Chemistry, 2006. **61**(6): p. 519.

134. Joshi, M., K. Rigsby, and J.R. Almirall, *Analysis of the headspace composition of smokeless powders using GC-MS, GC-uECD and ion mobility spectrometry*. Forensic Science International, 2011. **208**(1): p. 29-36.
135. Arndt, J., et al., *Preliminary evaluation of the persistence of organic gunshot residue*. Forensic Science International, 2012. **222**(1-3): p. 137-145.
136. Zalewska, A., W. Pawlowski, and W. Tomaszewski, *Limits of detection of explosives as determined with IMS and field asymmetric IMS vapour detectors*. Forensic Science International, 2013.
137. West, C., G. Baron, and J.J. Minet, *Detection of gunpowder stabilizers with ion mobility spectrometry*. Forensic Science International, 2007. **166**(2-3): p. 91-101.
138. Perr, J.M., K.G. Furton, and J.R. Almirall, *Solid phase microextraction ion mobility spectrometer interface for explosive and taggant detection*. Journal of Separation Science, 2005. **28**(2): p. 177-183.
139. Lai, H., et al., *Analysis of volatile components of drugs and explosives by solid phase microextraction-ion mobility spectrometry*. Journal of Separation Science, 2008. **31**(2): p. 402-412.
140. Yeager, B., et al., *Evaluation and validation of ion mobility spectrometry for presumptive testing targeting the organic constituents of firearms discharge residue*. Analytical Methods, 2015. **7**(22): p. 9683-9691.
141. Bell, S. and L. Seitzinger, *From binary presumptive assays to probabilistic assessments: Differentiation of shooters from non-shooters using IMS, OGSR, neural networks, and likelihood ratios*. Forensic Science International, 2016. **263**: p. 176-185.
142. Cook, G.W., et al., *Using Gas Chromatography with Ion Mobility Spectrometry to Resolve Explosive Compounds in the Presence of Interferents*. Journal of Forensic Sciences, 2010. **55**(6): p. 1582-1591.
143. Northrop, D.M., D.E. Martire, and W.A. MacCrehan, *Separation and Identification of Organic Gunshot and Explosive Constituents by Micellar Electrokinetic Capillary Electrophoresis*. Analytical Chemistry, 1991. **63**(10): p. 1038-1042.
144. de Perre, C., et al., *Separation and identification of smokeless gunpowder additives by capillary electrochromatography*. Journal of Chromatography A, 2012. **1267**: p. 259-265.
145. Bernal Morales, E. and A.L. Revilla Vazquez, *Simultaneous determination of inorganic and organic gunshot residues by capillary electrophoresis*. Journal of Chromatography A, 2004. **1061**(2): p. 225-233.
146. Cascio, O., et al., *Analysis of organic components of smokeless gunpowders: High-performance liquid chromatography vs. micellar electrokinetic capillary chromatography*. Electrophoresis, 2004. **25**(10B-Tj11): p. 1543-1547.
147. Romolo, F., et al., *Rapid, selective and quantitative determination of nitrite and nitrate ions with capillary electrophoresis: A new screening tool for gunshot residue detection*. Forensic Science International, 2003. **136**: p. 147-147.
148. Izake, E.L., *Forensic and homeland security applications of modern portable Raman spectroscopy*. Forensic Science International, 2010. **202**(1): p. 1-8.
149. Bueno, J. and I. Lednev, *Attenuated Total Reflectance-FT-IR Imaging for Rapid and Automated Detection of Gunshot Residue*. Analytical Chemistry, 2014. **86**(7): p. 3389-3396.
150. Bueno, J., V. Sikirzhyski, and I.K. Lednev, *Raman spectroscopic analysis of gunshot residue offering great potential for caliber differentiation*. Analytical Chemistry, 2012. **84**(10): p. 4334.
151. Konanur, N.K. and G.W. vanLoon, *Determination of lead and antimony in firearm discharge residues on hands by anodic stripping voltammetry*. Talanta, 1977. **24**(3): p. 184-187.
152. O'Mahony, A.M. and J. Wang, *Electrochemical Detection of Gunshot Residue for Forensic Analysis: A Review*. Electroanalysis, 2013. **25**(6): p. 1341-1358.
153. Vuki, M., et al., *Simultaneous electrochemical measurement of metal and organic propellant constituents of gunshot residues*. Analyst, 2012. **137**(14): p. 3265-3270.
154. O'Mahony, A.M., et al., *Orthogonal Identification of Gunshot Residue with Complementary Detection Principles of Voltammetry, Scanning Electron Microscopy, and Energy-Dispersive X-ray Spectroscopy: Sample, Screen, and Confirm*. Analytical Chemistry, 2014. **86**(16): p. 8031-8036.

155. Feeney, W., et al., *Detection of organic and inorganic gunshot residues from hands using complexing agents and LC-MS/MS*. Analytical Methods, 2021. **13**(27): p. 324-339.
156. Ott, C.E., et al., *Evaluation of the Simultaneous Analysis of Organic and Inorganic Gunshot Residues Within a Large Population Data Set Using Electrochemical Sensors*. Journal of Forensic Sciences, 2020. **65**(6): p. 1935-1944.
157. Maitre, M., et al., *Current perspectives in the interpretation of gunshot residues in forensic science: A review*. Forensic Science International, 2017. **270**: p. 1-11.
158. Laza, D., et al., *Development of a Quantitative LC-MS/MS Method for the Analysis of Common Propellant Powder Stabilizers in Gunshot Residue*. Journal of Forensic Sciences, 2007. **52**(4): p. 842-850.
159. Perret, D., et al., *LC-MS-MS determination of stabilizers and explosives residues in hand-swabs*. Chromatographia, 2008. **68**(7-8): p. 517-524.
160. Meng, H. and B. Caddy, *Gunshot Residue Analysis: A Review*. Journal of Forensic Sciences, 1997. **42**: p. 553-570.
161. Mach, M.H., A. Pallos, and P.F. Jones, *Feasibility of Gunshot Residue Detection Via Its Organic Constituents. Part II: A Gas Chromatography-Mass Spectrometry Method*. Journal of Forensic Sciences, 1978. **23**(3): p. 446-455.
162. Andrasko, J. and S. Ståhling, *Time Since Discharge of Pistols and Revolvers*. Journal of Forensic Sciences, 2003. **48**(2): p. 1-5.
163. Pigou, P., et al., *An investigation into artefacts formed during gas chromatography/mass spectrometry analysis of firearms propellant that contains diphenylamine as the stabiliser*. Forensic Science International, 2017.
164. Dalby, O. and J.W. Birkett, *The evaluation of solid phase micro-extraction fibre types for the analysis of organic components in unburned propellant powders*. Journal of Chromatography A, 2010. **1217**(46): p. 7183-7188.
165. Sauzier, G., et al., *Optimisation of recovery protocols for double-base smokeless powder residues analysed by total vaporisation (TV) SPME/GC-MS*. Talanta, 2016. **158**: p. 368-374.
166. Andrasko, J. and S. Ståhling, *Time Since Discharge of Rifles*. Journal of Forensic Sciences, 2000. **45**(6): p. 1250-1255.
167. Gallidabino, M., et al., *Development of a Novel Headspace Sorptive Extraction Method To Study the Aging of Volatile Compounds in Spent Handgun Cartridges*. Analytical Chemistry, 2014. **86**(9): p. 4471-4478.
168. Gallidabino, M., F.S. Romolo, and C. Weyermann, *Time since discharge of 9 mm cartridges by headspace analysis, part 1: comprehensive optimisation and validation of a headspace sorptive extraction (HSSE) method*. Forensic Science International, 2016. **272**: p. 159-170.
169. Weyermann, C., et al., *Analysis of organic volatile residues in 9 mm spent cartridges*. Forensic science international, 2009. **186**(1): p. 29-35.
170. Scherperel, G., G. Reid, and R. Waddell Smith, *Characterization of smokeless powders using nano-electrospray ionization mass spectrometry (nESI-MS)*. Analytical and Bioanalytical Chemistry, 2009. **394**(8): p. 2019-2028.
171. Mathis, J.A. and B.R. McCord, *Gradient reversed-phase liquid chromatographic-electrospray ionization mass spectrometric method for the comparison of smokeless powders*. Journal of Chromatography A, 2003. **988**(1): p. 107-116.
172. Kebarle, P. and U.H. Verkerk, *Electrospray: From ions in solution to ions in the gas phase, what we know now*. Mass Spectrometry Reviews, 2009. **28**: p. 898-917.
173. Thomas, J.L., D. Lincoln, and B.R. McCord, *Separation and Detection of Smokeless Powder Additives by Ultra Performance Liquid Chromatography with Tandem Mass Spectrometry (UPLC/MS/MS)*. Journal of Forensic Sciences, 2013. **58**(3): p. 609-615.
174. DeTata, D., P. Collins, and A. McKinley, *A fast liquid chromatography quadrupole time-of-flight mass spectrometry (LC-QToF-MS) method for the identification of organic explosives and propellants*. Forensic Science International, 2013. **233**(1): p. 63-74.

175. Taudte, R.V., C. Roux, and A. Beavis, *Stability of Smokeless Powder Compounds On Collection Devices*. Forensic Science International, 2016. **270**: p. 55-60.
176. Javanshad, R. and A.R. Venter, *Ambient ionization mass spectrometry: real-time, proximal sample processing and ionization*. Analytical Methods, 2017. **9**(34): p. 4896-497.
177. Green, F.M., et al., *Ambient mass spectrometry: advances and applications in forensics*. Surface and Interface Analysis, 2010. **42**(5): p. 347-357.
178. Correa, D.N., et al., *Forensic Chemistry and Ambient Mass Spectrometry: A Perfect Couple Destined for a Happy Marriage?* Analytical chemistry, 2016. **88**(5): p. 2515.
179. Takáts, Z., et al., *Mass spectrometry sampling under ambient conditions with desorption electrospray ionization*. Science (New York, N.Y.), 2004. **306**(5695): p. 471-473.
180. Cody, R.B., J.A. Laramee, and H.D. Durst, *Versatile New Ion Source for the Analysis of Materials in Open Air under Ambient Conditions*. Analytical Chemistry, 2005. **77**(8): p. 2297-2302.
181. Cooks, R.G., et al., *Ambient mass spectrometry*. Science, 2006. **311**(5767): p. 1566.
182. Takats, Z., J.M. Wiseman, and R.G. Cooks, *Ambient mass spectrometry using desorption electrospray ionization (DESI): instrumentation, mechanisms and applications in forensics, chemistry, and biology*. Journal of Mass Spectrometry, 2005. **40**(10): p. 1261-1275.
183. Wu, Z., et al., *Detection of N,N-diphenyl-N,N-dimethylurea (methyl centralite) in gunshot residues using MS-MS method*. Analyst, 1999. **124**(11): p. 1563-1567.
184. Tong, Y., et al., *Determination of diphenylamine stabilizer and its nitrated derivatives in smokeless gunpowder using a tandem MS method*. The Analyst, 2001. **126**(4): p. 480-484.
185. Morelato, M., et al., *Forensic applications of desorption electrospray ionisation mass spectrometry (DESI-MS)*. Forensic Science International, 2013. **226**(1-3).
186. Justes, D.R., et al., *Detection of explosives on skin using ambient ionization mass spectrometry*. Chemical Communications (Cambridge, England), 2007(21): p. 2142.
187. Siegel, J., *Forensic Chemistry : Fundamentals and Applications*. 2015, New York: New York: John Wiley & Sons, Incorporated.
188. Morelato, M., et al., *Screening of gunshot residues using desorption electrospray ionisation-mass spectrometry (DESI-MS)*. Forensic Science International, 2012. **217**(1-3): p. 101-106.
189. Pirro, V., et al., *Direct drug analysis from oral fluid using medical swab touch spray mass spectrometry*. Analytica Chimica Acta, 2015. **861**: p. 47-54.
190. Fedick, P.W. and R.M. Bain, *Swab touch spray mass spectrometry for rapid analysis of organic gunshot residue from human hand and various surfaces using commercial and fieldable mass spectrometry systems*. Forensic Chemistry, 2017. **5**: p. 53-57.
191. Ding, X. and Y. Duan, *Plasma-based ambient mass spectrometry techniques: The current status and future prospective*. Mass Spectrometry Reviews, 2015. **34**(4): p. 449-473.
192. Chen, J., et al., *Plasma-based ambient mass spectrometry: a step forward to practical applications*. Analytical Methods, 2017. **9**(34): p. 498-4923.
193. Gross, J., *Direct analysis in real time: a critical review on DART-MS*. Analytical and Bioanalytical Chemistry, 2014. **406**(1): p. 63-80.
194. Chen, H.-W., B. Hu, and X. Zhang, *Principle and Application of Ambient Mass Spectrometry for Direct Analysis of Complex Samples*. Chinese Journal of Analytical Chemistry, 2010. **38**(8): p. 1069-1088.
195. Brown, H., et al., *Direct Analysis in Real Time (DART) and a portable mass spectrometer for rapid identification of common and designer drugs on-site*. Forensic Chemistry, 2016. **1**: p. 66-73.
196. Sisco, E., et al., *Rapid detection of fentanyl, fentanyl analogues, and opioids for on-site or laboratory based drug seizure screening using thermal desorption DART-MS and ion mobility spectrometry*. Forensic Chemistry, 2017. **4**: p. 108-115.
197. Sisco, E., J. Dake, and C. Bridge, *Screening for trace explosives by AccuTOF-DART: An in-depth validation study*. Forensic Science International, 2013. **232**(1-3): p. 160-168.
198. Rowell, F., et al., *Detection of nitro-organic and peroxide explosives in latent fingerprints by DART- and SALDI-TOF-mass spectrometry*. Forensic Science International, 2012. **221**(1-3): p. 84-91.

199. Bridoux, M., et al., *Combined use of direct analysis in real-time/Orbitrap mass spectrometry and micro-Raman spectroscopy for the comprehensive characterization of real explosive samples*. Analytical and Bioanalytical Chemistry, 2016. **408**(21): p. 5677-5687.
200. Li, F., et al., *A method for rapid sampling and characterization of smokeless powder using sorbent-coated wire mesh and direct analysis in real time - mass spectrometry (DART-MS)*. Science & Justice, 2016. **56**(5): p. 321-328.
201. Williamson, R., et al., *The coupling of capillary microextraction of volatiles (CMV) dynamic air sampling device with DART-MS analysis for the detection of gunshot residues*. Forensic Chemistry, 2018. **8**: p. 49-56.
202. Black, O., et al., *Identification of polymers and organic gunshot residue in evidence from 3D-printed firearms using DART-mass spectrometry: A feasibility study*. Forensic Chemistry, 2017. **5**: p. 26-32.
203. Goudsmits, E., et al., *The analysis of organic and inorganic gunshot residue from a single sample*. Forensic Science International, 2019. **299**: p. 168-173.
204. Zeichner, A. and B. Eldar, *A Novel Method for Extraction and Analysis of Gunpowder Residues on Double-Side Adhesive Coated Stubs*. Journal of forensic sciences, 2004. **49**(6): p. JFS2004022-13.
205. Minziere, V., et al., *Combined Collection and Analysis of Inorganic and Organic Gunshot Residues*. Journal of Forensic Science, 2020.
206. Lucas, N., et al., *A study into the distribution of gunshot residue particles in the random population*. Forensic Science International, 2016. **262**: p. 150-155.
207. Gandy, L., et al., *A novel protocol for the combined detection of organic, inorganic gunshot residue*. Forensic chemistry, 2018. **8**: p. 1-10.
208. Maitre, M., et al., *Thinking beyond the lab: organic gunshot residues in an investigative perspective*. Australian Journal of Forensic Sciences, 2018. **50**(6): p. 659-665.
209. Dennis, D., J. Frisch, and Q. Price, *NCFS Sample Preparation and Instrumental Parameters*. 2010.
210. Sucecka, M., S.M. Musanic, and I.F. Houra, *Kinetics and enthalpy of nitroglycerin evaporation from double base propellants by isothermal thermogravimetry*. Thermochemica Acta, 2010. **510**(1-2): p. 9.
211. Lussier, L., E. Bergeron, and H. Gagnon, *Study of the Daughter Products of Akardite-II*. Propellants, Explosives, Pyrotechnics, 2006. **31**(4): p. 253-262.
212. De Klerk, W., *Assessment of Stability of Propellants and Safe Lifetimes*. Propellants, Explosives, Pyrotechnics, 2015. **40**(3): p. 388-393.
213. Lopez-Lopez, M. and C. Garcia-Ruiz, *Recent non-chemical approaches to estimate the shooting distance*. Forensic Science International, 2014. **239**: p. 79-85.
214. Plattner, T., et al., *Gunshot residue patterns on skin in angled contact and near contact gunshot wounds*. Forensic Science International, 2003. **138**(1): p. 68-74.
215. Cecchetto, G., et al., *MicroCT detection of gunshot residue in fresh and decomposed firearm wounds*. Int J Legal Med, 2011. **126**(3): p. 377-383.
216. Pircher, R., et al., *Bullet wipe on the uppermost textile layer of gunshot entrance sites: may it be absent due to pre-existing blood staining?* International Journal of Legal Medicine, 2019. **133**(5): p. 1437-1442.
217. Fabbris, S., et al., *Interaction of gunshot residues (GSR) with natural and synthetic textiles having different structural features*. Talanta Open, 2020. **2**: p. 100017.
218. Romolo, F. and P. Margot, *Identification of gunshot residue: a critical review*. Forensic Science International, 2001. **119**(2): p. 195-211.
219. *U.S. Attorney's Office, Middle District of North Carolina. Defendant Sentenced For Firearm Possession in Road Rage Incident*, in Targeted News Service. 2018, Targeted News Service: Washington, D.C.
220. Atwater, C.S., et al., *Visualization of Gunshot Residue Patterns on Dark Clothing*. Journal of Forensic Science, 2006. **51**(5): p. 1091-1095.
221. Grabmuller, M., et al., *RNA/DNA co-analysis on aged bloodstains from adhesive tapes used for gunshot residue collection from hands*. Forensic Science, Medicine and Pathology, 2017. **13**(2): p. 161-169.

222. Zuy, Y., et al., *HPLC detection of organic gunshot residues collected with silicone wristbands*. Analytical Methods, 2020. **12**(1): p. 85-90.
223. Bonnar, C., et al., *Tandem detection of organic and inorganic gunshot residues using LC–MS and SEM-EDS*. Forensic Science International, 2020. **314**: p. 110389.
224. Feeney, W., et al., *Trends in composition, collection, persistence, and analysis of IGSR and OGSR: A review*. Forensic Chemistry, 2020. **19**.
225. Shaw, A., *The role of the gunshot residue expert in case review — A case study*. Forensic Science International, 2019. **300**: p. 28-31.
226. Gialamas, D., E. Rhodes, and L. Sugarman, *Officers, Their Weapons and Their Hands: An Empirical Study of GSR on the Hands of Non-Shooting Police Officers*. Journal of Forensic Science, 1995. **40**(6): p. 1086-1089.
227. Northrop, D., *Gunshot Residue Analysis by Micellar Electrokinetic Capillary Electrophoresis: Assessment for Application to Casework. Part II*. Journal of Forensic Science, 2001. **46**(3): p. 560-572.
228. Cullum, H., et al., *A second survey of high explosives traces in public places*. Journal of Forensic Science, 2004. **49**(4): p. 684-90.
229. Lahoda, K.G., et al., *A Survey of Background Levels of Explosives and Related Compounds in the Environment*. Journal of Forensic Sciences, 2008. **53**(4): p. 802-806.
230. Lindsay, E., et al., *Observations of GSR on the hands of employees at firearms manufacturing facilities*. Canadian Society of Forensic Science Journal, 2011. **44**: p. 105-109.
231. Gerard, R.V., et al., *Observations of Gunshot Residue Associated with Police Officers, Their Equipment, and Their Vehicles*. Canadian Society of Forensic Science Journal, 2012. **45**(2): p. 57-63.
232. Hannigan, T.J., et al., *Evaluation of gunshot residue (GSR) evidence: Surveys of prevalence of GSR on clothing and frequency of residue types*. Forensic Science International, 2015. **257**: p. 177-181.
233. Manganelli, M., C. Weyermann, and A.-L. Gassner, *Surveys of organic gunshot residue prevalence: Comparison between civilian and police populations*. Forensic Science International, 2019. **298**: p. 48-57.
234. *Subcommittee for Ignitable Liquids, Explosives, and Gunshot Residue (2022). OSAC 2022-S-0003 Proposed Standard for comment, subject to change. Standard Practice for the Analysis of Organic Gunshot Residue by Liquid Chromatography-Mass Spectrometry*. Organization of Scientific Area Committees for Forensic Science.
235. Lafleche, D., et al., *Gunshot residue and airbags: Part I. Assessing the risk of deployed automotive airbags to produce particles similar to gunshot residue*. Journal of the Canadian Society of Forensic Science, 2018. **51**(2): p. 48-57.
236. Berk, R.E., *Automated SEM/EDS Analysis of Airbag Residue. II: Airbag Residue as a Source of Percussion Primer Residue Particles*. Journal of forensic sciences, 2009. **54**(1): p. 69-76.
237. Niewohner, L., *Final Workshop Report on the Application of the Bayesian Approach in Gunshot Residue Investigation 2014*, ENSFI.
238. ENSFI, *Guideline for Evaluative Reporting in Forensic Science*. 2015, European Network of Forensic Science Institutes: European Union. p. 1-128.
239. NIFS, *An introductory guide to evaluative reporting*. 2017, Australia New Zealand Policing Advisory Agency (ANZPAA). p. 1-26.
240. Cook, R., et al., *A hierarchy of propositions: deciding which level to address in casework*. Science & justice, 1998. **38**(4): p. 231-239.
241. *Australian Law Review Council. Traditional Rights and Freedoms—Encroachments by Commonwealth Laws (ALRC Report 129)*. 2015, ALRC.
242. Gittelsohn, S., et al., *A Practical Guide for the Formulation of Propositions in the Bayesian Approach to DNA Evidence Interpretation in an Adversarial Environment*. Journal of Forensic Science, 2016. **61**(1): p. 186-195.
243. Charles, S. and A. Jonckheere, *The use and understanding of forensic reports by judicial actors—The field of gunshot residue expertise as an example*. Forensic Science International, 2022. **335**: p. 111312-111312.

244. Martire, K.A., et al., *On the interpretation of likelihood ratios in forensic science evidence: Presentation formats and the weak evidence effect*. Forensic Science International, 2014. **240**: p. 61-68.
245. Morrison, G.S. and E. Enzinger, *What should a forensic practitioner's likelihood ratio be?* Science & Justice, 2016. **56**(5): p. 374-379.
246. Marquis, R., et al., *Discussion on how to implement a verbal scale in a forensic laboratory: Benefits, pitfalls and suggestions to avoid misunderstandings*. Science & justice, 2016. **56**(5): p. 364-370.
247. Aitken, C., P. Roberts, and G. Jackson, *Fundamentals of Probability and Statistical Evidence in Criminal Proceedings*. 2010.
248. Champod, C., et al., *ENFSI Guideline for Evaluative Reporting in Forensic Science: A Primer for Legal Practitioners*. Criminal Law & Justice Weekly, 2016. **180**(10): p. 189-193.
249. Taylor, D., B. Kokshoorn, and A. Biedermann, *Evaluation of forensic genetics findings given activity level propositions: A review*. Forensic Science International: Genetics, 2018. **36**: p. 34-49.
250. Aitken, C., et al., *Expressing evaluative opinions: A position statement*. Science & Justice, 2011. **51**(1): p. 1-2.
251. Bunch, S. and G. Wevers, *Application of likelihood ratios for firearm and toolmark analysis*. Science & Justice, 2013. **53**(2): p. 223-229.
252. Buckleton, J., et al., *A review of likelihood ratios in forensic science*. Forensic Science International, 2020. **310**: p. 110251-110251.
253. Berger, C.E.H., et al., *Evidence evaluation: A response to the court of appeal judgment in R v T*. Science & Justice, 2011. **51**(2): p. 43-49.
254. Fenton, N., M. Neil, and D. Berger, *Bayes and the Law*. Annual Review of Statistics and Its Application, 2016. **3**(1): p. 51-77.
255. Taroni, F., et al., *A general approach to Bayesian networks for the interpretation of evidence*. Forensic Science International, 2004. **139**(1): p. 5-16.
256. Lucas, N., et al., *A framework for the assessment of gunshot residue (GSR) evidence: transfer, contamination, and preservation*, in *American Academy of Forensic Sciences 70th Annual Meeting*. 2018.
257. Morrison, G.S. and N. Poh, *Avoiding overstating the strength of forensic evidence: Shrunk likelihood ratios/Bayes factors*. Sci Justice, 2018. **58**(3): p. 200-218.
258. Cardinetti, B., et al., *A proposal for statistical evaluation of the detection of gunshot residues on a suspect*. Scanning, 2006. **28**(3): p. 142-147.
259. Damary, N.K., et al., *Calculation of likelihood ratios for gunshot residue evidence-statistical aspects*. Law, Probability and Risk, 2016. **15**(2): p. 107-125.
260. Benzaquen, D., et al., *A Mixture Model for the Number of Gunshot Residues Found on Suspects' Hands*. Journal of Forensic Science, 2020. **65**(4): p. 1114-1119.
261. Maitre, M., et al., *An application example of the likelihood ratio approach to the evaluation of organic gunshot residues using a fictional scenario and recently published data*. Forensic Science International, 2022. **335**: p. 111267-111267.
262. Bovens, M., et al., *Chemometrics in forensic chemistry — Part I: Implications to the forensic workflow*. Forensic Science International, 2019. **301**: p. 82-90.
263. Matzen, T., et al., *Objectifying evidence evaluation for gunshot residue comparisons using machine learning on criminal case data*. Forensic Science International, 2022. **335**: p. 111293-111293.
264. Bolck, A., H. Ni, and M. Lopatka, *Evaluating score- and feature-based likelihood ratio models for multivariate continuous data: applied to forensic MDMA comparison*. Law, Probability and Risk, 2015. **14**(3): p. 243-266.
265. Lee, L.C., C.-Y. Liong, and A.A. Jemain, *Effects of data pre-processing methods on classification of ATR-FTIR spectra of pen inks using partial least squares-discriminant analysis (PLS-DA)*. Chemometrics and Intelligent Laboratory Systems, 2018. **182**: p. 90-100.
266. Marini, F., *Artificial neural networks in foodstuff analyses: Trends and Perspectives*. Analytica Chimica Acta, 2009. **635**(2): p. 121-131.

267. Feeney, W., et al., *Evaluation of organic and inorganic gunshot residues in various populations using LC-MS/MS*. Forensic Chemistry, 2022. **27**: p. 100389.
268. Gallidabino, M.D., et al., *Quantitative profile-profile relationship (QPPR) modelling: a novel machine learning approach to predict and associate chemical characteristics of unspent ammunition from gunshot residue*. Analyst, 2019. **144**(4): p. 1128-1139.
269. Skorupski, W.P. and H. Wainer, *The Bayesian flip: Correcting the prosecutor's fallacy*. Significance, 2015. **12**(4): p. 16-20.
270. Molinaro, A.M., *Diagnostic tests: how to estimate the positive predictive value*. Neuro-Oncology Practice, 2015. **2**(4): p. 162-166.
271. Mandell, B., *Clinical Decision Making: Understanding Medical Tests and Test Results*, in *MSD Manuals, Professional Version*. 2021, Merck & Co. Inc.: Kenilworth, NJ, USA.
272. Gigerenzer, G., et al., *Helping Doctors and Patients Make Sense of Health Statistics*. Psychological Science in the Public Interest, 2007. **8**(2): p. 53-96.
273. Westreich, D. and N. Iliinsky, *Epidemiology Visualized: The Prosecutor's Fallacy*. American Journal of Epidemiology, 2014. **179**(9): p. 1125-1127.
274. Thompson, W.C. and E.L. Schumann, *Interpretation of Statistical Evidence in Criminal Trials: The Prosecutor's Fallacy and the Defense Attorney's Fallacy*. Law and Human Behavior, 1987. **11**(3): p. 167-187.
275. Biedermann, A., S. Bozza, and F. Taroni, *Probabilistic evidential assessment of gunshot residue particle evidence (Part II): Bayesian parameter estimation for experimental count data*. Forensic Science International, 2010. **206**(1): p. 103-110.
276. Addinsoft, *XLSTAT statistical and data analysis solution*. 2022, Addinsoft New York, USA.
277. Biedermann, A. and F. Taroni, *A probabilistic approach to the joint evaluation of firearm evidence and gunshot residues*. Forensic science international, 2006. **163**(1): p. 18-33.
278. de Zoete, J. and M. Sjerps, *Combining multiple pieces of evidence using a lower bound for the LR*. Law, Probability and Risk, 2018. **17**(2): p. 163-178.
279. Addinsoft_Corporation, *XLStat Life Sciences Package*. 2022: Long Island, NY, USA. <https://www.xlstat.com/>. Accessed Online 01/12/2022.
280. O'Brien, R.M., *A caution regarding rules of thumb for variance inflation factors*. Quality & Quantity, 2007. **41**(5): p. 673-690.
281. *Supreme Court of Western Australia - Court of Appeal. Nicolaidis v Western Australia*. Australasian Legal Information Institute, 2007. **WASCA 203**.
282. Grigoratos, T. and G. Martini, *Brake wear particle emissions: a review*. Environmental Science and Pollution Research, 2014. **22**(4): p. 2491-2504.
283. Kukutschova, J., et al., *On airborne nano/micro-sized wear particles released from low-metallic automotive brakes*. Environmental Pollution, 2011. **159**(4): p. 998-1006.
284. Thorpe, A. and R.M. Harrison, *Sources and properties of non-exhaust particulate matter from road traffic: A review*. Science of the Total Environment, 2008. **400**(1): p. 270-282.
285. Iijima, A., et al., *Particle size and composition distribution analysis of automotive brake abrasion dusts for the evaluation of antimony sources of airborne particulate matter*. Atmospheric Environment, 2007. **41**(23): p. 4908-4919.
286. Poole, D.R., *Azide-free gas generant composition with easily filterable combustion products*, in *United States Patent and Trademark Office*. 1990, Automotive Systems Laboratory Inc.: USA.
287. Berk, R.E., *Automated SEM/EDS Analysis of Airbag Residue. I: Particle Identification*. Journal of Forensic Sciences, 2009. **54**(1): p. 60-68.
288. Ho, J.S., et al., *Distinguishing diphenylamine and N-nitrosodiphenylamine in hazardous waste samples by using high-performance liquid chromatography/thermospray/mass spectrometry*. Environmental Science & Technology, 1990. **24**(11): p. 1748-1751.
289. Canterberry, J., et al., *Ignition enhancement composition for an airbag inflator*, in *European Patent Office*. 1997, Breed Automotive Technology Inc.

290. Cataldo, F., *On the ozone protection of polymers having non-conjugated unsaturation*. Polymer Degradation and Stability, 2001. **72**(2): p. 287-296.
291. Gadd, J. and P. Kennedy, *Preliminary examination of organic compounds present in tyres, brake pads and road bitumen in New Zealand*. 2003.
292. Kole, P.J., et al., *Wear and Tear of Tyres: A Stealthy Source of Microplastics in the Environment*. International Journal of Environmental Research and Public Health, 2017. **14**(10): p. 1265.
293. Wik, A. and G. Dave, *Occurrence and effects of tire wear particles in the environment: A critical review and an initial risk assessment*. Environmental Pollution, 2009. **157**(1): p. 1-11.
294. Wagner, S., et al., *Tire wear particles in the aquatic environment - A review on generation, analysis, occurrence, fate and effects*. Water Research, 2018. **139**: p. 83-100.
295. Liu, R., et al., *Emerging aromatic secondary amine contaminants and related derivatives in various dust matrices in China*. Ecotoxicology and Environmental Safety, 2019. **170**: p. 657-663.
296. Dodd, D.E., et al., *Subchronic urinary bladder toxicity evaluation of N-Nitrosodiphenylamine in Fischer 344 rats*. Journal of Applied Toxicology, 2013. **33**(5): p. 383-389.
297. Gassner, A.-L. and C.I. Weyermann, *Prevalence of organic gunshot residues in police vehicles*. Science & Justice, 2020. **60**(2): p. 136-144.
298. Blakey, L., et al., *Fate and Behavior of Gunshot Residue: Recreational Shooter Vehicle Distribution*. Journal of Forensic Science, 2019. **64**(6): p. 1668-1672.
299. Burnett, B.R. and J. Lebieczik, *Discharge of a Pistol Out a Car Window with the Breech Within the Interior of the Car: Analysis of Gunshot Residue on a Car's Interior Surfaces*. Journal of Forensic Science, 2017. **62**(3): p. 768-772.
300. Burnett, B.R., *A case of alleged discharge of a firearm within a vehicle*. Forensic Science International, 2018. **289**: p. e1-e8.
301. Lafleche, D.J.N. and N.G.R. Hearn, *Gunshot residue and airbags: Part II. A case study*. Journal of the Canadian Society of Forensic Science, 2019. **52**(1): p. 26-32.
302. Bonnar, C., R. Popelka-Filcoff, and K.P. Kirkbride, *Armed with the Facts: A Method for the Analysis of Smokeless Powders by Ambient Mass Spectrometry*. Journal of the American Society for Mass Spectrometry, 2020. **31**(9): p. 1943-1956.
303. Heramb, R.M. and B.R. McCord, *The manufacture of smokeless powders and their forensic analysis: a brief review. (Research and Technology)*. Forensic Science Communications, 2002. **4**(2).
304. Wallace, C.L. and C.R. Midkiff, *Smokeless Powder Characterization: An Investigative Tool in Pipe Bombings*. Advances in Analysis and Detection of Explosives, 1993: p. 29-39.
305. Bors, D. and J. Goodpaster, *Mapping smokeless powder residue on PVC pipe bomb fragments using total vaporization solid phase microextraction*. Forensic Science International, 2017. **276**: p. 71-76.
306. Ewing, R.G., et al., *A Critical Review of Ion Mobility Spectrometry for the Detection of Explosives and Explosive Related Compounds*. Talanta, 2001. **54**(3).
307. Klapek, D.J., G. Czarnopys, and J. Pannuto, *Interpol review of detection and characterization of explosives and explosives residues 2016-2019*. Forensic Science International: Synergy.
308. Harris, G.A., L. Nyadong, and F.M. Fernandez, *Recent developments in ambient ionization techniques for analytical mass spectrometry*. The Analyst, 2008. **133**(10): p. 1297-1301.
309. Pavlovich, M.J., B. Musselman, and A.B. Hall, *Direct analysis in real time-mass spectrometry (DART-MS) in forensic and security applications*. Mass Spectrometry Reviews, 2018. **37**(2): p. 171-187.
310. Ifa, D., et al., *Forensic applications of ambient ionization mass spectrometry*. Analytical and Bioanalytical Chemistry, 2009. **394**(8): p. 1995-2008.
311. Hoffmann, W.D. and G.P. Jackson, *Forensic Mass Spectrometry*. Annual Review of Analytical Chemistry, 2015. **8**(1): p. 419-440.
312. Forbes, T.P. and E. Sisco, *Recent advances in ambient mass spectrometry of trace explosives*. Analyst, 2018. **143**(9): p. 1948-1969.
313. Chen, H.-W., et al., *Instrumentation and Characterization of Surface Desorption Atmospheric Pressure Chemical Ionization Mass Spectrometry*. Fenxi Huaxue - Chinese Journal of Analytical Chemistry, 2007. **35**(8): p. 1233-1240.

314. Winter, G., J. Wilhide, and W. LaCourse, *Characterization of a Direct Sample Analysis (DSA) Ambient Ionization Source*. Journal of The American Society for Mass Spectrometry, 2015. **26**(9): p. 1502-1507.
315. NATA, *General Accreditation Guidance: Validation and Verification of Quantitative and Qualitative Test Methods*. 2018.
316. Habib, A., et al., *Detection of explosives using a hollow cathode discharge ion source*. Rapid communications in mass spectrometry, 2015. **29**(7): p. 601-610.
317. Sekimoto, K. and M. Takayama, *Dependence of negative ion formation on inhomogeneous electric field strength in atmospheric pressure negative corona discharge*. The European physical journal. D, Atomic, molecular, and optical physics, 2008. **50**(3): p. 297-305.
318. Sekimoto, K. and M. Takayama, *Negative ion formation and evolution in atmospheric pressure corona discharges between point-to-plane electrodes with arbitrary needle angle*. The European physical journal. D, Atomic, molecular, and optical physics, 2010. **60**(3): p. 589-599.
319. Nagato, K., et al., *An analysis of the evolution of negative ions produced by a corona ionizer in air*. International journal of mass spectrometry, 2006. **248**(3): p. 142-147.
320. PerkinElmer, *Streamline and Simplify Your Forensics Workflow*. Forensics Reference Notebook of LC/MS Applications, 2014: p. 50-51.
321. Nilles, J.M., et al., *Explosives Detection Using Direct Analysis in Real Time (DART) Mass Spectrometry*. Propellants, Explosives, Pyrotechnics, 2010. **35**(5): p. 446-451.
322. Stoneham, M., *Comprehensive Handbook of Chemical Bond Energies*. 2009. **50**: p. 494.
323. Gonzalez-Mendez, R. and C. Mayhew, *Applications of Direct Injection Soft Chemical Ionisation-Mass Spectrometry for the Detection of Pre-blast Smokeless Powder Organic Additives*. Journal of The American Society for Mass Spectrometry, 2019. **30**(4): p. 615-624.
324. Godfrey, A. and A. Brenton, *Accurate mass measurements and their appropriate use for reliable analyte identification*. Analytical and Bioanalytical Chemistry, 2012. **404**(4): p. 1159-1164.
325. Sisco, E. and T.P. Forbes, *Forensic applications of DART-MS: A review of recent literature*. Forensic Chemistry, 2021. **22**: p. 100294.
326. Hodgman, S.S., et al., *Metastable helium: A new determination of the longest atomic excited-state lifetime*. Physical Review Letters, 2009. **103**(5): p. 053002-053002.
327. Song, L., et al., *Ionization Mechanism of Positive-Ion Nitrogen Direct Analysis in Real Time*. Journal of The American Society for Mass Spectrometry, 2018. **29**(4): p. 640-650.
328. Pitman, C.N. and W.R. LaCourse, *Desorption atmospheric pressure chemical ionization: A review*. Analytica Chimica Acta, 2020. **1130**: p. 146-154.
329. Wells, J.M., et al., *Implementation of DART and DESI Ionization on a Fieldable Mass Spectrometer*. Journal of The American Society for Mass Spectrometry, 2008. **19**(10): p. 1419-1424.
330. Mess, A., et al., *Qualitative Analysis of Tackifier Resins in Pressure Sensitive Adhesives Using Direct Analysis in Real Time Time-of-Flight Mass Spectrometry*. Analytical Chemistry, 2011. **83**(19): p. 7323-7330.

8.3 Appendices

Appendix 2-1

Detection status of OGSR compounds above respective LODs, in samples taken after progressively longer delays post-shooting. The substrates (silicone sheeting) were kept as stationary as practical during the interval.

T= (hrs)	Rep	DPA	n(NO).DPA	(NO ₂).DPA	(NO ₂) ₂ .DPA	AK	EC
0	R1	✓	✓	✓	x	✓	✓
	R2	✓	✓	✓	x	✓	✓
	R3	✓	✓	✓	✓	✓	✓
1	R1	✓	✓	✓	x	✓	✓
	R2	x	x	x	x	✓	✓
	R3	✓	✓	✓	x	✓	✓
2	R1	x	x	x	x	x	x
	R2	x	x	x	x	✓	✓
	R3	✓	✓	✓	x	✓	✓
3	R1	✓	✓	✓	✓	✓	✓
	R2	✓	✓	✓	x	✓	✓
	R3	✓	✓	✓	✓	✓	✓
4	R1	✓	✓	✓	✓	✓	✓
	R2	x	x	x	x	✓	✓
	R3	x	x	x	x	✓	✓
5	R1	✓	x	x	x	✓	✓
	R2	✓	✓	✓	x	✓	✓
	R3	✓	✓	✓	x	✓	✓
6	R1	✓	✓	✓	x	✓	✓
	R2	✓	✓	✓	✓	✓	✓
	R3	x	✓	✓	x	✓	✓
8	R1	✓	✓	✓	x	✓	✓
	R2	x	x	x	x	x	✓
	R3	x	x	x	x	✓	✓
12	R1	✓	✓	✓	✓	✓	✓
	R2	✓	✓	✓	✓	✓	✓
	R3	x	x	x	x	✓	✓
24	R1	✓	✓	✓	x	✓	✓
	R2	✓	✓	✓	x	✓	✓
	R3	x	x	x	x	✓	✓

Appendix 3-1

IGSR particle examination results for survey samples (respondents' hands)

3-1 a) Non-shooter sub-population				Characteristic		Characteristic Pb-Free /Non-Toxic		Consistent						Consistent Pb-Free /Non-Toxic		Environmental
Sample Name	Search Duration (mins)	Total (Characteristic)	Total (Consistent)	Pb Sb Ba	Pb Ba Ca Si Sn	Gd Ti Zn	Ga Cu Sn	Sb Ba	Pb Sb	Pb Ba	Pb Ba Si	Ba Ca Si	Ba Al	Ti Zn	Sr	(total only)
HS 051	163	0	0	0	0	0	0	0	0	0	0	0	0	0	0	428
HS 052	211	0	0	0	0	0	0	0	0	0	0	0	0	0	0	245
HS 053	305	0	0	0	0	0	0	0	0	0	0	0	0	0	0	596
HS 054	483	0	2	0	0	0	0	0	0	0	0	0	2	2	1	18,666
HS 055	164	0	2	0	0	0	0	0	0	0	0	0	2	2	1	808
HS 056	149	0	0	0	0	0	0	0	0	0	0	0	0	0	0	391
HS 057	165	0	0	0	0	0	0	0	0	0	0	0	0	0	0	829
HS 058	171	0	0	0	0	0	0	0	0	0	0	0	0	0	1	922
HS 059	190	0	0	0	0	0	0	0	0	0	0	0	0	0	0	1,615
HS 060	151	0	3	0	0	0	0	0	3	0	0	0	0	0	0	472
HS 061	165	0	1	0	0	0	0	0	1	0	0	0	0	0	1	854
HS 062	177	1*	1	1	0	0	0	0	0	1	0	0	0	7	0	1,080
HS 063	327	0	1	0	0	0	0	0	1	0	0	0	0	0	0	6,148
HS 064	140	0	0	0	0	0	0	0	0	0	0	0	0	0	0	300
HS 065	147	0	2	0	0	0	0	0	2	0	0	0	0	0	0	391
HS 066	181	0	0	0	0	0	0	0	0	0	0	0	0	0	0	1,398
HS 067	145	0	0	0	0	0	0	0	0	0	0	0	0	0	0	333
HS 068	163	0	0	0	0	0	0	0	0	0	0	0	0	0	1	853
HS 069	146	0	1	0	0	0	0	0	1	0	0	0	0	0	0	347
HS 070	159	0	0	0	0	0	0	0	0	0	0	0	0	0	2	832
HS 071	144	0	0	0	0	0	0	0	0	0	0	0	0	0	0	302
HS 072	159	0	0	0	0	0	0	0	0	0	0	0	0	0	0	674
HS 073	135	0	0	0	0	0	0	0	0	0	0	0	0	0	0	38
HS 074	145	0	8	0	0	0	0	0	5	0	0	3	0	3	4	266
HS 075	185	0	1	0	0	0	0	0	0	0	0	1	0	0	1	1,907
HS 076	139	0	3	0	0	0	0	0	3	0	0	0	0	0	0	297
HS 077	155	0	3	0	0	0	0	0	2	0	0	0	1	0	7	850
HS 078	135	0	2	0	0	0	0	0	2	0	0	0	0	0	0	290
HS 079	133	0	0	0	0	0	0	0	0	0	0	0	0	0	0	170
HS 080	222	0	1	0	0	0	0	0	1	0	0	0	0	0	1	3,174

3-1 b) Shooter sub-population				Characteristic		Characteristic Pb-Free /Non-Toxic		Consistent					Consistent Pb-Free/Non-Toxic		Environmental	
Sample Name	Search Duration (mins)	Total (Characteristic)	Total (Consistent)	Pb Sb Ba	Pb Ba Ca Si Sn	Gd Ti Zn	Ga Cu Sn	Sb Ba	Pb Sb	Pb Ba	Pb Ba Si	Ba Ca Si	Ba Al	Ti Zn	Sr	(total only)
HS 081	241	414	634	414	0	0	0	10	446	24	2	5	147	1	1	4,303
HS 082	149	135	480	135	0	0	0	6	367	10	1	6	90	0	0	2,591
HS 083	480	119	170	119	0	0	0	2	117	15	4	0	32	0	0	1,008
HS 084	480	35	94	35	0	0	0	3	64	4	2	1	20	0	2	1,303
HS 085	481	186	706	183	3	0	0	18	510	59	7	16	96	11	105	4,224
HS 086	483	209	563	206	3	0	0	6	479	24	7	5	42	0	2	3,094
HS 087	331	118	316	118	0	0	0	6	213	11	3	1	82	0	0	1,168
HS 088	240	437	555	437	0	0	0	43	338	12	1	4	157	0	1	4,660
HS 089	299	103	168	103	0	0	0	0	149	19	0	0	0	0	0	920
HS 090	240	55	103	55	0	0	0	0	80	19	2	0	2	0	0	1,136
HS 091	240	163	241	163	0	0	0	3	221	15	0	0	2	0	0	943
HS 092	240	155	222	155	0	0	0	0	204	17	1	0	0	0	4	1,178
HS 093	240	79	216	79	0	0	0	1	198	6	0	2	9	0	2	5,807
HS 094	241	129	172	129	0	0	0	2	153	14	0	0	3	0	4	834
HS 095	244	1,501	198	1,501	0	0	0	0	189	5	0	0	4	0	0	201
HS 096	242	400	124	400	0	0	0	3	117	2	0	0	2	0	3	1,366
HS 097	185	68	210	68	0	0	0	2	183	24	1	0	0	0	1	1,437
HS 098	240	102	61	102	0	0	0	1	55	4	0	0	1	2	0	1,095
HS 099	240	302	584	302	0	0	0	0	484	96	0	0	4	0	0	1,944
HS 100	240	299	329	299	0	0	0	0	268	61	0	0	0	0	0	826
HS 101	242	769	1,250	769	0	0	0	1	1,248	0	0	0	1	0	0	161
HS 102	241	1,824	746	1,824	0	0	0	28	712	2	0	0	4	0	2	1,926
HS 103	240	28	295	28	0	0	0	0	286	6	1	1	1	0	3	1,229
HS 104	240	1,147	566	1,147	0	0	0	54	501	3	0	0	8	0	0	1,872
HS 105	240	50	124	50	0	0	0	3	100	19	1	1	0	0	0	1,671
HS 106	241	74	156	74	0	0	0	0	149	7	0	0	0	0	3	844
HS 107	240	1,127	490	1,127	0	0	0	34	452	3	0	0	1	0	7	2,253
HS 108	240	1,250	355	1,250	0	0	0	38	310	3	0	0	4	0	1	2,663
HS 109	240	1,545	637	1,545	0	0	0	57	575	0	0	0	5	0	0	1,842
HS 110	241	1,671	723	1,671	0	0	0	82	630	4	0	0	7	0	3	2,299

Appendix 5-1

Information and instructions provided to participants in survey and sample collection



Sampling Instructions

Dear Volunteer,

Thank you for agreeing to take part in this research. In this kit you should have received a short survey and five adhesive stubs in plastic holders. We ask that you use one of these stubs to collect residues from your hands and use the remaining stubs to collect residues from four surfaces within your car as indicated below. The purpose of doing this is to see if residues from your hands or your car may give a positive result if tested for gunshot residue. This could occur because you have used a firearm for legitimate reasons, have come into contact someone else who has, or there is an unrelated substance causing a false positive.



In order to collect each sample of residue, you will need to unscrew the plastic cap and dab the adhesive against the relevant surface approximately 50 times or until it is no longer sticky. This shouldn't leave any noticeable residue behind. Please try to dab the stub straight up and down onto the surface it is sampling and press the stub flat as dragging the adhesive may cause it to tear or separate from its' aluminum backing. Once each sample has been collected, replace the plastic screw caps to avoid further contamination and put all samples together in the return envelope.

For samples collected from your hands, please use a single stub for both hands and focus on the webbing between thumb and forefinger as indicated in the pictures below.





If you are providing residues from your vehicle, there are four target areas that we request you sample:

- A) control surfaces – steering wheel, handbrake & gear levers using the same stub.
- B) front dashboard.
- C) driver's seat and seat-back.
- D) rear storage.

A visual guide is included below. On textile surfaces and the dashboard the sampling stub is likely to lose its stickiness quite rapidly. Therefore, in order to ensure maximum coverage of the large areas in B), C) and D), we suggest that you widely space your dabs across each surface.

Once the samples have been collected, double check that all five stubs are placed in the envelope alongside the completed questionnaire. Posting the kit for return will conclude your direct participation in the research, as your samples will be separated from any identifying information before analysis.

Once again, we thank you for your valuable contribution of time to this project.



Appendix 5-2

GSR examination results for shooters' and non-shooters' vehicle samples

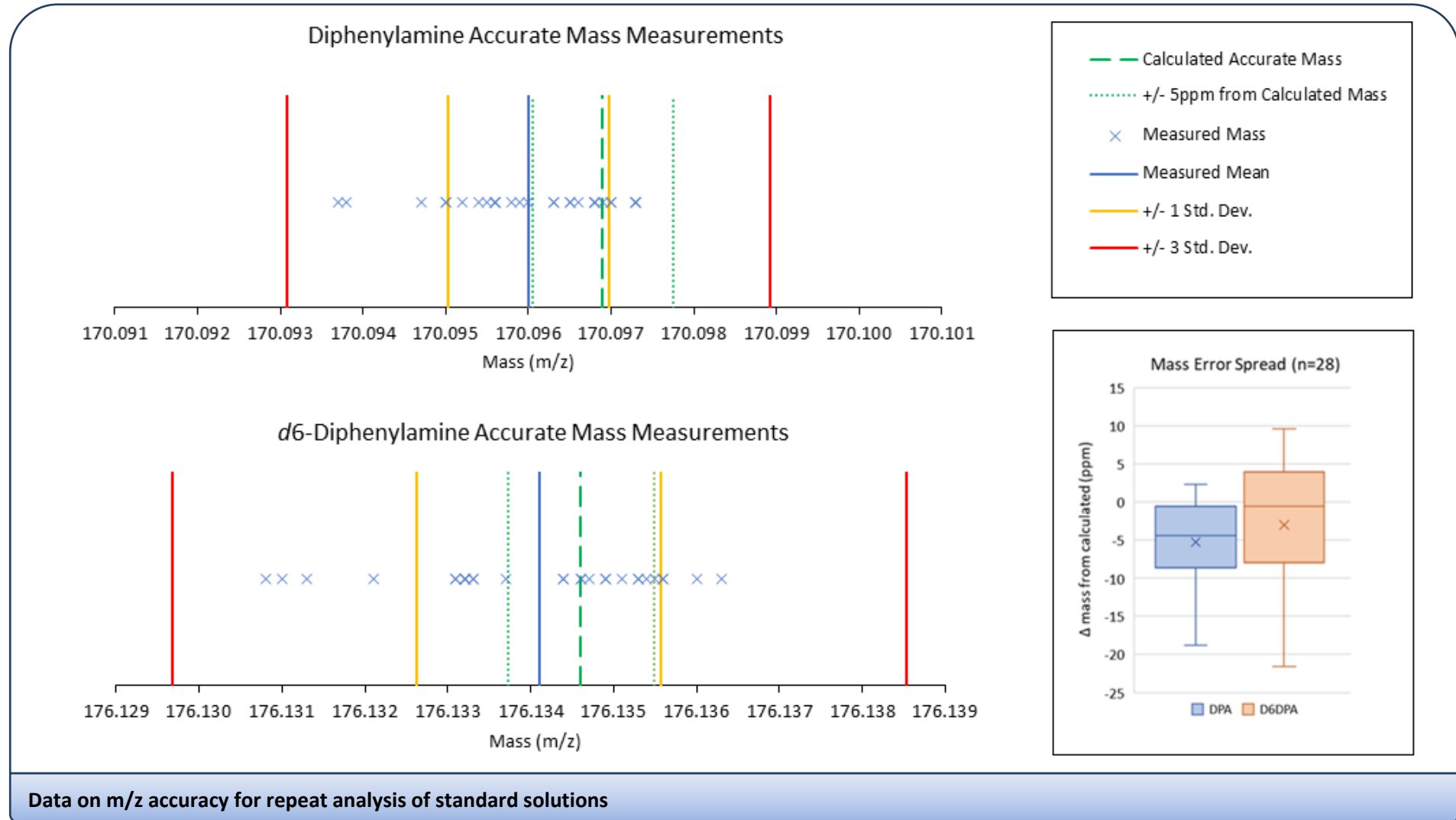
With Recent Firearm Association		IGSR Particle Count		OGSR compound concentration (ppb)						OGSR Count	OGSR Report:	
Sample ID		Characteristic	Consistent	DPA	NO.DPA	(NO2).DPA	(NO2)2.DPA	Ak	MC			EC
LODS (ppb):		x	x	27	57	0.9	4	0.2	0.02	0.2		
V21 - "sport shooting, every two weeks, 9mm & 0.22LR pistol". Last Fired >1 month, last handled >1 week Last transported ~2 weeks	A	7	2								0	Neg
	B	11	0								0	Neg
	C	3	0								0	Neg
	D	0	0								0	Neg
	E	0	0								0	Neg
V26 - "sport shooting, every two weeks, 9mm & 0.22LR pistol". Last Fired >1 month, last handled >1 week Last transported >1 year	A	0	0								0	Neg
	B	2	1					4.8			1	Inconclusive
	C	0	0								0	Neg
	D	0	0					2.4			1	Inconclusive
	E	0	0								0	Neg
V28 - "Sports/target shooting. Used weekly until Covid lockdown. Mainly 9mm luger/45 ACP." Last Fired >1 month, last handled >1 month Last transported never	A	948	1,000+						0.08	5.1	2	Characteristic
	B	18	1								0	Neg
	C	2	14								0	Neg
	D	0	0								0	Neg
	E	0	0					4.3			1	Inconclusive
V25 - Infrequent shooter. Last fired >1 month, last handled >1 month, last transported ~6 months.	A	0	1								0	Neg
	B	2	7								0	Neg
	C	0	2								0	Neg
	D	1	4								0	Neg
	E	0	0								0	Neg
V41 - "Target shooting, 3 x week, revolvers in various cal up to 0.45." Last fired 30 mins, last handled 90 mins, last transported earlier that day	A	96	149								0	Neg
	B	17	33								0	Neg
	C	177	128								0	Neg
	D	498	502	41	1725	3.2	28			5.1	5	Characteristic
	E	73	157								0	Neg
V42 - "Sports/target shooting 3 x week, 22LR semi auto pistol & revolver + 38sp revolver." Last fired, handled and transported firearms 2 days ago	A	55	94								0	Neg
	B	207	362								0	Neg
	C	169	189								0	Neg
	D	59	49								0	Neg
	E	97	100								0	Neg
43 - Sports/target shooting, no details on firearm(s) provided. Last fired, handled and transported firearms 2 hrs earlier	A	53	65								0	Neg
	B	45	464								0	Neg
	C	73	340	56	310	4.2					3	Characteristic
	D	122	804	99	553	8.6	14			4.8	4	Characteristic
	E	215	1,000+						0.8	1.0	2	Consistent

Without Recent Firearm Association		IGSR Particle Count		OGSR compound concentration (ppb)						OGSR Count	OGSR Report:	
Sample ID		Characteristic	Consistent	DPA	NO.DPA	(NO2).DPA	(NO2)2.DPA	Ak	MC			EC
LODS (ppb):		x	x	27	57	0.9	4	0.2	0.02	0.2		
V20 - No association declared	A	0	0								0	Neg
	B	0	2 x BaAl								0	Neg
	C	0	0								0	Neg
	D	0	0								0	Neg
	E	0	1 x BaAl								0	Neg
V23 - No association declared	A	0	1 x BaAl, 1 x TiZn								0	Neg
	B	0	0								0	Neg
	C	0	1 x BaAl								0	Neg
	D	0	1 x PbSb								0	Neg
	E	0	1 x BaAl								0	Neg
V24 - No association declared	A	0	0								0	Neg
	B	0	0								0	Neg
	C	0	1 x BaAl								0	Neg
	D	0	1 x BaAl								0	Neg
	E	0	3 x BaAl								0	Neg
V22 - No association declared	A	0	0								0	Neg
	B	0	0								0	Neg
	C	0	0					6.1			1	Inconclusive
	D	0	0								0	Neg
	E	0	0								0	Neg

27 - No association declared	A	0	0						0	Neg
	B	0	0						0	Neg
	C	0	1 x Sr					2.6	1	Inconclusive
	D	0	0					1.3	1	Inconclusive
	E	0	0				4.9		1	Inconclusive
V31 - minor association, last handled firearm materials >1 month ago	A	0	0						0	Neg
	B	0	0						0	Neg
	C	0	0						0	Neg
	D	0	0						0	Neg
	E	0	0						0	Neg
V32 - No association declared	A	0	0						0	Neg
	B	0	1 x Sr						0	Neg
	C	0	1 x PbSb						0	Neg
	D	0	0						0	Neg
	E	0	0						0	Neg
V33 - No association declared	A	0	1 x PbSb						0	Neg
	B	0	1 x PbBa, 1 x PbSb, 1 x Sr						0	Neg
	C	0	0						0	Neg
	D	0	0				90.3		1	Inconclusive
	E	0	0						0	Neg
V34 - minor association, last handled firearm materials >1 month ago	A	0	1 x Sr						0	Neg
	B	0	0						0	Neg
	C	0	0						0	Neg
	D	0	0						0	Neg
	E	0	1 x Sr						0	Neg
V35 - No association declared	A	0	1 x PbSb						0	Neg
	B	0	0						0	Neg
	C	0	0					3.2	1	Inconclusive
	D	0	0				2.5		1	Inconclusive
	E	0	20 x PbSb, 1 x Sr					1.8	1	Inconclusive
V36 - No association declared	A	0	0					7.0	1	Inconclusive
	B	0	0					8.1	1	Inconclusive
	C	0	0					6.2	1	Inconclusive
	D	0	1 x PbSb				2.2	7.0	2	Consistent
	E	0	1 x PbSb						0	Neg
V37 - No association declared	A	0	0						0	Neg
	B	1 x PbBaSb	0						0	Neg
	C	0	0						0	Neg
	D	0	0						0	Neg
	E	0	0					3.3	1	Inconclusive
V38 - minor association, last handled firearm materials >1 month ago	A	0	0						0	Neg
	B	0	1 x PbBa						0	Neg
	C	0	1 x PbBa						0	Neg
	D	0	0						0	Neg
	E	0	0						0	Neg
V39 - No association declared	A	0	0						0	Neg
	B	0	0						0	Neg
	C	0	0						0	Neg
	D	0	1 x BaAl						0	Neg
	E	0	0						0	Neg
V40 - No association declared	A	0	1 x PbSb						0	Neg
	B	0	0						0	Neg
	C	0	1 x BaAl						0	Neg
	D	0	1 x BaAl						0	Neg
	E	0	0					0.03	1	Inconclusive

Appendix 6-1

Data on mass accuracy for repeat analysis of standard solutions:



Appendix 6-2

Additional figures of merit describing instrument performance for quantitative measurement:

Quantitative Accuracy (DPA Recovery Curve)		
DPA on mesh (ng, by microbalance and dilution, normalized to I.S.)	mean ratio between peak areas (n=4)	% recovery
0.248	0.283	115.6%
0.499	0.527	99.4%
0.739	0.730	90.8%
0.997	1.026	92.7%
1.519	1.755	102.0%
2.003	2.228	97.7%
2.547	2.862	98.2%

Quantitative Precision	
nominal DPA mass	Coefficient of Variation (Std Dev / mean, n=4)
0.25 ng	8.7%
0.5 ng	6.6%
0.75 ng	2.2%
1 ng	4.8%
1.5 ng	6.3%
2 ng	4.0%
2.5 ng	4.7%

Linearity	
Linear Regression:	$y=1.144x-0.0535$
R ² :	0.9972
Standard error of regression (S):	0.0393

Calculated analytical limits	
$LOD = \frac{3 \times S}{m}$:	0.105 ng
$LOQ = \frac{10 \times S}{m}$:	0.347 ng